Lecture Notes in Physics 937

Guido Altarelli

Collider Physics within the Standard Model

A Primer

Edited by James Wells

With a Foreword by Gian Giudice

Springer Open

Lecture Notes in Physics

Volume 937

Founding Editors

W. Beiglböck
J. Ehlers
K. Hepp
H. Weidenmüller

Editorial Board

M. Bartelmann, Heidelberg, Germany
B.-G. Englert, Singapore, Singapore
P. Hänggi, Augsburg, Germany
M. Hjorth-Jensen, Oslo, Norway
R.A.L. Jones, Sheffield, UK
M. Lewenstein, Barcelona, Spain
H. von Löhneysen, Karlsruhe, Germany
J.-M. Raimond, Paris, France
A. Rubio, Hamburg, Germany
M. Salmhofer, Heidelberg, Germany
W. Schleich, Ulm, Germany
S. Theisen, Potsdam, Germany
D. Vollhardt, Augsburg, Germany
J.D. Wells, Ann Arbor, USA
G.P. Zank, Huntsville, USA

The Lecture Notes in Physics

The series Lecture Notes in Physics (LNP), founded in 1969, reports new developments in physics research and teaching-quickly and informally, but with a high quality and the explicit aim to summarize and communicate current knowledge in an accessible way. Books published in this series are conceived as bridging material between advanced graduate textbooks and the forefront of research and to serve three purposes:

- to be a compact and modern up-to-date source of reference on a well-defined topic
- to serve as an accessible introduction to the field to postgraduate students and nonspecialist researchers from related areas
- to be a source of advanced teaching material for specialized seminars, courses and schools

Both monographs and multi-author volumes will be considered for publication. Edited volumes should, however, consist of a very limited number of contributions only. Proceedings will not be considered for LNP.

Volumes published in LNP are disseminated both in print and in electronic formats, the electronic archive being available at springerlink.com. The series content is indexed, abstracted and referenced by many abstracting and information services, bibliographic networks, subscription agencies, library networks, and consortia.

Proposals should be sent to a member of the Editorial Board, or directly to the managing editor at Springer:

Christian Caron
Springer Heidelberg
Physics Editorial Department I
Tiergartenstrasse 17
69121 Heidelberg/Germany
christian.caron@springer.com

More information about this series at http://www.springer.com/series/5304

Guido Altarelli

Collider Physics within the Standard Model

A Primer

Edited by James Wells

Springer Open

Author
Guido Altarelli (deceased)
CERN
Geneva, Switzerland

Editor
James Wells
Physics Department
University of Michigan
Ann Arbor, MI
USA

ISSN 0075-8450 ISSN 1616-6361 (electronic)
Lecture Notes in Physics
ISBN 978-3-319-51919-7 ISBN 978-3-319-51920-3 (eBook)
DOI 10.1007/978-3-319-51920-3

Library of Congress Control Number: 2017934490

© The Editor(s) (if applicable) and The Author(s) 2017. This book is an open access publication.
Open Access This book is licensed under the terms of the Creative Commons Attribution 4.0 International License (http://creativecommons.org/licenses/by/4.0/), which permits use, sharing, adaptation, distribution and reproduction in any medium or format, as long as you give appropriate credit to the original author(s) and the source, provide a link to the Creative Commons license and indicate if changes were made.
The images or other third party material in this book are included in the book's Creative Commons license, unless indicated otherwise in a credit line to the material. If material is not included in the book's Creative Commons license and your intended use is not permitted by statutory regulation or exceeds the permitted use, you will need to obtain permission directly from the copyright holder.
The use of general descriptive names, registered names, trademarks, service marks, etc. in this publication does not imply, even in the absence of a specific statement, that such names are exempt from the relevant protective laws and regulations and therefore free for general use.
The publisher, the authors and the editors are safe to assume that the advice and information in this book are believed to be true and accurate at the date of publication. Neither the publisher nor the authors or the editors give a warranty, express or implied, with respect to the material contained herein or for any errors or omissions that may have been made. The publisher remains neutral with regard to jurisdictional claims in published maps and institutional affiliations.

Printed on acid-free paper

This Springer imprint is published by Springer Nature
The registered company is Springer International Publishing AG
The registered company address is: Gewerbestrasse 11, 6330 Cham, Switzerland

Foreword

Guido Altarelli was a leading figure in establishing the Standard Model as the emerging description of the elementary particle world. Not only was he a mastermind behind the success of the theory, but I would say that he really incarnated its very essence. The same perfect synthesis of elegance, purity, and genius that defines the Standard Model also characterised Guido's scientific life. One of his most striking qualities was always his ability to identify the essence of a physics problem, to ask the right question, and to express the answer in a clear and penetrating way. So it is no surprise that Guido was in high demand as a speaker for summary talks at major conferences and as a lecturer in physics schools. Few others could match his ability in giving lucid overviews of a field, focusing on the critical issues and explaining in simple terms the most complicated concepts. His vision of the progress of particle physics has been an illuminating guide for generations of physicists, both theorists and experimentalists.

Guido Altarelli was born in Rome in 1941. After graduating from the university La Sapienza in Rome in 1963, he followed his advisor, Raoul Gatto, to Florence. There, he became part of the "Gattini", as the Florentine group of Gatto's students was affectionately known, after a nickname coined by Sidney Coleman during a Physics School at Erice. Besides Guido, the "Gattini" included some of today's most renowned Italian theoreticians such as Luciano Maiani, Giuliano Preparata, Franco Buccella, Gabriele Veneziano, and Roberto Casalbuoni, all of them of the same age within a year's difference. Towards the end of the 1960s, the Florentine group dispersed, as the various members left for different destinations. Guido went to the United States, staying at New York University (1968–1969) and Rockefeller University (1969–1970), where he worked on various aspects of strong interactions.

In 1970, he was appointed professor at La Sapienza in Rome. Those were the years in which the Standard Model was taking shape, after the proof of renormalisability by Veltman and 't Hooft and the discovery of asymptotic freedom by Gross, Wilczek, and Politzer. Then Guido turned his interests to the interplay between the strong and weak interactions. In particular, he made seminal contributions to the QCD corrections of non-leptonic weak interactions, proposing them as an explanation for the observed $\Delta I = 1/2$ rule. Together with Nicola

Cabibbo, Luciano Maiani, Giorgio Parisi, Guido Martinelli, Keith Ellis, and Roberto Petronzio, Guido succeeded in bringing back to Rome the splendour of the time of Enrico Fermi and the Via Panisperna boys. However, Guido's most celebrated work was not done in Rome. In 1977, he was in Paris, on leave at the École Normale Supérieure, while Giorgio Parisi was at the Institut des Hautes Études Scientifiques. Together, they wrote the famous paper "Asymptotic Freedom in Parton Language", which contains the QCD equation describing how parton densities vary with the energy scale, known today as DGLAP or, more simply, the Altarelli–Parisi equation.

In 1987, Guido moved to the CERN Theory Division, still keeping academic links with Rome, first teaching at La Sapienza and then at the University of Roma Tre. His scientific output at CERN was remarkable. In 1988, after a surprising result from the EMC measurement of the first moment of the polarised proton structure function, he emphasised, together with Graham Ross, the role of the gluon anomaly as a resolution of the apparent violation of quark model expectations. In the early 1990s, in a series of papers with Riccardo Barbieri, Francesco Caravaglios, and Stanislaw Jadach, he developed a model-independent parameterisation of new physics effects in electroweak observables. These studies were extremely influential in the interpretation of LEP data and are still used today for the construction of realistic theories beyond the Standard Model. During the last period of his scientific career, while continuing his research in QCD and the electroweak theory, Guido pursued with great interest the physics of neutrinos, as a tool to infer information about new structures coming from grand unified theories.

Besides his scientific contributions, Guido had a significant impact on CERN's experimental programme by bridging the activities between the theoretical and experimental communities. A famous example goes back to the time in which UA1 presented some unexpected mono-jet events, believed to be the first signal of supersymmetry. In the midst of the general excitement, he realised that, although any individual Standard Model process could not justify the data, when combined together in the so-called Altarelli cocktail, they could give a more mundane explanation of the observed excess. His sober scepticism prompted the experimentalists to reconsider the Standard Model interpretation, and, eventually, his explanation turned out to be the right one. Guido's leading role in advising and guiding the experimental community became even more prominent during the construction and operation of LEP and, later, of the LHC.

These lecture notes are a beautiful example of Guido's unique pedagogical abilities and scientific vision. They give a clear and accurate account of our present knowledge of the particle world, synthesised in the Standard Model. The reader is led from the basic framework of gauge theories to the structure of QCD to weak interactions and the Higgs sector, along a path which is a necessary prerequisite for any researcher interested in particle physics and which actually corresponds to the itinerary followed by Guido during his scientific life. Although today there are several textbooks on the Standard Model, it is difficult to match these lecture notes in terms of conciseness, clarity, and depth. These notes provide a unique resource for researchers—theorists and experimentalists alike—who want to approach the field, especially from the collider point of view, giving a global but complete picture

of the Standard Model and bringing the reader up to the very frontier of present knowledge.

The most touching aspect of these lecture notes is that reading them is just like listening to Guido. His style was direct and essential, and his logical thinking was always clear, profound, and focused on concepts rather than technicalities. From these lecture notes, the reader will not only learn about the Standard Model but also a way to approach physics. They are a faithful portrait of Guido, not only because they cover the field of his vast scientific activity but also because they convey his pragmatic and concrete vision of the world of physics. Guido's intellectual brilliance and physics intuition are perfectly reflected. They will be used regularly by generations of physicists and will remain as a tribute to an original and creative mind who did so much to shape the field of particle physics.

Geneva, Switzerland
June 2016

Gian Francesco Giudice

Preface

When editing this material, most of which dates from 2013, we felt that it was not the aim of this predominantly theoretical text to update the experimental data to the very latest results. After all, what endures at the core of this material are the principles of the Standard Model of particle physics, which Prof. Altarelli so skillfully elucidates. Up-to-date results and values can easily be looked up in the open-access literature which is now inherently part of high-energy physics.

Yet, the devil being typically in the details, we were confronted with plots included by Prof. Altarelli of quite various degrees of "publishability". Sometimes they were taken from internal notes or unpublished proceedings. In those cases, and depending most of the time on the preferences of the authors, they could be published as such, had to be removed altogether, or had to be replaced by more up-to-date figures, such as was the case with a few figures labelled "preliminary" by the large collaborations.

In short, we would like to draw to the reader's attention the fact that the references to experimental data mostly form a snapshot in time as selected by Prof. Altarelli in 2013. Above all, we opted for a minimalistic upgrade in referencing so as to make this exceptional material formally publishable with all permissions required in the first place.

Last but not least, we gratefully acknowledge the support by Monica Pepe-Altarelli for releasing this material and CERN for sponsoring the publication as an open-access book. We further thank Stephen Lyle for the technical editing of the manuscript.

Ann Arbor, MI, USA — James Wells
Heidelberg, Germany — Christian Caron

Acknowledgements

I am very grateful to Giuseppe Degrassi, Ferruccio Feruglio, Paolo Gambino, Mario Greco, Martin Grunewald, Vittorio Lubicz, Richard Ball, Keith Ellis, Stefano Forte, Ashutosh Kotwal, Lorenzo Magnea, Michelangelo Mangano, Luca Merlo, Silvano Simula, and Graham Watt for their help and advice.

This work has been partly supported by the Italian Ministero dell'Università e della Ricerca Scientifica, under the COFIN programme (PRIN 2008), by the European Commission, under the networks "LHCPHENONET" and "Invisibles".

Geneva, Switzerland Guido Altarelli

Contents

Chapter 1
Gauge Theories and the Standard Model

1.1 An Overview of the Fundamental Interactions

A possible goal of fundamental physics is to reduce all natural phenomena to a set of basic laws and theories which, at least in principle, can quantitatively reproduce and predict experimental observations. At the microscopic level all the phenomenology of matter and radiation, including molecular, atomic, nuclear, and subnuclear physics, can be understood in terms of three classes of fundamental interactions: strong, electromagnetic, and weak interactions. For all material bodies on the Earth and in all geological, astrophysical, and cosmological phenomena, a fourth interaction, the gravitational force, plays a dominant role, but this remains negligible in atomic and nuclear physics. In atoms, the electrons are bound to nuclei by electromagnetic forces, and the properties of electron clouds explain the complex phenomenology of atoms and molecules. Light is a particular vibration of electric and magnetic fields (an electromagnetic wave). Strong interactions bind the protons and neutrons together in nuclei, being so strongly attractive at short distances that they prevail over the electric repulsion due to the like charges of protons. Protons and neutrons, in turn, are composites of three quarks held together by strong interactions occur between quarks and gluons (hence these particles are called "hadrons" from the Greek word for "strong"). The weak interactions are responsible for the beta radioactivity that makes some nuclei unstable, as well as the nuclear reactions that produce the enormous energy radiated by the stars, and in particular by our Sun. The weak interactions also cause the disintegration of the neutron, the charged pions, and the lightest hadronic particles with strangeness, charm, and beauty (which are "flavour" quantum numbers), as well as the decay of the top quark and the heavy charged leptons (the muon μ^- and the tau τ^-). In addition, all observed neutrino interactions are due to these weak forces.

All these interactions (with the possible exception of gravity) are described within the framework of quantum mechanics and relativity, more precisely by a local relativistic quantum field theory. To each particle, treated as pointlike, is associated

© The Author(s) 2017

G. Altarelli, *Collider Physics within the Standard Model*,
Lecture Notes in Physics 937, DOI 10.1007/978-3-319-51920-3_1

a field with suitable (depending on the particle spin) transformation properties under the Lorentz group (the relativistic spacetime coordinate transformations). It is remarkable that the description of all these particle interactions is based on a common principle: "gauge" invariance. A "gauge" symmetry is invariance under transformations that rotate the basic internal degrees of freedom, but with rotation angles that depend on the spacetime point. At the classical level, gauge invariance is a property of the Maxwell equations of electrodynamics, and it is in this context that the notion and the name of gauge invariance were introduced. The prototype of all quantum gauge field theories, with a single gauged charge, is quantum electrodynamics (QED), developed in the years from 1926 until about 1950, which is indeed the quantum version of Maxwell's theory. Theories with gauge symmetry in four spacetime dimensions are renormalizable and are completely determined given the symmetry group and the representations of the interacting fields. The whole set of strong, electromagnetic, and weak interactions is described by a gauge theory with 12 gauged non-commuting charges. This is called the "Standard Model" of particle interactions (SM). Actually, only a subgroup of the SM symmetry is directly reflected in the spectrum of physical states. A part of the electroweak symmetry is hidden by the Higgs mechanism for spontaneous symmetry breaking of the gauge symmetry.

The theory of general relativity is a classical description of gravity (in the sense that it is non-quantum mechanical). It goes beyond the static approximation described by Newton's law and includes dynamical phenomena like, for example, gravitational waves. The problem of formulating a quantum theory of gravitational interactions is one of the central challenges of contemporary theoretical physics. But quantum effects in gravity only become important for energy concentrations in spacetime which are not in practice accessible to experimentation in the laboratory. Thus the search for the correct theory can only be done by a purely speculative approach. All attempts at a description of quantum gravity in terms of a well defined and computable local field theory along similar lines to those used for the SM have so far failed to lead to a satisfactory framework. Rather, at present, the most complete and plausible description of quantum gravity is a theory formulated in terms of non-pointlike basic objects, the so-called "strings", extended over much shorter distances than those experimentally accessible and which live in a spacetime with 10 or 11 dimensions. The additional dimensions beyond the familiar 4 are, typically, compactified, which means that they are curled up with a curvature radius of the order of the string dimensions. Present string theory is an all-comprehensive framework that suggests a unified description of all interactions including gravity, in which the SM would be only a low energy or large distance approximation.

A fundamental principle of quantum mechanics, the Heisenberg uncertainty principle, implies that, when studying particles with spatial dimensions of order Δx or interactions taking place at distances of order Δx, one needs as a probe a beam of particles (typically produced by an accelerator) with impulse $p \gtrsim \hbar/\Delta x$, where $\hbar$ is the reduced Planck constant ($\hbar = h/2\pi$). Accelerators presently in operation, like the Large Hadron Collider (LHC) at CERN near Geneva, allow us to study collisions

between two particles with total center of mass energy up to $2E \sim 2pc \lesssim 7$–$14\,\text{TeV}$. These machines can, in principle, study physics down to distances $\Delta x \gtrsim 10^{-18}\,\text{cm}$. Thus, on the basis of results from experiments at existing accelerators, we can indeed confirm that, down to distances of that order of magnitude, electrons, quarks, and all the fundamental SM particles do not show an appreciable internal structure, and look elementary and pointlike. We certainly expect quantum effects in gravity to become important at distances $\Delta x \leq 10^{-33}\,\text{cm}$, corresponding to energies up to $E \sim M_{\text{Planck}}c^2 \sim 10^{19}\,\text{GeV}$, where M_{Planck} is the Planck mass, related to Newton's gravitational constant by $G_{\text{N}} = \hbar c/M_{\text{Planck}}^2$. At such short distances the particles that so far appeared as pointlike may well reveal an extended structure, as would strings, and they may be described by a more detailed theoretical framework for which the local quantum field theory description of the SM would be just a low energy/large distance limit.

From the first few moments of the Universe, just after the Big Bang, the temperature of the cosmic background gradually went down, starting from $kT \sim M_{\text{Planck}}c^2$, where $k = 8.617 \times 10^{-5}\,\text{eV}\,\text{K}^{-1}$ is the Boltzmann constant, down to the present situation where $T \sim 2.725\,\text{K}$. Then all stages of high energy physics from string theory, which is a purely speculative framework, down to the SM phenomenology, which is directly accessible to experiment and well tested, are essential for the reconstruction of the evolution of the Universe starting from the Big Bang. This is the basis for the ever increasing connection between high energy physics and cosmology.

1.2 The Architecture of the Standard Model

The Standard Model (SM) is a gauge field theory based on the symmetry group $SU(3) \bigotimes SU(2) \bigotimes U(1)$. The transformations of the group act on the basic fields. This group has $8 + 3 + 1 = 12$ generators with a nontrivial commutator algebra (if all generators commute, the gauge theory is said to be "Abelian", while the SM is a "non-Abelian" gauge theory). $SU(2) \bigotimes U(1)$ describes the electroweak (EW) interactions [225, 316, 359] and the electric charge Q, the generator of the QED gauge group $U(1)_Q$, is the sum of T_3, one of the $SU(2)$ generators and of $Y/2$, where Y is the $U(1)$ generator: $Q = T_3 + Y/2$. $SU(3)$ is the "colour" group of the theory of strong interactions (quantum chromodynamics QCD [215, 234, 360]).

In a gauge theory,[1] associated with each generator T is a vector boson (also called a gauge boson) with the same quantum numbers as T, and if the gauge symmetry is unbroken, this boson is of vanishing mass. These vector bosons (i.e., of spin 1) act as mediators of the corresponding interactions. For example, in QED the vector boson associated with the generator Q is the photon γ. The interaction between two charged particles in QED, for example two electrons, is mediated by the exchange of

[1] Much of the material in this chapter is a revision and update of [32].

one (or occasionally more than one) photon emitted by one electron and reabsorbed by the other. Similarly, in the SM there are 8 gluons associated with the $SU(3)$ colour generators, while for $SU(2) \bigotimes U(1)$ there are four gauge bosons W^+, W^-, Z^0, and γ. Of these, only the gluons and the photon γ are massless, because the symmetry induced by the other three generators is actually spontaneously broken. The masses of W^+, W^-, and Z^0 are very large indeed on the scale of elementary particles, with values $m_W \sim 80.4\,\text{GeV}$ and $m_Z \sim 91.2\,\text{GeV}$, whence they are as heavy as atoms of intermediate size, like rubidium and molybdenum, respectively.

In the electroweak theory, the breaking of the symmetry is of a particular type, referred to as spontaneous symmetry breaking. In this case, charges and currents are as dictated by the symmetry, but the fundamental state of minimum energy, the vacuum, is not unique and there is a continuum of degenerate states that all respect the symmetry (in the sense that the whole vacuum orbit is spanned by applying the symmetry transformations). The symmetry breaking is due to the fact that the system (with infinite volume and an infinite number of degrees of freedom) is found in one particular vacuum state, and this choice, which for the SM occurred in the first instants of the life of the Universe, means that the symmetry is violated in the spectrum of states. In a gauge theory like the SM, the spontaneous symmetry breaking is realized by the Higgs mechanism [189, 236, 243, 261] (described in detail in Sect. 1.7): there are a number of scalar (i.e., zero spin) Higgs bosons with a potential that produces an orbit of degenerate vacuum states. One or more of these scalar Higgs particles must necessarily be present in the spectrum of physical states with masses very close to the range so far explored. The Higgs particle has now been found at the LHC with $m_\text{H} \sim 126\,\text{GeV}$ [341, 345], thus making a big step towards completing the experimental verification of the SM. The Higgs boson acts as the mediator of a new class of interactions which, at the tree level, are coupled in proportion to the particle masses and thus have a very different strength for, say, an electron and a top quark.

The fermionic matter fields of the SM are quarks and leptons (all of spin 1/2). Each type of quark is a colour triplet (i.e., each quark flavour comes in three colours) and also carries electroweak charges, in particular electric charges $+2/3$ for up-type quarks and $-1/3$ for down-type quarks. So quarks are subject to all SM interactions. Leptons are colourless and thus do not interact strongly (they are not hadrons) but have electroweak charges, in particular electric charges -1 for charged leptons (e^-, μ^- and τ^-) and charge 0 for neutrinos (ν_e, ν_μ and ν_τ). Quarks and leptons are grouped in 3 "families" or "generations" with equal quantum numbers but different masses. At present we do not have an explanation for this triple repetition of fermion families:

$$\begin{bmatrix} u & u & u & \nu_e \\ d & d & d & e \end{bmatrix}, \qquad \begin{bmatrix} c & c & c & \nu_\mu \\ s & s & s & \mu \end{bmatrix}, \qquad \begin{bmatrix} t & t & t & \nu_\tau \\ b & b & b & \tau \end{bmatrix}. \tag{1.1}$$

The QCD sector of the SM (see Chap. 2) has a simple structure but a very rich dynamical content, including the observed complex spectroscopy with a large

number of hadrons. The most prominent properties of QCD are asymptotic freedom and confinement. In field theory, the effective coupling of a given interaction vertex is modified by the interaction. As a result, the measured intensity of the force depends on the square Q^2 of the four-momentum Q transferred among the participants. In QCD the relevant coupling parameter that appears in physical processes is $\alpha_s = e_s^2/4\pi$, where e_s is the coupling constant of the basic interaction vertices of quarks and gluons: qqg or ggg [see (1.28)–(1.31)].

Asymptotic freedom means that the effective coupling becomes a function of Q^2, and in fact $\alpha_s(Q^2)$ decreases for increasing Q^2 and vanishes asymptotically. Thus, the QCD interaction becomes very weak in processes with large Q^2, called hard processes or deep inelastic processes (i.e., with a final state distribution of momenta and a particle content very different than those in the initial state). One can prove that in four spacetime dimensions all pure gauge theories based on a non-commuting symmetry group are asymptotically free, and conversely. The effective coupling decreases very slowly at large momenta, going as the reciprocal logarithm of Q^2, i.e., $\alpha_s(Q^2) = 1/b \log(Q^2/\Lambda^2)$, where b is a known constant and Λ is an energy of order a few hundred MeV. Since in quantum mechanics large momenta imply short wavelengths, the result is that at short distances (or $Q > \Lambda$) the potential between two colour charges is similar to the Coulomb potential, i.e., proportional to $\alpha_s(r)/r$, with an effective colour charge which is small at short distances.

In contrast, the interaction strength becomes large at large distances or small transferred momenta, of order $Q < \Lambda$. In fact, all observed hadrons are tightly bound composite states of quarks (baryons are made of qqq and mesons of $q\bar{q}$), with compensating colour charges so that they are overall neutral in colour. In fact, the property of confinement is the impossibility of separating colour charges, like individual quarks and gluons or any other coloured state. This is because in QCD the interaction potential between colour charges increases linearly in r at long distances. When we try to separate a quark and an antiquark that form a colour neutral meson, the interaction energy grows until pairs of quarks and antiquarks are created from the vacuum. New neutral mesons then coalesce and are observed in the final state, instead of free quarks. For example, consider the process $e^+e^- \to q\bar{q}$ at large center-of-mass energies. The final state quark and antiquark have high energies, so they move apart very fast. But the colour confinement forces create new pairs between them. What is observed is two back-to-back jets of colourless hadrons with a number of slow pions that make the exact separation of the two jets impossible. In some cases, a third, well separated jet of hadrons is also observed: these events correspond to the radiation of an energetic gluon from the parent quark–antiquark pair.

In the EW sector, the SM (see Chap. 3) inherits the phenomenological successes of the old $(V - A) \otimes (V - A)$ four-fermion low-energy description of weak interactions, and provides a well-defined and consistent theoretical framework that includes weak interactions and quantum electrodynamics in a unified picture. The weak interactions derive their name from their strength. At low energy, the strength of the effective four-fermion interaction of charged currents is determined by the Fermi coupling constant G_F. For example, the effective interaction for muon decay

is given by

$$\mathscr{L}_{\text{eff}} = \frac{G_{\text{F}}}{\sqrt{2}}\left[\bar{\nu}_\mu \gamma_\alpha (1-\gamma_5)\mu\right]\left[\bar{e}\gamma^\alpha(1-\gamma_5)\nu_e\right] , \tag{1.2}$$

with [307]

$$G_{\text{F}} = 1.166\,378\,7(6) \times 10^{-5}\ \text{GeV}^{-2} . \tag{1.3}$$

In natural units $\hbar = c = 1$, G_{F} (which we most often use in this work) has dimensions of (mass)$^{-2}$. As a result, the strength of weak interactions at low energy is characterized by $G_{\text{F}}E^2$, where E is the energy scale for a given process ($E \approx m_\mu$ for muon decay). Since

$$G_{\text{F}}E^2 = G_{\text{F}}m_{\text{p}}^2(E/m_{\text{p}})^2 \approx 10^{-5}(E/m_{\text{p}})^2 , \tag{1.4}$$

where m_{p} is the proton mass, the weak interactions are indeed weak at low energies (up to energies of order a few tens of GeV). Effective four-fermion couplings for neutral current interactions have comparable intensity and energy behaviour. The quadratic increase with energy cannot continue for ever, because it would lead to a violation of unitarity. In fact, at high energies, propagator effects can no longer be neglected, and the current–current interaction is resolved into current–W gauge boson vertices connected by a W propagator. The strength of the weak interactions at high energies is then measured by g_W, the W–μ–ν_μ coupling, or even better, by $\alpha_W = g_W^2/4\pi$, analogous to the fine-structure constant α of QED (in Chap. 3, g_W is simply denoted by g or g_2). In the standard EW theory, we have

$$\alpha_W = \sqrt{2}G_{\text{F}}m_W^2/\pi \approx 1/30 . \tag{1.5}$$

That is, at high energies the weak interactions are no longer so weak.

The range r_W of weak interactions is very short: it was only with the experimental discovery of the W and Z gauge bosons that it could be demonstrated that r_W is non-vanishing. Now we know that

$$r_W = \frac{\hbar}{m_W c} \approx 2.5 \times 10^{-16}\ \text{cm} , \tag{1.6}$$

corresponding to $m_W \approx 80.4\,\text{GeV}$. This very high value for the W (or the Z) mass makes a drastic difference, compared with the massless photon and the infinite range of the QED force. The direct experimental limit on the photon mass is [307] $m_\gamma < 10^{-18}\,\text{eV}$. Thus, on the one hand, there is very good evidence that the photon is massless, and on the other, the weak bosons are very heavy. A unified theory of EW interactions has to face this striking difference.

Another apparent obstacle in the way of EW unification is the chiral structure of weak interactions: in the massless limit for fermions, only left-handed quarks and

leptons (and right-handed antiquarks and antileptons) are coupled to W particles. This clearly implies parity and charge-conjugation violation in weak interactions.

The universality of weak interactions and the algebraic properties of the electromagnetic and weak currents [conservation of vector currents (CVC), partial conservation of axial currents (PCAC), the algebra of currents, etc.] were crucial in pointing to the symmetric role of electromagnetism and weak interactions at a more fundamental level. The old Cabibbo universality [120] for the weak charged current, viz.,

$$J_\alpha^{\text{weak}} = \bar{\nu}_\mu \gamma_\alpha (1-\gamma_5)\mu + \bar{\nu}_e \gamma_\alpha (1-\gamma_5) e + \cos\theta_c \bar{u}\gamma_\alpha (1-\gamma_5) d + \sin\theta_c \bar{u}\gamma_\alpha (1-\gamma_5) s + \cdots , \tag{1.7}$$

suitably extended, is naturally implied by the standard EW theory. In this theory the weak gauge bosons couple to all particles with couplings that are proportional to their weak charges, in the same way as the photon couples to all particles in proportion to their electric charges. In (1.7), $d' = d\cos\theta_c + s\sin\theta_c$ is the weak isospin partner of u in a doublet. The (u, d') doublet has the same couplings as the (ν_e, ℓ) and (ν_μ, μ) doublets.

Another crucial feature is that the charged weak interactions are the only known interactions that can change flavour: charged leptons into neutrinos or up-type quarks into down-type quarks. On the other hand, there are no flavour-changing neutral currents at tree level. This is a remarkable property of the weak neutral current, which is explained by the introduction of the Glashow–Iliopoulos–Maiani (GIM) mechanism [226] and led to the successful prediction of charm.

The natural suppression of flavour-changing neutral currents, the separate conservation of e, μ, and τ leptonic flavours that is only broken by the small neutrino masses, the mechanism of CP violation through the phase in the quark-mixing matrix [269], are all crucial features of the SM. Many examples of new physics tend to break the selection rules of the standard theory. Thus the experimental study of rare flavour-changing transitions is an important window on possible new physics.

The SM is a renormalizable field theory, which means that the ultraviolet divergences that appear in loop diagrams can be eliminated by a suitable redefinition of the parameters already appearing in the bare Lagrangian: masses, couplings, and field normalizations. As will be discussed later, a necessary condition for a theory to be renormalizable is that only operator vertices of dimension not greater than 4 (that is m^4, where m is some mass scale) appear in the Lagrangian density $\mathscr{L}$ (itself of dimension 4, because the action S is given by the integral of $\mathscr{L}$ over d^4x and is dimensionless in natural units such that $\hbar = c = 1$). Once this condition is added to the specification of a gauge group and of the matter field content, the gauge theory Lagrangian density is completely specified. We shall see the precise rules for writing down the Lagrangian of a gauge theory in the next section.

1.3 The Formalism of Gauge Theories

In this section we summarize the definition and the structure of a Yang–Mills gauge theory [371]. We will list here the general rules for constructing such a theory. Then these results will be applied to the SM.

Consider a Lagrangian density $\mathscr{L}[\phi, \partial_\mu \phi]$ which is invariant under a D dimensional continuous group Γ of transformations:

$$\phi'(x) = U(\theta^A)\phi(x) \qquad (A = 1, 2, \ldots, D) \,, \tag{1.8}$$

with

$$U(\theta^A) = \exp\left[\mathrm{i}g \sum_A \theta^A T^A\right] \sim 1 + \mathrm{i}g \sum_A \theta^A T^A + \cdots \,. \tag{1.9}$$

The quantities θ^A are numerical parameters, like angles in the particular case of a rotation group in some internal space. The approximate expression on the right is valid for θ^A infinitesimal. Then, g is the coupling constant and T^A are the generators of the group Γ of transformations (1.8) in the (in general reducible) representation of the fields ϕ. Here we restrict ourselves to the case of internal symmetries, so the T^A are matrices that are independent of the spacetime coordinates, and the arguments of the fields ϕ and ϕ' in (1.8) are the same.

If U is unitary, then the generators T^A are Hermitian, but this need not be the case in general (although it is true for the SM). Similarly, if U is a group of matrices with unit determinant, then the traces of the T^A vanish, i.e., $\mathrm{tr}(T^A) = 0$. In general, the generators satisfy the commutation relations

$$[T^A, T^B] = \mathrm{i}C_{ABC}T^C \,. \tag{1.10}$$

For $A, B, C, \ldots$, up or down indices make no difference, i.e., $T^A = T_A$, etc. The structure constants C_{ABC} are completely antisymmetric in their indices, as can be easily seen. Recall that if all generators commute, the gauge theory is said to be "Abelian" (in this case all the structure constants C_{ABC} vanish), while the SM is a "non-Abelian" gauge theory.

We choose to normalize the generators T^A in such a way that, for the lowest dimensional non-trivial representation of the group Γ (we use t^A to denote the generators in this particular representation), we have

$$\mathrm{tr}\left(t^A t^B\right) = \frac{1}{2}\delta^{AB} \,. \tag{1.11}$$

A normalization convention is needed to fix the normalization of the coupling g and the structure constants C_{ABC}. In the following, for each quantity f^A, we define

$$\mathbf{f} = \sum_A T^A f^A \ . \tag{1.12}$$

For example, we can rewrite (1.9) in the form

$$U(\theta^A) = \exp(\mathrm{i}g\boldsymbol{\theta}) \sim 1 + \mathrm{i}g\boldsymbol{\theta} + \cdots \ . \tag{1.13}$$

If we now make the parameters θ^A depend on the spacetime coordinates, whence $\theta^A = \theta^A(x_\mu)$, then $\mathscr{L}[\phi, \partial_\mu\phi]$ is in general no longer invariant under the gauge transformations $U[\theta^A(x_\mu)]$, because of the derivative terms. Indeed, we then have $\partial_\mu\phi' = \partial_\mu(U\phi) \neq U\partial_\mu\phi$. Gauge invariance is recovered if the ordinary derivative is replaced by the covariant derivative

$$D_\mu = \partial_\mu + ig\mathbf{V}_\mu \ , \tag{1.14}$$

where V_μ^A are a set of D gauge vector fields (in one-to-one correspondence with the group generators), with the transformation law

$$\mathbf{V}'_\mu = U\mathbf{V}_\mu U^{-1} - \frac{1}{\mathrm{i}g}(\partial_\mu U)U^{-1}. \tag{1.15}$$

For constant θ^A, $\mathbf{V}$ reduces to a tensor of the adjoint (or regular) representation of the group:

$$\mathbf{V}'_\mu = U\mathbf{V}_\mu U^{-1} \approx \mathbf{V}_\mu + \mathrm{i}g[\boldsymbol{\theta}, \mathbf{V}_\mu] + \cdots \ , \tag{1.16}$$

which implies that

$$V'^C_\mu = V^C_\mu - gC_{ABC}\theta^A V^B_\mu + \cdots \ , \tag{1.17}$$

where repeated indices are summed over.

As a consequence of (1.14) and (1.15), $D_\mu\phi$ has the same transformation properties as ϕ :

$$(D_\mu\phi)' = U(D_\mu\phi) \ . \tag{1.18}$$

In fact,

$$\begin{aligned}(D_\mu\phi)' &= (\partial_\mu + ig\mathbf{V}'_\mu)\phi' \\ &= (\partial_\mu U)\phi + U\partial_\mu\phi + igU\mathbf{V}_\mu\phi - (\partial_\mu U)\phi = U(D_\mu\phi) \ .\end{aligned} \tag{1.19}$$

Thus $\mathscr{L}[\phi, D_\mu\phi]$ is indeed invariant under gauge transformations. But at this stage the gauge fields V_μ^A appear as external fields that do not propagate. In order to construct a gauge invariant kinetic energy term for the gauge fields V_μ^A, we consider

$$[D_\mu, D_\nu]\phi = \mathrm{i}g\{\partial_\mu \mathbf{V}_\nu - \partial_\nu \mathbf{V}_\mu + \mathrm{i}g[\mathbf{V}_\mu, \mathbf{V}_\nu]\}\phi \equiv \mathrm{i}g\mathbf{F}_{\mu\nu}\phi \ , \tag{1.20}$$

which is equivalent to

$$F_{\mu\nu}^A = \partial_\mu V_\nu^A - \partial_\nu V_\mu^A - gC_{ABC}V_\mu^B V_\nu^C \ . \tag{1.21}$$

From (1.8), (1.18), and (1.20), it follows that the transformation properties of $F_{\mu\nu}^A$ are those of a tensor of the adjoint representation:

$$\mathbf{F}'_{\mu\nu} = U\mathbf{F}_{\mu\nu}U^{-1} \ . \tag{1.22}$$

The complete Yang–Mills Lagrangian, which is invariant under gauge transformations, can be written in the form

$$\mathscr{L}_{\mathrm{YM}} = -\frac{1}{2}Tr\mathbf{F}_{\mu\nu}\mathbf{F}^{\mu\nu} + \mathscr{L}[\phi, D_\mu\phi] = -\frac{1}{4}\sum_A F_{\mu\nu}^A F^{A\mu\nu} + \mathscr{L}[\phi, D_\mu\phi] \ . \tag{1.23}$$

Note that the kinetic energy term is an operator of dimension 4. Thus if $\mathscr{L}$ is renormalizable, so also is $\mathscr{L}_{\mathrm{YM}}$. If we give up renormalizability, then more gauge invariant higher dimensional terms could be added. It is already clear at this stage that no mass term for gauge bosons of the form $m^2 V_\mu V^\mu$ is allowed by gauge invariance.

1.4 Application to QED and QCD

For an Abelian theory like QED, the gauge transformation reduces to $U[\theta(x)] = \exp[\mathrm{i}eQ\theta(x)]$, where Q is the charge generator (for more commuting generators, one simply has a product of similar factors). According to (1.15), the associated gauge field (the photon) transforms as

$$V'_\mu = V_\mu - \partial_\mu\theta(x) \ , \tag{1.24}$$

and the familiar gauge transformation is recovered, with addition of a 4-gradient of a scalar function. The QED Lagrangian density is given by

$$\mathscr{L} = -\frac{1}{4}F^{\mu\nu}F_{\mu\nu} + \sum_\psi \bar{\psi}(\mathrm{i}\not{D} - m_\psi)\psi \ . \tag{1.25}$$

Here $\not{D} = D_\mu \gamma^\mu$, where γ^μ are the Dirac matrices and the covariant derivative is given in terms of the photon field A_μ and the charge operator Q by

$$D_\mu = \partial_\mu + \mathrm{i}eA_\mu Q \tag{1.26}$$

and

$$F_{\mu\nu} = \partial_\mu A_\nu - \partial_\nu A_\mu \ . \tag{1.27}$$

Note that in QED one usually takes e^- to be the particle, so that $Q = -1$ and the covariant derivative is $D_\mu = \partial_\mu - \mathrm{i}eA_\mu$ when acting on the electron field. In the Abelian case, the $F_{\mu\nu}$ tensor is linear in the gauge field V_μ, so that in the absence of matter fields the theory is free. On the other hand, in the non-Abelian case, the $F^A_{\mu\nu}$ tensor contains both linear and quadratic terms in V^A_μ, so the theory is non-trivial even in the absence of matter fields.

According to the formalism of the previous section, the statement that QCD is a renormalizable gauge theory based on the group $SU(3)$ with colour triplet quark matter fields fixes the QCD Lagrangian density to be

$$\mathscr{L} = -\frac{1}{4}\sum_{A=1}^{8} F^{A\mu\nu}F^A_{\mu\nu} + \sum_{j=1}^{n_\mathrm{f}} \bar{q}_j(i\not{D} - m_j)q_j \ . \tag{1.28}$$

Here q_j are the quark fields with n_f different flavours and mass m_j, and D_μ is the covariant derivative of the form

$$D_\mu = \partial_\mu + \mathrm{i}e_\mathrm{s}\mathbf{g}_{\boldsymbol{\mu}} \ , \tag{1.29}$$

with gauge coupling e_s. Later, in analogy with QED, we will mostly use

$$\alpha_\mathrm{s} = \frac{e_\mathrm{s}^2}{4\pi} \ . \tag{1.30}$$

In addition, $\mathbf{g}_{\boldsymbol{\mu}} = \sum_A t^A g^A_\mu$, where g^A_μ, $A = 1, \ldots, 8$, are the gluon fields and t^A are the $SU(3)$ group generators in the triplet representation of the quarks (i.e., t_A are 3×3 matrices acting on q). The generators obey the commutation relations $[t^A, t^B] = \mathrm{i}C_{ABC}t^C$, where C_{ABC} are the completely antisymmetric structure constants of $SU(3)$. The normalizations of C_{ABC} and e_s are specified by those of the generators t^A, i.e., $\mathrm{Tr}[t^A t^B] = \delta^{AB}/2$ [see (1.11)]. Finally, we have

$$F^A_{\mu\nu} = \partial_\mu g^A_\nu - \partial_\nu g^A_\mu - e_\mathrm{s}C_{ABC}g^B_\mu g^C_\nu \ . \tag{1.31}$$

Chapter 2 is devoted to a detailed description of QCD as the theory of strong interactions. The physical vertices in QCD include the gluon–quark–antiquark vertex, analogous to the QED photon–fermion–antifermion coupling, but also the

3-gluon and 4-gluon vertices, of order e_s and e_s^2 respectively, which have no analogue in an Abelian theory like QED. In QED the photon is coupled to all electrically charged particles, but is itself neutral. In QCD the gluons are coloured, hence self-coupled. This is reflected by the fact that, in QED, $F_{\mu\nu}$ is linear in the gauge field, so that the term $F_{\mu\nu}^2$ in the Lagrangian is a pure kinetic term, while in QCD, $F_{\mu\nu}^A$ is quadratic in the gauge field, so that in $F_{\mu\nu}^{A2}$, we find cubic and quartic vertices beyond the kinetic term. It is also instructive to consider a scalar version of QED:

$$\mathscr{L} = -\frac{1}{4}F^{\mu\nu}F_{\mu\nu} + (D_\mu\phi)^\dagger(D^\mu\phi) - m^2(\phi^\dagger\phi) \ . \tag{1.32}$$

For $Q = 1$, we have

$$(D_\mu\phi)^\dagger(D^\mu\phi) = (\partial_\mu\phi)^\dagger(\partial^\mu\phi) + \mathrm{i}eA_\mu\big[(\partial^\mu\phi)^\dagger\phi - \phi^\dagger(\partial^\mu\phi)\big] + e^2A_\mu A^\mu\phi^\dagger\phi \ . \tag{1.33}$$

We see that for a charged boson in QED, given that the kinetic term for bosons is quadratic in the derivative, there is a gauge–gauge–scalar–scalar vertex of order e^2. We understand that in QCD the 3-gluon vertex is there because the gluon is coloured, and the 4-gluon vertex because the gluon is a boson.

1.5 Chirality

We recall here the notion of chirality and related issues which are crucial for the formulation of the EW Theory. The fermion fields can be described through their right-handed (RH) (chirality $+1$) and left-handed (LH) (chirality -1) components:

$$\psi_{\mathrm{L,R}} = [(1 \mp \gamma_5)/2]\psi \ , \quad \bar\psi_{\mathrm{L,R}} = \bar\psi[(1 \pm \gamma_5)/2] \ , \tag{1.34}$$

where γ_5 and the other Dirac matrices are defined as in the book by Bjorken and Drell [102]. In particular, $\gamma_5^2 = 1$, $\gamma_5^\dagger = \gamma_5$. Note that (1.34) implies

$$\bar\psi_{\mathrm{L}} = \psi_{\mathrm{L}}^\dagger\gamma_0 = \psi^\dagger[(1-\gamma_5)/2]\gamma_0 = \bar\psi\gamma_0[(1-\gamma_5)/2]\gamma_0 = \bar\psi[(1+\gamma_5)/2] \ .$$

The matrices $P_\pm = (1 \pm \gamma_5)/2$ are projectors. They satisfy the relations $P_\pm P_\pm = P_\pm$, $P_\pm P_\mp = 0$, $P_+ + P_- = 1$. They project onto fermions of definite chirality. For massless particles, chirality coincides with helicity. For massive particles, a chirality $+1$ state only coincides with a $+1$ helicity state up to terms suppressed by powers of m/E.

The 16 linearly independent Dirac matrices (Γ) can be divided into γ_5-even (Γ_{E}) and γ_5-odd (Γ_{O}) according to whether they commute or anticommute with γ_5. For

the γ_5-even, we have

$$\bar{\psi}\Gamma_{\mathrm{E}}\psi = \bar{\psi}_{\mathrm{L}}\Gamma_{\mathrm{E}}\psi_{\mathrm{R}} + \bar{\psi}_{\mathrm{R}}\Gamma_{\mathrm{E}}\psi_{\mathrm{L}} \qquad (\Gamma_{\mathrm{E}} \equiv 1, \mathrm{i}\gamma_5, \sigma_{\mu\nu}) \,, \tag{1.35}$$

whilst for the γ_5-odd,

$$\bar{\psi}\Gamma_{\mathrm{O}}\psi = \bar{\psi}_{\mathrm{L}}\Gamma_{\mathrm{O}}\psi_{\mathrm{L}} + \bar{\psi}_{\mathrm{R}}\Gamma_{\mathrm{O}}\psi_{\mathrm{R}} \qquad (\Gamma_{\mathrm{O}} \equiv \gamma_\mu, \gamma_\mu\gamma_5) \,. \tag{1.36}$$

We see that in a gauge Lagrangian, fermion kinetic terms and interactions of gauge bosons with vector and axial vector fermion currents all conserve chirality, while fermion mass terms flip chirality. For example, in QED, if an electron emits a photon, the electron chirality is unchanged. In the ultrarelativistic limit, when the electron mass can be neglected, chirality and helicity are approximately the same and we can state that the helicity of the electron is unchanged by the photon emission. In a massless gauge theory, the LH and the RH fermion components are uncoupled and can be transformed separately. If in a gauge theory the LH and RH components transform as different representations of the gauge group, one speaks of a chiral gauge theory, while if they have the same gauge transformations, one has a vector gauge theory. Thus, QED and QCD are vector gauge theories because, for each given fermion, ψ_{L} and ψ_{R} have the same electric charge and the same colour. Instead, the standard EW theory is a chiral theory, in the sense that ψ_{L} and ψ_{R} behave differently under the gauge group (so that parity and charge conjugation non-conservation are made possible in principle). Thus, mass terms for fermions (of the form $\bar{\psi}_{\mathrm{L}}\psi_{\mathrm{R}}$ + h.c.) are forbidden in the EW gauge-symmetric limit. In particular, in the Minimal Standard Model (MSM), i.e., the model that only includes all observed particles plus a single Higgs doublet, all ψ_{L} are $SU(2)$ doublets, while all ψ_{R} are singlets.

1.6 Quantization of a Gauge Theory

The Lagrangian density $\mathscr{L}_{\mathrm{YM}}$ in (1.23) fully describes the theory at the classical level. The formulation of the theory at the quantum level requires us to specify procedures of quantization, regularization and, finally, renormalization. To start with, the formulation of Feynman rules is not straightforward. A first problem, common to all gauge theories, including the Abelian case of QED, can be realized by observing that the free equations of motion for V^A_μ, as obtained from (1.21) and (1.23), are given by

$$\left(\partial^2 g_{\mu\nu} - \partial_\mu\partial_\nu\right)V^{A\nu} = 0 \,. \tag{1.37}$$

Normally the propagator of the gauge field should be determined by the inverse of the operator $\partial^2 g_{\mu\nu} - \partial_\mu\partial_\nu$. However, it has no inverse, being a projector over the transverse gauge vector states. This difficulty is removed by fixing a particular

gauge. If one chooses a covariant gauge condition $\partial^\mu V_\mu^A = 0$, then a gauge fixing term of the form

$$\Delta\mathscr{L}_{\rm GF} = -\frac{1}{2\lambda}\sum_A |\partial^\mu V_\mu^A|^2 \tag{1.38}$$

has to be added to the Lagrangian ($1/\lambda$ acts as a Lagrangian multiplier). The free equations of motion are then modified as follows:

$$\left[\partial^2 g_{\mu\nu} - (1-1/\lambda)\partial_\mu\partial_\nu\right]V^{A\nu} = 0\,. \tag{1.39}$$

This operator now has an inverse whose Fourier transform is given by

$$D_{\mu\nu}^{AB}(q) = \frac{\mathrm{i}}{q^2+\mathrm{i}\epsilon}\left[-g_{\mu\nu} + (1-\lambda)\frac{q_\mu q_\nu}{q^2+\mathrm{i}\epsilon}\right]\delta^{AB}\,, \tag{1.40}$$

which is the propagator in this class of gauges. The parameter λ can take any value and it disappears from the final expression of any gauge invariant, physical quantity. Commonly used particular cases are $\lambda = 1$ (Feynman gauge) and $\lambda = 0$ (Landau gauge).

While in an Abelian theory the gauge fixing term is all that is needed for a correct quantization, in a non-Abelian theory the formulation of complete Feynman rules involves a further subtlety. This is formally taken into account by introducing a set of D fictitious ghost fields that must be included as internal lines in closed loops (Faddeev–Popov ghosts [197]). Given that gauge fields connected by a gauge transformation describe the same physics, there are clearly fewer physical degrees of freedom than gauge field components. Ghosts appear, in the form of a transformation Jacobian in the functional integral, in the process of elimination of the redundant variables associated with fields on the same gauge orbit [14]. By performing some path integral acrobatics, the correct ghost contributions can be translated into an additional term in the Lagrangian density. For each choice of the gauge fixing term, the ghost Lagrangian is obtained by considering the effect of an infinitesimal gauge transformation $V_\mu'^C = V_\mu^C - gC_{ABC}\theta^A V_\mu^B - \partial_\mu\theta^C$ on the gauge fixing condition. For $\partial^\mu V_\mu^C = 0$, one obtains

$$\partial^\mu V_\mu'^C = \partial^\mu V_\mu^C - gC_{ABC}\partial^\mu(\theta^A V_\mu^B) - \partial^2\theta^C = -\left[\partial^2\delta_{AC} + gC_{ABC}V_\mu^B\partial^\mu\right]\theta^A\,, \tag{1.41}$$

where the gauge condition $\partial^\mu V_\mu^C = 0$ has been taken into account in the last step. The ghost Lagrangian is then given by

$$\Delta\mathscr{L}_{\rm Ghost} = \bar\eta^C\left[\partial^2\delta_{AC} + gC_{ABC}V_\mu^B\partial^\mu\right]\eta^A\,, \tag{1.42}$$

where η^A is the ghost field (one for each index A) which has to be treated as a scalar field, except that a factor -1 has to be included for each closed loop, as for fermion fields.

Starting from non-covariant gauges, one can construct ghost-free gauges. An example, also important in other respects, is provided by the set of "axial" gauges $n^\mu V^A_\mu = 0$, where n_μ is a fixed reference 4-vector (actually, for n_μ spacelike, one has an axial gauge proper, for $n^2 = 0$, one speaks of a light-like gauge, and for n_μ timelike, one has a Coulomb or temporal gauge). The gauge fixing term is of the form

$$\Delta\mathscr{L}_{\rm GF} = -\frac{1}{2\lambda}\sum_A |n^\mu V^A_\mu|^2 \,. \tag{1.43}$$

With a procedure that can be found in QED textbooks [102], the corresponding propagator in Fourier space is found to be

$$D^{AB}_{\mu\nu}(q) = \frac{\mathrm{i}}{q^2 + \mathrm{i}\epsilon}\left[-g_{\mu\nu} + \frac{n_\mu q_+ n_\nu q_\mu}{(nq)} - \frac{n^2 q_\mu q_\nu}{(nq)^2}\right]\delta^{AB} \,. \tag{1.44}$$

In this case there are no ghost interactions because $n^\mu V'^A_\mu$, obtained by a gauge transformation from $n^\mu V^A_\mu$, contains no gauge fields, once the gauge condition $n^\mu V^A_\mu = 0$ has been taken into account. Thus the ghosts are decoupled and can be ignored.

The introduction of a suitable regularization method that preserves gauge invariance is essential for the definition and the calculation of loop diagrams and for the renormalization programme of the theory. The method that is currently adopted is dimensional regularization [334], which consists in the formulation of the theory in n dimensions. All loop integrals have an analytic expression that is actually valid also for non-integer values of n. Writing the results for $n = 4 - \epsilon$ the loops are ultraviolet finite for $\epsilon > 0$ and the divergences reappear in the form of poles at $\epsilon = 0$.

1.7 Spontaneous Symmetry Breaking in Gauge Theories

The gauge symmetry of the SM was difficult to discover because it is well hidden in nature. The only observed gauge boson that is massless is the photon. The gluons are presumed massless but cannot be directly observed because of confinement, and the W and Z weak bosons carry a heavy mass. Indeed a major difficulty in unifying the weak and electromagnetic interactions was the fact that electromagnetic interactions have infinite range ($m_\gamma = 0$), whilst the weak forces have a very short range, owing to $m_{W,Z} \neq 0$. The solution to this problem lies in the concept of spontaneous symmetry breaking, which was borrowed from condensed matter physics.

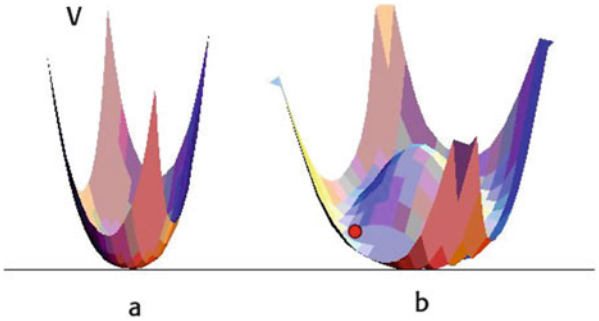

Fig. 1.1 The potential $V = \mu^2\mathbf{M}^2/2 + \lambda(\mathbf{M}^2)^2/4$ for positive (**a**) or negative μ^2 (**b**) (for simplicity, **M** is a 2-dimensional vector). The *small sphere* indicates a possible choice for the direction of **M**

Consider a ferromagnet at zero magnetic field in the Landau–Ginzburg approximation. The free energy in terms of the temperature T and the magnetization **M** can be written as

$$F(\mathbf{M}, T) \simeq F_0(T) + \frac{1}{2}\mu^2(T)\mathbf{M}^2 + \frac{1}{4}\lambda(T)(\mathbf{M}^2)^2 + \cdots . \tag{1.45}$$

This is an expansion which is valid at small magnetization. The neglect of terms of higher order in $\mathbf{M}^2$ is the analogue in this context of the renormalizability criterion. Furthermore, $\lambda(T) > 0$ is assumed for stability, and F is invariant under rotations, i.e., all directions of **M** in space are equivalent. The minimum condition for F reads

$$\partial F/\partial M_i = 0 , \quad \left[\mu^2(T) + \lambda(T)\mathbf{M}^2\right]\mathbf{M} = 0 . \tag{1.46}$$

There are two cases, shown in Fig. 1.1. If $\mu^2 \gtrsim 0$, then the only solution is $\mathbf{M} = 0$, there is no magnetization, and the rotation symmetry is respected. In this case the lowest energy state (in a quantum theory the vacuum) is unique and invariant under rotations. If $\mu^2 < 0$, then another solution appears, which is

$$|\mathbf{M}_0|^2 = -\mu^2/\lambda . \tag{1.47}$$

In this case there is a continuous orbit of lowest energy states, all with the same value of $|\mathbf{M}|$, but different orientations. A particular direction chosen by the vector $\mathbf{M}_0$ leads to a breaking of the rotation symmetry.

For a piece of iron we can imagine bringing it to high temperature and letting it melt in an external magnetic field **B**. The presence of **B** is an explicit breaking of the rotational symmetry and it induces a nonzero magnetization **M** along its direction. Now we lower the temperature while keeping **B** fixed. Both λ and μ^2 depend on the temperature. With lowering T, μ^2 goes from positive to negative values. The critical

temperature $T_{\rm crit}$ (Curie temperature) is where $\mu^2(T)$ changes sign, i.e., $\mu^2(T_{\rm crit})=0$. For pure iron, $T_{\rm crit}$ is below the melting temperature. So at $T = T_{\rm crit}$ iron is a solid. Below $T_{\rm crit}$ we remove the magnetic field. In a solid the mobility of the magnetic domains is limited and a non-vanishing M_0 remains. The form of the free energy is again rotationally invariant as in (1.45). But now the system allows a minimum energy state with non-vanishing **M** in the direction of **B**. As a consequence the symmetry is broken by this choice of one particular vacuum state out of a continuum of them.

We now prove the Goldstone theorem [228]. It states that when spontaneous symmetry breaking takes place, there is always a zero-mass mode in the spectrum. In a classical context this can be proven as follows. Consider a Lagrangian

$$\mathscr{L} = \frac{1}{2}|\partial_\mu \phi|^2 - V(\phi) \ . \tag{1.48}$$

The potential $V(\phi)$ can be kept generic at this stage, but in the following we will be mostly interested in a renormalizable potential of the form

$$V(\phi) = -\frac{1}{2}\mu^2\phi^2 + \frac{1}{4}\lambda\phi^4 \ , \tag{1.49}$$

with no more than quartic terms. Here by ϕ we mean a column vector with real components ϕ_i $(1 = 1, 2, \ldots, N)$ (complex fields can always be decomposed into a pair of real fields), so that, for example, $\phi^2 = \sum_i \phi_i^2$. This particular potential is symmetric under an $N \times N$ orthogonal matrix rotation $\phi' = O\phi$, where O is an $SO(N)$ transformation. For simplicity, we have omitted odd powers of ϕ, which means that we have assumed an extra discrete symmetry under $\phi \leftrightarrow -\phi$. Note that, for positive μ^2, the mass term in the potential has the "wrong" sign: according to the previous discussion this is the condition for the existence of a non-unique lowest energy state. Further, we only assume here that the potential is symmetric under the infinitesimal transformations

$$\phi \to \phi' = \phi + \delta\phi \ , \quad \delta\phi_i = \mathrm{i}\delta\theta^A t^A_{ij}\phi_j \ , \tag{1.50}$$

where $\delta\theta^A$ are infinitesimal parameters and t^A_{ij} are the matrices that represent the symmetry group on the representation carried by the fields ϕ_i (a sum over A is understood). The minimum condition on V that identifies the equilibrium position (or the vacuum state in quantum field theory language) is

$$\frac{\partial V}{\partial \phi_i}(\phi_i = \phi_i^0) = 0 \ . \tag{1.51}$$

The symmetry of V implies that

$$\delta V = \frac{\partial V}{\partial \phi_i}\delta\phi_i = \mathrm{i}\delta\theta^A \frac{\partial V}{\partial \phi_i} t^A_{ij}\phi_j = 0 \,. \tag{1.52}$$

By taking a second derivative at the minimum $\phi_i = \phi_i^0$ of both sides of the previous equation, we obtain that, for each A,

$$\frac{\partial^2 V}{\partial \phi_k \partial \phi_i}(\phi_i = \phi_i^0) t^A_{ij}\phi_j^0 + \frac{\partial V}{\partial \phi_i}(\phi_i = \phi_i^0) t^A_{ik} = 0 \,. \tag{1.53}$$

The second term vanishes owing to the minimum condition (1.51). We then find

$$\frac{\partial^2 V}{\partial \phi_k \partial \phi_i}(\phi_i = \phi_i^0) t^A_{ij}\phi_j^0 = 0 \,. \tag{1.54}$$

The second derivatives $M^2_{ki} = (\partial^2 V/\partial\phi_k\partial\phi_i)(\phi_i = \phi_i^0)$ define the squared mass matrix. Thus the above equation in matrix notation can be written as

$$M^2 t^A \phi^0 = 0 \,. \tag{1.55}$$

In the case of no spontaneous symmetry breaking, the ground state is unique, and all symmetry transformations leave it invariant, so that, for all A, $t^A\phi^0 = 0$. On the other hand, if for some values of A the vectors $(t^A\phi^0)$ are non-vanishing, i.e., there is some generator that shifts the ground state into some other state with the same energy (whence the vacuum is not unique), then each $t^A\phi^0 \neq 0$ is an eigenstate of the squared mass matrix with zero eigenvalue. Therefore, a massless mode is associated with each broken generator. The charges of the massless modes (their quantum numbers in quantum language) differ from those of the vacuum (usually all taken as zero) by the values of the t^A charges: one says that the massless modes have the same quantum numbers as the broken generators, i.e., those that do not annihilate the vacuum.

The previous proof of the Goldstone theorem has been given for the classical case. In the quantum case, the classical potential corresponds to the tree level approximation of the quantum potential. Higher order diagrams with loops introduce quantum corrections. The functional integral formulation of quantum field theory [14, 250] is the most appropriate framework to define and compute, in a loop expansion, the quantum potential which specifies the vacuum properties of the quantum theory in exactly the way described above. If the theory is weakly coupled, e.g., if λ is small, the tree level expression for the potential is not too far from the truth, and the classical situation is a good approximation. We shall see that this is the situation that occurs in the electroweak theory with a moderately light Higgs particle (see Sect. 3.5).

We note that for a quantum system with a finite number of degrees of freedom, for example, one described by the Schrödinger equation, there are no degenerate vacua: the vacuum is always unique. For example, in the one-dimensional Schrödinger problem with a potential

$$V(x) = -\frac{\mu^2}{2}x^2 + \frac{\lambda}{4}x^4 \,, \tag{1.56}$$

there are two degenerate minima at $x = \pm x_0 = (\mu^2/\lambda)^{1/2}$, which we denote by $|+\rangle$ and $|-\rangle$. But the potential is not diagonal in this basis: the off-diagonal matrix elements

$$\langle +|V|-\rangle = \langle -|V|+\rangle \sim \exp(-khd) = \delta \tag{1.57}$$

are different from zero due to the non-vanishing amplitude for a tunnel effect between the two vacua given in (1.57), proportional to the exponential of minus the product of the distance d between the vacua and the height h of the barrier, with k a constant (see Fig. 1.2). After diagonalization the eigenvectors are $(|+\rangle + |-\rangle)/\sqrt{2}$ and $(|+\rangle - |-\rangle)/\sqrt{2}$, with different energies (the difference being proportional to δ). Suppose now that we have a sum of n equal terms in the potential, i.e., $V = \sum_i V(x_i)$. Then the transition amplitude would be proportional to δ^n and would vanish for infinite n: the probability that all degrees of freedom together jump over the barrier vanishes. In this example there is a discrete number of minimum points. The case of a continuum of minima is obtained, still in the Schrödinger context, if we take

$$V = \frac{1}{2}\mu^2\mathbf{r}^2 + \frac{1}{4}\lambda(\mathbf{r}^2)^2 \,, \tag{1.58}$$

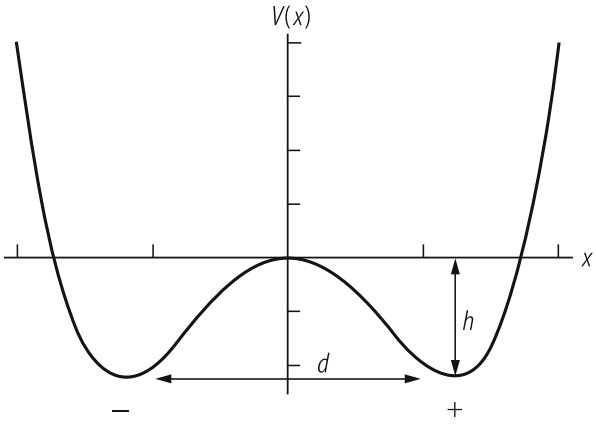

Fig. 1.2 A Schrödinger potential $V(x)$ analogous to the Higgs potential

with $\mathbf{r} = (x, y, z)$. The ground state is also unique in this case: it is given by a state with total orbital angular momentum zero, i.e., an s-wave state, whose wave function only depends on $|\mathbf{r}|$, i.e., it is independent of all angles. This is a superposition of all directions with the same weight, analogous to what happened in the discrete case. But again, if we replace a single vector $\mathbf{r}$, with a vector field $\mathbf{M}(\mathbf{x})$, that is, a different vector at each point in space, the amplitude to go from a minimum state in one direction to another in a different direction goes to zero in the limit of infinite volume. Put simply, the vectors at all points in space have a vanishingly small amplitude to make a common rotation, all together at the same time. In the infinite volume limit, all vacua along each direction have the same energy, and spontaneous symmetry breaking can occur.

A massless Goldstone boson corresponds to a long range force. Unless the massless particles are confined, as for the gluons in QCD, these long range forces would be easily detectable. Thus, in the construction of the EW theory, we cannot accept physical massless scalar particles. Fortunately, when spontaneous symmetry breaking takes place in a gauge theory, the massless Goldstone modes exist, but they are unphysical and disappear from the spectrum. In fact, each of them becomes the third helicity state of a gauge boson that takes mass. This is the Higgs mechanism [189, 236, 243, 261] (it should be called the Englert–Brout–Higgs mechanism, because of the simultaneous paper by Englert and Brout). Consider, for example, the simplest Higgs model described by the Lagrangian [243, 261]

$$\mathscr{L} = -\frac{1}{4}F_{\mu\nu}^2 + \left|(\partial_\mu + \mathrm{i}eA_\mu Q)\phi\right|^2 + \mu^2\phi^*\phi - \frac{\lambda}{2}(\phi^*\phi)^2 \,. \tag{1.59}$$

Note the "wrong" sign in front of the mass term for the scalar field ϕ, which is necessary for the spontaneous symmetry breaking to take place. The above Lagrangian is invariant under the $U(1)$ gauge symmetry

$$A_\mu \to A'_\mu = A_\mu - \partial_\mu\theta(x) \,, \qquad \phi \to \phi' = \exp\bigl[\mathrm{i}eQ\theta(x)\bigr]\phi \,. \tag{1.60}$$

For the U(1) charge Q, we take $Q\phi = -\phi$, as in QED, where the particle is e^-. Let $\phi^0 = v \neq 0$, with v real, be the ground state that minimizes the potential and induces the spontaneous symmetry breaking. In our case v is given by $v^2 = \mu^2/\lambda$. Exploiting gauge invariance, we make the change of variables

$$\begin{aligned} \phi(x) &\to \left[v + \frac{h(x)}{\sqrt{2}}\right]\exp\left[-\mathrm{i}\frac{\zeta(x)}{v\sqrt{2}}\right], \\ A_\mu(x) &\to A_\mu - \partial_\mu\frac{\zeta(x)}{ev\sqrt{2}}. \end{aligned} \tag{1.61}$$

Then the position of the minimum at $\phi^0 = v$ corresponds to $h = 0$, and the Lagrangian becomes

$$\mathscr{L} = -\frac{1}{4}F_{\mu\nu}^2 + e^2v^2A_\mu^2 + \frac{1}{2}e^2h^2A_\mu^2 + \sqrt{2}e^2hvA_\mu^2 + \mathscr{L}(h) \,. \tag{1.62}$$

The field $\zeta(x)$ is the would-be Goldstone boson, as can be seen by considering only the ϕ terms in the Lagrangian, i.e., setting $A_\mu = 0$ in (1.59). In fact, in this limit the kinetic term $\partial_\mu\zeta\partial^\mu\zeta$ remains but with no ζ^2 mass term. Instead, in the gauge case of (1.59), after changing variables in the Lagrangian, the field $\zeta(x)$ completely disappears (not even the kinetic term remains), whilst the mass term $e^2v^2A_\mu^2$ for A_μ is now present: the gauge boson mass is $M = \sqrt{2}ev$. The field h describes the massive Higgs particle. Leaving a constant term aside, the last term in (1.62) is now

$$\mathscr{L}(h) = \frac{1}{2}\partial_\mu h\partial^\mu h - h^2\mu^2 + \cdots \,, \tag{1.63}$$

where the dots stand for cubic and quartic terms in h. We see that the h mass term has the "right" sign, due to the combination of the quadratic tems in h which, after the shift, arise from the quadratic and quartic terms in ϕ. The h mass is given by $m_h^2 = 2\mu^2$.

The Higgs mechanism is realized in well-known physical situations. It was actually discovered in condensed matter physics by Anderson [58]. For a superconductor in the Landau–Ginzburg approximation, the free energy can be written as

$$F = F_0 + \frac{1}{2}\mathbf{B}^2 + \frac{1}{4m}\left|(\nabla - 2ie\mathbf{A})\phi\right|^2 - \alpha|\phi|^2 + \beta|\phi|^4 \,. \tag{1.64}$$

Here $\mathbf{B}$ is the magnetic field, $|\phi|^2$ is the Cooper pair (e^-e^-) density, and $2e$ and $2m$ are the charge and mass of the Cooper pair. The "wrong" sign of α leads to $\phi \neq 0$ at the minimum. This is precisely the non-relativistic analogue of the Higgs model of the previous example. The Higgs mechanism implies the absence of propagation of massless phonons (states with dispersion relation $\omega = kv$, with constant v). Moreover, the mass term for $\mathbf{A}$ is manifested by the exponential decrease of $\mathbf{B}$ inside the superconductor (Meissner effect). However, in condensed matter examples, the Higgs field is not elementary, but rather a condensate of elementary fields (like for the Cooper pairs).

1.8 Quantization of Spontaneously Broken Gauge Theories: R_ξ Gauges

In Sect. 1.6 we discussed the problems arising in the quantization of a gauge theory and in the formulation of the correct Feynman rules (gauge fixing terms, ghosts, etc.). Here we give a concise account of the corresponding results for spontaneously broken gauge theories. In particular, we describe the R_ξ gauge formalism [14, 207, 250]: in this formalism the interplay of transverse and longitudinal gauge boson degrees of freedom is made explicit and their combination leads to the cancellation of the gauge parameter ξ from physical quantities. We work out in detail an Abelian example that will be easy to generalize later to the non-Abelian case.

We go back to the Abelian model of (1.59) (with $Q = -1$). In the treatment presented there, the would-be Goldstone boson $\zeta(x)$ was completely eliminated from the Lagrangian by a nonlinear field transformation formally identical to a gauge transformation corresponding to the $U(1)$ symmetry of the Lagrangian. In that description, in the new variables, we eventually obtain a theory with only physical fields: a massive gauge boson A_μ with mass $M = \sqrt{2}ev$ and a Higgs particle h with mass $m_h = \sqrt{2}\mu$. This is called a "unitary" gauge, because only physical fields appear. But if we work out the propagator of the massive gauge boson, viz.,

$$\mathrm{i}D_{\mu\nu}(k) = -\mathrm{i}\frac{g_{\mu\nu} - k_\mu k_\nu/M^2}{k^2 - M^2 + \mathrm{i}\epsilon} , \tag{1.65}$$

we find that it has a bad ultraviolet behaviour due to the second term in the numerator. This choice does not prove to be the most convenient for a discussion of the ultraviolet behaviour of the theory. Alternatively, one can go to a different formulation where the would-be Goldstone boson remains in the Lagrangian, but the complication of keeping spurious degrees of freedom is compensated by having all propagators with good ultraviolet behaviour ("renormalizable" gauges). To this end we replace the nonlinear transformation for ϕ in (1.61) by its linear equivalent (after all, perturbation theory deals with small oscillations around the minimum):

$$\phi(x) \to \left[v + \frac{h(x)}{\sqrt{2}}\right] \exp\left[-\mathrm{i}\frac{\zeta(x)}{v\sqrt{2}}\right] \sim \left[v + \frac{h(x)}{\sqrt{2}} - \mathrm{i}\frac{\zeta(x)}{\sqrt{2}}\right] . \tag{1.66}$$

Here we have only applied a shift by the amount v and separated the real and imaginary components of the resulting field with vanishing vacuum expectation value. If we leave A_μ as it is and simply replace the linearized expression for ϕ, we obtain the following quadratic terms (those important for propagators):

$$\begin{aligned}\mathscr{L}_{\text{quad}} = &-\frac{1}{4}\sum_A F^A_{\mu\nu}F^{A\mu\nu} + \frac{1}{2}M^2 A_\mu A^\mu \\ &+\frac{1}{2}(\partial_\mu\zeta)^2 + MA_\mu\partial^\mu\zeta + \frac{1}{2}(\partial_\mu h)^2 - h^2\mu^2 .\end{aligned} \tag{1.67}$$

The mixing term between A_μ and $\partial_\mu \zeta$ does not allow us to write diagonal mass matrices directly. But this mixing term can be eliminated by an appropriate modification of the covariant gauge fixing term given in (1.38) for the unbroken theory. We now take

$$\Delta\mathscr{L}_{\rm GF} = -\frac{1}{2\xi}(\partial^\mu A_\mu - \xi M\zeta)^2 \,. \tag{1.68}$$

By adding $\Delta\mathscr{L}_{\rm GF}$ to the quadratic terms in (1.67), the mixing term cancels (apart from a total derivative that can be omitted) and we have

$$\begin{aligned}\mathscr{L}_{\rm quad} = &-\frac{1}{4}\sum_A F^A_{\mu\nu}F^{A\mu\nu} + \frac{1}{2}M^2 A_\mu A^\mu - \frac{1}{2\xi}(\partial^\mu A_\mu)^2 \\ &+\frac{1}{2}(\partial_\mu\zeta)^2 - \frac{\xi}{2}M^2\zeta^2 + \frac{1}{2}(\partial_\mu h)^2 - h^2\mu^2 \,.\end{aligned} \tag{1.69}$$

We see that the ζ field appears with a mass $\sqrt{\xi}M$ and its propagator is

$$\mathrm{i}D_\zeta = \frac{\mathrm{i}}{k^2 - \xi M^2 + \mathrm{i}\epsilon} \,. \tag{1.70}$$

The propagators of the Higgs field h and of gauge field A_μ are

$$\mathrm{i}D_h = \frac{\mathrm{i}}{k^2 - 2\mu^2 + \mathrm{i}\epsilon} \,, \tag{1.71}$$

$$\mathrm{i}D_{\mu\nu}(k) = \frac{-\mathrm{i}}{k^2 - M^2 + \mathrm{i}\epsilon}\left[g_{\mu\nu} - (1-\xi)\frac{k_\mu k_\nu}{k^2 - \xi M^2}\right] \,. \tag{1.72}$$

As anticipated, all propagators have good behaviour at large k^2. This class of gauges are called "R_ξ gauges" [207]. Note that for $\xi = 1$ we have a sort of generalization of the Feynman gauge with a Goldstone boson of mass M and a gauge propagator:

$$\mathrm{i}D_{\mu\nu}(k) = \frac{-\mathrm{i}g_{\mu\nu}}{k^2 - M^2 + \mathrm{i}\epsilon} \,. \tag{1.73}$$

Furthermore, for $\xi \to \infty$ the unitary gauge description is recovered, since the would-be Goldstone propagator vanishes and the gauge propagator reproduces that of the unitary gauge in (1.65). All ξ dependence present in individual Feynman diagrams, including the unphysical singularities of the ζ and A_μ propagators at $k^2 = \xi M^2$, must cancel in the sum of all contributions to any physical quantity.

An additional complication is that a Faddeev–Popov ghost is also present in R_ξ gauges (while it is absent in an unbroken Abelian gauge theory). In fact, under an

infinitesimal gauge transformation with parameter $\theta(x)$, we have the transformations

$$A_\mu \to A_\mu - \partial_\mu \theta,$$
$$\phi \to (1 - \mathrm{i}e\theta)\left[v + \frac{h(x)}{\sqrt{2}} - \mathrm{i}\frac{\zeta(x)}{\sqrt{2}}\right],$$

so that

$$\delta A_\mu = -\partial_\mu \theta\ , \quad \delta h = -e\zeta\theta\ , \quad \delta\zeta = e\theta\sqrt{2}\left(v + \frac{h}{\sqrt{2}}\right)\ . \tag{1.74}$$

The gauge fixing condition $\partial_\mu A^\mu - \xi M\zeta = 0$ undergoes the variation

$$\partial_\mu A^\mu - \xi M\zeta \ \to\ \partial_\mu A^\mu - \xi M\zeta - \left[\partial^2 + \xi M^2\left(1 + \frac{h}{v\sqrt{2}}\right)\right]\theta\ , \tag{1.75}$$

where we have used $M = \sqrt{2}ev$. From this, recalling the discussion in Sect. 1.6, we see that the ghost is not coupled to the gauge boson (as usual for an Abelian gauge theory), but has a coupling to the Higgs field h. The ghost Lagrangian is

$$\Delta\mathscr{L}_{\text{Ghost}} = \bar{\eta}\left[\partial^2 + \xi M^2\left(1 + \frac{h}{v\sqrt{2}}\right)\right]\eta\ . \tag{1.76}$$

The ghost mass is seen to be $m_{\text{gh}} = \sqrt{\xi}M$ and its propagator is

$$\mathrm{i}D_{\text{gh}} = \frac{\mathrm{i}}{k^2 - \xi M^2 + \mathrm{i}\epsilon}\ . \tag{1.77}$$

The detailed Feynman rules follow for all the basic vertices involving the gauge boson, the Higgs, the would-be Goldstone boson, and the ghost, and are easily derived, with some algebra, from the total Lagrangian including the gauge fixing and ghost additions. The generalization to the non-Abelian case is in principle straightforward, with some formal complications involving the projectors over the space of the would-be Goldstone bosons and over the orthogonal space of the Higgs particles. But for each gauge boson that takes mass M_a, we still have a corresponding would-be Goldstone boson and a ghost with mass $\sqrt{\xi}M_a$. The Feynman diagrams, both for the Abelian and the non-Abelian case, are listed explicitly, for example, in the textbook by Cheng and Li [250].

We conclude that the renormalizability of non-Abelian gauge theories, also in the presence of spontaneous symmetry breaking, was proven in the fundamental work by t'Hooft and Veltman [358], and is discussed in detail in [278].

Open Access This chapter is licensed under the terms of the Creative Commons Attribution 4.0 International License (http://creativecommons.org/licenses/by/4.0/), which permits use, sharing, adaptation, distribution and reproduction in any medium or format, as long as you give appropriate credit to the original author(s) and the source, provide a link to the Creative Commons license and indicate if changes were made.

The images or other third party material in this chapter are included in the chapter's Creative Commons license, unless indicated otherwise in a credit line to the material. If material is not included in the chapter's Creative Commons license and your intended use is not permitted by statutory regulation or exceeds the permitted use, you will need to obtain permission directly from the copyright holder.

Chapter 2
QCD: The Theory of Strong Interactions

2.1 Introduction

This chapter is devoted to a concise introduction to quantum chromodynamics (QCD), the theory of strong interactions [215, 234, 360] (for a number of dedicated books on QCD, see [173], and also [33]). The main emphasis will be on ideas without too many technicalities. As an introduction we present here a broad overview of the strong interactions (for reviews of the subject, see, for example, [29, 30]). Then some methods of non-perturbative QCD will be briefly described, including both analytic approaches and simulations of the theory on a discrete spacetime lattice. Then we shall proceed to the main focus of the chapter, that is, the principles and applications of perturbative QCD, which will be discussed in detail.

As mentioned in Chap. 1, the QCD theory of strong interactions is an unbroken gauge theory based on the colour group $SU(3)$. The eight massless gauge bosons are the gluons g_μ^A and the matter fields are colour triplets of quarks q_i^a (in different flavours i). Quarks and gluons are the only fundamental fields of the Standard Model (SM) with strong interactions (hadrons). The QCD Lagrangian was introduced in (1.28)–(1.31) of Sect. 1.4. For quantization the classical Lagrangian in (1.28) must be extended to contain gauge fixing and ghost terms, as described in Chap. 1. The Feynman rules of QCD are listed in Fig. 2.1. The physical vertices in QCD include the gluon–quark–antiquark vertex, analogous to the QED photon–fermion–antifermion coupling, but also the 3-gluon and 4-gluon vertices, of order e_s and e_s^2 respectively, which have no analogue in an Abelian theory like QED.

Why $SU(N_C = 3)_{\text{colour}}$? The choice of $SU(3)$ as colour gauge group is unique in view of a number of constraints:

- The group must admit complex representations because it must be able to distinguish a quark from an antiquark [214]. In fact, there are meson states made up of $q\bar{q}$ but not analogous qq bound states. Among simple groups, this restricts

© The Author(s) 2017

G. Altarelli, *Collider Physics within the Standard Model*,
Lecture Notes in Physics 937, DOI 10.1007/978-3-319-51920-3_2

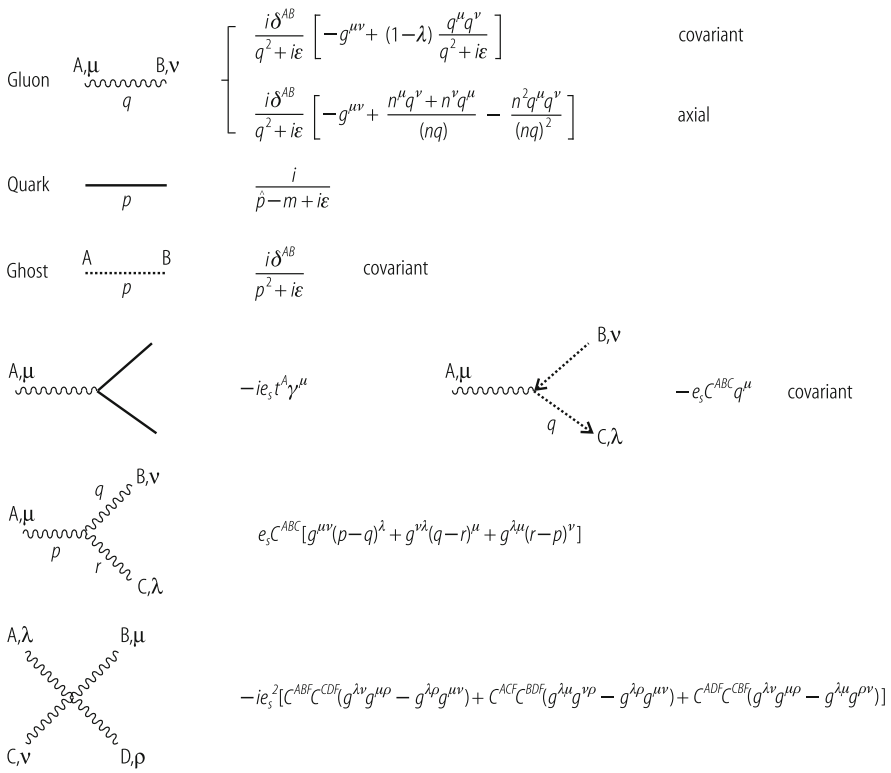

Fig. 2.1 Feynman rules for QCD. *Solid lines* represent the quarks, *curly lines* the gluons, and *dotted lines* the ghosts (see Chap. 1). The gauge parameter is denoted by λ. The 3-gluon vertex is written as if all gluon lines are outgoing

the choice to $SU(N)$ with $N \geq 3$, $SO(4N+2)$ with $N \geq 2$ [taking into account the fact that $SO(6)$ has the same algebra as $SU(4)$], and $E(6)$.

- The group must admit a completely antisymmetric colour singlet baryon made up of three quarks, viz., qqq. In fact, from the study of hadron spectroscopy, we know that the low-lying baryons, completing an octet and a decuplet of (flavour) $SU(3)$ (the approximate symmetry that rotates the three light quarks u, d, and s), are made up of three quarks and are colour singlets. The qqq wave function must be completely antisymmetric in colour in order to agree with Fermi statistics. Indeed, if we consider, for example, a N^{*++} with spin z-component +3/2, this is made up of $(u \uparrow u \uparrow u \uparrow)$ in an s-state. Thus its wave function is totally symmetric in space, spin, and flavour, so that complete antisymmetry in colour is required by Fermi statistics. In QCD this requirement is very simply satisfied by $\epsilon_{abc}q^a q^b q^c$, where a, b, c are $SU(3)_{\text{colour}}$ indices.
- The choice of $SU(N_{\text{C}} = 3)_{\text{colour}}$ is confirmed by many processes that directly measure N_{C}. Some examples are listed here.

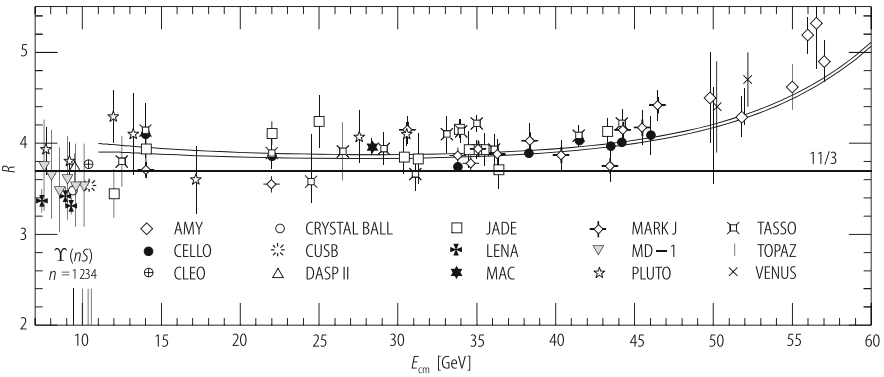

Fig. 2.2 Comparison of the data on $R = \sigma(e^+e^- \to \text{hadrons})/\sigma_{\text{point}}(e^+e^- \to \mu^+\mu^-)$ with the QCD prediction (adapted from [306]). $N_C = 3$ is indicated by the data points above ∼10 GeV (the $b\bar{b}$ threshold) and ∼40 GeV, where the rise due to the Z_0 resonance becomes appreciable

The total rate for hadronic production in e^+e^- annihilation is linear in N_C. More precisely, if we consider $R = R_{e^+e^-} = \sigma(e^+e^- \to \text{hadrons})/\sigma_{\text{point}}(e^+e^- \to \mu^+\mu^-)$ above the $b\bar{b}$ threshold and below m_Z, and if we neglect small computable radiative corrections (which will be discussed in Sect. 2.7), we have a sum of individual contributions (proportional to Q^2, where Q is the electric charge in units of the proton charge) from $q\bar{q}$ final states with $q = u,\ c,\ d,\ s,\ b$:

$$R \approx N_C \left(2 \times \frac{4}{9} + 3 \times \frac{1}{9}\right) \approx N_C \frac{11}{9} . \tag{2.1}$$

The data neatly indicate $N_C = 3$, as can be seen from Fig. 2.2 [306]. The slight excess of the data with respect to the value 11/3 is due to QCD radiative corrections (see Sect. 2.7).

Similarly, we can consider the branching ratio $B(W^- \to e^-\bar{\nu})$, again in the Born approximation. The possible fermion–antifermion ($f\bar{f}$) final states are for $f = e^-$, μ^-, τ^-, d, s (there is no $f = b$ because the top quark is too heavy for $b\bar{t}$ to occur). Each channel gives the same contribution, except that for quarks we have N_C colours:

$$B(W^- \to e^-\bar{\nu}) \approx \frac{1}{3 + 2N_C} . \tag{2.2}$$

For $N_C = 3$, we obtain $B = 11\%$ and the experimental number is $B = 10.7\%$.

Another analogous example is the branching ratio $B(\tau^- \to e^-\bar{\nu}_e\nu_\tau)$. From the final state channels with $f = e^-, \mu^-, d$, we find

$$B(\tau^- \to e^-\bar{\nu}_e\nu_\tau) \approx \frac{1}{2 + N_C} . \tag{2.3}$$

For $N_C = 3$, we obtain $B = 20\%$ and the experimental number is $B = 18\%$ (the lower accuracy in this case is explained by the larger radiative and phase-space corrections, because the mass of τ^- is much smaller than m_W).

An important process that is quadratic in N_C is the rate $\Gamma(\pi^0 \to 2\gamma)$. This rate can be reliably calculated from a theorem in field theory which has to do with the chiral anomaly:

$$\Gamma(\pi^0 \to 2\gamma) \approx \left(\frac{N_C}{3}\right)^2 \frac{\alpha^2 m_{\pi^0}^3}{32\pi^3 f_\pi^2} = (7.73 \pm 0.04)\left(\frac{N_C}{3}\right)^2 \text{eV}\,, \tag{2.4}$$

where the prediction is obtained for $f_\pi = (130.7 \pm 0.37)$ MeV. The experimental result is $\Gamma = (7.7 \pm 0.5)$ eV, in remarkable agreement with $N_C = 3$.

There are many more experimental confirmations that $N_C = 3$. For example, the rate for Drell–Yan processes (see Sect. 2.9) is inversely proportional to N_C.

2.2 Non-perturbative QCD

The QCD Lagrangian in (1.28) has a simple structure, but a very rich dynamical content. It gives rise to a complex spectrum of hadrons, implies the striking properties of confinement and asymptotic freedom, is endowed with an approximate chiral symmetry which is spontaneously broken, has a highly nontrivial topological vacuum structure (instantons, $U(1)_A$ symmetry breaking, strong CP violation which is a problematic item in QCD possibly connected with new physics, like axions, and so on), and an intriguing phase transition diagram (colour deconfinement, quark–gluon plasma, chiral symmetry restoration, colour superconductivity, and so on).

How do we get testable predictions from QCD? On the one hand there are non-perturbative methods. The most important at present is the technique of lattice simulations (for a recent review, see [272]): it is based on first principles, it has produced very valuable results on confinement, phase transitions, bound states, hadronic matrix elements, and so on, and it is by now an established basic tool. The main limitation is from computing power, so there is continuous progress and good prospects for the future.

Another class of approaches is based on effective Lagrangians, which provide simpler approximations than the full theory, valid in some definite domain of physical conditions. Typically at energies below a given scale L, particles with mass greater than L cannot be produced, and thus only contribute short distance effects as virtual states in loops. Under suitable conditions one can write down a simplified effective Lagrangian, where the heavy fields have been eliminated (one says "integrated out"). Virtual heavy particle short distance effects are absorbed into the coefficients of the various operators in the effective Lagrangian. These coefficients are determined in a matching procedure, by requiring that the effective theory reproduce the matrix elements of the full theory up to power corrections.

Chiral Lagrangians are based on soft pion theorems [362] and are valid for suitable processes at energies below 1 GeV (for a recent, concise review, see [212] and references therein). Heavy quark effective theories [178] are obtained by expanding in inverse powers of the heavy quark mass and are mainly important for the study of b and, to lesser accuracy, c decays (for reviews, see, for example, [301]).

Soft-collinear effective theories (SCET) [84], are valid for processes where quarks have energies much greater than their mass. Light energetic quarks not only emit soft gluons, but also collinear gluons (a gluon in the same direction as the original quark), without changing their virtuality. In SCET, the logs associated with these soft and collinear gluons are resummed.

The approach using QCD sum rules [298, 325] has led to interesting results but now appears not to offer much potential for further development. On the other hand, the perturbative approach, based on asymptotic freedom, still remains the main quantitative connection to experiment, due to its wide range of applicability to all sorts of "hard" processes.

2.2.1 Progress in Lattice QCD

One of the main approaches to non-perturbative problems in QCD is by simulations of the theory on a lattice, a technique initiated by K. Wilson in 1974 [366] which has shown continuous progress over the last decades. In this approach the QCD theory is reformulated on a discrete space time, a hypercubic lattice of sites (in the simplest realizations) with spacing a and 4-volume L^4. On each side, there are N sites with $L = Na$. Over the years we have learned how to efficiently describe a field theory on a discrete spacetime and how to implement gauge symmetry, chiral symmetry, and so on (for a recent review see, for example, [272]).

Gauge and matter fields are specified on the lattice sites and the path integral is computed numerically as a sum over the field configurations. Much more powerful computers than in the past now allow for a number of essential improvements. As one is eventually interested in the continuum limit $a \to 0$, it is important to work with as fine a lattice spacing a as possible. Methods have been developed for "improving" the Lagrangian in such a way that the discretization errors vanish faster than linearly in a. A larger lattice volume (i.e., large L or N) is also useful since the dimensions of the lattice should be as large as possible in comparison with the dimensions of the hadrons to be studied. In many cases the volume corrections are exponentially damped, but this is not always the case. Lattice simulation is limited to large enough masses of light quarks: in fact, heavier quarks have shorter wavelengths and can be accommodated in a smaller volume. In general, computations are done for quark and pion masses heavier than in reality, and then extrapolated to the physical values, but at present one can work with smaller quark masses than in the past. One can also take advantage of the chiral effective theory in order to control the chiral logs $\log(m_q/4\pi f_\pi)$ and guide the extrapolation.

A big step that has been taken recently, made possible by the availability of more powerful dedicated computers, is the evolution from quenched (i.e., with no dynamical fermions) to unquenched calculations. In doing this, an evident improvement is obtained in the agreement between predictions and data. For example [272], modern unquenched simulations reproduce the hadron spectrum quite well. Calculations with dynamical fermions (which take into account the effects of virtual quark loops) involve evaluation of the quark determinant, which is a difficult task. Just how difficult depends on the particular calculation method. There are several approaches (Wilson, twisted mass, Kogut–Susskind staggered, Ginsparg–Wilson fermions), each with its own advantages and disadvantages (including the time it takes to run the simulation on a computer). A compromise between efficiency and theoretical purity is needed. The most reliable lattice calculations are today for $2+1$ light quarks (degenerate up and down quarks and a heavier strange quark s). The first calculations for $2+1+1$ including charm quarks are starting to appear.

Lattice QCD is becoming increasingly predictive and plays a crucial role in different domains. For example, in flavour physics it is essential for computing the relevant hadronic matrix elements. In high temperature QCD the most illuminating studies of the phase diagram, the critical temperature, and the nature of the phase transitions are obtained by lattice QCD: as we now discuss, the best arguments to prove that QCD implies confinement come from the lattice.

2.2.2 *Confinement*

Confinement is the property that no isolated coloured charge can exist. One only sees colour singlet particles. Our understanding of the confinement mechanism has much improved thanks to lattice simulations of QCD at finite temperatures and densities (for reviews see, e.g., [85, 162, 199]). For example, the potential between a quark and an antiquark has been studied on the lattice [256]. It has a Coulomb part at short range and a linearly increasing term at long range:

$$V_{q\bar{q}} \approx C_{\mathrm{F}} \left[\frac{\alpha_{\mathrm{s}}(r)}{r} + \cdots + \sigma r \right] , \tag{2.5}$$

where

$$C_{\mathrm{F}} = \frac{1}{N_{\mathrm{C}}} \sum_{\mathrm{A}} t^A t^A = \frac{N_{\mathrm{C}}^2 - 1}{2N_{\mathrm{C}}} \tag{2.6}$$

with N_{C} the number of colours ($N_{\mathrm{C}} = 3$ in QCD). The scale dependence of α_{s} (the distance r is Fourier-conjugate to the momentum transfer) will be explained in detail later. The slope decreases with increasing temperature until it vanishes at a critical temperature T_{C}. Then above T_{C} the slope remains zero, as shown in Fig. 2.3. The value of the critical temperature is estimated to be around $T_{\mathrm{C}} \sim 175\,\mathrm{MeV}$.

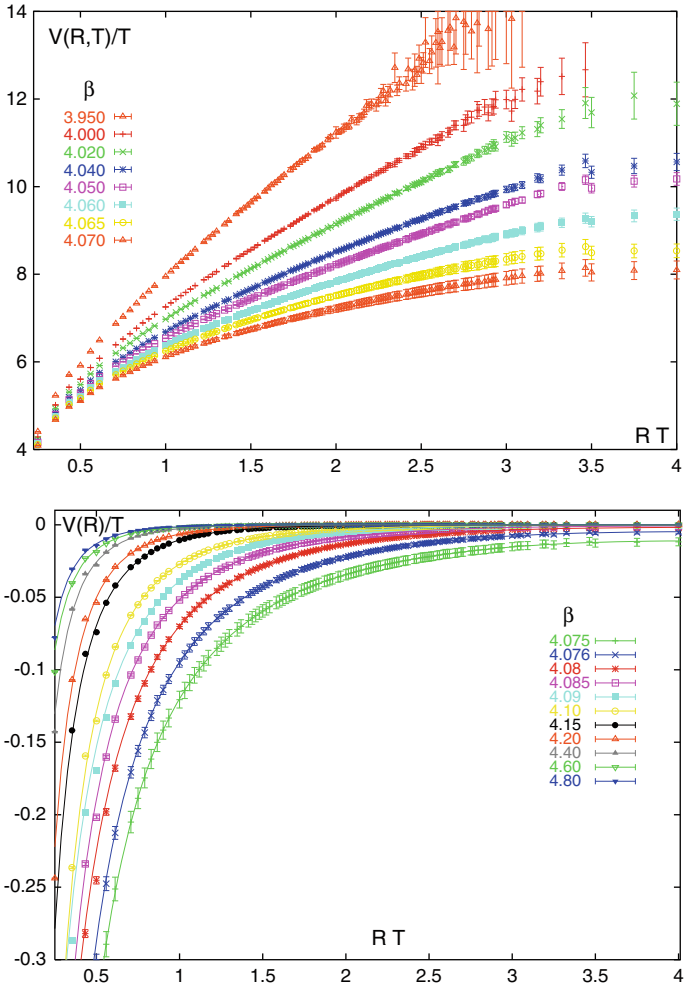

Fig. 2.3 The potential between a quark and an antiquark computed on the lattice in the quenched approximation [256]. The *upper panel* shows that the slope of the linearly rising term decreases with temperature and vanishes at the critical temperature T_C. At $T \geq T_C$ the slope remains at zero (*lower panel*)

The linearly increasing term in the potential makes it energetically impossible to separate a $q\bar{q}$ pair. If the pair is created at one spacetime point, for example in e^+e^- annihilation, and then the quark and the antiquark start moving away from each other in the center-of-mass frame, it soon becomes energetically favourable to create additional pairs, smoothly distributed in rapidity between the two leading charges, which neutralize colour and allow the final state to be reorganized into two jets of colourless hadrons that communicate in the central region by a number of

"wee" hadrons with small energy. It is just like the familiar example of the broken magnet: if you try to isolate a magnetic pole by stretching a dipole, the magnet breaks down and two new poles appear at the breaking point.

Confinement is essential to explain why nuclear forces have very short range while massless gluon exchange would be long range. Nucleons are colour singlets and they cannot exchange colour octet gluons but only colourless states. The lightest colour singlet hadronic particles are pions. So the range of nuclear forces is fixed by the pion mass $r \simeq m_\pi^{-1} \approx 10^{-13}$ cm, since $V \approx \exp(-m_\pi r)/r$.

The phase transitions of colour deconfinement and of chiral restoration appear to happen together on the lattice [85, 162, 199, 272] (see Fig. 2.4). A rapid transition is observed in lattice simulations where the energy density $\epsilon(T)$ is seen to increase sharply near the critical temperature for deconfinement and chiral restoration

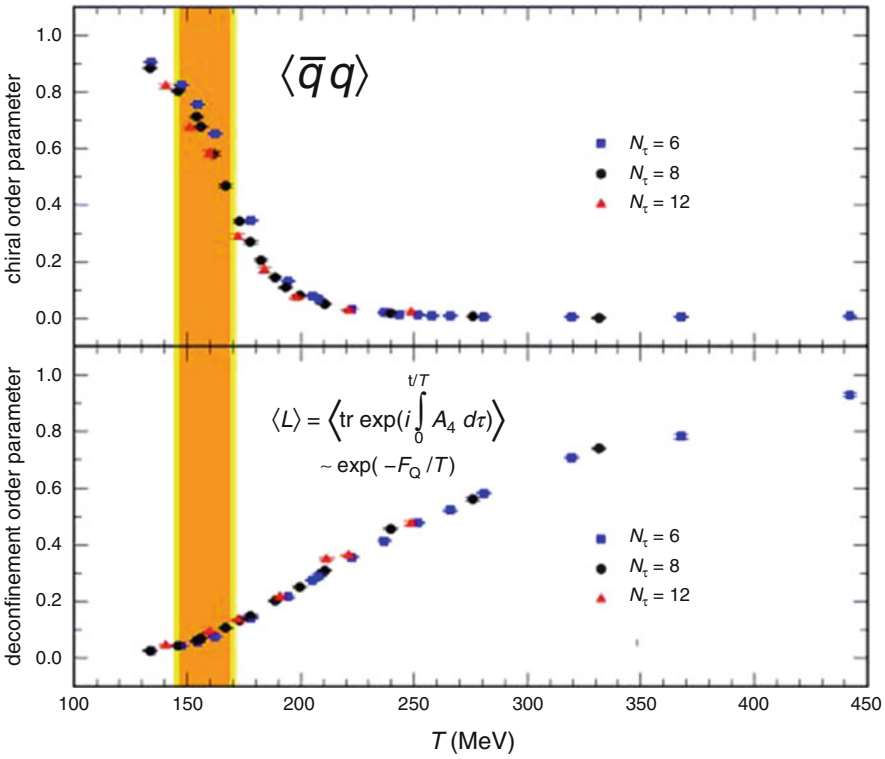

Fig. 2.4 Order parameters for deconfinement (*bottom*) and chiral symmetry restoration (*top*), as a function of temperature [85, 272]. On a finite lattice the singularities associated with phase transitions are not present, but their development is indicated by a rapid rate of change. With increasing temperature, the vacuum expectation value of the quark–antiquark condensate goes from the finite value that breaks chiral symmetry down to zero, where chiral symmetry is restored. In a comparable temperature range, the Wilson plaquette, the order parameter for deconfinement, goes from zero to a finite value. Figure reproduced with permission. Copyright (c) 2012 by *Annual Reviews*

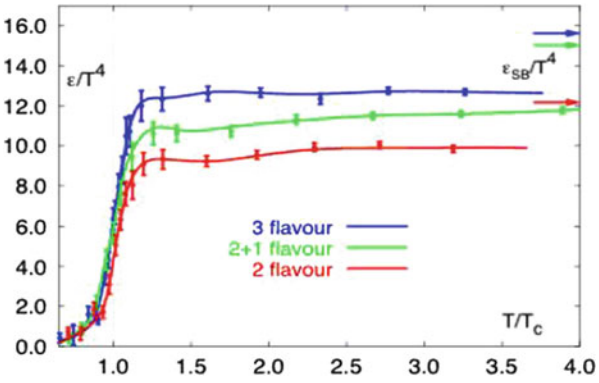

Fig. 2.5 The energy density divided by the fourth power of the temperature, computed on the lattice with different numbers of sea flavours, shows a marked rise near the critical temperature (adapted from [85] and [272]). The *arrows* on top show the limit for a perfect Bose gas (while the hot dense hadronic fluid is not expected to be a perfect gas)

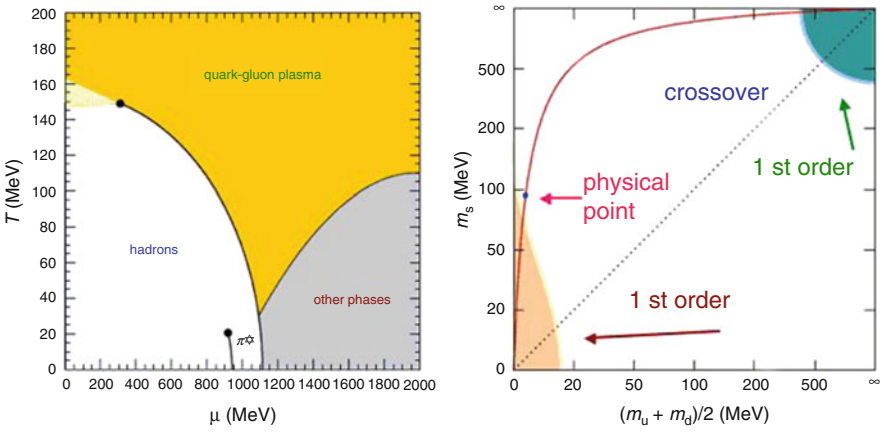

Fig. 2.6 *Left*: a schematic view of the QCD phase diagram. *Right*: on the lattice the nature of the phase transition depends on the number of quark flavours and their masses as indicated [272]. Figure reproduced with permission. Copyright (c) 2012 by *Annual Reviews*

(see Fig. 2.5). The critical parameters and the nature of the phase transition depend on the number of quark flavours n_f and on their masses (see Fig. 2.6). For example, for $n_f = 2$ or $2+1$ (i.e., 2 light u and d quarks and 1 heavier s quark), $T_C \sim 175\,\text{MeV}$ and $\epsilon(T_C) \sim 0.5$–$1.0\,\text{GeV/fm}^3$. For realistic values of the masses m_s and $m_{u,d}$, the two phases are connected by a smooth crossover, while the phase transition becomes first order for very small or very large $m_{u,d,s}$. Accordingly, the hadronic phase and the deconfined phase are separated by a crossover region at small densities and by a critical line at high densities that ends with a critical point. Determining the exact location of the critical point in T and μ_B is an important challenge for theory and

is also important for the interpretation of heavy ion collision experiments. At high densities, the colour superconducting phase is also present, with bosonic diquarks acting as Cooper pairs.

A large investment is being made in heavy ion collision experiments with the aim of finding some evidence of the quark–gluon plasma phase. Many exciting results have been found at the CERN SPS in the past few years, more recently at RHIC and now at the LHC, in dedicated heavy ion runs [296] (the ALICE detector is especially designed for the study of heavy ion collisions).

2.2.3 Chiral Symmetry in QCD and the Strong CP Problem

In the QCD Lagrangian (1.28), the quark mass terms are of the general form $[m\bar{\psi}_{\rm L}\psi_{\rm R}+{\rm h.c.}]$ (recall the definition of $\psi_{\rm L,R}$ in Sect. 1.5 and the related discussion). These terms are the only ones that show a chirality flip. In the absence of these terms, i.e., for $m=0$, the QCD Lagrangian would be invariant under independent unitary transformations acting separately on $\psi_{\rm L}$ and $\psi_{\rm R}$. Thus, if the masses of the $N_{\rm f}$ lightest quarks are neglected, the QCD Lagrangian is invariant under a global $U(N_{\rm f})_{\rm L}\bigotimes U(N_{\rm f})_{\rm R}$ chiral group.

Consider $N_{\rm f}=2$. Then $SU(2)_{\rm V}$ corresponds to the observed approximate isospin symmetry and $U(1)_{\rm V}$ to the portion of baryon number associated with u and d quarks. Since no approximate parity doubling of light quark bound states is observed, the $U(2)_{\rm A}$ symmetry must be spontaneously broken (for example, no opposite parity analogues of protons and neutrons exist with a few tens of MeV separation in mass from the ordinary nucleons). The breaking of chiral symmetry is induced by the VEV of a quark condensate. For $N_{\rm f}=2$ this is $[\bar{u}_{\rm L}u_{\rm R}+\bar{d}_{\rm L}d_{\rm R}+{\rm h.c.}]$. A recent lattice calculation [208] has given for this condensate the value $[234\pm 18\,{\rm MeV}]^3$ (in $\overline{\rm MS}$, $N_{\rm f}=2+1$, with the physical m_s value, at the scale of 2 GeV). This scalar operator is an isospin singlet, so it preserves $U(2)_{\rm V}$, but breaks $U(2)_{\rm A}$. In fact, it transforms like (1/2,1/2) under $U(2)_{\rm L}\bigotimes U(2)_{\rm R}$, but is a singlet under the diagonal group $U(2)_{\rm V}$.

The pseudoscalar mesons are obvious candidates for the would-be Goldstone bosons associated with the breakdown of the axial group, in that they have the quantum number of the broken generators: the three pions are the approximately massless Goldstone bosons (exactly massless in the limit of vanishing u and d quark masses) associated with the breaking of three generators of $U(2)_{\rm L}\bigotimes U(2)_{\rm R}$ down to $SU(2)_{\rm V}\bigotimes U(1)_{\rm V}\bigotimes U(1)_{\rm A}$. The couplings of Goldstone bosons are very special: in particular only derivative couplings are allowed. The pions as pseudo-Goldstone bosons have couplings that satisfy strong constraints. An effective chiral Lagrangian formalism [362] allows one to systematically reproduce the low energy theorems implied by the approximate status of Goldstone particles for the pion, and successfully describes QCD for energies at scales below $\sim$1 GeV.

The breaking mechanism for the remaining $U(1)_{\rm A}$ arises from an even subtler mechanism. A state in the η–η' space cannot be the associated Goldstone particle because the masses are too large [361] and the η' mass does not vanish in the chiral limit [367]. Rather, the conservation of the singlet axial current $j_5^\mu = \sum \bar{q}_i \gamma^\mu \gamma_5 q_i$ is broken by the Adler–Bell–Jackiw anomaly [19]:

$$\partial_\mu j_5^\mu \equiv I(x) = N_{\rm f} \frac{\alpha_{\rm s}}{4\pi} \sum_{\rm A} F^A_{\mu\nu} \tilde{F}^{A\mu\nu} = N_{\rm f} \frac{\alpha_{\rm s}}{2\pi} {\rm Tr}(\mathbf{F}_{\boldsymbol{\mu\nu}} \tilde{\mathbf{F}}^{\boldsymbol{\mu\nu}}) \ , \tag{2.7}$$

recalling that $\mathbf{F}_{\boldsymbol{\mu\nu}} = \sum F^A_{\mu\nu} t^A$ and the normalization is ${\rm Tr}(t^A t^B) = 1/2\delta^{AB}$, with $F^A_{\mu\nu}$ given in (1.31) and j_5^μ the $u + d$ singlet axial current (the factor of $N_{\rm f}$, in this case $N_{\rm f} = 2$, in front of the right-hand side takes into account the fact that $N_{\rm f}$ flavours are involved), and

$$\tilde{F}^A_{\mu\nu} = \frac{1}{2} \epsilon_{\mu\nu\rho\sigma} F^{A\rho\sigma} \ . \tag{2.8}$$

An important point is that the pseudoscalar quantity $I(x)$ is a four-divergence. More precisely, one can check that

$${\rm Tr}(\mathbf{F}_{\boldsymbol{\mu\nu}} \tilde{\mathbf{F}}^{\boldsymbol{\mu\nu}}) = \partial^\mu k_\mu \ , \tag{2.9}$$

with

$$k_\mu = \epsilon_{\mu\nu\lambda\sigma} {\rm Tr} \left[\mathbf{A}^\nu \left(\mathbf{F}^{\lambda\sigma} - \frac{2}{3} {\rm i} e_{\rm s} \mathbf{A}^\lambda \mathbf{A}^\sigma \right) \right] \ . \tag{2.10}$$

As a consequence the modified current $\tilde{j}_5^\mu$ and its associated charge $\tilde{Q}_5$ still appear to be conserved, viz.,

$$\partial_\mu \tilde{j}_5^\mu = \partial_\mu \left(j_5^\mu - N_{\rm f} \frac{\alpha_{\rm s}}{2\pi} k^\mu \right) = 0 \ , \tag{2.11}$$

and could act as a modified chiral current and charge with an additional gluonic component. But actually this charge is not conserved due to the topological structure of the QCD vacuum (instantons) as discussed in the following (for an introduction, see [308]).

The configuration where all gauge fields are zero $A^A_\mu = 0$ can be called "the vacuum". However, all configurations connected to $A^A_\mu = 0$ by a gauge transformation must also correspond to the same physical vacuum. For example, in an Abelian theory all gauge fields that can be written as the gradient of a scalar, i.e., $A^A_\mu = \partial_\mu \chi(x)$, are equivalent to $A^A_\mu = 0$. In non-Abelian gauge theories, there are some "large" gauge transformations that are topologically nontrivial and correspond to non-vanishing integer values of a topological charge, the "winding number". Taking $SU(2)$ for simplicity, although in QCD it could be any such

subgroup of colour $SU(3)$, we can consider the following time-independent gauge transformation:

$$\Omega_1(\mathbf{x}) = \frac{\mathbf{x}^2 - d^2 + 2\mathrm{i}d\boldsymbol{\tau}\cdot\mathbf{x}}{\mathbf{x}^2 + d^2} \,, \tag{2.12}$$

where d is a positive constant. Note that $\Omega_1^{-1} = \Omega_1^*$. Starting from $\mathbf{A}_\mu = (A_0, A_i) = (0,0)$ $(i = 1,2,3)$, with $\mathbf{A}_\mu = \sum A_\mu^a \tau^a/2$ and recalling the general expression of a gauge transformation in (1.15), the gauge transform of the potential by Ω_1 is

$$\mathbf{A}_\mathbf{j}^{(\mathbf{1})} = -\frac{\mathrm{i}}{e_\mathrm{s}}\big[\nabla_j \Omega_1(\mathbf{x})\big]\Omega_1^{-1}(\mathbf{x}) \,. \tag{2.13}$$

For the vector potential $\mathbf{A}^{(\mathbf{1})}$, which is a pure gauge and hence part of the "vacuum", the winding number n, defined in general by

$$n = \frac{\mathrm{i}e_\mathrm{s}^3}{24\pi^2}\int \mathrm{d}^3x\,\mathrm{Tr}\big[\mathbf{A_i}(\mathbf{x})\mathbf{A_j}(\mathbf{x})\mathbf{A_k}(\mathbf{x})\big]\epsilon^{ijk} \,, \tag{2.14}$$

is equal to 1, i.e., $n = 1$. Similarly, for $\mathbf{A}^{(\mathbf{m})}$ obtained from $\Omega_m = [\Omega_1]^m$, one has $n = m$. Given (2.9), we might expect the integrated four-divergence to vanish, but instead one finds

$$\frac{\alpha_\mathrm{s}}{4\pi}\int \mathrm{d}^4x\,\mathrm{Tr}(\mathbf{F}_{\boldsymbol{\mu\nu}}\tilde{\mathbf{F}}^{\boldsymbol{\mu\nu}}) = \frac{\alpha_\mathrm{s}}{4\pi}\int \mathrm{d}^4x\,\partial_\mu k^\mu = \frac{\alpha_\mathrm{s}}{4\pi}\left[\int \mathrm{d}^3x\,k_0\right]_{-\infty}^{+\infty} = n_+ - n_- \,, \tag{2.15}$$

for a configuration of gauge fields that vanish fast enough on the space sphere at infinity, and the winding numbers are $n_\mp$ at time $t = \mp\infty$ ("instantons").

From the above discussion it follows that in QCD all gauge fields can be classified in sectors with different n: there is a vacuum for each n, $|n\rangle$, and $\Omega_1|n\rangle = |n+1\rangle$ (not gauge invariant!). The true vacuum must be gauge invariant (up to a phase) and is obtained as a superposition of all $|n\rangle$:

$$|\theta\rangle = \sum_{-\infty}^{+\infty} \mathrm{e}^{-in\theta}|n\rangle \,. \tag{2.16}$$

In fact,

$$\Omega_1|\theta\rangle = \sum \mathrm{e}^{-\mathrm{i}n\theta}|n+1\rangle = \mathrm{e}^{\mathrm{i}\theta}|\theta\rangle \,. \tag{2.17}$$

If we compute the expectation value of any operator O in the θ vacuum, we find

$$\langle\theta|O|\theta\rangle = \sum_{m,n} \mathrm{e}^{\mathrm{i}(m-n)\theta}\langle m|O|n\rangle \,. \tag{2.18}$$

The path integral describing the O vacuum matrix element at $\theta = 0$ must be modified to reproduce the extra phase, taking (2.15) into account:

$$\langle\theta|O|\theta\rangle = \int \mathrm{d}A\mathrm{d}\bar{\psi}\mathrm{d}\psi O \exp\left[\mathrm{i}S_{\mathrm{QCD}} + \mathrm{i}\theta\frac{\alpha_{\mathrm{s}}}{4\pi}\int \mathrm{d}^4x\,\mathrm{Tr}(\mathbf{F}_{\mu\nu}\tilde{\mathbf{F}}^{\mu\nu})\right] . \tag{2.19}$$

This is equivalent to adding a θ term to the QCD Lagrangian:

$$\mathscr{L}_{\mathrm{QCD}} = \theta\frac{\alpha_{\mathrm{s}}}{4\pi}\int \mathrm{d}^4x\,\mathrm{Tr}(\mathbf{F}_{\mu\nu}\tilde{\mathbf{F}}^{\mu\nu}) . \tag{2.20}$$

The θ term is parity (P) odd and charge conjugation (C) even, so it introduces CP violation in the theory (and also time reversal (T) violation). A priori one would expect $\tilde{\theta}$ to be $O(1)$. But it would contribute to the neutron electric dipole moment, according to $d_n(e{\cdot}\mathrm{cm}) \sim 3\times 10^{-16}\tilde{\theta}$. The strong experimental bounds on d_n, viz., $d_n(e{\cdot}\mathrm{cm}) \leq 3\times 10^{-26}$ [307], imply that $\tilde{\theta}$ must be very small, viz., $\tilde{\theta} \leq 10^{-10}$. The so-called "strong CP problem" or "θ-problem" consists in finding an explanation for such a small value [263, 308]. An important point that is relevant for a possible solution is that a chiral transformation translates θ by a fixed amount. By recalling (2.11), we have

$$\mathrm{e}^{\mathrm{i}\delta\tilde{Q}_5}|\theta\rangle = |\theta - 2N_{\mathrm{f}}\delta\rangle . \tag{2.21}$$

To prove this relation we first observe that $\tilde{Q}_5$ is not gauge invariant under Ω_1, because it involves k_0 :

$$\Omega_1\tilde{Q}_5\Omega_1^{-1} = Q_5 - \Omega_1 2N_{\mathrm{f}}\frac{\alpha_{\mathrm{s}}}{4\pi}\left[\int \mathrm{d}^3x\,k_0\right]\Omega_1^{-1} = \tilde{Q}_5 - 2N_{\mathrm{f}} . \tag{2.22}$$

It then follows that

$$\Omega_1\mathrm{e}^{\mathrm{i}\delta\tilde{Q}_5}|\theta\rangle = \Omega_1\mathrm{e}^{\mathrm{i}\delta\tilde{Q}_5}\Omega_1^{-1}\Omega_1|\theta\rangle = \mathrm{e}^{\mathrm{i}(\theta-2N_{\mathrm{f}}\delta)}\mathrm{e}^{\mathrm{i}\delta\tilde{Q}_5}|\theta\rangle , \tag{2.23}$$

which implies (2.21). Thus in a chiral invariant theory, one could dispose of θ. For this it would be sufficient for a single quark mass to be zero, and the obvious candidate would be $m_u = 0$. But apparently this possibility has been excluded [263]. For non-vanishing quark masses, the transformation $m \to U_{\mathrm{L}}^{\dagger}mU_{\mathrm{R}}$ needed to make the mass matrix Hermitian (which implies γ_5-free) and diagonal involves a chiral transformation that affects θ. Considering that $U(N) = U(1)\bigotimes SU(N)$ and that for Hermitian m the argument of the determinant vanishes, i.e., $\arg\det m = 0$, the transformation from a generic m' to a real and diagonal m gives

$$\begin{aligned}\arg\det m = 0 &= \arg\det\ U_{\mathrm{L}}^{*} + \arg\det m' + \arg\det U_{\mathrm{R}}\\ &= -2N_{\mathrm{f}}(\delta_{\mathrm{L}} - \delta_{\mathrm{R}}) + \arg\det m' .\end{aligned} \tag{2.24}$$

From this equation one derives the phase $\delta_R - \delta_L$ of the chiral transformation and then, by (2.21), the important result for the effective θ value:

$$\theta_{\text{eff}} = \theta + \arg \det m' \,. \tag{2.25}$$

As we have seen the small empirical value of θ_{eff} poses a serious naturalness problem for the SM. Among the possible solutions, perhaps the most interesting option is a mechanism proposed by Peccei and Quinn [309]. One assumes that the SM or an enlarged theory is invariant under an additional chiral symmetry $U(1)_{PQ}$ acting on the fields of the theory. This symmetry is spontaneously broken by the vacuum expectation value v_{PQ} of a scalar field. The associated Goldstone boson, the axion, is actually not massless, because of the chiral anomaly. The parameter θ is canceled by the vacuum expectation value of the axion field due to the properties of the associated potential, also determined by the anomaly. Axions could contribute to the dark matter in the Universe, if their mass falls in a suitable narrow range (for a recent review, see, for example, [262]).

Alternative solutions to the θ-problem have also been suggested. Some of them can probably be discarded (for example, the idea that the up quark is exactly massless), while others are still possible: for example, in supersymmetric theories, if the smallness of θ could be guaranteed at the Planck scale by some feature of the more fundamental theory valid there, then the non-renormalization theorems of supersymmetry would preserve its small value throughout the transition down to low energy.

2.3 Massless QCD and Scale Invariance

As discussed in Chap. 2, the QCD Lagrangian in (1.28) only specifies the theory at the classical level. The procedure for quantizing gauge theories involves a number of complications that arise from the fact that not all degrees of freedom of gauge fields are physical because of the constraints from gauge invariance which can be used to eliminate the dependent variables. This is already true for Abelian theories and one is familiar with the QED case. One introduces a gauge fixing term (an additional term in the Lagrangian density that acts as a Lagrange multiplier in the action extremization). One can choose to preserve manifest Lorentz invariance. In this case, one adopts a covariant gauge, like the Lorentz gauge, and in QED one proceeds according to the formalism of Gupta and Bleuler [102]. Or one can give up explicit formal covariance and work in a non-covariant gauge, like the Coulomb or the axial gauges, and only quantize the physical degrees of freedom (in QED the transverse components of the photon field).

While this is all for an Abelian gauge theory, in the non-Abelian case some additional complications arise, in particular the need to introduce ghosts for the formulation of Feynman rules. As we have seen, there are in general as many ghost fields as gauge bosons, and they appear in the form of a transformation Jacobian

in the Feynman functional integral. Ghosts only propagate in closed loops and their vertices with gluons can be included as additional terms in the Lagrangian density, these being fixed once the gauge fixing terms and their infinitesimal gauge transformations are specified. Finally, the complete Feynman rules can be obtained in either the covariant or the axial gauges, and they appear in Fig. 2.1.

Once the Feynman rules are derived, we have a formal perturbative expansion, but loop diagrams generate infinities. First a regularization must be introduced, compatible with gauge symmetry and Lorentz invariance. This is possible in QCD. In principle, one can introduce a cutoff K (with dimensions of energy), for example, as done by Pauli and Villars [102]. But at present, the universally adopted regularization procedure is dimensional regularization, which we will describe briefly later on.

After regularization, the next step is renormalization. In a renormalizable theory (which is the case for all gauge theories in four spacetime dimensions and for QCD in particular), the dependence on the cutoff can be completely reabsorbed in a redefinition of particle masses, gauge coupling(s), and wave function normalizations. Once renormalization is achieved, the perturbative definition of the quantum theory that corresponds to a classical Lagrangian like (1.28) is completed.

In the QCD Lagrangian of (1.28), quark masses are the only parameters with physical dimensions (we work in the natural system of units $\hbar = c = 1$). Naively, we would expect massless QCD to be scale invariant. This is actually true at the classical level. Scale invariance implies that dimensionless observables should not depend on the absolute scale of energy, but only on ratios of energy-dimensional variables. The massless limit should be relevant for the large asymptotic energy limit of processes which are non-singular for $m \to 0$.

The naive expectation that massless QCD should be scale invariant is false in the quantum theory. The scale symmetry of the classical theory is unavoidably destroyed by the regularization and renormalization procedure, which introduce a dimensional parameter into the quantum version of the theory. When a symmetry of the classical theory is necessarily destroyed by quantization, regularization, and renormalization one talks of an "anomaly". So in this sense, scale invariance in massless QCD is anomalous.

While massless QCD is not in the end scale invariant, the departures from scaling are asymptotically small, logarithmic, and computable. In massive QCD, there are additional mass corrections suppressed by powers of m/E, where E is the energy scale (for processes that are non-singular in the limit $m \to 0$). At the parton level (q and g), we can consider applying the asymptotic predictions of massless QCD to processes and observables (we use the word "processes" for both) with the following properties ("hard processes"):

- All relevant energy variables must be large:

$$E_i = z_i Q \,, \quad Q \gg m_j \,, \quad z_i \text{ scaling variables } O(1) \,. \tag{2.26}$$

- There should be no infrared singularities (one talks of "infrared safe" processes).
- The processes concerned must be finite for $m \to 0$ (no mass singularities).

To have any chance of satisfying these criteria, processes must be as "inclusive" as possible: one should include all final states with massless gluon emission and add all mass degenerate final states (given that quarks are massless, $q\bar{q}$ pairs can also be massless if "collinear", that is moving together in the same direction at a common speed, the speed of light).

In perturbative QCD one computes inclusive rates for partons (the fields in the Lagrangian, that is, in QCD, quarks and gluons) and takes them as equal to rates for hadrons. Partons and hadrons are considered as two equivalent sets of complete states. This is called "global duality", and it is rather safe in the rare instance of a totally inclusive final state. It is less so for distributions, like distributions in the invariant mass M ("local duality"), where it can be reliable only if smeared over a sufficiently wide bin in M.

Let us discuss infrared and collinear safety in more detail. Consider, for example, a quark virtual line that ends up in a real quark plus a real gluon (Fig. 2.7). For the propagator we have

$$\text{propagator} = \frac{1}{(p+k)^2 - m^2} = \frac{1}{2(p \cdot k)} = \frac{1}{2E_k E_p} \cdot \frac{1}{1 - \beta_p \cos\theta} \,. \tag{2.27}$$

Since the gluon is massless, E_k can vanish and this corresponds to an infrared singularity. Remember that we have to take the square of the amplitude and integrate it over the final state phase space, resulting in this case with $\mathrm{d}E_k/E_k$. Indeed, we get $1/E_k^2$ from the squared amplitude and $\mathrm{d}^3k/E_k \sim E_k \mathrm{d}E_k$ from the phase space. Further, for $m \to 0$, $\beta_p = \sqrt{1 - m^2/E_p^2} \to 1$ and $1 - \beta_p \cos\theta$ vanishes at $\cos\theta = 1$, leading to a collinear mass singularity.

There are two very important theorems on infrared and mass singularities. The first one is the Bloch–Nordsieck theorem [103]: infrared singularities cancel between real and virtual diagrams (see Fig. 2.8) when all resolution-indistinguishable final states are added up. For example, for each real detector there is a minimum energy of gluon radiation that can be detected. For the cancellation of infrared divergences, one should add all possible gluon emission with a total energy below the detectable minimum.

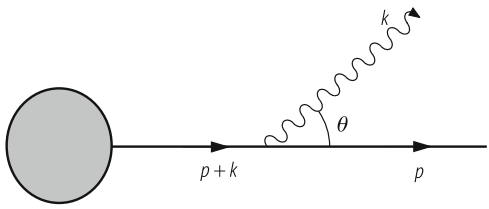

Fig. 2.7 The splitting of a virtual quark into a quark and a gluon

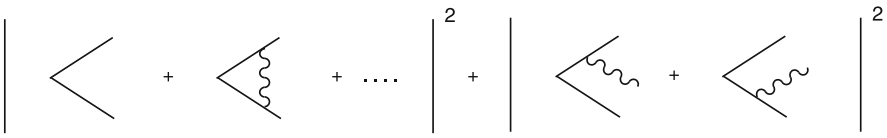

Fig. 2.8 Diagrams contributing to the total cross-section $e^+e^- \to$ hadrons at order α_s. For simplicity, only the final state quarks and (virtual or real) gluons are drawn

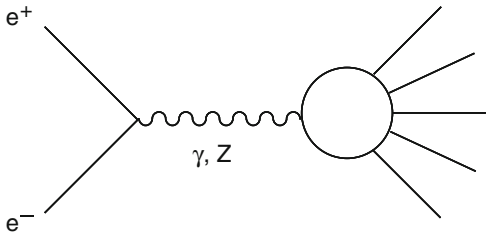

Fig. 2.9 Total cross-section $e^+e^- \to$ hadrons

The second one is the Kinoshita–Lee–Nauenberg theorem [265]: mass singularities connected with an external particle of mass m are canceled if all degenerate states (that is, with the same mass) are summed up. Hence, for a final state particle of mass m, we should add all final states that have the same mass in the limit $m \to 0$, including also gluons and massless pairs. If a completely inclusive final state is taken, only the mass singularities from the initial state particles remain (we shall see that they will be absorbed inside the non-perturbative parton densities, which are probability densities for finding the given parton in the initial hadron).

Hard processes to which the massless QCD asymptotics may possibly apply must be infrared and collinear safe, that is they must satisfy the requirements of the Bloch–Nordsieck and the Kinoshita–Lee–Nauenberg theorems. We now give some examples of important hard processes. One of the simplest hard processes is the totally inclusive cross-section for hadron production in e^+e^- annihilation (see Fig. 2.9), parameterized in terms of the already mentioned dimensionless observable $R = \sigma(e^+e^- \to \text{hadrons})/\sigma_{\text{point}}(e^+e^- \to \mu^+\mu^-)$. The pointlike cross-section in the denominator is given by $\sigma_{\text{point}} = 4\pi\alpha^2/3s$, where $s = Q^2 = 4E^2$ is the squared total center of mass energy and Q is the mass of the exchanged virtual gauge boson.

At parton level, the final state is $q\bar{q} + ng + n'q'\bar{q}'$, and n and n' are limited at each order of perturbation theory. It is assumed that the conversion of partons into hadrons does not affect the rate (it happens with probability 1). We have already mentioned that, in order for this to be true within a given accuracy, averaging over a sufficiently large bin of Q must be understood. The binning width is larger in the vicinity of thresholds: for example, when one goes across the charm $c\bar{c}$ threshold, the physical cross-section shows resonance bumps that are absent in the smooth partonic counterpart, which, however, gives an average of the cross-section.

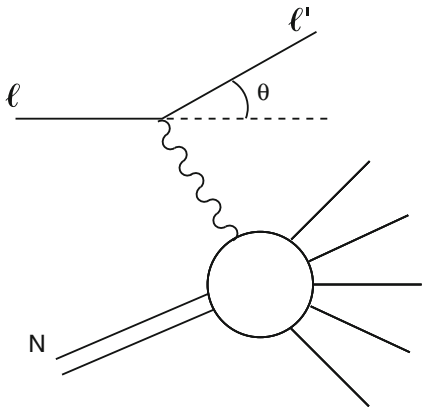

Fig. 2.10 Deep inelastic lepto-production

A very important class of hard processes is deep inelastic scattering (DIS):

$$l + N \to l' + X\,, \qquad l = e^{\pm},\, \mu^{\pm},\, \nu,\, \bar{\nu}\,. \tag{2.28}$$

This has played, and still plays, a very important role in our understanding of QCD and nucleon structure. For the processes in (2.28) (see Fig. 2.10), in the lab system where the nucleon of mass m is at rest, we have

$$Q^2 = -q^2 = -(k-k')^2 = 4EE' \sin^2\frac{\theta}{2}\,, \quad m\nu = (p.q)\,, \quad x = \frac{Q^2}{2m\nu}\,. \tag{2.29}$$

In this case the virtual momentum q of the gauge boson is spacelike. x is the familiar Bjorken variable. The DIS processes in QCD will be discussed extensively in Sect. 2.8.

2.4 The Renormalization Group and Asymptotic Freedom

In this section we aim to provide a reasonably detailed introduction to the renormalization group formalism and the concept of running coupling, which leads to the result that QCD has the property of asymptotic freedom. We start with a summary of how renormalization works.

In the simplest conceptual situation imagine that we implement regularization of divergent integrals by introducing a dimensional cutoff K that respects gauge and Lorentz invariance. The dependence of renormalized quantities on K is eliminated by absorbing it into a redefinition of m, the quark mass (for simplicity we assume a single flavour here), the gauge coupling e (which can be e in QED or e_s in QCD), and the wave function renormalization factors $Z_{q,g}^{1/2}$ for q and g, using suitable renormalization conditions (that is, precise definitions of m, g, and Z that can be

implemented order by order in perturbation theory). For example, we can define the renormalized mass m as the position of the pole in the quark propagator, and similarly, the normalization Z_q as the residue at the pole:

$$\text{propagator} = \frac{Z_q}{p^2 - m^2} + \text{no-pole terms}\,. \tag{2.30}$$

The renormalized coupling e can be defined in terms of a renormalized 3-point vertex at some specified values of the external momenta. More precisely, we consider a one-particle irreducible vertex (1PI). We recall that a connected Green function is the sum of all connected diagrams, while 1PI Green functions are the sum of all diagrams that cannot be separated into two disconnected parts by cutting only one line.

We now become more specific, by concentrating on the case of massless QCD. If we start from a vanishing mass at the classical (or "bare") level $m_0 = 0$, the mass is not renormalized because it is protected by a symmetry, namely, chiral symmetry. The conserved currents of chiral symmetry are axial currents: $\bar{q}\gamma_\mu\gamma_5 q$. Using the Dirac equation, divergence of the axial current gives $\partial^\mu(\bar{q}\gamma_\mu\gamma_5 q) = 2m\bar{q}\gamma_5 q$. So the axial current and the corresponding axial charge are conserved in the massless limit. Actually, the singlet axial current is not conserved due to the anomaly, but since QCD is a vector theory, we do not have to worry about chiral anomalies in the present context. As there are no γ_5 factors around, the chosen regularization preserves chiral symmetry as well as gauge and Lorentz symmetry, and the renormalized mass remains zero. The renormalized propagator has the form (2.30) with $m = 0$.

The renormalized coupling e_s can be defined from the renormalized 1PI 3-gluon vertex at a scale $-\mu^2$ (Fig. 2.11):

$$V_{\text{bare}}(p^2, q^2, r^2) = ZV_{\text{ren}}(p^2, q^2, r^2)\,, \quad Z = Z_g^{-3/2}\,, \quad V_{\text{ren}}(-\mu^2, -\mu^2, -\mu^2) \to e_s\,. \tag{2.31}$$

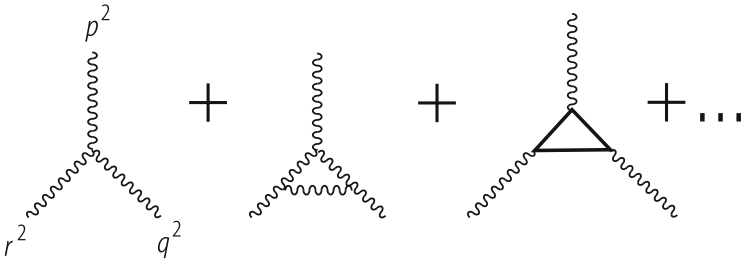

Fig. 2.11 Diagrams contributing to the 1PI 3-gluon vertex at the one-loop approximation level

We could just as well use the quark–gluon vertex or any other vertex which coincides with e_{s0} in lowest order (even the ghost–gluon vertex, if we want). With a regularization and renormalization that preserves gauge invariance, we can be sure that all these different definitions are equivalent.

Here V_{bare} is what is obtained from computing the Feynman diagrams including, for example, the 1-loop corrections at the lowest non-trivial order. V_{bare} is defined as the scalar function multiplying the 3-gluon vertex tensor (given in Fig. 2.1), normalized in such a way that it coincides with e_{s0} in lowest order. V_{bare} contains the cutoff K, but does not know about μ. Z is a factor that depends both on the cutoff and on μ, but not on momenta. Because of infrared singularities, the defining scale μ cannot vanish. The negative value $-\mu^2 < 0$ is chosen to stay away from physical cuts (a gluon with negative virtual mass cannot decay). Similarly, in the massless theory, we can define Z_g^{-1} as the inverse gluon propagator (the 1PI 2-point function) at the same scale $-\mu^2$ (the vanishing mass of the gluon is guaranteed by gauge invariance).

After computing all 1-loop diagrams indicated in Fig. 2.11, we have

$$\begin{aligned} V_{\text{bare}}(p^2,p^2,p^2) &= e_{s0}\left(1 + c\alpha_{s0}\log\frac{K^2}{p^2} + \cdots\right) \\ &= \left(1 + c\alpha_s \log\frac{K^2}{-\mu^2} + \ldots\right) e_{s0}\left(1 + c\alpha_{s0}\log\frac{-\mu^2}{p^2}\right) \\ &= Z_V^{-1} e_{s0}\left(1 + c\alpha_s \log\frac{-\mu^2}{p^2}\right) \\ &= \left(1 + d\alpha_s \log\frac{K^2}{-\mu^2} + \cdots\right) e_s\left(1 + c\alpha_s \log\frac{-\mu^2}{p^2}\right) \\ &= Z_g^{-3/2} V_{\text{ren}}\,. \end{aligned} \tag{2.32}$$

Note the replacement of α_{s0} with α_s in the second step, as we work at 1-loop accuracy. Then we change e_{s0} into e_s, given by $e_0 = Z_g^{-3/2} Z_V e$, and this implies changing c into d in the first bracket. The definition of e_s requires precise specification of what is included in Z. For this, in a given renormalization scheme, a prescription is fixed to specify the finite terms that go into Z, i.e., the terms of order α_s that accompany $\log K^2$. Then V_{ren} is specified and the renormalized coupling is defined from it according to (2.31). For example, in the momentum subtraction scheme we define $V_{\text{ren}}(p^2,p^2,p^2) = e_s + V_{\text{bare}}(p^2,p^2,p^2) - V_{\text{bare}}(-\mu^2,-\mu^2,-\mu^2)$, which is equivalent to saying that, at 1-loop, all finite terms that do not vanish at $p^2 = -\mu^2$ are included in Z.

A crucial observation is that V_{bare} depends on K, but not on μ, which is only introduced when Z, V_{ren}, and hence α_s are defined. (From here on, for simplicity, we write α to indicate either the QED coupling or the QCD coupling α_s.) Similarly, for

a generic Green function G, we have more generally

$$G_{\text{bare}}(K^2, \alpha_0, p_i^2) = Z_G G_{\text{ren}}(\mu^2, \alpha, p_i^2) \ , \tag{2.33}$$

whence

$$\frac{\mathrm{d}G_{\text{bare}}}{\mathrm{d}\log\mu^2} = \frac{\mathrm{d}}{\mathrm{d}\log\mu^2}(Z_G G_{\text{ren}}) = 0 \ , \tag{2.34}$$

or

$$Z_G \left(\frac{\partial}{\partial \log\mu^2} + \frac{\partial\alpha}{\partial\log\mu^2}\frac{\partial}{\partial\alpha} + \frac{1}{Z_G}\frac{\partial Z_G}{\partial\log\mu^2} \right) G_{\text{ren}} = 0 \ . \tag{2.35}$$

Finally, the renormalization group equation (RGE) can be written as

$$\left[\frac{\partial}{\partial \log\mu^2} + \beta(\alpha)\frac{\partial}{\partial\alpha} + \gamma_G(\alpha) \right] G_{\text{ren}} = 0 \ , \tag{2.36}$$

where

$$\beta(\alpha) = \frac{\partial\alpha}{\partial\log\mu^2} \tag{2.37}$$

and

$$\gamma_G(\alpha) = \frac{\partial \log Z_G}{\partial\log\mu^2} \ . \tag{2.38}$$

Note that $\beta(\alpha)$ does not depend on which Green function G we are considering. Actually, it is a property of the theory and of the renormalization scheme adopted, while $\gamma_G(\alpha)$ also depends on G. Strictly speaking the RGE as written above is only valid in the Landau gauge ($\lambda = 0$). In other gauges, an additional term that takes the variation of the gauge fixing parameter λ into account should also be included. We omit this term, for simplicity, as it is not relevant at the 1-loop level.

Suppose we want to apply the RGE to some hard process at a large scale Q, related to a Green function G that we can always take to be dimensionless (by multiplying by a suitable power of Q). Since the interesting dependence on Q will be logarithmic, we introduce the variable t as

$$t = \log\frac{Q^2}{\mu^2} \ . \tag{2.39}$$

Then we can write $G_{\text{ren}} \equiv F(t, \alpha, x_i)$, where x_i are scaling variables (we shall often omit them in the following). In the naive scaling limit, F should be independent of

t, according to the classical intuition that massless QCD is scale invariant. To find the actual dependence on t, we must solve the RGE

$$\left[-\frac{\partial}{\partial t}+\beta(\alpha)\frac{\partial}{\partial \alpha}+\gamma_G(\alpha)\right]G_{\text{ren}}=0\,, \tag{2.40}$$

with a given boundary condition at $t=0$ (or $Q^2=\mu^2$), viz., $F(0,\alpha)$.

We first solve the RGE in the simplest case, i.e., when $\gamma_G(\alpha)=0$. This is not an unphysical case. For example, it applies to

$$R=R_{e^+e^-}=\frac{\sigma(e^+e^-\to \text{hadrons})}{\sigma_{\text{point}}(e^+e^-\to \mu^+\mu^-)}\,,$$

where the vanishing of γ is related to the non-renormalization of the electric charge in QCD (otherwise the proton and the electron charge would not exactly balance, something we explain in Sect. 2.7). So we consider the equation

$$\left[-\frac{\partial}{\partial t}+\beta(\alpha)\frac{\partial}{\partial \alpha}\right]G_{\text{ren}}=0\,. \tag{2.41}$$

The solution is simply

$$F(t,\alpha)=F[0,\alpha(t)]\,, \tag{2.42}$$

where the "running coupling" $\alpha(t)$ is defined by

$$t=\int_{\alpha}^{\alpha(t)}\frac{1}{\beta(\alpha')}\mathrm{d}\alpha'\,. \tag{2.43}$$

Note that from this definition it follows that $\alpha(0)=\alpha$, so that the boundary condition is also satisfied. To prove that $F[0,\alpha(t)]$ is indeed the solution, we first take derivatives with respect of t and α (the two independent variables) of both sides of (2.43). By taking $\mathrm{d}/\mathrm{d}t$ we obtain

$$1=\frac{1}{\beta(\alpha(t))}\frac{\partial\alpha(t)}{\partial t}\,. \tag{2.44}$$

We then take $\mathrm{d}/\mathrm{d}\alpha$ and obtain

$$0=-\frac{1}{\beta(\alpha)}+\frac{1}{\beta(\alpha(t))}\frac{\partial\alpha(t)}{\partial\alpha}\,. \tag{2.45}$$

These two relations make explicit the dependence of the running coupling on t and α:

$$\frac{\partial \alpha(t)}{\partial t} = \beta(\alpha(t)) \ , \qquad \frac{\partial \alpha(t)}{\partial \alpha} = \frac{\beta(\alpha(t))}{\beta(\alpha)} \ . \tag{2.46}$$

Using these two equations, one immediately checks that $F[0, \alpha(t)]$ is indeed the solution.

Similarly, one finds that the solution of the more general equation (2.40) with $\gamma \neq 0$ is given by

$$F(t, \alpha) = F[0, \alpha(t)] \exp \int_{\alpha}^{\alpha(t)} \frac{\gamma(\alpha')}{\beta(\alpha')} \mathrm{d}\alpha' \ . \tag{2.47}$$

In fact the sum of the two derivatives acting on the factor $F[0, \alpha(t)]$ vanishes (as we have just seen), and the exponential is by itself a solution of the complete equation. Note that the boundary condition is also satisfied.

The important point is the appearance of the running coupling that determines the asymptotic departures from scaling. The next step is to study the functional form of the running coupling. From (2.46) we see that the rate of change of the running coupling with respect to t is determined by the function β. In turn, $\beta(\alpha)$ is determined by the μ dependence of the renormalized coupling through (2.37). Clearly, there is no dependence of the basic 3-gluon vertex on μ to lowest order (order e). The dependence starts at 1-loop, that is at order e^3 (one extra gluon has to be emitted and reabsorbed). Thus we find that, in perturbation theory,

$$\frac{\partial e}{\partial \log \mu^2} \propto e^3 \ . \tag{2.48}$$

Recalling that $\alpha = e^2/4\pi$, we have

$$\frac{\partial \alpha}{\partial \log \mu^2} \propto 2e \frac{\partial e}{\partial \log \mu^2} \propto e^4 \propto \alpha^2 \ . \tag{2.49}$$

Thus the behaviour of $\beta(\alpha)$ in perturbation theory is

$$\beta(\alpha) = \pm b \alpha^2 (1 + b' \alpha + \cdots) \ . \tag{2.50}$$

Since the sign of the leading term is crucial in the following discussion, we stipulate that $b > 0$ and we make the sign explicit in front.

Let us make the procedure more precise for computing the 1-loop beta function in QCD (or, similarly, in QED). The result of the 1-loop 1PI diagrams for $V_{\rm ren}$ can be written as

$$V_{\rm ren} = e\left(1 + \alpha B_{3g} \log \frac{\mu^2}{-p^2}\right) . \tag{2.51}$$

$V_{\rm ren}$ satisfies the RGE

$$\left[\frac{\partial}{\partial \log \mu^2} + \beta(\alpha)\frac{\partial e}{\partial \alpha}\frac{\partial}{\partial e} - \frac{3}{2}\gamma_g(\alpha)\right] V_{\rm ren} = 0 . \tag{2.52}$$

With respect to (2.36), the beta function term has been rewritten taking into account the fact that $V_{\rm ren}$ starts with e, and the anomalous dimension term arises from a factor $Z_g^{-1/2}$ for each gluon leg. In general, for an n-leg 1PI Green function $V_{n,\rm bare} = Z_g^{-n/2} V_{n,\rm ren}$, if all external legs are gluons. Note that, in the particular case of $V = V_3$ that is used to define e, other Z factors are absorbed in the replacement $Z_{\rm V}^{-1} Z_g^{3/2} e_0 = e$. At 1-loop accuracy, we replace $\beta(\alpha) = -b\alpha^2$ and $\gamma_g(\alpha) = \gamma_g^{(1)}\alpha$. One thus obtains

$$b = 2\left[B_{3g} - \frac{3}{2}\gamma_g^{(1)}\right] . \tag{2.53}$$

Similarly, we can write the diagrammatic expression and the RGE for the 1PI 2-gluon Green function, which is the inverse gluon propagator Π (a scalar function after removing the gauge invariant tensor):

$$\Pi_{\rm ren} = \left(1 + \alpha B_{2g} \log \frac{\mu^2}{-p^2} + \cdots\right) \tag{2.54}$$

and

$$\left[\frac{\partial}{\partial \log \mu^2} + \beta(\alpha)\frac{\partial}{\partial \alpha} - \gamma_g(\alpha)\right] \Pi_{\rm ren} = 0 . \tag{2.55}$$

Notice that the normalization and the phase of Π are specified by the lowest order term being 1. In this case the β function term is negligible, being of order α^2 (because Π is a function of e only through α) and we obtain

$$\gamma_g^{(1)} = B_{2g} . \tag{2.56}$$

Thus, finally,

$$b = 2\left(B_{3g} - \frac{3}{2}B_{2g}\right) . \tag{2.57}$$

By direct calculation at 1-loop level, one finds

$$\text{QED} \qquad \beta(\alpha) \sim +b\alpha^2 + \cdots , \quad b = \sum_i \frac{N_C Q_i^2}{3\pi} , \tag{2.58}$$

where $N_C = 3$ for quarks and $N_C = 1$ for leptons, and the sum runs over all fermions of charge $Q_i e$ that are coupled. One also finds

$$\text{QCD} \qquad \beta(\alpha) \sim -b\alpha^2 + \cdots , \quad b = \frac{11N_C - 2n_f}{12\pi} , \tag{2.59}$$

where, as usual, n_f is the number of coupled (see below) flavours of quarks (we assume here that $n_f \leq 16$, so that $b > 0$ in QCD).

If $\alpha(t)$ is small, we can compute $\beta(\alpha(t))$ in perturbation theory. The sign in front of b then decides the slope of the coupling: $\alpha(t)$ increases with t (or Q^2) if β is positive at small α (QED), or $\alpha(t)$ decreases with t (or Q^2) if β is negative at small α (QCD). A theory like QCD in which the running coupling vanishes asymptotically at large Q^2 is said to be (ultraviolet) "asymptotically free". An important result that has been proven [145] is that, in four spacetime dimensions, all and only non-Abelian gauge theories are asymptotically free.

Going back to (2.43), we replace $\beta(\alpha) \sim \pm b\alpha^2$, do the integral, and perform some simple algebra to find

$$\text{QED} \qquad \alpha(t) \sim \frac{\alpha}{1 - b\alpha t} \tag{2.60}$$

and

$$\text{QCD} \qquad \alpha(t) \sim \frac{\alpha}{1 + b\alpha t} . \tag{2.61}$$

A slightly different form is often used in QCD. Defining $1/\alpha = b \log \mu^2/\Lambda_{\text{QCD}}^2$, we can write

$$\alpha(t) \sim \frac{1}{\frac{1}{\alpha} + bt} = \frac{1}{b \log \frac{\mu^2}{\Lambda_{\text{QCD}}^2} + b \log \frac{Q^2}{\mu^2}} = \frac{1}{b \log \frac{Q^2}{\Lambda_{\text{QCD}}^2}} . \tag{2.62}$$

The parameter μ has been traded for the parameter Λ_{QCD}. We see that $\alpha(t)$ decreases logarithmically with Q^2 and that one can introduce a dimensional parameter Λ_{QCD} that replaces μ. In the following we will often simply write Λ for Λ_{QCD}. Note that it is clear that Λ depends on the particular definition of α, not only on the defining scale μ, but also on the renormalization scheme (see, for example, the discussion in the next section). Through the parameter b, and in general through the function β, it also depends on the number n_f of coupled flavours.

It is very important to note that QED and QCD are theories with "decoupling", i.e., up to the scale Q, only quarks with masses $m \ll Q$ contribute to the running of α. This is clearly very important, given that all applications of perturbative QCD so far apply to energies below the top quark mass m_t. For the validity of the decoupling theorem [60], the theory in which all the heavy particle internal lines are eliminated must still be renormalizable and the coupling constants must not vary with the mass. These requirements are satisfied for the masses of heavy quarks in QED and QCD, but they are not satisfied in the electroweak theory where the elimination of the top would violate $SU(2)$ symmetry (because the t and b left-handed quarks are in a doublet) and the quark couplings to the Higgs multiplet (hence to the longitudinal gauge bosons) are proportional to the mass.

In conclusion, in QED and QCD, quarks with $m \gg Q$ do not contribute to n_f in the coefficients of the relevant β function. The effects of heavy quarks are power suppressed and can be taken into account separately. For example, in e^+e^- annihilation for $2m_c < Q < 2m_b$, the relevant asymptotics is for $n_\mathrm{f} = 4$, while for $2m_b < Q < 2m_t$, it is for $n_\mathrm{f} = 5$. Going across the b threshold, the β function coefficients change, so the slope of $\alpha(t)$ changes. But $\alpha(t)$ is continuous, whence Λ changes so as to keep $\alpha(t)$ constant at the matching point at $Q \sim O(2m_b)$. The effect on Λ is large: approximately $\Lambda_5 \sim 0.65\Lambda_4$, where $\Lambda_{4,5}$ are for $n_\mathrm{f} = 4, 5$.

Note the presence of a pole at $\pm b\alpha t = 1$ in (2.60) and (2.61). This is called the Landau pole, since Landau had already realised its existence in QED in the 1950s. For $\mu \sim m_e$ (in QED), the pole occurs beyond the Planck mass. In QCD, the Landau pole is located for negative t or at $Q < \mu$ in the region of light hadron masses. Clearly the issue of the definition and the behaviour of the physical coupling (which is always finite, when defined in terms of some physical process) in the region around the perturbative Landau pole is a problem that lies outside the scope of perturbative QCD.

The non-leading terms in the asymptotic behaviour of the running coupling can in principle be evaluated by going back to (2.50) and computing b' at 2-loops and so on. But in general the perturbative coefficients of $\beta(\alpha)$ depend on the definition of the renormalized coupling α (the renormalization scheme), so one wonders whether it is worthwhile to do a complicated calculation to get b', if it must then be repeated for a different definition or scheme. In this respect it is interesting to note that both b and b' are actually independent of the definition of α, while higher order coefficients do depend on that. Here is the simple proof. Two different perturbative definitions of α are related by $\alpha' \sim \alpha(1 + c_1\alpha + \cdots)$. Then we have

$$\begin{aligned}\beta(\alpha') = \frac{\mathrm{d}\alpha'}{\mathrm{d}\log\mu^2} &= \frac{\mathrm{d}\alpha}{\mathrm{d}\log\mu^2}(1 + 2c_1\alpha + \cdots) \\ &= \beta(\alpha)(1 + 2c_1\alpha + \ldots) \\ &= \pm b\alpha^2(1 + b'\alpha + \cdots)(1 + 2c_1\alpha + \cdots) \\ &= \pm b\alpha'^2(1 + b'\alpha' + \cdots)\,, \end{aligned} \tag{2.63}$$

which shows that, up to the first subleading order, $\beta(\alpha')$ has the same form as $\beta(\alpha)$.

In QCD ($N_C = 3$), it has been shown that [131]

$$b' = \frac{153 - 19n_f}{2\pi(33 - 2n_f)} . \tag{2.64}$$

By taking b' into account, one can write the expression for the running coupling at next to the leading order (NLO):

$$\alpha(Q^2) = \alpha_{LO}(Q^2)\left[1 - b'\alpha_{LO}(Q^2)\log\log\frac{Q^2}{\Lambda^2} + \cdots\right] , \tag{2.65}$$

where $\alpha_{LO}^{-1} = b\log Q^2/\Lambda^2$ is the LO result (actually at NLO, the definition of Λ is modified according to $b\log\mu^2/\Lambda^2 = 1/\alpha + b'\log b\alpha$).

Summarizing, we started from massless classical QCD which is scale invariant. But we have seen that the procedure of quantization, regularization, and renormalization necessarily breaks scale invariance. In the quantum QCD theory, there is a scale of energy Λ. From experiment, this is of the order of a few hundred MeV, its precise value depending on the definition, as we shall see in detail. Dimensionless quantities depend on the energy scale through the running coupling, which is a logarithmic function of Q^2/Λ^2. In QCD the running coupling decreases logarithmically at large Q^2 (asymptotic freedom), while in QED the coupling has the opposite behaviour.

2.5 More on the Running Coupling

In the last section we introduced the renormalized coupling α in terms of the 3-gluon vertex at $p^2 = -\mu^2$ (momentum subtraction). The Ward identities of QCD then ensure that the coupling defined from other vertices like the $\bar{q}qg$ vertex are renormalized in the same way and the finite radiative corrections are related. But at present the universally adopted definition of α_s is in terms of dimensional regularization [333], because of computational simplicity, which is essential given the great complexity of present day calculations. So we now briefly review the principles of dimensional regularization and the definition of minimal subtraction (MS) [335] and modified minimal subtraction ($\overline{\text{MS}}$) [82]. The $\overline{\text{MS}}$ definition of α_s is the one most commonly adopted in the literature, and values quoted for it normally refer to this definition.

Dimensional regularization (DR) is a gauge and Lorentz invariant regularization that consists in formulating the theory in $D < 4$ spacetime dimensions in order to make loop integrals ultraviolet finite. In DR one rewrites the theory in D dimensions (D is integer at the beginning, but then one realizes that the expression calculated from diagrams makes sense for all D, except for isolated singularities). The metric tensor is extended to a $D \times D$ matrix $g_{\mu\nu} = \text{diag}(1, -1, -1, \ldots, -1)$ and 4-vectors are given by $k^\mu = (k^0, k^1, \ldots, k^{D-1})$. The Dirac γ^μ are $f(D) \times f(D)$ matrices and

the precise form of the function $f(D)$ is not important. It is sufficient to extend the usual algebra in a straightforward way like $\{\gamma_\mu, \gamma_\nu\} = 2g_{\mu,\nu}I$, where I is the D-dimensional identity matrix, $\gamma^\mu\gamma^\nu\gamma_\mu = -(D-2)\gamma^\nu$, or $\mathrm{Tr}(\gamma^\mu\gamma^\nu) = f(D)g_{\mu\nu}$.

The physical dimensions of fields change in D dimensions, and as a consequence the gauge couplings become dimensional $e_D = \mu^\epsilon e$, where e is dimensionless, $D = 4-2\epsilon$, and μ is a mass scale (this is how a scale of mass is introduced in the DR of massless QCD). In fact, the dimension of the fields is determined by requiring the action $S = \int \mathrm{d}^D x \mathscr{L}$ to be dimensionless. By inserting terms like $m\bar{\Psi}\Psi$ or $m^2\phi^\dagger\phi$ or $e\bar{\Psi}\gamma^\mu\Psi A_\mu$ for $\mathscr{L}$, the dimensions of the fields and couplings m, Ψ, ϕ, A_μ, and e are determined as 1, $(D-1)/2$, $(D-2)/2$, $(D-2)/2$, and $(4-D)/2$, respectively. The formal expression of loop integrals can be written for any D. For example,

$$\int \frac{\mathrm{d}^D k}{(2\pi)^D} \frac{1}{(k^2-m^2)^2} = \frac{\Gamma(2-D/2)(-m^2)^{D/2-2}}{(4\pi)^{D/2}} \,. \tag{2.66}$$

For $D = 4-2\epsilon$, one can expand using

$$\Gamma(\epsilon) = \frac{1}{\epsilon} - \gamma_\mathrm{E} + O(\epsilon) \,, \quad \gamma_\mathrm{E} = 0.5772\ldots \,. \tag{2.67}$$

For some Green function G, normalized to 1 in lowest order (like V/e, with V the 3-gluon vertex function at the symmetric point $p^2 = q^2 = r^2$, considered in the previous section), we typically find, at the 1-loop level,

$$G_\mathrm{bare} = 1 + \alpha_0 \left(\frac{-\mu^2}{p^2}\right)^\epsilon \left[B\left(\frac{1}{\epsilon} + \log 4\pi - \gamma_\mathrm{E}\right) + A + O(\epsilon)\right] \,. \tag{2.68}$$

In $\overline{\mathrm{MS}}$, one rewrites this as (diagram by diagram, a virtue of the method)

$$\begin{aligned} G_\mathrm{bare} &= Z G_\mathrm{ren} \,, \\ Z &= 1 + \alpha\left[B\left(\frac{1}{\epsilon} + \log 4\pi - \gamma_\mathrm{E}\right)\right] \,, \\ G_\mathrm{ren} &= 1 + \alpha\left(B \log\frac{-\mu^2}{p^2} + A\right) \,. \end{aligned} \tag{2.69}$$

Here Z stands for the relevant product of renormalization factors. In the original MS prescription, only $1/\epsilon$ was subtracted (and this clearly plays the role of a cutoff), while $\log 4\pi$ and γ_E were not. Later, since these constants always appear in the expansion of Γ functions, it was decided to modify MS into $\overline{\mathrm{MS}}$. Note that the $\overline{\mathrm{MS}}$ definition of α is different than that in the momentum subtraction scheme, because the finite terms (those beyond logs) are different. In particular, the order α correction to G_ren does not vanish at $p^2 = -\mu^2$.

The third [337] and fourth [357] coefficients of the QCD β function are also known in the $\overline{\text{MS}}$ prescription (recall that only the first two coefficients are scheme-independent). The calculation of the last term involved the evaluation of some 50,000 four-loop diagrams. Translated in numbers, for $n_\text{f} = 5$, one obtains

$$\beta(\alpha) = -0.610\alpha^2\left[1 + 1.261\ldots\frac{\alpha}{\pi} + 1.475\ldots\left(\frac{\alpha}{\pi}\right)^2 + 9.836\ldots\left(\frac{\alpha}{\pi}\right)^3 + \cdots\right]. \tag{2.70}$$

It is interesting to remark that the expansion coefficients are of order 1 or 10 (only for the last one), so that the $\overline{\text{MS}}$ expansion looks reasonably well behaved.

2.6 On the Non-convergence of Perturbative Expansions

It is important to keep in mind that, after renormalization, all the coefficients in the QED and QCD perturbative series are finite, but the expansion does not converge. Actually, the perturbative series is not even Borel summable (for reviews see, for example, [31]). After the Borel resummation, for a given process, one is left with a result that is ambiguous up to terms typically going as $\exp(-n/b\alpha)$, where n is an integer and b the absolute value of the first β function coefficient. In QED, these corrective terms are extremely small and not very important in practice. However, in QCD, $\alpha = \alpha_\text{s}(Q^2) \sim 1/b\log(Q^2/\Lambda^2)$ and the ambiguous terms are of order $(1/Q^2)^n$, that is, they are power suppressed. It is interesting that, through this mechanism, the perturbative version of the theory is somehow able to take into account the power-suppressed corrections. A sequence of diagrams with factorial growth at large order n is constructed by dressing gluon propagators by any number of quark bubbles together with their gauge completions (renormalons). The problem of the precise relation between the ambiguities of the perturbative expansion and the power-suppressed corrections has been discussed in recent years, also for processes without light cone operator expansion [31, 324].

2.7 e^+e^- Annihilation and Related Processes

2.7.1 $R_{e^+e^-}$

The simplest hard process is

$$R = R_{e^+e^-} = \frac{\sigma(e^+e^- \to \text{hadrons})}{\sigma_\text{point}(e^+e^- \to \mu^+\mu^-)},$$

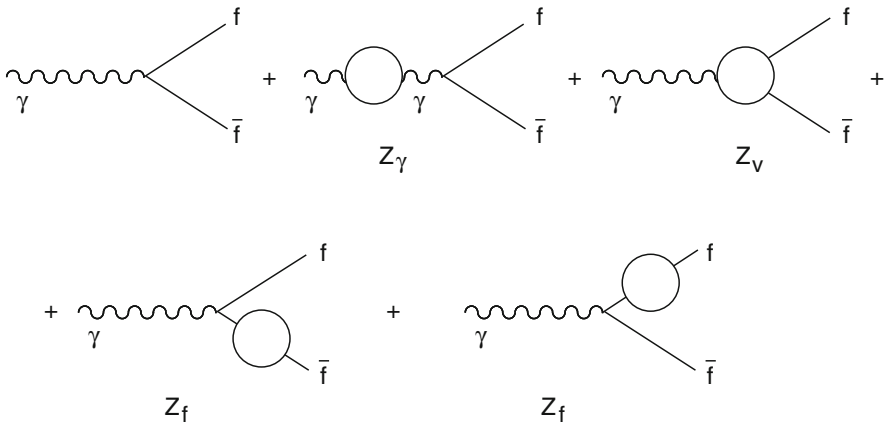

Fig. 2.12 Diagrams for charge renormalization in QED at 1-loop (the blob in each diagram represents the loop)

which we have already introduced. R is dimensionless and is given in perturbation theory by[1] $R = N_C \sum_i Q_i^2 F(t, \alpha_s)$, where $F = 1 + O(\alpha_s)$. We have already mentioned that for this process the "anomalous dimension" function vanishes, i.e., $\gamma(\alpha_s) = 0$, because of electric charge non-renormalization by strong interactions. Let us recall how this happens in detail.

The diagrams that are relevant for charge renormalization in QED at 1-loop are shown in Fig. 2.12. The Ward identity that follows from gauge invariance in QED requires the vertex (Z_V) and the self-energy (Z_f) renormalization factors to cancel, and the only divergence remains in Z_γ, the vacuum polarization of the photon. Hence, the charge is only renormalized by the photon vacuum polarization blob, and it is thus universal (the same factor for all fermions, independent of their charge) and not affected by QCD at 1-loop. It is true that at higher orders the photon vacuum polarization diagram is affected by QCD (for example, at 2-loops we can exchange a gluon between the quarks in the loop), but the renormalization induced by the divergent logs from the vacuum polarization diagram remain independent of the nature of the fermion to which the photon line is attached. The gluon contributions to the vertex (Z_V) and to the self-energy (Z_f) cancel, because they have exactly the same structure as in QED, and there is no gluon contribution to the photon blob at 1-loop, so that $\gamma(\alpha_s) = 0$.

At the 1-loop level, the diagrams relevant for the computation of R are shown in Fig. 2.13. There are virtual diagrams and also real diagrams with one additional gluon in the final state. Infrared divergences cancel between the interference term of the virtual diagrams and the absolute square of the real diagrams, according to the

[1] Actually, starting from order α_s^2, there are some "singlet" terms proportional to $(\sum_i Q_i)^2$. These small terms are included in F by dividing and multiplying by $\sum_i Q_i^2$.

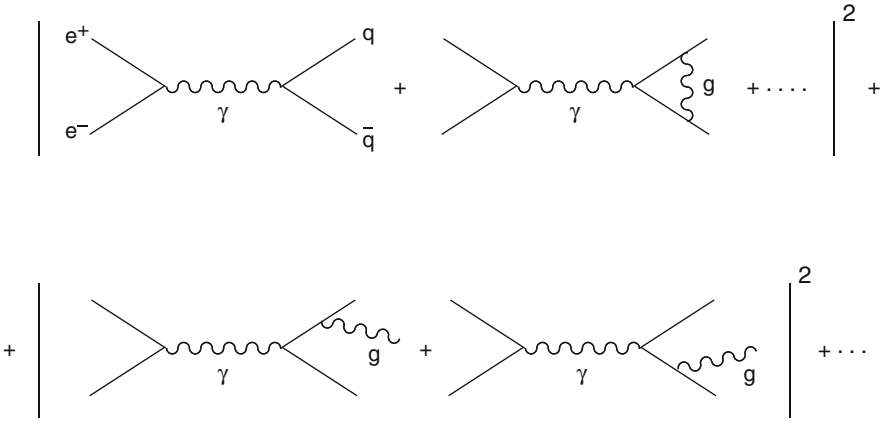

Fig. 2.13 Real and virtual diagrams relevant for the computation of R at 1-loop accuracy (the initial e^+e^- has been omitted to make the drawing simpler)

Bloch–Nordsieck theorem. Similarly, there are no mass singularities, in agreement with the Kinoshita–Lee–Nauenberg theorem, because the initial state is purely leptonic and all degenerate states that can appear at the given order are included in the final state. Given that $\gamma(\alpha_s) = 0$, the RGE prediction is simply given, as we have already seen, by $F(t, \alpha_s) = F[0, \alpha_s(t)]$. This means that, if we do, for example, a 2-loop calculation, we must obtain a result of the form

$$F(t, \alpha_s) = 1 + c_1\alpha_s(1 - b\alpha_s t) + c_2\alpha_s^2 + O(\alpha_s^3) \,. \tag{2.71}$$

In fact, taking into account the expression for the running coupling in (2.61), viz.,

$$\alpha_s(t) \sim \frac{\alpha_s}{1 + b\alpha_s t} \sim \alpha_s(1 - b\alpha_s t + \cdots) \,, \tag{2.72}$$

Eq. (2.71) can be rewritten as

$$F(t, \alpha_s) = 1 + c_1\alpha_s(t) + c_2\alpha_s^2(t) + O(\alpha_s^3(t)) = F[0, \alpha_s(t)] \,. \tag{2.73}$$

The content of the RGE prediction is, at this order, that there are no $\alpha_s t$ and $(\alpha_s t)^2$ terms (the leading log sequence must be absent), and the term of order $\alpha_s^2 t$ has the appropriate coefficient to be reabsorbed in the transformation of α_s into $\alpha_s(t)$.

At present the first four coefficients $c_1, \ldots, c_4$ have been computed in the $\overline{\text{MS}}$ scheme. The references are as follows: for c_2 [138], for c_3 [230], and for c_4 [74]. Clearly, $c_1 = 1/\pi$ does not depend on the definition of α_s, but the c_n with $n \geq 2$ do. The subleading coefficients also depend on the scale choice: if instead of expanding in $\alpha_s(Q)$, we decide to choose $\alpha_s(Q/2)$, the coefficients c_n $n \geq 2$ will change. In the $\overline{\text{MS}}$ scheme, for γ exchange and $n_f = 5$, which are good approximations for

$2m_b \ll Q \ll m_Z$, one has

$$F[0,\alpha_s(t)] = 1 + \frac{\alpha_s(t)}{\pi} + 1.409\ldots\left[\frac{\alpha_s(t)}{\pi}\right]^2 - 12.8\ldots\left[\frac{\alpha_s(t)}{\pi}\right]^3 - 80.0\ldots\left[\frac{\alpha_s(t)}{\pi}\right]^4 + \cdots . \tag{2.74}$$

Similar perturbative results at 3-loop accuracy also exist for

$$R_Z = \frac{\Gamma(Z \to \text{hadrons})}{\Gamma(Z \to \text{leptons})} , \qquad R_\tau = \frac{\Gamma(\tau \to \nu_\tau + \text{hadrons})}{\Gamma(\tau \to \nu_\tau + \text{leptons})} ,$$

and so on. We will discuss these results in Sect. 2.10, where we deal with measurements of α_s.

The perturbative expansion in powers of $\alpha_s(t)$ takes into account all contributions that are suppressed by powers of logarithms of the large scale Q^2 ("leading twist" terms). In addition, there are corrections suppressed by powers of the large scale Q^2 ("higher twist" terms). The pattern of power corrections is controlled by the light-cone operator product expansion (OPE) [112, 365], which leads (schematically) to

$$F = \text{pert.} + r_2\frac{m^2}{Q^2} + r_4\frac{\langle 0|\text{Tr}[\mathbf{F_{\mu\nu}F^{\mu\nu}}]|0\rangle}{Q^4} + \cdots + r_6\frac{\langle 0|O_6|0\rangle}{Q^6} + \cdots . \tag{2.75}$$

Here m^2 generically indicates mass corrections, for example from b quarks, beyond the b threshold, while top quark mass corrections only arise from loops, vanish in the limit $m_t \to \infty$, and are included in the coefficients like those in (2.74) and the analogous ones for higher twist terms; $\mathbf{F_{\mu\nu}} = \sum_A F^A_{\mu\nu} t^A$, O_6 is typically a 4-fermion operator, etc. For each possible gauge invariant operator, the corresponding negative power of Q^2 is fixed by dimensions.

We now consider the light-cone OPE in more detail. $R_{e^+e^-} \sim \Pi(Q^2)$, where $\Pi(Q^2)$ is the scalar spectral function related to the hadronic contribution to the imaginary part of the photon vacuum polarization $T_{\mu\nu}$:

$$T_{\mu\nu} = (-g_{\mu\nu}Q^2 + q_\mu q_\nu)\Pi(Q^2) = \int \mathrm{d}^4x \exp \mathrm{i}(q\cdot x)\langle 0|J^\dagger_\mu(x)J_\nu(0)|0\rangle$$
$$= \sum_n \langle 0|J^\dagger_\mu(0)|n\rangle\langle n|J_\nu(0)|0\rangle(2\pi)^4\delta^4(q-p_n) . \tag{2.76}$$

For $Q^2 \to \infty$, the $x^2 \to 0$ region is dominant. The light cone OPE is valid to all orders in perturbation theory. Schematically and dropping Lorentz indices for simplicity, near $x^2 \sim 0$, we have

$$J^\dagger(x)J(0) = I(x^2) + E(x^2)\sum_{n=0}^{\infty} c_n(x^2)x^{\mu_1}\ldots x^{\mu_n}\,O^n_{\mu_1\ldots\mu_n}(0) + \text{less sing. terms} . \tag{2.77}$$

Here $I(x^2)$, $E(x^2)$, ..., $c_n(x^2)$ are c-number singular functions and O^n is a string of local operators. $E(x^2)$ is the singularity of free field theory, while $I(x^2)$ and $c_n(x^2)$ in the interacting theory contain powers of $\log(\mu^2 x^2)$. Some O^n are already present in free field theory, while others appear when interactions are switched on. Given that $\Pi(Q^2)$ is related to the Fourier transform of the vacuum expectation value of the product of currents, less singular terms in x^2 lead to power-suppressed terms in $1/Q^2$. The perturbative terms, like those in (2.73), come from $I(x^2)$, which is the leading twist term, and the dominant logarithmic scaling violations induced by the running coupling are the logs in $I(x^2)$.

2.7.2 The Final State in e^+e^- Annihilation

Experiments on e^+e^- annihilation at high energy provide a remarkable opportunity for systematically testing the distinct signatures predicted by QCD for the structure of the final state averaged over a large number of events. Typical of asymptotic freedom is the hierarchy of configurations emerging as a consequence of the smallness of $\alpha_s(Q^2)$. When all corrections of order $\alpha_s(Q^2)$ are neglected, one recovers the naive parton model prediction for the final state: almost collinear events with two back-to-back jets with limited transverse momentum and an angular distribution $1 + \cos^2\theta$ with respect to the beam axis (typical of spin 1/2 parton quarks, while scalar quarks would lead to a $\sin^2\theta$ distribution). To order $\alpha_s(Q^2)$, a tail of events is predicted to appear with large transverse momentum $p_T \sim Q/2$ with respect to a suitably defined jet axis (for example, the thrust axis, see below). This small fraction of events with large p_T consists mainly of three-jet events with almost planar topology. The skeleton of a three-jet event, to leading order in $\alpha_s(Q^2)$, is formed by three hard partons $q\bar{q}g$, the third being a gluon emitted by a quark or antiquark line. To order $\alpha_s^2(Q^2)$, a hard perturbative non-planar component starts to build up, and a small fraction of four-jet events $q\bar{q}gg$ or $q\bar{q}q\bar{q}$ appear, and so on.

Event shape variables defined from the set of 4-momenta of final state particles are introduced to describe the topological structure of the final state energy flow in a quantitative manner [154]. The best known event shape variable is thrust (T) [192], defined as

$$T = \max \frac{\sum_i |\mathbf{p_i} \cdot \mathbf{n_T}|}{\sum_i |\mathbf{p_i}|} , \tag{2.78}$$

where the maximization is in terms of the axis defined by the unit vector n_T: the thrust axis is the axis that maximizes the sum of the absolute values of the longitudinal momenta of the final state particles. The thrust T varies between 1/2, for a spherical event, to 1 for a collinear (2-jet) event. Event shape variables are important for QCD tests and measurements of α_s, and also for more practical purposes, like a laboratory for assessing the reliability of event simulation programmes and a tool for the separation of signals and background.

A quantitatively specified definition of jets and of the number of jets in one event (jet counting) must be introduced for precise QCD tests and measurement of α_s, which must be infrared safe (i.e., not altered by soft particle emission or collinear splittings of massless particles) in order to be computable at the parton level and as insensitive as possible to the transformation of partons into hadrons (see, for example, [294]). For e^+e^- physics, one can use a jet algorithm based on a resolution parameter $y_{\rm cut}$ and a suitable pair variable. For example [172],

$$y_{ij} = \frac{2\min(E_i^2, E_j^2)(1-\cos\theta_{ij})}{s} \,. \tag{2.79}$$

Note that $1-\cos\theta_{ij} \sim \theta_{ij}^2/2$, so that the relative transverse momentum $k_{\rm T}^2$ is involved (hence, the name $k_{\rm T}$ algorithm). The particles i,j belong to different jets for $y_{ij} > y_{\rm cut}$. Clearly, the number of jets becomes a function of $y_{\rm cut}$, and in fact there are more jets for smaller $y_{\rm cut}$.

Recently, motivated by the LHC experiments, there has been a flurry of improved jet algorithm studies: it is essential that correct jet finding should be implemented by LHC experiments for optimal matching of theory and experiment [185, 317]. In particular, existing sequential recombination algorithms like $k_{\rm T}$ [132, 172] and Cambridge/Aachen [174] have been generalized. In these recursive definitions, one introduces distances d_{ij} between particles or clusters of particles i and j, and d_{iB} between i and the beam (B). The inclusive clustering proceeds by identifying the smallest of the distances and, if it is a d_{ij}, by recombining particles i and j, while if it is d_{iB}, calling i a jet and removing it from the list. The distances are recalculated and the procedure repeated until no i and j are left.

The extension relative to the $k_{\rm T}$ [132] and Cambridge/Aachen [174] algorithms lies in the definition of the distance measures:

$$d_{ij} = \min(k_{Ti}^{2p}, k_{Tj}^{2p})\frac{\Delta_{ij}^2}{R^2} \,, \tag{2.80}$$

where $\Delta_{ij}^2 = (y_i - y_j)^2 + (\phi_i - \phi_j)^2$ and k_{Ti}, y_i, and ϕ_i are the transverse momentum, rapidity, and azimuth of particle i, respectively. R is the radius of the jet, i.e., the radius of a cone which, by definition, contains the jet. The exponent p fixes the relative power of the energy versus geometrical (Δ_{ij}) scales.

For $p = 1$, one has the inclusive k_T algorithm. It can be shown in general that for $p \geq 0$ the behaviour of the jet algorithm with respect to soft radiation is rather similar to that observed for the k_T algorithm. The case $p = 0$ is special, and it corresponds to the inclusive Cambridge/Aachen algorithm [174]. Surprisingly (at first sight), taking p to be negative also yields an algorithm that is infrared and collinear safe and has sensible phenomenological behaviour. For $p = -1$, one obtains the recently introduced "anti-k_T" jet-clustering algorithm [126], which has particularly stable jet boundaries with respect to soft radiation and is suitable for practical use in experiments.

2.8 Deep Inelastic Scattering

Deep inelastic scattering (DIS) processes have played, and still play, a very important role in our understanding of QCD and of nucleon structure. This set of processes actually provides us with a rich laboratory for theory and experiment. There are several structure functions $F_i(x, Q^2)$ that can be studied, each a function of two variables. This is true separately for different beams and targets and different polarizations. Depending on the charges of ℓ and ℓ' [see (2.28)], we can have neutral currents (γ, Z) or charged currents in the ℓ–ℓ' channel (Fig. 2.10). In the past, DIS processes were crucial for establishing QCD as the theory of strong interactions and quarks and gluons as the QCD partons.

At present DIS remains very important for quantitative studies and tests of QCD. The theory of scaling violations for totally inclusive DIS structure functions, based on operator expansion or diagrammatic techniques and renormalization group methods, is crystal clear and the predicted Q^2 dependence can be tested at each value of x. The measurement of quark and gluon densities in the nucleon, as functions of x at some reference value of Q^2, which is an essential starting point for the calculation of all relevant hadronic hard processes, is performed in DIS processes. At the same time one measures $\alpha_s(Q^2)$, and the DIS values of the running coupling can be compared with those obtained from other processes. At all times new theoretical challenges arise from the study of DIS processes. Recent examples (see the following) are the so-called "spin crisis" in polarized DIS and the behaviour of singlet structure functions at small x, as revealed by HERA data. In the following we review the past successes and the present open problems in the physics of DIS.

The cross-section $\sigma \sim L^{\mu\nu} W_{\mu\nu}$ is given in terms of the product of a leptonic ($L^{\mu\nu}$) and a hadronic ($W_{\mu\nu}$) tensor. While $L^{\mu\nu}$ is simple and easily obtained from the lowest order electroweak (EW) vertex plus QED radiative corrections, the complicated strong interaction dynamics is contained in $W_{\mu\nu}$. The latter is proportional to the Fourier transform of the forward matrix element between the nucleon target states of the product of two EW currents:

$$W_{\mu\nu} = \int \mathrm{d}^4 y \, \exp \mathrm{i}(q \cdot y) \langle p | J_\mu^\dagger(y) J_\nu(0) | p \rangle \, . \tag{2.81}$$

Structure functions are defined starting from the general form of $W_{\mu\nu}$, given Lorentz invariance and current conservation. For example, for EW currents between unpolarized nucleons, we have

$$W_{\mu\nu} = \left(-g_{\mu\nu} + \frac{q_\mu q_\nu}{q^2} \right) W_1(\nu, Q^2) + \left(p_\mu - \frac{m\nu}{q^2} q_\mu \right) \left(p_\nu - \frac{m\nu}{q^2} q_\nu \right) \frac{W_2(\nu, Q^2)}{m^2}$$
$$- \frac{\mathrm{i}}{2m^2} \epsilon_{\mu\nu\lambda\rho} p^\lambda q^\rho W_3(\nu, Q^2) \, .$$

where variables are defined as in (2.28) and (2.29), and W_3 arises from VA interference and is absent for pure vector currents. In the limit $Q^2 \gg m^2$, with the Bjorken variable x fixed, the structure functions obey approximate Bjorken scaling, which is in fact broken by logarithmic corrections that can be computed in QCD:

$$mW_1(\nu, Q^2) \to F_1(x) \,, \qquad \nu W_{2,3}(\nu, Q^2) \to F_{2,3}(x) \,. \tag{2.82}$$

The γ–N cross-section is given by

$$\frac{\mathrm{d}\sigma^{\gamma}}{\mathrm{d}Q^2\mathrm{d}\nu} = \frac{4\pi\alpha^2 E'}{Q^4 E}\left(2\sin^2\frac{\theta}{2}W_1 + \cos^2\frac{\theta}{2}W_2\right) \,, \tag{2.83}$$

with $W_i = W_i(Q^2, \nu)$, while for the ν–N or $\bar{\nu}$–N cross-section one has

$$\frac{\mathrm{d}\sigma^{\nu,\bar{\nu}}}{\mathrm{d}Q^2\mathrm{d}\nu} = \frac{G_F^2 E'}{2\pi E}\left(\frac{m_W^2}{Q^2 + m_W^2}\right)^2\left(2\sin^2\frac{\theta}{2}W_1 + \cos^2\frac{\theta}{2}W_2 \pm \frac{E+E'}{m}\sin^2\frac{\theta}{2}W_3\right) \,, \tag{2.84}$$

with W_i for photons, and ν and $\bar{\nu}$ are all different, as we shall see in a moment.

In the scaling limit the longitudinal and transverse cross-sections are given by

$$\sigma_{\mathrm{L}} \sim \frac{1}{s}\left[\frac{F_2(x)}{2x} - F_1(x)\right] \,, \quad \sigma_{\mathrm{RH,LH}} \sim \frac{1}{s}\big[F_1(x) \pm F_3(x)\big] \,, \quad \sigma_{\mathrm{T}} = \sigma_{\mathrm{RH}} + \sigma_{\mathrm{LH}} \,, \tag{2.85}$$

where L, RH, LH refer to the helicity 0, 1, -1, respectively, of the exchanged gauge vector boson. For the photon case, $F_3 = 0$ and $\sigma_{\mathrm{RH}} = \sigma_{\mathrm{LH}}$.

In the 1960s the demise of hadrons from the status of fundamental particles to that of bound states of constituent quarks was the breakthrough that made possible the construction of a renormalizable field theory for strong interactions. The presence of an unlimited number of hadrons species, many of them with high spin values, presented an obvious dead-end for a manageable field theory. The evidence for constituent quarks emerged clearly from the systematics of hadron spectroscopy. The complications of the hadron spectrum could be explained in terms of the quantum numbers of spin 1/2, fractionally charged u, d, and s quarks. The notion of colour was introduced to reconcile the observed spectrum with Fermi statistics.

However, confinement, which forbids the observation of free quarks, was a clear obstacle towards the acceptance of quarks as real constituents and not just as fictitious entities describing some mathematical pattern (a doubt expressed even by Gell-Mann at the time). The early measurements of DIS at SLAC dissipated all doubts: the observation of Bjorken scaling and the success of Feynman's "naive" (not so much after all) parton model imposed quarks as the basic fields for describing the nucleon structure (parton quarks).

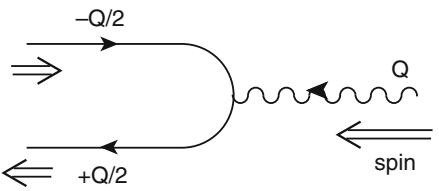

Fig. 2.14 Schematic diagram for the interaction of the virtual photon with a parton quark in the Breit frame

In the language of Bjorken and Feynman, the virtual γ (or, in general, any gauge boson) sees the quark partons inside the nucleon target as quasi-free, because their (Lorentz dilated) QCD interaction time is much longer than $\tau_\gamma \sim 1/Q$, the duration of the virtual photon interaction. Since the virtual photon 4-momentum is spacelike, we can go to a Lorentz frame where $E_\gamma = 0$ (Breit frame). In this frame $q = (E_\gamma = 0, 0, 0, Q)$ and the nucleon momentum, neglecting the mass $m \ll Q$, is $p = (Q/2x, 0, 0, -Q/2x)$. We note that this gives $q^2 = -Q^2$ and $x = Q^2/2(p \cdot q)$, as it should.

Consider the interaction of the photon with a quark (see Fig. 2.14) carrying a fraction y of the nucleon 4-momentum: $p_q = yp$ (we are neglecting the transverse components of p_q which are of order m). The incoming parton with $p_q = yp$ absorbs the photon and the final parton has 4-momentum p'_q. Since in the Breit frame the photon carries no energy, but only a longitudinal momentum Q, the photon can only be absorbed by those partons with $y = x$. Then the longitudinal component of $p_q = yp$ is $-yQ/2x = -Q/2$, and can be flipped into $+Q/2$ by the photon. As a result, the photon longitudinal momentum $+Q$ disappears, the parton quark momentum changes sign from $-Q/2$ to $+Q/2$ and the energy is not changed. So the structure functions are proportional to the density of partons with fraction x of the nucleon momentum, weighted by the squared charge.

Furthermore, recall that the helicity of a massless quark is conserved in a vector (or axial vector) interaction (see Sect. 1.5). So when the momentum is reversed, the spin must also flip. Since the process is collinear there is no orbital contribution, and only a photon with helicity ± 1 (transverse photon) can be absorbed. Alternatively, if partons were spin zero, only longitudinal photons would then contribute.

Using these results, which are maintained in QCD at leading order, the quantum numbers of the quarks were confirmed by early experiments. The observation that $R = \sigma_{\rm L}/\sigma_{\rm T} \to 0$ implies that the charged partons have spin 1/2. The quark charges were derived from the data on the electron and neutrino structure functions:

$$\begin{aligned} F_{ep} &= \frac{4}{9}u(x) + \frac{1}{9}d(x) + \cdots , \qquad & F_{en} &= \frac{4}{9}d(x) + \frac{1}{9}u(x) + \cdots , \\ F_{\nu p} &= F_{\bar{\nu} n} = 2d(x) + \cdots , \qquad & F_{\nu n} &= F_{\bar{\nu} p} = 2u(x) + \cdots , \end{aligned} \tag{2.86}$$

where $F \sim 2F_1 \sim F_2/x$ and $u(x)$, $d(x)$ are the parton number densities in the proton (with fraction x of the proton longitudinal momentum), which, in the scaling limit, do not depend on Q^2. The normalization of the structure functions and the parton densities are such that the charge relations hold:

$$\int_0^1 \big[u(x) - \bar{u}(x)\big]\mathrm{d}x = 2\ , \quad \int_0^1 \big[d(x) - \bar{d}(x)\big]\mathrm{d}x = 1\ , \quad \int_0^1 \big[s(x) - \bar{s}(x)\big]\mathrm{d}x = 0\ . \tag{2.87}$$

Furthermore, it was proven by experiment that, at values of Q^2 of a few GeV^2, in the scaling region, about half of the nucleon momentum, given by the momentum sum rule

$$\int_0^1 \Big[\sum_i \big[q_i(x) + \bar{q}_i(x)\big] + g(x)\Big]x\mathrm{d}x = 1\ , \tag{2.88}$$

is carried by neutral partons (gluons).

In QCD there are calculable log scaling violations induced by $\alpha_\mathrm{s}(t)$. The parton rules in (2.86) can be summarized in the schematic formula

$$F(x,t) = \int_x^1 \mathrm{d}y \frac{q_0(y)}{y} \sigma_\mathrm{point}\big(x/y, \alpha_\mathrm{s}(t)\big) + O(1/Q^2)\ . \tag{2.89}$$

Before QCD corrections $\sigma_\mathrm{point} = e^2\delta(x/y - 1)$ and $F = e^2 q_0(x)$ (here e denotes the charge of the quark in units of the positron charge, i.e., $e = 2/3$ for the u quark). QCD modifies σ_point at order α_s via the diagrams of Fig. 2.15. From a direct computation of the diagrams, one obtains a result of the following form:

$$\sigma_\mathrm{point}\big(z, \alpha_\mathrm{s}(t)\big) \simeq e^2\left[\delta(z-1) + \frac{\alpha_\mathrm{s}}{2\pi}\big[tP(z) + f(z)\big]\right]\ . \tag{2.90}$$

Note that the y integral in (2.89) is from x to 1, because the energy can only be lost by radiation before interacting with the photon (which eventually wants to find a fraction x, as we have explained). For $y > x$ the correction arises from diagrams with real gluon emission. Only the sum of the two real-gluon diagrams in Fig. 2.15 is gauge invariant, so the contribution of one given diagram will be gauge dependent. But in an axial gauge, which for this reason is sometimes also called the

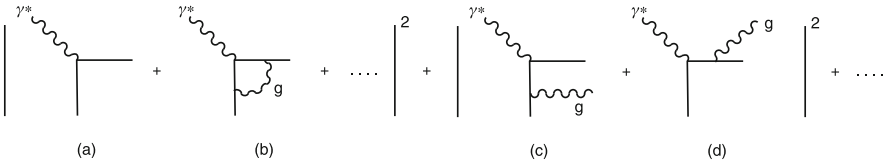

Fig. 2.15 First order QCD corrections to the virtual photon–quark cross-section. (**a**) Tree level, (**b**) vertex correction, (**c**) final-state radiation of one leg, (**d**) final-state radiation off the other leg

"physical gauge", the diagram of Fig. 2.15c, among real diagrams, gives the whole t-proportional term at $0 < x < 1$. It is obviously not essential to go to this gauge, but this diagram has a direct physical interpretation: a quark in the proton has a fraction $y > x$ of the parent 4-momentum; it then radiates a gluon and loses energy down to a fraction x, before interacting with the photon. The log arises from the virtual quark propagator, according to the discussion of collinear mass singularities in (2.27). In fact, in the massless limit, one has (k and h are the 4-momenta of the initial quark and the emitted gluon, respectively):

$$\begin{aligned} \text{propagator} &= \frac{1}{r^2} = \frac{1}{(k-h)^2} = \frac{-1}{2E_k E_h} \frac{1}{1-\cos\theta} \\ &= \frac{-1}{4E_k E_h} \frac{1}{\sin^2\theta/2} \propto \frac{-1}{p_{\mathrm{T}}^2} , \end{aligned} \tag{2.91}$$

where p_{T} is the transverse momentum of the virtual quark. So the square of the propagator goes like $1/p_{\mathrm{T}}^4$. But there is a p_{T}^2 factor in the numerator, because in the collinear limit, when $\theta = 0$ and the initial and final quarks and the emitted gluon are all aligned, the quark helicity cannot flip (vector interaction), so that the gluon should carry zero helicity, while a real gluon can only have ± 1 helicity. Thus the numerator vanishes as p_{T}^2 in the forward direction and the cross-section behaves as

$$\sigma \sim \int^{Q^2} \frac{1}{p_{\mathrm{T}}^2} \mathrm{d}p_{\mathrm{T}}^2 \sim \log Q^2 . \tag{2.92}$$

Actually, the log should be read as $\log Q^2/m^2$, because in the massless limit a genuine mass singularity appears. In fact, the mass singularity connected with the initial quark line is not cancelled, because we do not have the sum of all degenerate initial states [265], but only a single quark. But in correspondence with the initial quark, we have the (bare) quark density $q_0(y)$ which appears in the convolution integral. This is a non-perturbative quantity determined by the nucleon wave function. So we can factorize the mass singularity in a redefinition of the quark density: we replace $q_0(y) \to q(y,t) = q_0(y) + \Delta q(y,t)$ with

$$\Delta q(x,t) = \frac{\alpha_{\mathrm{s}}}{2\pi} t \int_x^1 \mathrm{d}y \frac{q_0(y)}{y} P(x/y) . \tag{2.93}$$

Here the factor of t is a bit symbolic: it stands for $\log Q^2/m^2$, but what exactly we put under Q^2 depends on the definition of the renormalized quark density, which also fixes the exact form of the finite term $f(z)$ in (2.90).

The effective parton density $q(y,t)$ that we have defined is now scale dependent. In terms of this scale dependent density, we have the following relations, where we have also replaced the fixed coupling with the running coupling according to the

prescription derived from the RGE:

$$F(x,t) = \int_x^1 \mathrm{d}y \frac{q(y,t)}{y} e^2 \left[\delta\left(\frac{x}{y}-1\right) + \frac{\alpha_\mathrm{s}(t)}{2\pi} f\left(\frac{x}{y}\right)\right] = e^2 q(x,t) + O\big(\alpha_\mathrm{s}(t)\big),$$
$$\frac{\mathrm{d}}{\mathrm{d}t} q(x,t) = \frac{\alpha_\mathrm{s}(t)}{2\pi} \int_x^1 \mathrm{d}y \frac{q(y,t)}{y} P\left(\frac{x}{y}\right) + O\big(\alpha_\mathrm{s}(t)^2\big). \tag{2.94}$$

We see that at lowest order we reproduce the naive parton model formulae for the structure functions in terms of effective parton densities that are scale dependent. The evolution equations for the parton densities are written down in terms of kernels (the "splitting functions" [40]), which can be expanded in powers of the running coupling. At leading order, we can interpret the evolution equation by saying that the variation of the quark density at x is given by the convolution of the quark density at y and the probability of emitting a gluon with fraction x/y of the quark momentum.

It is interesting that the integro-differential QCD evolution equation for densities can be transformed into an infinite set of ordinary differential equations for Mellin moments [234]. The Mellin moment f_n of a density $f(x)$ is defined by

$$f_n = \int_0^1 \mathrm{d}x\, x^{n-1} f(x)\ . \tag{2.95}$$

By taking moments of both sides of the second equation in (2.94), and changing the order of integration, one finds the simpler equation for the n th moment:

$$\frac{\mathrm{d}}{\mathrm{d}t} q_n(t) = \frac{\alpha_\mathrm{s}(t)}{2\pi} P_n q_n(t)\ . \tag{2.96}$$

To solve this equation we observe that it is equivalent to

$$\log \frac{q_n(t)}{q_n(0)} = \frac{P_n}{2\pi} \int_0^t \alpha_\mathrm{s}(t)\mathrm{d}t = \frac{P_n}{2\pi} \int_{\alpha_\mathrm{s}}^{\alpha_\mathrm{s}(t)} \frac{\mathrm{d}\alpha'}{-b\alpha'}\ . \tag{2.97}$$

To see the equivalence just take the t derivative of both sides. Here we used (2.46) to change the integration variable from $\mathrm{d}t$ to $\mathrm{d}\alpha(t)$ (denoted $\mathrm{d}\alpha'$) and

$$\beta(\alpha) \simeq -b\alpha^2 + \cdots\ .$$

Finally, the solution is

$$q_n(t) = \left[\frac{\alpha_\mathrm{s}}{\alpha_\mathrm{s}(t)}\right]^{P_n/2\pi b} q_n(0)\ . \tag{2.98}$$

The connection between these results and the RGE general formalism occurs via the light cone OPE [recall (2.81) for $W_{\mu\nu}$ and (2.77) for the OPE of two currents]. In the case of DIS, the c-number term $I(x^2)$ does not contribute, because we are interested in the connected part of the matrix element $\langle p|\ldots|p\rangle - \langle 0|\ldots|0\rangle$. The relevant terms are

$$J^\dagger(x)J(0) = E(x^2)\sum_{n=0}^{\infty} c_n(x^2)x^{\mu_1}\ldots x^{\mu_n}O^n_{\mu_1\ldots\mu_n}(0) + \text{less singular terms}\,. \tag{2.99}$$

A formally intricate but conceptually simple argument based on the analyticity properties of the forward virtual Compton amplitude shows that the Mellin moments M_n of structure functions are related to the individual terms in the OPE, in fact, precisely to the Fourier transform $c_n(Q^2)$, which we will write as $c_n(t,\alpha)$, of the coefficient $c_n(x^2)$ times a reduced matrix element h_n from the operators O^n: $\langle p|O^n_{\mu_1\ldots\mu_n}(0)|p\rangle = h_n p_{\mu_1}\ldots p_{\mu_n}$:

$$c_n\langle p|O^n|p\rangle \longrightarrow M_n = \int_0^1 \mathrm{d}x\, x^{n-1}F(x)\,. \tag{2.100}$$

Since the matrix element of the products of currents satisfy the RGE, so do the moments M_n. Hence, the general form of the Q^2 dependence is given by the RGE solution [see (2.47)]:

$$M_n(t,\alpha) = c_n[0,\alpha(t)]\exp\int_\alpha^{\alpha(t)}\frac{\gamma_n(\alpha')}{\beta(\alpha')}\mathrm{d}\alpha' h_n(\alpha)\,. \tag{2.101}$$

At lowest order, in the simplest case, identifying M_n with q_n, we have

$$\gamma_n(\alpha) = \frac{P_n}{2\pi}\alpha + \cdots\,, \quad \beta(\alpha) = -b\alpha^2 + \cdots\,, \tag{2.102}$$

and

$$q_n(t) = q_n(0)\exp\int_\alpha^{\alpha(t)}\frac{\gamma_n(\alpha')}{\beta(\alpha')}\mathrm{d}\alpha' = \left[\frac{\alpha_s}{\alpha_s(t)}\right]^{P_n/2\pi b} q_n(0)\,, \tag{2.103}$$

which exactly coincides with (2.98).

Up to this point we have implicitly restricted our attention to non-singlet (under the flavour group) structure functions. The Q^2 evolution equations become non-diagonal as soon as we take into account the presence of gluons in the target. In fact, the quark which is seen by the photon can be generated by a gluon in the target (Fig. 2.16). The quark evolution equation becomes:

$$\frac{\mathrm{d}}{\mathrm{d}t}q_i(x,t) = \frac{\alpha_s(t)}{2\pi}[q_i \otimes P_{qq}] + \frac{\alpha_s(t)}{2\pi}[g \otimes P_{qg}]\,, \tag{2.104}$$

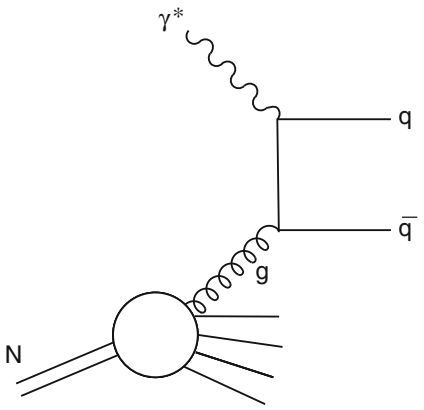

Fig. 2.16 Lowest order diagram for the interaction of the virtual photon with a parton gluon

where we have introduced the shorthand notation

$$[q \otimes P] = [P \otimes q] = \int_x^1 \mathrm{d}y \frac{q(y,t)}{y} P(x/y) \; . \tag{2.105}$$

It is easy to check that the convolution defined in this way is commutative, like an ordinary product. At leading order, the interpretation of (2.104) is simply that the variation of the quark density is due to the convolution of the quark density at a higher energy times the probability of finding a quark in a quark (with the right energy fraction) plus the gluon density at a higher energy times the probability of finding a quark (of the given flavour i) in a gluon. The evolution equation for the gluon density, needed to close the system,[2] can be obtained by suitably extending the same line of reasoning to a gedanken probe sensitive to colour charges, for example,

[2]The evolution equations are now often called the DGLAP equations (after Dokshitzer, Gribov, Lipatov, Altarelli, and Parisi). The first article by Gribov and Lipatov was published in 1972 [233] (even before the works by Gross and Wilczek and by Politzer!), and was followed in 1974 by a paper by Lipatov [283] (these dates correspond to the publication in Russian). All these articles refer to an Abelian vector theory (treated in parallel with a pseudoscalar theory). Seen from the point of view of the evolution equations, these papers, in the context of the Abelian theory, ask the right question and extract the relevant logarithmic terms from the dominant class of diagrams. But from their formal presentation, the relation to real physics is somewhat hidden (in this respect the 1974 paper by Lipatov makes some progress and explicitly refers to the parton model). The article by Dokshitser [171] was exactly contemporary to that by Altarelli and Parisi [40]. It now refers to the non-Abelian theory (with running coupling), and the discussion is more complete and explicit than in the Gribov–Lipatov articles. But, for example, the connection to the parton model, the notion of the evolution as a branching process, and the independence of the kernels from the process are not emphasized.

a virtual gluon. The resulting equation is of the form

$$\frac{\mathrm{d}}{\mathrm{d}t}g(x,t) = \frac{\alpha_\mathrm{s}(t)}{2\pi}\left[\sum_i (q_i + \bar{q}_i) \otimes P_{gq}\right] + \frac{\alpha_\mathrm{s}(t)}{2\pi}[g \otimes P_{\mathrm{gg}}] \,. \tag{2.106}$$

The explicit form of the splitting functions in lowest order [40, 171, 233] can be directly derived from the QCD vertices [40]. They are a property of the theory and do not depend on the particular process the parton density is taking part in. The results are as follows:

$$\begin{aligned}
P_{qq} &= \frac{4}{3}\left[\frac{1+x^2}{(1-x)_+} + \frac{3}{2}\delta(1-x)\right] + O(\alpha_\mathrm{s}),\\
P_{gq} &= \frac{4}{3}\frac{1+(1-x)^2}{x} + O(\alpha_\mathrm{s}),\\
P_{qg} &= \frac{1}{2}\left[x^2 + (1-x)^2\right] + O(\alpha_\mathrm{s}),\\
P_{\mathrm{gg}} &= 6\left[\frac{x}{(1-x)_+} + \frac{1-x}{x} + x(1-x)\right] + \frac{33-2n_\mathrm{f}}{6}\delta(1-x) + O(\alpha_\mathrm{s}).
\end{aligned} \tag{2.107}$$

For a generic non-singular weight function $f(x)$, the "+" distribution is defined as

$$\int_0^1 \frac{f(x)}{(1-x)_+}\mathrm{d}x = \int_0^1 \frac{f(x)-f(1)}{1-x}\mathrm{d}x \,. \tag{2.108}$$

The $\delta(1-x)$ terms arise from the virtual corrections to the lowest order tree diagrams. Their coefficient can be simply obtained by imposing the validity of charge and momentum sum rules. In fact, from the request that the charge sum rules in (2.87) are not affected by the Q^2 dependence, one derives

$$\int_0^1 P_{qq}(x)\mathrm{d}x = 0 \,, \tag{2.109}$$

which can be used to fix the coefficient of the $\delta(1-x)$ terms of P_{qq}. Similarly, by taking the t derivative of the momentum sum rule in (2.88) and requiring it to vanish for generic q_i and g, one obtains

$$\int_0^1 \left[P_{qq}(x) + P_{gq}(x)\right]x\mathrm{d}x = 0 \,, \quad \int_0^1 \left[2n_\mathrm{f}P_{qg}(x) + P_{\mathrm{gg}}(x)\right]x\mathrm{d}x = 0 \,. \tag{2.110}$$

At higher orders, the evolution equations are easily generalized, but the calculation of the splitting functions rapidly becomes very complicated. For many years the splitting functions were only completely known at NLO accuracy [198], that is, $\alpha_s P \sim \alpha_s P_1 + \alpha_s^2 P_2 + \cdots$. But in recent years, the NNLO results P_3 were first derived in analytic form for the first few moments, and then the full NNLO analytic calculation, a really monumental work, was completed in 2004 by Moch et al. [292].

Beyond leading order, a precise definition of parton densities should be specified. One can take a physical definition: for example, quark densities can be defined so as to keep the LO expression for the structure function F_2 valid at all orders, the so-called DIS definition [42], and the gluon density can be defined starting from F_L, the longitudinal structure function. Alternatively, one can adopt a more abstract specification, for example, in terms of the $\overline{\text{MS}}$ prescription. Once the definition of parton densities is fixed, the coefficients that relate the different structure functions to the parton densities at each fixed order can be computed. Similarly, the higher order splitting functions also depend, to some extent, on the definition of parton densities, and a consistent set of coefficients and splitting functions must be used at each order.

The scaling violations are clearly observed by experiment (Fig. 2.17), and their pattern is well reproduced by QCD fits at NLO (Figs. 2.18 and 2.19) [349]. These fits provide an impressive confirmation of a quantitative QCD prediction, a measurement of $q_i(x, Q_0^2)$ and $g(x, Q_0^2)$, at some reference value Q_0^2 of Q^2, and a precise measurement of $\alpha_s(Q^2)$.

2.8.1 The Longitudinal Structure Function

After SLAC established the dominance of the transverse cross-section it took about 40 years to get meaningful data on the longitudinal structure function F_L [see (2.85)]! These data are an experimental highlight of recent years. They were obtained by H1 at HERA [237]. The data are shown in Fig. 2.20. For spin 1/2 charged partons, F_L vanishes asymptotically. In QCD F_L starts at order $\alpha_s(Q^2)$. At LO the simple 30-year-old formula is valid (for $N_f = 4$) [39]:

$$F_L(x, Q^2) = \frac{\alpha_s(Q^2)}{2\pi} x^2 \int_x^1 \frac{dy}{y^3} \left[\frac{8}{3} F_2(y, Q^2) + \frac{40}{9} y g(y, Q^2) \left(1 - \frac{x}{y}\right) \right] . \tag{2.111}$$

The $O(\alpha_s^2)$ [372] and $O(\alpha_s^3)$ [293] corrections are now also known. One would not have expected it to take such a long time to have a meaningful test of this simple prediction! And in fact better data would be highly desirable. But how and when they will be obtained is at present not clear at all.

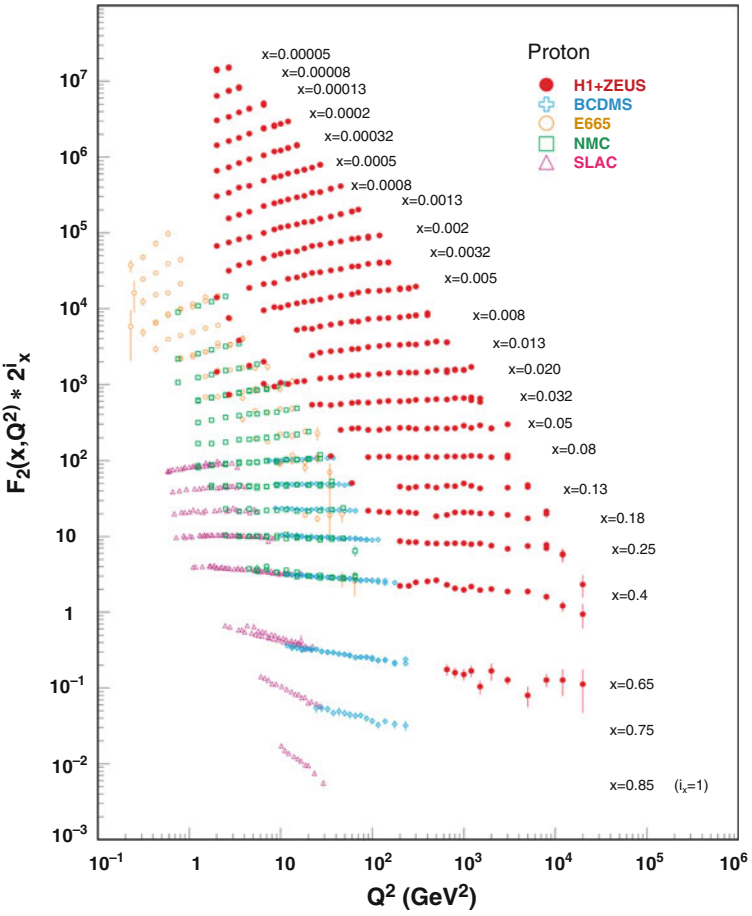

Fig. 2.17 A representative selection of data on the proton electromagnetic structure function F_2^p, from collider (HERA) and fixed target experiments [307], clearly showing the pattern of scaling violations. Figure reproduced with permission. Copyright (c) 2012 by *American Physical Society*

2.8.2 *Large and Small x Resummations for Structure Functions*

At values of x either near 0 or near 1 (with Q^2 large), those terms of higher order in α_s, in both the coefficients or the splitting functions, which are multiplied by powers of $\log 1/x$ or $\log(1-x)$ eventually become important and should be taken into account. Fortunately, the sequences of leading and subleading logs can be evaluated at all orders by special techniques, and resummed to all orders.

For $x \sim 1$ resummation [329], I refer to the recent papers [202, 211] (the latter also involving higher twist corrections, which are important at large x), where a

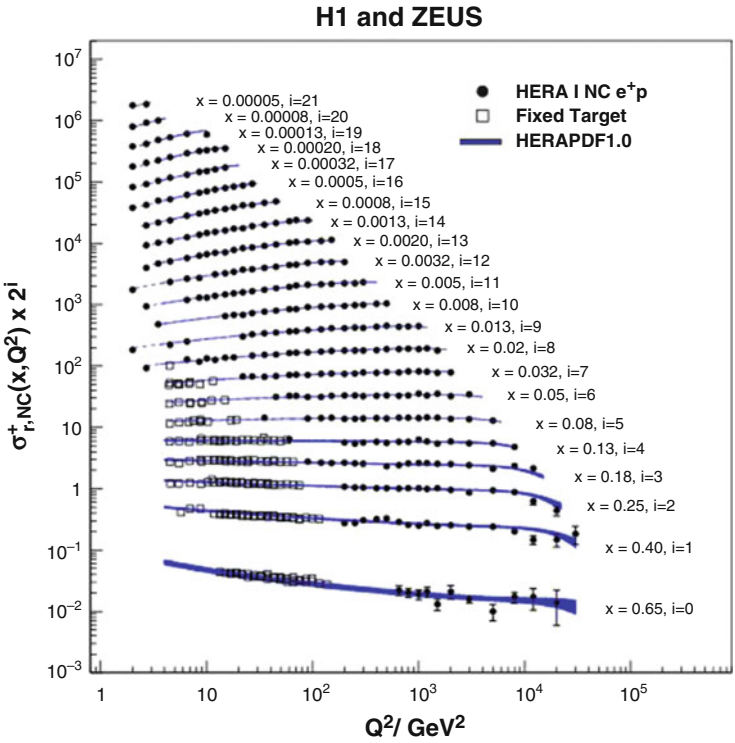

Fig. 2.18 NLO QCD fit to the combined HERA data with $Q^2 \geq 3.5\,\mathrm{GeV}^2$: $\chi^2/\mathrm{dof} = 574/582$ [349]

list of references to previous work can be found. More important is the small x resummation because, the singlet structure functions are large in this domain of x (while all structure functions vanish near $x = 1$). Here we briefly summarize the small-x case for the singlet structure function, which is the dominant channel at HERA, dominated by the sharp rise of the gluon and sea parton densities at small x.

The small x data collected by HERA can be fitted reasonably well, even at the smallest measured values of x, by the NLO QCD evolution equations, so that there is no dramatic evidence in the data for departures. This is surprising also in view of the fact that the NNLO effects in the evolution have recently become available and are quite large [292]. Resummation effects have been shown to resolve this apparent paradox. For the singlet splitting function, the coefficients of all LO and NLO corrections of order $[\alpha_s(Q^2)\log 1/x]^n$ and $\alpha_s(Q^2)[\alpha_s(Q^2)\log 1/x]^n$, respectively, are explicitly known from the Balitski, Fadin, Kuraev, Lipatov (BFKL) analysis of virtual gluon–virtual gluon scattering [191, 284]. But the simple addition of these higher order terms to the perturbative result (with subtraction of all double counting) does not lead to a converging expansion (the NLO logs completely override the LO logs in the relevant domain of x and Q^2).

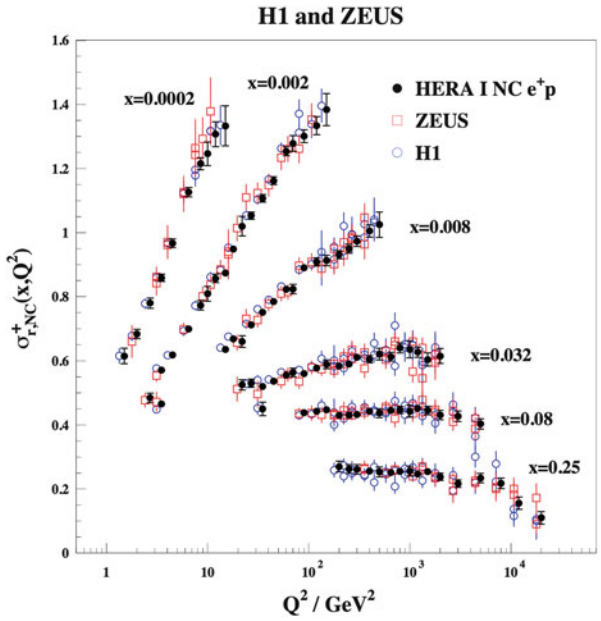

Fig. 2.19 More detailed view of the NLO QCD fit to a selection of the HERA data [349]

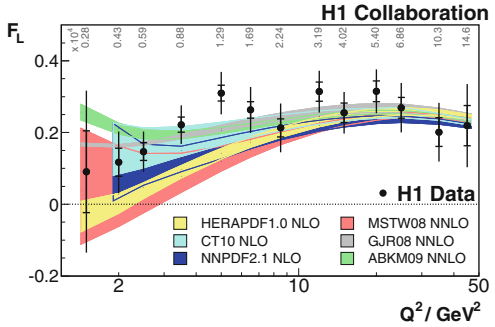

Fig. 2.20 Longitudinal structure function F_L measured by H1 at HERA, as a function of Q^2 for different values of x. The theoretical curves are obtained from different sets of parton densities as indicated

A sensible expansion is only obtained by a proper treatment of momentum conservation constraints, also using the underlying symmetry of the BFKL kernel under exchange of the two external gluons, and especially, of the running coupling effects (see the analysis in [49, 141] and references therein). In Fig. 2.21, we present the results for the dominant singlet splitting function $xP_{gg}(x, \alpha_s(Q^2))$ for $\alpha_s(Q^2) \sim 0.2$. We see that, while the NNLO perturbative splitting function deviates sharply from the NLO approximation at small x, the resummed result only shows a moderate dip with respect to the NLO perturbative splitting function in the region

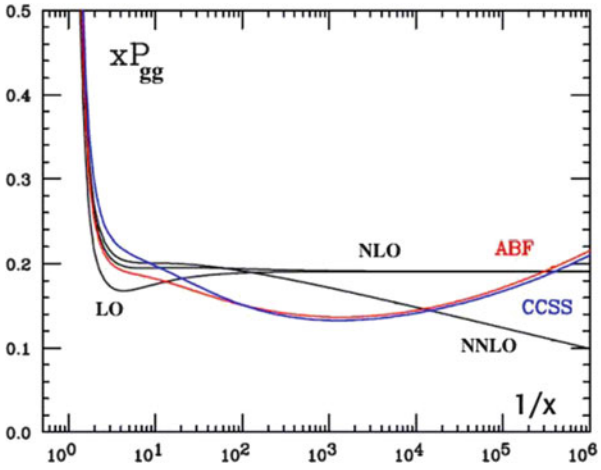

Fig. 2.21 Dominant singlet splitting function $xP_{gg}(x, \alpha_s(Q^2))$ for $\alpha_s(Q^2) \sim 0.2$. The resummed results from [49] (labeled ABF) and from [141] (CCSS), which are in good mutual agreement, are compared with the LO, NLO, and NNLO perturbative results (adapted from [49] and [141])

of HERA data, and the full effect of the true small x asymptotics is only felt at much smaller values of x. The related effects are not very important for most processes at the LHC, but could become relevant for the next generation of hadron colliders.

2.8.3 Polarized Deep Inelastic Scattering

Polarized DIS is a subject where our knowledge is still far from satisfactory, in spite of a great experimental effort (for recent reviews, see, for example, [24]). One major question is how the proton helicity is distributed among quarks, gluons, and orbital angular momentum:

$$\frac{1}{2}\Delta\Sigma + \Delta g + L_z = \frac{1}{2}\,. \tag{2.112}$$

Experiments with polarized leptons on polarized nucleons are sensitive to the polarized parton densities $\Delta q = q_+ - q_-$, the difference of quark densities with helicity plus and minus, in a proton with helicity plus. These differences are related to the quark matrix elements of the axial current. The polarized densities satisfy evolution equations analogous to (2.104) and (2.106), but with modified splitting functions that were derived in [40] (the corresponding anomalous dimensions were obtained in [22]).

Measurements have shown that the quark moment $\Delta\Sigma$ is small. This is the "spin crisis" started by [65]: values from recent fits [104, 159, 244, 277, 303, 326] lie in

the range $\Delta\Sigma \sim 0.2$–0.3. In any case, it is a less pronounced crisis than it used to be in the past. From the spin sum rule, one finds that either $\Delta g + L_z$ is relatively large or there are contributions to $\Delta\Sigma$ at very small x, outside of the measured region. Denoting the first moment of the net helicity carried by the sum $q + \bar{q}$ by Δq, we have the relations [104, 159]

$$a_3 = \Delta u - \Delta d = (F + D)(1 + \epsilon_2) = 1.269 \pm 0.003 \,, \tag{2.113}$$

$$a_8 = \Delta u + \Delta d - 2\Delta s = (3F - D)(1 + \epsilon_3) = 0.586 \pm 0.031 \,, \tag{2.114}$$

where the F and D couplings are defined in the $SU(3)$ flavour symmetry limit, and ϵ_2 and ϵ_3 describe the $SU(2)$ and $SU(3)$ breakings, respectively. From the measured first moment of the structure function g_1, one obtains the value of $a_0 = \Delta\Sigma$:

$$\Gamma_1 = \int \mathrm{d}x\, g_1(x) = \frac{1}{12}\left[a_3 + \frac{1}{3}(a_8 + 4a_0)\right] \,, \tag{2.115}$$

with the result, at $Q^2 \sim 4\,\mathrm{GeV}^2$,

$$a_0 = \Delta\Sigma = \Delta u + \Delta d + \Delta s = a_8 + 3\Delta s \sim 0.25 \,. \tag{2.116}$$

In turn, in the $SU(3)$ limit $\epsilon_2 = \epsilon_3 = 0$, one then obtains

$$\Delta u \sim 0.82 \,, \qquad \Delta d \sim -0.45 \,, \qquad \Delta s \sim -0.11 \,. \tag{2.117}$$

This is an important result! Given F, D, and Γ_1, we know Δu, Δd, Δs, and $\Delta\Sigma$ in the $SU(3)$ limit, which should be reasonably accurate. The x distribution of g_1 is known down to $x \sim 10^{-4}$ on proton and deuterium, and the first moment of g_1 does not seem to get much from the unmeasured range at small x (also, theoretically, g_1 should be smooth at small x [190]).

The value of $\Delta s \sim -0.11$ from totally inclusive data and $SU(3)$ appears to be at variance with the value extracted from single-particle inclusive DIS (SIDIS), where one obtains a nearly vanishing result for Δs in a fit to all data [159, 326] that leads to puzzling results. There is, in fact, an apparent tension between the first moments as determined by using the approximate $SU(3)$ symmetry and from fitting the data on SIDIS ($x \geq 0.001$) (in particular for the strange density). But the adequacy of the SIDIS data is questionable (in particular the kaon data which fix Δs) and so is their theoretical treatment (for example, the application of parton results at too low an energy and the ambiguities in the kaon fragmentation function).

$\Delta\Sigma$ is conserved in perturbation theory at LO (i.e., it does not evolve with Q^2). Regarding conserved quantities, we would expect them to be the same for constituent and for parton quarks. But actually, the conservation of $\Delta\Sigma$ is broken by the axial anomaly and, in fact, in perturbation theory beyond LO, the conserved density is actually $\Delta\Sigma' = \Delta\Sigma + \Delta g(n_\mathrm{f}/2\pi\alpha_\mathrm{s})$ [41]. Note also that $\alpha_\mathrm{s}\Delta g$ is conserved in LO, that is $\Delta g \sim \log Q^2$. This behaviour is not controversial, but it will

be a long time before the log growth of Δg is confirmed by experiment! However, by establishing this behaviour, one would show that the extraction of Δg from the data is correct and that the QCD evolution works as expected.

If Δg were large enough, it could account for the difference between partons ($\Delta\Sigma$) and constituents ($\Delta\Sigma'$). From the spin sum rule it is clear that the log increase should cancel between Δg and L_z. This cancelation is automatic, as a consequence of helicity conservation in the basic QCD vertices. Δg can be measured indirectly by scaling violations and directly from asymmetries, e.g., in SIDIS. Existing measurements by HERMES, COMPASS, and at RHIC are still crude, but show no hint of a large Δg at accessible values of x and Q^2. Present data, affected by large errors (see, in particular, [303] for a discussion of this point) are consistent [104, 159, 244, 277, 303, 326] with a sizable contribution of Δg to the spin sum rule in (2.112), but there is no indication that $\alpha_s \Delta g$ effects can explain the difference between constituents and parton quarks.

2.9 Hadron Collider Processes and Factorization

There are three classes of hard processes: those with no hadronic particles in the initial state, like e^+e^- annihilation, those initiated by a lepton and a hadron, like DIS, and those with two incoming hadrons. The parton densities, defined and measured in DIS, are instrumental to compute hard processes initiated by collisions of two hadrons, like $p\bar{p}$ (Tevatron) or pp (LHC). Suppose we have a hadronic process of the form $h_1 + h_2 \to X + \text{all}$, where h_i are hadrons and X is some triggering particle, or pair of particles, or one or more jets which specify the large scale Q^2 relevant for the process, in general somewhat, but not much, smaller than s, the total centre-of-mass squared mass. For example, X can be a $W^\pm$, or a Z, or a virtual photon with large Q^2 (Drell–Yan processes), or a jet with large transverse momentum p_T, or a quark–antiquark pair with heavy components (of mass M). By "all" we mean a totally inclusive collection of hadronic particles. The factorization theorem (FT) states that, for the total cross-section or some other sufficiently inclusive distribution, we can write, apart from power-suppressed corrections, the expression (see also Fig. 2.22)

$$\sigma(s,\tau) = \sum_{AB} \int \mathrm{d}x_1 \mathrm{d}x_2 p_{1A}(x_1, Q^2) p_{2B}(x_2, Q^2) \sigma_{AB}(x_1 x_2 s, \tau) \ . \tag{2.118}$$

Here $\tau = Q^2/s$ is a scaling variable, p_{iA} are the densities for a parton of type A inside the hadron h_i, and σ_{AB} is the partonic cross-section for

$$\text{parton } A + \text{parton } B \to X + \text{ all}' \ .$$

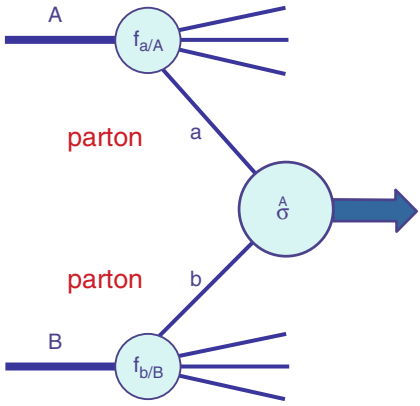

Fig. 2.22 Diagram for the factorization theorem

Here all′ is the partonic version of "all", i.e., a totally inclusive collection of quarks, antiquarks, and gluons. This result is based on the fact that the mass singularities associated with the initial legs are of universal nature, so that one can reproduce the same modified parton densities by absorbing these singularities into the bare parton densities, as in DIS. Once the parton densities and α_s are known from other measurements, the prediction of the rate for a given hard process is obtained without much ambiguity (e.g., from scale dependence or hadronization effects).

At least an NLO calculation of the reduced partonic cross-section σ_{AB} is needed in order to correctly specify the scale, and in general also the definition of the parton densities and of the running coupling in the leading term. The residual scale and scheme dependence is often the most important source of theoretical error. It is important to ask to what extent the FT has been proven? In perturbation theory up to NNLO, it has been explicitly checked to hold for many processes: if corrections exist we already know that they must be small (we stress that we are only considering totally inclusive processes). At all orders, the most in-depth discussions have been carried out in [146], in particular for Drell–Yan processes. The LHC experiments offer a wonderful opportunity for testing the FT by comparing precise theoretical predictions with accurate data on a wide variety of processes (for a recent review, see, for example, [119]).

A great effort has been and is being devoted to the theoretical preparation and interpretation of the LHC experiments. For this purpose very, difficult calculations are needed at NLO and beyond because the strong coupling, even at the large Q^2 values involved, is not that small. Further powerful techniques for amplitude calculations have been devised.

An interesting development at the interface between string theory and QCD is twistor calculus. A precursor was the Parke–Taylor result in 1986 [305] on the amplitudes for n incoming gluons with given $\pm$ helicities [91]. Inspired by dual models, they derived a compact formula for the maximum non-vanishing helicity-violating amplitude (with $n-2$ plus and 2 minus helicities) in terms of spinor products. In 2003, using the relation between strings and gauge theories in

twistor space, Witten developed [368] a formalism in terms of effective vertices and propagators that allows one to compute all helicity amplitudes. The method, alternative to other modern techniques for the evaluation of Feynman diagrams [163], leads to very compact results.

Since then, there has been rapid progress (for reviews, see [128]). The method was extended to include massless external fermions [217] and also external EW vector bosons [96] and Higgs particles [167]. The level attained is already important for multijet events at the LHC. The study of loop diagrams came next. The basic idea is that loops can be fully reconstructed from their unitarity cuts. First proposed by Bern et al. [95], the technique was revived by Britto et al. [114] and then perfected by Ossola et al. [304] and further extended to massive particles in [186]. For a recent review of these new methods see [188].

In parallel with this, activity on event simulation has received a big boost from preparations at the LHC (see, for example, the review [130]). Powerful techniques have been developed to generate numerical results at NLO for processes with complicated final states: matrix element calculation has been matched with modeling of parton showers in packages like Black Hat [92] (on-shell methods for loops), used in association with Sherpa [227] (for real emission), or POWHEG BOX [299] or aMC@NLO [203], the automated version of the general framework MC@NLO [206]. In a complete simulation, the matrix element calculation, improved by resummation of large logs, provides the hard skeleton (with large p_{T} branchings), while the parton shower is constructed by a sequence of factorized collinear emissions fixed by the QCD splitting functions. In addition, at low scales, a model of hadronization completes the simulation. The importance of all the components, matrix element, parton shower, and hadronization, can be appreciated in simulations of hard events compared with Tevatron and LHC data. One can say that the computation of NLO corrections in perturbative QCD has now been completely automated.

A partial list of examples of recent NLO calculations in pp collisions, obtained with these techniques is: $W + 3$ jets [187], Z, $\gamma^* + 3$ jets [93], W, $Z + 4$ jets [94], $W + 5$ jets [97], $t\bar{t}b\bar{b}$ [113], $t\bar{t} + 2$ jets [100], $t\bar{t}\,W$ [129], $WW + 2$ jets [289], $WWb\bar{b}$ [161], $b\bar{b}b\bar{b}$ [232], etc. In the following we shall detail a number of the most important and simplest examples, without any pretension to completeness.

2.9.1 Vector Boson Production

Drell–Yan processes which include lepton pair production via virtual γ, W, or Z exchange, offer a particularly good opportunity to test QCD. This process, among those quadratic in parton densities with a totally inclusive final state, is perhaps the simplest one from a theoretical point of view. The large scale is specified and measured by the invariant mass squared Q^2 of the lepton pair, which is not itself strongly interacting (so there are no dangerous hadronization effects). The improved QCD parton model leads directly to a prediction for the total rate as a function of

s and $\tau = Q^2/s$. The value of the LO cross-section is inversely proportional to the number of colours N_C, because a quark of given colour can only annihilate with an antiquark of the same colour to produce a colourless lepton pair. The order $\alpha_s(Q^2)$ NLO corrections to the total rate were computed long ago [42, 273] and found to be particularly large, when the quark densities are defined from the structure function F_2 measured in DIS at $q^2 = -Q^2$. The ratio $\sigma_{corr}/\sigma_{LO}$ of the corrected and the Born cross-sections was called the K-factor [28], because it is almost a constant in rapidity. More recently, the NNLO full calculation of the K-factor was completed in a truly remarkable calculation [240].

Over the years the QCD predictions for W and Z production, a better testing ground than the older fixed-target Drell–Yan experiments, have been compared with experiments at CERN $Sp\bar{p}S$ and Tevatron energies and now at the LHC. $Q \sim m_{W,Z}$ is large enough to make the prediction reliable (with a not too large K-factor) and the ratio $\sqrt{\tau} = Q/\sqrt{s}$ is not too small. Recall that, in lowest order, one has $x_1 x_2 s = Q^2$, so that the parton densities are probed at x values around $\sqrt{\tau}$. We have $\sqrt{\tau} = 0.13$–0.15 (for W and Z production, respectively) at $\sqrt{s} = 630\,\text{GeV}$ (CERN $Sp\bar{p}S$ collider) and $\sqrt{\tau} = 0.04$–0.05 at the Tevatron. At the LHC at 8 TeV or at 14 TeV, one has $\sqrt{\tau} \sim 10^{-2}$ or $\sim 6 \times 10^{-3}$, respectively (for both W and Z production). A comparison of the experimental total rates for W and Z with the QCD predictions at hadron colliders [327] is shown in Fig. 2.23. It is also important to mention that the cross-sections for di-boson production (i.e., WW, WZ, ZZ, $W\gamma$, $Z\gamma$) have been measured at the Tevatron and the LHC and are in fair agreement with the SM prediction (see, for example, the summary in [285] and references therein). The typical precision is comparable to or better than the size of NLO corrections.

The calculation of the W/Z p_T distribution is a classic challenge in QCD. For large p_T, for example $p_T \sim O(m_W)$, the p_T distribution can be reliably computed in perturbation theory, and this was done up to NLO in the late 1970s and early 1980s [183]. A problem arises in the intermediate range $\Lambda_{QCD} \ll p_T \ll m_W$, where the bulk of the data is concentrated, because terms of order $\alpha_s(p_T^2) \log m_W^2/p_T^2$ become

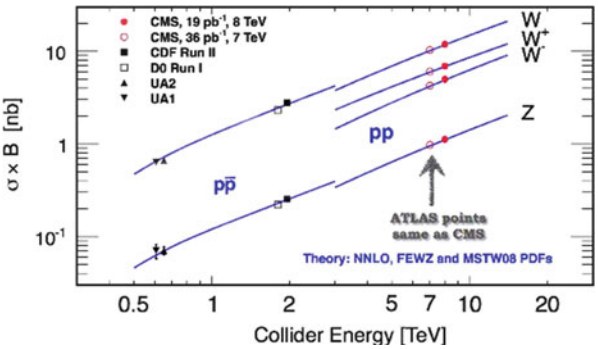

Fig. 2.23 Data vs. theory for W and Z production at hadron colliders [327] (included with permission)

of order 1 and should be included to all orders [330]. At order α_s, we have

$$\frac{1}{\sigma_0}\frac{d\sigma_0}{dp_T^2} = (1+A)\delta(p_T^2) + \frac{B}{p_T^2}\log\frac{m_W^2}{(p_T^2)_+} + \frac{C}{(p_T^2)_+} + D(p_T^2)\ , \tag{2.119}$$

where A, B, C, D are coefficients of order α_s. The "+" distribution is defined in complete analogy with (2.108):

$$\int_0^{p_{T\,MAX}^2} g(z)f(z)_+ dz = \int_0^{p_{T\,MAX}^2} \big[g(z)-g(0)\big]f(z)dz\ . \tag{2.120}$$

The content of this, at first sight mysterious, definition is that the singular "+" terms do not contribute to the total cross-section. In fact, for the cross-section, the weight function is $g(z) = 1$ and we obtain

$$\sigma = \sigma_0\left[(1+A) + \int_0^{p_{T\,MAX}^2} D(z)dz\right]\ . \tag{2.121}$$

The singular terms, of infrared origin, are present at the not completely inclusive level, but disappear in the total cross-section. Solid arguments have been given [330] to suggest that these singularities exponentiate. Explicit calculations in low order support the exponentiation, and this leads to the following expression:

$$\frac{1}{\sigma_0}\frac{d\sigma_0}{dp_T^2} = \int \frac{d^2b}{4\pi}\exp(-ib\cdot p_T)(1+A)\exp S(b)\ , \tag{2.122}$$

with

$$S(b) = \int_0^{p_{T\,MAX}} \frac{d^2k_T}{2\pi}\big[\exp(ik_T\cdot b) - 1\big]\left(\frac{B}{k_T^2}\log\frac{m_W^2}{k_T^2} + \frac{C}{k_T^2}\right)\ . \tag{2.123}$$

At large p_T the perturbative expansion is recovered. At intermediate p_T the infrared p_T singularities are resummed (the Sudakov log terms, which are typical of vector gluons, are related to the fact that for a charged particle in acceleration, it is impossible not to radiate, so that the amplitude for no soft gluon emission is exponentially suppressed). A delicate procedure for matching perturbative and resummed terms is needed [43]. However, this formula has problems at small p_T, for example, because of the presence of α_s under the integral for $S(b)$. Presumably, the relevant scale is of order k_T^2. So it must be completed by some non-perturbative ansatz or an extrapolation into the soft region [330].

All the formalism has been extended to NLO accuracy [64], where one starts from the perturbative expansion at order α_s^2, and generalises the resummation to include also NLO terms of order $\alpha_s(p_T^2)^2\log m_W^2/p_T^2$. The comparison with the data is very impressive. Figure 2.24 shows the p_T distribution as predicted in QCD (with

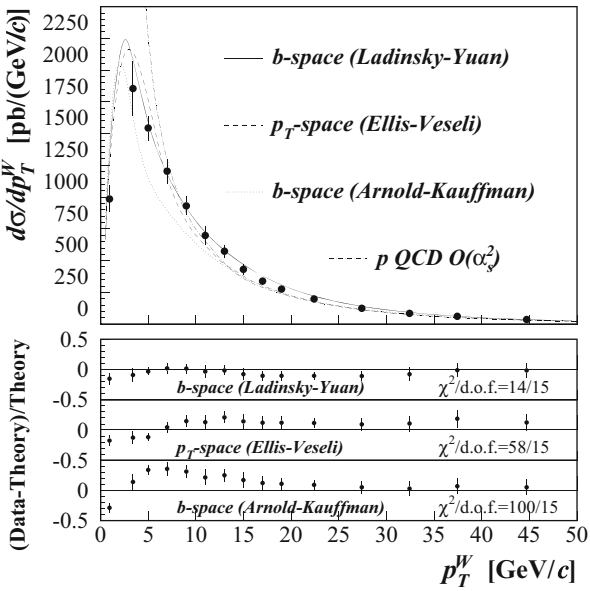

Fig. 2.24 QCD predictions for the W p_T distribution compared with recent D0 data at the Tevatron ($\sqrt{s} = 1.8$ TeV) (adapted from [64, 347])

a number of variants that differ mainly in the approach to the soft region) compared with some recent data at the Tevatron [347]. The W and Z p_T distributions have also been measured at the LHC and are in fair agreement with the theoretical expectation [343].

The rapidity distributions of the produced W and Z have also been measured with fair accuracy at the Tevatron and at the LHC, and predicted at NLO [55]. A representative example of great significance is provided by the combined LHC results for the W charge asymmetry, defined as $A \sim (W^+ - W^-)/(W^+ + W^-)$, as a function of the pseudo-rapidity η [340]. These data combine the ATLAS and CMS results at smaller values of η with those of the LHCb experiments at larger η (in the forward direction). This is very important input for the disentangling of the different quark parton densities.

2.9.2 *Jets at Large Transverse Momentum*

Another simple and important process at hadron colliders is the inclusive production of jets at high energy $\sqrt{s}$ and transverse momentum p_T. A comparison of the data with the QCD NLO predictions [147, 180] in pp or $p\bar{p}$ collisions is shown in Fig. 2.25 [369]. This is a particularly significant test because the rates at different centre-of-mass energies and, for each energy, at different values of p_T, span many orders of magnitude. This steep behaviour is determined by the sharp drop in the parton densities with increasing x. Moreover, the corresponding values of $\sqrt{s}$ and

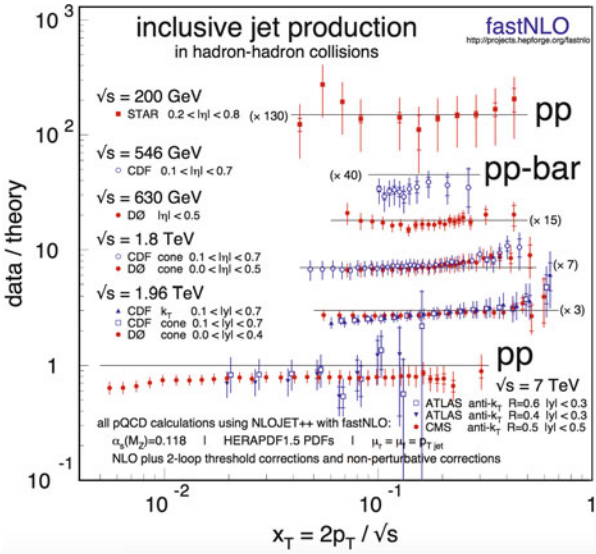

Fig. 2.25 Jet production cross-section at pp or $p\bar{p}$ colliders, as a function of p_T [369]. Theoretical predictions are from NLO perturbative calculations with state-of-the-art parton densities with the corresponding value of α_s plus a non-perturbative correction factor due to hadronization and the underlying event, obtained using Monte Carlo event generators (included with permission)

p_T are large enough to be well inside the perturbative region. The overall agreement of the data from ISR, UA1,2, STAR (at RHIC), CDF/D0, and now ATLAS/CMS, is indeed spectacular. In fact, the uncertainties in the resulting experiment/theory ratio, due to systematics and to ambiguities in the parton densities, the value of α_s, the scale choice, and so on, which can reach a factor of 2–3, are much smaller than the spread of the cross-section values over many orders of magnitude.

Similar results also hold for the production of photons at large p_T. The ATLAS data [342], shown in Fig. 2.26, are in fair agreement with the theoretical predictions. For the same process, a less clear situation was found with fixed target data. Here, first of all, the experimental results show some internal discrepancies. Moreover, the accessible values of p_T being smaller, the theoretical uncertainties are greater.

2.9.3 Heavy Quark Production

We now discuss heavy quark production at colliders. The totally inclusive cross-sections have been known at NLO for a long time [300]. The resummation of leading and next-to-leading logarithmically enhanced effects in the vicinity of the threshold region have also been studied [108]. The bottom production at the Tevatron has represented a problem for some time: the total rate and the

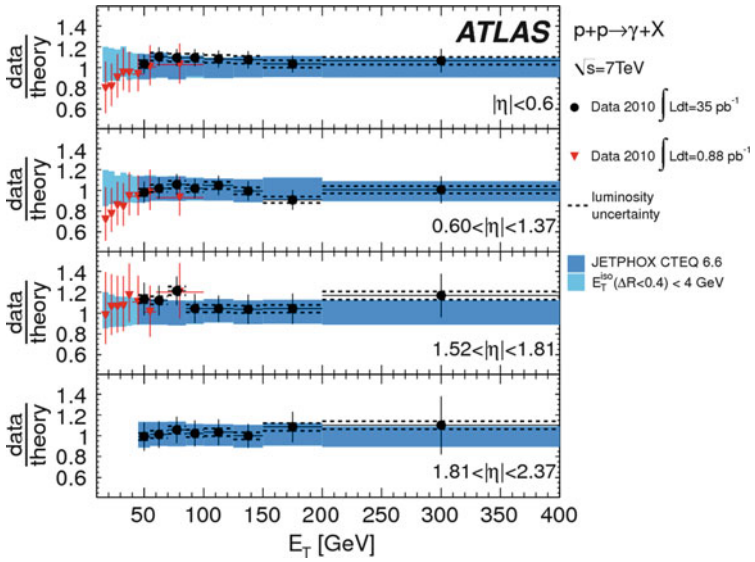

Fig. 2.26 Single-photon production in $p\bar{p}$ colliders as a function of p_T [342] (included with permission)

p_T distribution of b quarks observed at CDF and D0 appeared in excess of the prediction, up to the highest measured values of p_T [83, 124]. But this is a complicated problem, with different scales present at the same time: $\sqrt{s}, p_T, m_b$. The discrepancy was finally explained by more carefully taking into account a number of small effects from resummation of large logarithms, the difference between b hadrons and b partons, the inclusion of better fragmentation functions, etc. [125]. At present the LHC data on b production are in satisfactory agreement with the theoretical predictions (Fig. 2.27 [67]).

The top quark is really special: its mass is of the order of the Higgs VEV or its Yukawa coupling is of order 1, and in this sense, it is the only "normal" case among all quarks and charged leptons. Due to its heavy mass, it decays so fast that it has no time to be bound in a hadron: thus it can be studied as a quark. It is very important to determine its mass and couplings for different precision predictions of the SM. The top quark may be particularly sensitive to new heavy states or have a connection to the Higgs sector when we go beyond the SM theories.

Top quark physics has thus attracted much attention, both from the experimental side, at hadron colliders, and from the theoretical point of view. In particular, the top–antitop inclusive cross-section has been measured in $p\bar{p}$ collisions at the Tevatron [15], and now in pp collisions at the LHC [339, 346]. The QCD prediction is at present completely known at NNLO [150]. Soft gluon resummation has also been performed at NNLL [127]. The agreement between theory and experiment is good for the best available parton density functions together with the values of α_s

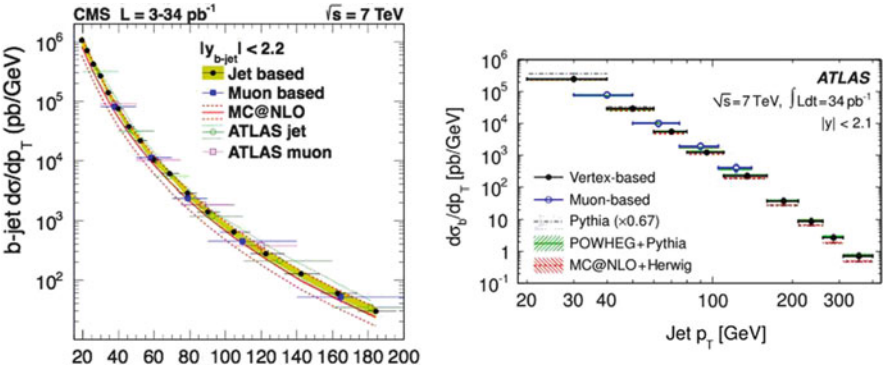

Fig. 2.27 The b production p_{T} distribution at the LHC [67]

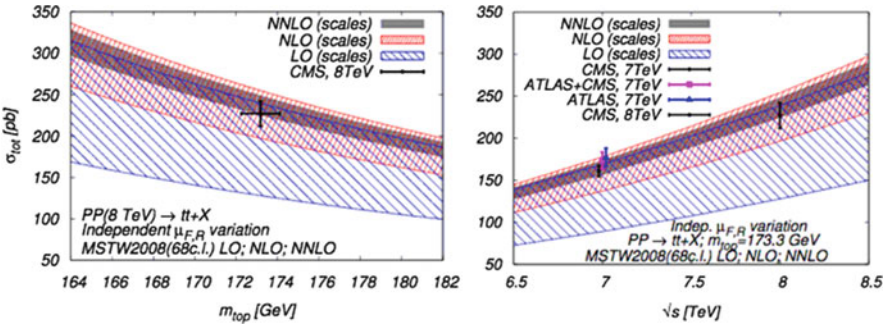

Fig. 2.28 The $t\bar{t}$ production cross-section at the LHC collider. Scale dependence of the total cross-section at LO (*blue*), NLO (*red*), and NNLO (*black*) as a function of m_{top} (*left*) or $\sqrt{s}$ (*right*) at the LHC 8 TeV [150] (included with permission)

and m_t measured separately (the top mass is measured from the invariant mass of the decay products), as can be seen from Fig. 2.28 [150].

The mass of the top (and the value of α_{s}) can be determined from the cross-section, assuming that QCD is correct, and compared with the more precise value from the final decay state. The value of the top pole mass derived in [27] from the cross-section data, using the best available parton densities with the correlated value of α_{s}, is $m_t^{\mathrm{pole}} = 173.3 \pm 2.8\,\mathrm{GeV}$. This is to be compared with the value measured at the Tevatron by the CDF and D0 collaborations, viz., $m_t^{\mathrm{exp}} = 173.2 \pm 0.9\,\mathrm{GeV}$. This quoted error is clearly too optimistic, especially if one identifies this value with the pole mass which it resembles. This error is only adequate within the specific procedure used by the experimental collaborations to define their mass (including Montecarlo, with assumptions about higher order terms, non-perturbative effects, etc.). The problem is how to export this value to other processes. Leaving aside the thorny issue of the precise relation between m_t^{exp} with m_t^{pole}, it is clear that there is good overall consistency.

The inclusive forward–backward asymmetry, $A_{\rm FB}$, in the $t\bar{t}$ rest frame has been measured by both the CDF [6] and D0 [9] collaborations, and found to be in excess of the SM prediction, by about 2σ [247]. For CDF the discrepancy increases at large $t\bar{t}$ invariant mass, and reaches about 2.5σ for $M_{t\bar{t}} \geq 450\,\text{GeV}$. Recently, CDF has obtained [7] the first measurement of the top quark pair production differential cross-section as a function of $\cos\theta$, with θ the production angle of the top quark. The coefficient of the $\cos\theta$ term in the differential cross-section, viz., $a_1 = 0.40 \pm 0.12$, is found to be in excess of the NLO SM prediction, viz., $0.15^{+0.07}_{-0.03}$, while all other terms are in good agreement with the NLO SM prediction, and $A_{\rm FB}$ is dominated by this excess linear term. Is this a real discrepancy? The evidence is far from compelling, but this effect has received much attention from theorists [321]. A related observable at the LHC is the charge asymmetry $A_{\rm C}$ in $t\bar{t}$ production. In contrast to $A_{\rm FB}$, the combined value of $A_{\rm C}$ reported by ATLAS [1] and CMS [144] agrees with the SM, within the still limited accuracy of the data.

2.9.4 Higgs Boson Production

We now turn to the discussion of the SM Higgs inclusive production cross-section (for a review and a list of references, see [165]). The most important Higgs production modes are gluon fusion, vector boson fusion, Higgs strahlung, and associated production with top quark pairs. Some typical Feynman diagrams for these different modes are depicted in Fig. 2.29. The predicted rates are shown in Fig. 2.30 [168].

The most important channel at the LHC is Higgs production via $g + g \to H$. The amplitude is dominated by the top quark loop [216]. The NLO corrections turn out to be particularly large [156], as can be seen in Fig. 2.31. Higher order corrections can be computed either in the effective Lagrangian approach, where the heavy top is integrated away and the loop is shrunk down to a point [182] (the coefficient of the effective vertex is known to $\alpha_{\rm s}^4$ accuracy [139]), or in the full theory. At the NLO, the two approaches agree very well for the rate as a function of $m_{\rm H}$ [270]. The NNLO corrections have been computed in the effective vertex approximation [133] (see Fig. 2.31). Beyond fixed order, resummation of large logs has been carried out [134]. Further, the NLO EW contributions have been computed [20]. Rapidity (at NNLO) [56] and $p_{\rm T}$ distributions (at NLO) [158] have also been evaluated. At smaller $p_{\rm T}$, the large logarithms $[\text{Log}(p_{\rm T}/m_{\rm H})]^n$ have been resummed in analogy with what was done long ago for W and Z production [110]. For additional recent works on Higgs physics at colliders, see, for example, [184].

So far we have seen examples of resummation of large logs. This is a very important chapter of modern QCD. The resummation of soft gluon logs enter into different problems, and the related theory is subtle. The reader is referred here to some recent papers where additional references can be found [77]. A particularly interesting related development has to do with the so-called non-global logs (see, for example, [153]). If in the measurement of an observable some experimental cuts

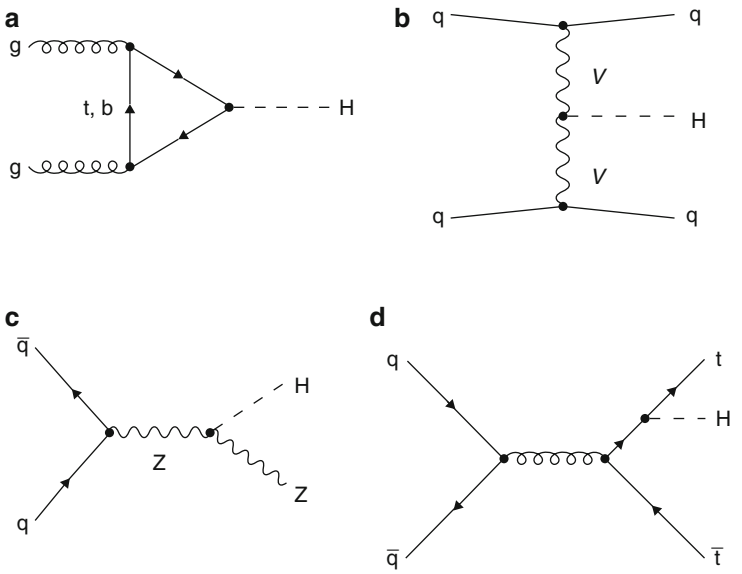

Fig. 2.29 Representative Feynman diagrams for the Higgs production cross-section mechanisms. (**a**) Gluon fusion. (**b**) Vector boson fusion ($V = W, Z$). (**c**) Higgs strahlung from a Z boson (an analogous diagram can be drawn for the W boson). (**d**) $t\bar{t}$ associated production

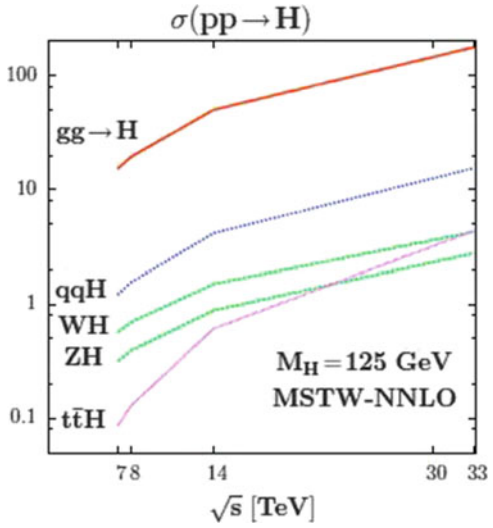

Fig. 2.30 Production cross-sections at the LHC for a Higgs with mass $M_{\mathrm{H}} \sim 125\,\mathrm{GeV}$ for different centre-of-mass energies [168]

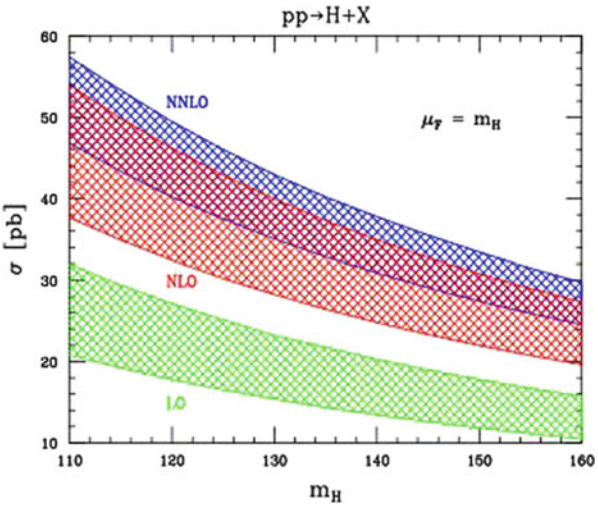

Fig. 2.31 Higgs gluon fusion cross-section in LO, NLO, and NLLO [57]. Figure reproduced with permission. Copyright (c) 2005 by *American Physical Society*

are introduced, which is very often the case, then a number of large logs can arise from the corresponding breaking of inclusiveness. It is also important to mention the development of software for the automated implementation of resummation (see, for example, [78]).

2.10 Measurements of α_s

Very precise and reliable measurements of $\alpha_s(m_Z)$ are obtained from e^+e^- colliders (in particular LEP), from deep inelastic scattering, and from the hadron colliders (Tevatron and LHC). The "official" compilation due to Bethke [99, 311], included in the 2012 edition of the PDG [307], is reproduced here in Fig. 2.32. The agreement among so many different ways of measuring α_s is a strong quantitative test of QCD. However, for some entries the stated error is taken directly from the original works and is not transparent enough when viewed from the outside (e.g., the lattice determination). In my opinion one should select a few of the theoretically cleanest processes for measuring α_s and consider all other ways as tests of the theory. Note that, in QED, α is measured from a single very precise and theoretically clean observable (one possible calibration process is at present the electron $g-2$ [242]). The cleanest processes for measuring α_s are the totally inclusive ones (no hadronic corrections) with light cone dominance, like Z decay, scaling violations in DIS, and perhaps τ decay (but for τ the energy scale is dangerously low). We will review these cleanest methods for measuring α_s in the following.

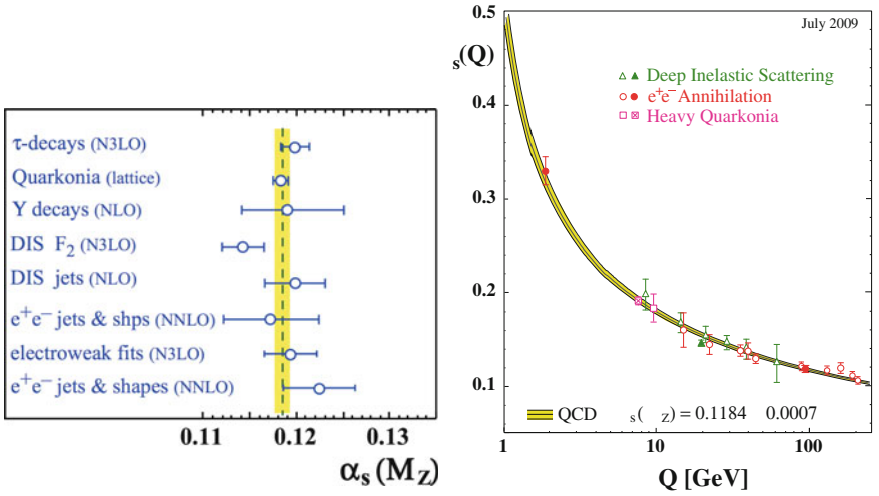

Fig. 2.32 *Left*: Summary of measurements of $\alpha_s(m_Z)$. The *yellow band* is the proposed average: $\alpha_s(m_Z) = 0.1184 \pm 0.0007$. *Right*: Summary of measurements of α_s as a function of the respective energy scale Q. Figures from [99]

2.10.1 α_s from e^+e^- Colliders

The totally inclusive processes for measuring α_s at e^+e^- colliders are hadronic Z decays (R_l, σ_h, σ_l, Γ_Z) and hadronic τ decays. As we have seen in Sect. 2.7.1, for a quantity like R_l we can write a general expression of the form

$$R_l = \frac{\Gamma(Z, \tau \to \text{hadrons})}{\Gamma(Z, \tau \to \text{leptons})} \sim R^{EW}(1 + \delta_{QCD} + \delta_{NP}) \,, \tag{2.124}$$

where R^{EW} is the electroweak-corrected Born approximation, and δ_{QCD}, δ_{NP} are the perturbative (logarithmic) and non-perturbative (power suppressed) QCD corrections. For a measurement of α_s (in the following we always refer to the $\overline{MS}$ definition of α_s) at the Z resonance peak, one can use all the information from R_l, $\Gamma_Z = 3\Gamma_l + \Gamma_h + \Gamma_{inv}$, and $\sigma_F = 12\pi\Gamma_l\Gamma_F/(m_Z^2\Gamma_Z^2)$, where F stands for h or l.

In the past, the measurement from R_l was preferred (taken by itself it leads to $\alpha_s(m_Z) = 0.1226 \pm 0.0038$, a bit on the large side), but after LEP there is no reason for this preference. In all these quantities α_s enters through Γ_h, but the measurements of, say, Γ_Z, R_l, and σ_l are really independent, as they are affected by entirely different systematics: Γ_Z is extracted from the line shape, and R_l and σ_l are measured at the peak, but R_l does not depend on the absolute luminosity, while σ_l does. The most sensitive single quantity is σ_l. It gives $\alpha_s(m_Z) = 0.1183 \pm 0.0030$. The combined value from the measurements at the Z (assuming the validity of the SM and the

observed Higgs mass) is [268]

$$\alpha_s(m_Z) = 0.1187 \pm 0.0027 \,. \tag{2.125}$$

Similarly, by adding all other electroweak precision tests (in particular m_W), one finds [350]

$$\alpha_s(m_Z) = 0.1186 \pm 0.0026 \,. \tag{2.126}$$

These results have been obtained from the $\delta_{\rm QCD}$ expansion up to and including the c_3 term of order α_s^3. But by now the c_4 term (NNNLO!) has also been computed [74] for inclusive hadronic Z and τ decay. For $n_f = 5$ and $a_s = \alpha_s(m_Z)/\pi$, this remarkable calculation of about 20,000 diagrams for the inclusive hadronic Z width leads to the result

$$\delta_{\rm QCD} = 1 + a_s + 0.76264 a_s^2 - 15.49 a_s^3 - 68.2 a_s^4 + \cdots \,. \tag{2.127}$$

This result can be used to improve the value of $\alpha_s(m_Z)$ from the EW fit given in (2.126), which becomes

$$\alpha_s(m_Z) = 0.1190 \pm 0.0026 \,. \tag{2.128}$$

Note that the error shown is dominated by the experimental errors. Ambiguities from higher perturbative orders [328], from power corrections, and also from uncertainties on the Bhabha luminometer (which affect $\sigma_{\rm h,l}$) [157] are very small. In particular, the fact of having now fixed m_H does not decrease the error significantly [73] (Grunewald, M., for the LEP EW Group, private communication). The main source of error is the assumption of no new physics, for example, in the $Zb\bar{b}$ vertex, which may affect the Γ_h prediction.

We now consider the measurement of $\alpha_s(m_Z)$ from τ decay. R_τ has a number of advantages which, at least in part, tend to compensate for the smallness of $m_\tau = 1.777\,\text{GeV}$. First, R_τ is maximally inclusive, more so than $R_{e^+e^-}(s)$, because one also integrates over all values of the invariant hadronic squared mass:

$$R_\tau = \frac{1}{\pi} \int_0^{m_\tau^2} \frac{{\rm d}s}{m_\tau^2} \left(1 - \frac{s}{m_\tau^2}\right)^2 {\rm Im}\, \Pi_\tau(s) \,. \tag{2.129}$$

As we have seen, the perturbative contribution is now known at NNNLO [74]. Analyticity can be used to transform the integral into one on the circle at $|s| = m_\tau^2$:

$$R_\tau = \frac{1}{2\pi {\rm i}} \oint_{|s|=m_\tau^2} \frac{{\rm d}s}{m_\tau^2} \left(1 - \frac{s}{m_\tau^2}\right)^2 \Pi_\tau(s) \,. \tag{2.130}$$

Furthermore, the factor $(1 - s/m_\tau^2)^2$ is important to kill the sensitivity in the region $\mathrm{Re}[s] = m_\tau^2$ where the physical cut and the associated thresholds are located. However, the sensitivity to hadronic effects in the vicinity of the cut is still a non-negligible source of theoretical error which the formulation of duality violation models tries to decrease. But the main feature that has attracted attention to τ decays for the measurement of $\alpha_s(m_Z)$ is that even a rough determination of $\Lambda_{\rm QCD}$ at a low scale $Q \sim m_\tau$ leads to a very precise prediction of α_s at the scale m_Z, just because in $\log Q/\Lambda_{\rm QCD}$ the value of $\Lambda_{\rm QCD}$ counts less and less as Q increases. The absolute error in α_s shrinks by a factor of about one order of magnitude in going from $\alpha_s(m_\tau)$ to $\alpha_s(m_Z)$.

Still it seems a little suspicious that, in order to obtain a better measurement of $\alpha_s(m_Z)$, we have to go down to lower and lower energy scales. And in fact, in general, one finds that the decreased control of higher order perturbative and non-perturbative corrections makes the apparent advantage totally illusory. For α_s from R_τ, the quoted amazing precision is obtained by taking for granted that corrections suppressed by $1/m_\tau^2$ are negligible. The argument is that, in the massless theory, the light cone expansion is given by

$$\delta_{\rm NP} = \frac{\rm ZERO}{m_\tau^2} + c_4 \frac{\langle O_4 \rangle}{m_\tau^4} + c_6 \frac{\langle O_6 \rangle}{m_\tau^6} + \cdots . \tag{2.131}$$

In fact there are no 2D Lorentz and gauge invariant operators. For example, $\mathrm{Tr}[\mathbf{g}_\mu \mathbf{g}^\mu]$ [recall (1.12)] is not gauge invariant. In the massive theory, ZERO here is replaced by the light quark mass-squared m^2. This is still negligible if m is taken as a Lagrangian mass of a few MeV. If on the other hand the mass were taken to be the constituent mass of order $\Lambda_{\rm QCD}$, this term would not be negligible at all, and would substantially affect the result [note that $\alpha_s(m_\tau)/\pi \sim 0.1 \sim (0.6\,\mathrm{GeV}/m_\tau)^2$ and that $\Lambda_{\rm QCD}$ for three flavours is large]. The principle that coefficients in the operator expansion can be computed from the perturbative theory in terms of parton masses has never really been tested (due to ambiguities in the determination of condensates) and this particular case with a ZERO there is unique in making the issue crucial. Many distinguished theorists believe the optimistic version. I am not convinced that the gap is not filled up by ambiguities in $O(\Lambda_{\rm QCD}^2/m_\tau^2)$ from $\delta_{\rm pert}$ [45].

There is a vast and sophisticated literature on α_s from τ decay. Unbelievably small errors are obtained in one or the other of several different procedures and assumptions that have been adopted to end up with a specified result. With time there has been an increasing awareness of the problem of controlling higher orders and non-perturbative effects. In particular, fixed order perturbation theory (FOPT) has been compared with resummation of leading beta function effects in the so-called contour-improved perturbation theory (CIPT). The results are sizeably different in the two cases, and there have been many arguments in the literature about which method is best.

One important piece of progress comes from the experimental measurement of moments of the τ decay mass distributions, defined by modifying the weight function in the integral in (2.129). In principle, one can measure α_s from the

sum rules obtained from different weight functions that emphasize different mass intervals and different operator dimensions in the light cone operator expansion. A thorough study of the dependence of the measured value of α_s on the choice of the weight function, and in general of higher order and non-perturbative corrections, has appeared in [89], and the interested reader is advised to look at that paper and the references therein.

We consider here the recent evaluations of α_s from τ decay based on the NNNLO perturbative calculations [74] and different procedures for estimating the different kinds of corrections. From the papers given in [90], we obtain an average value and error that agrees with the Erler and Langacker's values as given in PDG 12 [307]:

$$\alpha_s(m_\tau) = 0.3285 \pm 0.018 \,, \tag{2.132}$$

or

$$\alpha_s(m_Z) = 0.1194 \pm 0.0021 \,. \tag{2.133}$$

In any case, one can discuss the error, but what is true and remarkable is that the central value of α_s from τ decay, obtained at very small Q^2, is in good agreement with all other precise determinations of α_s at more typical LEP values of Q^2.

2.10.2 α_s from Deep Inelastic Scattering

In principle, DIS is expected to be an ideal laboratory for the determination of α_s, but in practice the outcome is still to some extent unsatisfactory. QCD predicts the Q^2 dependence of $F(x, Q^2)$ at each fixed x, not the x shape. But the Q^2 dependence is related to the x shape by the QCD evolution equations. For each x bin, the data can be used to extract the slope of an approximately straight line in $\mathrm{d}\log F(x, Q^2)/\mathrm{d}\log Q^2$, i.e., the log slope. The Q^2 span and the precision of the data are not very sensitive to the curvature, for most x values. A single value of Λ_{QCD} must be fitted to reproduce the collection of the log slopes. For the determination of α_s, the scaling violations of non-singlet structure functions would be ideal, because of the minimal impact of the choice of input parton densities. We can write the non-singlet evolution equations in the form

$$\frac{\mathrm{d}}{\mathrm{d}t}\log F(x,t) = \frac{\alpha_s(t)}{2\pi}\int_x^1 \frac{\mathrm{d}y}{y}\frac{F(y,t)}{F(x,t)}P_{qq}\left(\frac{x}{y}, \alpha_s(t)\right) \,, \tag{2.134}$$

where P_{qq} is the splitting function. At present, NLO and NNLO corrections are known. It is clear from this form that, for example, the normalization error on the input density drops out, and the dependence on the input is reduced to a minimum (indeed, only a single density appears here, while in general there are quark and gluon densities).

Unfortunately, the data on non-singlet structure functions are not very accurate. If we take the difference $F_{\rm p} - F_p$ in the data on protons and neutrons, experimental errors add up and become large in the end. The $F_{3\nu{\rm N}}$ data are directly non-singlet, but are not very precise. Another possibility is to neglect sea and glue in F_2 at sufficiently large x. But by only taking data at $x > x_0$, one decreases the sample and introduces a dependence on x_0 and an error from residual singlet terms. A recent fit to non singlet structure functions in electron or muon production extracted from proton and deuterium data, neglecting sea and gluons at $x > 0.3$ (error to be evaluated), has led to the results [105]:

$$\alpha_{\rm s}(m_Z) = 0.1148 \pm 0.0019({\rm exp}) + ? \quad ({\rm NLO}) \,, \tag{2.135}$$

$$\alpha_{\rm s}(m_Z) = 0.1134 \pm 0.0020({\rm exp}) + ? \quad ({\rm NNLO}) \,. \tag{2.136}$$

The central values are rather low and there is not much difference between NLO and NNLO. The question marks refer to the uncertainties from the residual singlet component at $x > 0.3$, and also to the fact that the old BCDMS data, whose systematics has been questioned, are very important at $x > 0.3$ and push the fit towards small values of $\alpha_{\rm s}$.

When one measures $\alpha_{\rm s}$ from scaling violations in F_2, measured with e or μ beams, the data are abundant, the statistical errors are small, the ambiguities from the treatment of heavy quarks and the effects of the longitudinal structure function $F_{\rm L}$ can be controlled, but there is an increased dependence on input parton densities, and most importantly a strong correlation between the result on $\alpha_{\rm s}$ and the adopted parametrization of the gluon density. In the following we restrict our attention to recent determinations of $\alpha_{\rm s}$ from scaling violations at NNLO accuracy, such as those in [26, 254] which report the results:

$$\alpha_{\rm s}(m_Z) = 0.1134 \pm 0.0011({\rm exp}) + ? \,, \tag{2.137}$$

$$\alpha_{\rm s}(m_Z) = 0.1158 \pm 0.0035 \,. \tag{2.138}$$

In the first line the question mark refers to the issue of the $\alpha_{\rm s}$–gluon correlation. In fact, $\alpha_{\rm s}$ tends to slide towards low values ($\alpha_{\rm s} \sim 0.113$–$0.116$) if the gluon input problem is not fixed. Indeed, in the second line, taken from [254], the large error also includes an estimate of the ambiguity from the gluon density parametrization. One way to restrict the gluon density is to use the Tevatron and LHC high $p_{\rm T}$ jet data to fix the gluon parton density at large x. Via the momentum conservation sum rule, this also constrains the small x values of the same density. Of course, in this way one has to go outside the pure domain of DIS. Further, the jet rates have been computed at NLO only. In a simultaneous fit of $\alpha_{\rm s}$ and the parton densities from a set of data which, although dominated by DIS data, also contains Tevatron jets and Drell–Yan production, the result was [287]

$$\alpha_{\rm s}(m_Z) = 0.1171 \pm 0.0014 + ? \,. \tag{2.139}$$

The authors of [287] attribute their higher value of α_s to a more flexible parametrization of the gluon and the inclusion of Tevatron jet data, which are important to fix the gluon at large x.

An alternative way to cope with the gluon problem is to drastically suppress the gluon parametrization rigidity by adopting the neural network approach. With this method, the following value was obtained, in [76], from DIS data alone, treated at NNLO accuracy:

$$\alpha_s(m_Z) = 0.1166 \pm 0.0008(\text{exp}) \pm 0.0009(\text{th}) + ? \,, \tag{2.140}$$

where the stated theoretical error is that quoted by the authors within their framework, while the question mark has to do with possible additional systematics from the method adopted. Interestingly, in the same approach, not much difference is found by also including the Tevatron jets and the Drell–Yan data:

$$\alpha_s(m_Z) = 0.1173 \pm 0.0007(\text{exp}) \pm 0.0009(\text{th}) + ? \,. \tag{2.141}$$

We see that, when the gluon input problem is suitably addressed, the fitted value of α_s is increased.

As we have seen there is some spread of results, even among the most recent determinations based on NNLO splitting functions. We tend to favour determinations from the whole DIS set of data (i.e., beyond the pure non-singlet case) and with attention paid to the gluon ambiguity problem (even if some non DIS data from Tevatron jets at NLO have to be included). A conservative proposal for the resulting value of α_s from DIS which emerges from the above discussion would be something like

$$\alpha_s(m_Z) = 0.1165 \pm 0.0020 \,. \tag{2.142}$$

The central value is below those obtained from Z and τ decays, but perfectly compatible with those results.

2.10.3 Recommended Value of $\alpha_s(m_Z)$

According to my proposal to calibrate $\alpha_s(m_Z)$ from the theoretically cleanest and most transparent methods, identified as the totally inclusive, light cone operator expansion dominated processes, I collect here my understanding of the results:

- From Z decays and EW precision tests, i.e., (2.126):

$$\alpha_s(m_Z) = 0.1190 \pm 0.0026 \,. \tag{2.143}$$

- From scaling violations in DIS, i.e., (2.142):

$$\alpha_s(m_Z) = 0.1165 \pm 0.0020 \,. \tag{2.144}$$

- From R_τ (2.133):

$$\alpha_s(m_Z) = 0.1194 \pm 0.0021. \tag{2.145}$$

If one wants to be on the safe side, one can take the average of Z decay and DIS, i.e.,

$$\alpha_s(m_Z) = 0.1174 \pm 0.0016\ . \tag{2.146}$$

This is my recommended value. If one adds to the average the rather conservative R_τ value and error given above in (2.145), which takes into account the dangerously low energy scale of the process, one obtains

$$\alpha_s(m_Z) = 0.1184 \pm 0.0011\ . \tag{2.147}$$

Note that this essentially coincides with the "official" average, with a moderate increase in the error.

2.10.4 Other $\alpha_s(m_Z)$ Measurements as QCD Tests

There are a number of other determinations of α_s that are important because they arise from qualitatively different observables and methods. Here I will give a few examples of the most interesting measurements.

A classic set of measurements comes from a number of infrared-safe observables related to event rates and jet shapes in e^+e^- annihilation. One important feature of these measurements is that they can be repeated at different energies in the same detector, like the JADE detector in the energy range of PETRA (most of the intermediate energy points in the right-hand panel of Fig. 2.32 are from this class of measurements) or the LEP detectors from LEP1 to LEP2 energies. As a result, one obtains a striking direct confirmation of the running of the coupling according to the renormalization group prediction. The perturbative part is known at NNLO [213], and resummations of leading logs arising from the vicinity of cuts and/or boundaries have been performed in many cases using effective field theory methods. The main problem with these measurements is the possibly large impact of non-perturbative hadronization effects on the result, and therefore on the theoretical error.

According to [99], a summarizing result that takes into account the central values and the spread from the JADE measurements at PETRA, in the range 14–46 GeV, is

$$\alpha_s(m_Z) = 0.1172 \pm 0.0051\ ,$$

while from the ALEPH data at LEP, in the range 90–206 GeV, the reported value [164] is

$$\alpha_s(m_Z) = 0.1224 \pm 0.0039\ .$$

It is amazing to note that among the related works there are a couple of papers by Abbate et al. [10, 11] where an extremely sophisticated formalism is developed for the thrust distribution, based on NNLO perturbation theory with resummations at NNNLL plus a data/theory-based estimate of non-perturbative corrections. The final quoted results are unbelievably precise:

$$\alpha_s(m_Z) = 0.1135 \pm 0.0011 \,,$$

from the tail of the thrust distribution [10], and

$$\alpha_s(m_Z) = 0.1140 \pm 0.0015 \,,$$

from the first moment of the thrust distribution [11]. I think that this is a good example of an underestimated error which is obtained within a given machinery without considering the limits of the method itself.

Another allegedly very precise determination of $\alpha_s(m_Z)$ is obtained from lattice QCD by several groups [288] with different methods and compatible results. A value that summarizes these different results is [307]

$$\alpha_s(m_Z) = 0.1185 \pm 0.0007 \,.$$

With all due respect to the lattice community, I think this small error is totally unrealistic. But we have shown that a sufficiently precise measurement of $\alpha_s(m_Z)$ can be obtained, viz., (2.146) and (2.147), by using only the simplest processes, where the control of theoretical errors is maximal. One is left free to judge whether a further restriction of theoretical errors is really on solid ground.

The value of Λ (for $n_f = 5$) which corresponds to (2.146) is

$$\Lambda_5 = 202 \pm 18\,\text{MeV} \,, \tag{2.148}$$

while the value from (2.147) is

$$\Lambda_5 = 213 \pm 13\,\text{MeV} \,. \tag{2.149}$$

Λ is the scale of mass that finally appears in massless QCD. It is the scale where $\alpha_s(\Lambda)$ is of order 1. Hadron masses are determined by Λ. Actually, the ρ mass or the nucleon mass receive little contribution from the quark masses (the case of pseudoscalar mesons is special, as they are the pseudo-Goldstone bosons of broken chiral invariance). Hadron masses would be almost the same in massless QCD.

2.11 Conclusion

We have seen that perturbative QCD based on asymptotic freedom offers a rich variety of tests, and we have described some examples in detail. QCD tests are not as precise as for the electroweak sector. But the number and diversity of such tests has established a very firm experimental foundation for QCD as a theory of strong interactions. The physics content of QCD is very large and our knowledge, especially in the non-perturbative domain, is still very limited, but progress both from experiment (Tevatron, RHIC, LHC, etc.) and from theory is continuing at a healthy rate. And all the QCD predictions that we have been able to formulate and to test appear to be in very good agreement with experiment.

The field of QCD appears to be one of great maturity, but also of robust vitality, with many rich branches and plenty of new blossoms. I may mention the very exciting explorations of supersymmetric extensions of QCD and the connections with string theory (for a recent review and a list of references, see [166]). In particular, $N = 4$ SUSY QCD (that is, with four spinor charge generators) has a vanishing beta function and is loop-finite. In the limit $N_C \to \infty$ with $\lambda = e_s^2 N_C$ fixed, planar diagrams are dominant. There is progress towards a solution of planar $N = 4$ SUSY QCD. The large λ limit corresponds by the AdS/CFT duality (anti-de Sitter/conformal field theory), a string theory concept, to the weakly coupled string (gravity) theory on $AdS_5 \times S_5$ (the 10 dimensions are compactified in a 5-dimensional anti-de Sitter space times a 5-dimensional sphere). By moving along this very tentative route, one can transfer some results (assumed to be of sufficiently universal nature) from the computable weak limit of the associated string theory to the non-perturbative ordinary QCD domain. Further along this line of investigation, there are studies of $N = 8$ supergravity, related to $N = 4$ SUSY Yang–Mills, which has been proven finite up to four loops. It could possibly lead to a finite field theory of gravity in four dimensions.

Open Access This chapter is licensed under the terms of the Creative Commons Attribution 4.0 International License (http://creativecommons.org/licenses/by/4.0/), which permits use, sharing, adaptation, distribution and reproduction in any medium or format, as long as you give appropriate credit to the original author(s) and the source, provide a link to the Creative Commons license and indicate if changes were made.

The images or other third party material in this chapter are included in the chapter's Creative Commons license, unless indicated otherwise in a credit line to the material. If material is not included in the chapter's Creative Commons license and your intended use is not permitted by statutory regulation or exceeds the permitted use, you will need to obtain permission directly from the copyright holder.

Chapter 3
The Theory of Electroweak Interactions

3.1 Introduction

In this chapter, we summarize the structure of the standard EW theory[1] and specify the couplings of the intermediate vector bosons $W^{\pm}$ and Z and those of the Higgs particle with the fermions and among themselves, as dictated by the gauge symmetry plus the observed matter content and the requirement of renormalizability. We discuss the realization of spontaneous symmetry breaking and the Higgs mechanism. We then review the phenomenological implications of the EW theory for collider physics, that is, we leave aside the classic low energy processes that are well described by the "old" weak interaction theory (see, for example, [148]).

For this discussion, we split the Lagrangian into two parts by separating the terms with the Higgs field:

$$\mathscr{L} = \mathscr{L}_{\text{gauge}} + \mathscr{L}_{\text{Higgs}} \,. \tag{3.1}$$

Both terms are written down as prescribed by the $SU(2) \bigotimes U(1)$ gauge symmetry and renormalizability, but the Higgs vacuum expectation value (VEV) induces the spontaneous symmetry breaking responsible for the non-vanishing vector boson and fermion masses.

[1] Some recent textbooks are listed in [276]. See also [34, 313].

© The Author(s) 2017

G. Altarelli, *Collider Physics within the Standard Model*,
Lecture Notes in Physics 937, DOI 10.1007/978-3-319-51920-3_3

3.2 The Gauge Sector

We start by specifying $\mathscr{L}_{\text{gauge}}$, which involves only gauge bosons and fermions, according to the general formalism of gauge theories discussed in Chap. 1:

$$\mathscr{L}_{\text{gauge}} = -\frac{1}{4}\sum_{A=1}^{3} F^A_{\mu\nu}F^{A\mu\nu} - \frac{1}{4}B_{\mu\nu}B^{\mu\nu} + \bar{\psi}_{\text{L}}\text{i}\gamma^\mu D_\mu \psi_{\text{L}} + \bar{\psi}_{\text{R}}\text{i}\gamma^\mu D_\mu \psi_{\text{R}} \ . \tag{3.2}$$

This is the Yang–Mills Lagrangian for the gauge group $SU(2) \otimes U(1)$ with fermion matter fields. Here

$$B_{\mu\nu} = \partial_\mu B_\nu - \partial_\nu B_\mu \ , \qquad F^A_{\mu\nu} = \partial_\mu W^A_\nu - \partial_\nu W^A_\mu - g\epsilon_{ABC}\, W^B_\mu W^C_\nu \ , \tag{3.3}$$

are the gauge antisymmetric tensors constructed out of the gauge field B_μ associated with $U(1)$ and W^A_μ corresponding to the three $SU(2)$ generators, while ϵ_{ABC} are the group structure constants [see (3.5) and (3.6)], which, for $SU(2)$, coincide with the totally antisymmetric Levi-Civita tensor, with $\epsilon_{123} = 1$ (recall the familiar angular momentum commutators). The normalization of the $SU(2)$ gauge coupling g is therefore specified by (3.3).

As discussed in Sect. 1.5, the standard EW theory is a chiral theory, in the sense that ψ_{L} and ψ_{R} behave differently under the gauge group (so that parity and charge conjugation non-conservation are made possible in principle). Thus, mass terms for fermions (of the form $\bar{\psi}_{\text{L}}\psi_{\text{R}} + \text{h.c.}$) are forbidden in the symmetric limit. In the following, $\psi_{\text{L,R}}$ are column vectors, including all fermion types in the theory that span generic reducible representations of $SU(2) \otimes U(1)$.

In the absence of mass terms, there are only vector and axial vector interactions in the Lagrangian, and these have the property of not mixing ψ_{L} and ψ_{R}. Fermion masses will be introduced, together with $W^\pm$ and Z masses, by the mechanism of symmetry breaking. The covariant derivatives $D_\mu\psi_{\text{L,R}}$ are given explicitly by

$$D_\mu \psi_{\text{L,R}} = \left(\partial_\mu + \text{i}g\sum_{A=1}^{3} t^A_{\text{L,R}} W^A_\mu + \text{i}g'\frac{1}{2}Y_{\text{L,R}}B_\mu\right)\psi_{\text{L,R}} \ , \tag{3.4}$$

where $t^A_{\text{L,R}}$ and $Y_{\text{L,R}}/2$ are the $SU(2)$ and $U(1)$ generators, respectively, in the reducible representations $\psi_{\text{L,R}}$. The commutation relations of the $SU(2)$ generators are given by

$$\left[t^A_{\text{L}}, t^B_{\text{L}}\right] = \text{i}\epsilon_{ABC}t^C_{\text{L}} \ , \quad \left[t^A_{\text{R}}, t^B_{\text{R}}\right] = \text{i}\epsilon_{ABC}t^C_{\text{R}} \ . \tag{3.5}$$

We use the normalization in (1.11) [in the fundamental representation of $SU(2)$]. The electric charge generator Q (in units of e, the positron charge) is given by

$$Q = t_{\rm L}^3 + \frac{1}{2}Y_{\rm L} = t_{\rm R}^3 + \frac{1}{2}Y_{\rm R} \ . \tag{3.6}$$

Note that the normalization of the $U(1)$ gauge coupling g' in (3.4) is now specified as a consequence of (3.6). Note also that $t_{\rm R}^i \psi_{\rm R} = 0$, given that, for all known quarks and leptons, $\psi_{\rm R}$ is a singlet. But in the following, we keep $t_{\rm R}^i \psi_{\rm R}$ for generality, in case one day a non-singlet right-handed fermion is discovered.

3.3 Couplings of Gauge Bosons to Fermions

All fermion couplings of the gauge bosons can be derived directly from (3.2) and (3.4). The charged W_μ fields are described by $W_\mu^{1,2}$, while the photon A_μ and weak neutral gauge boson Z_μ are obtained from combinations of W_μ^3 and B_μ. The charged-current (CC) couplings are the simplest. One starts from the $W_\mu^{1,2}$ terms in (3.2) and (3.4), which can be written as

$$\begin{aligned} g(t^1 W_\mu^1 + t^2 W_\mu^2) &= g\left[\frac{1}{\sqrt{2}}(t^1 + {\rm i}t^2)\frac{1}{\sqrt{2}}(W_\mu^1 - {\rm i}W_\mu^2) + {\rm h.c.}\right] \\ &= g\left(\frac{1}{\sqrt{2}}t^+ W_\mu^- + {\rm h.c.}\right) \ , \end{aligned} \tag{3.7}$$

where $t^\pm = t^1 \pm {\rm i}t^2$ and $W^\pm = (W^1 \pm {\rm i}W^2)/\sqrt{2}$. By applying this generic relation to L and R fermions separately, we obtain the vertex

$$V_{\bar\psi\psi W} = g\bar\psi\gamma_\mu\left[\frac{1}{\sqrt{2}}t_{\rm L}^+\frac{1}{2}(1-\gamma_5) + \frac{1}{\sqrt{2}}t_{\rm R}^+\frac{1}{2}(1+\gamma_5)\right]\psi W_\mu^- + {\rm h.c.} \tag{3.8}$$

Given that $t_{\rm R} = 0$ for all fermions in the SM, the charged current is pure $V-A$. In the neutral current (NC) sector, the photon A_μ and the mediator Z_μ of the weak NC are orthogonal and normalized linear combinations of B_μ and W_μ^3:

$$\begin{aligned} A_\mu &= \cos\theta_{\rm W} B_\mu + \sin\theta_{\rm W} W_\mu^3 \ , \\ Z_\mu &= -\sin\theta_{\rm W} B_\mu + \cos\theta_{\rm W} W_\mu^3 \ , \end{aligned} \tag{3.9}$$

whence

$$\begin{aligned} W_\mu^3 &= \sin\theta_{\rm W} A_\mu + \cos\theta_{\rm W} Z_\mu \ , \\ B_\mu &= \cos\theta_{\rm W} A_\mu - \sin\theta_{\rm W} Z_\mu \ . \end{aligned} \tag{3.10}$$

Equations (3.9) define the weak mixing angle $\theta_{\rm W}$. We can rewrite the W^3_μ and B_μ terms in (3.2) and (3.4) as follows:

$$gt^3 W^3_\mu + \frac{1}{2} g' Y B_\mu = \left[gt^3 \sin\theta_{\rm W} + g'(Q - t^3)\cos\theta_{\rm W} \right] A_\mu + \left[gt^3 \cos\theta_{\rm W} - g'(Q - t^3)\sin\theta_{\rm W} \right] Z_\mu \,, \tag{3.11}$$

where (3.6) was also used for the charge matrix Q. The photon is characterized by equal couplings to left and right fermions, with a strength equal to the electric charge. Thus we immediately obtain

$$g \sin\theta_{\rm W} = g' \cos\theta_{\rm W} = e \,, \tag{3.12}$$

so that

$$\tan\theta_{\rm W} = g'/g \,. \tag{3.13}$$

Once $\theta_{\rm W}$ has been fixed by the photon couplings, it is a matter of simple algebra to derive the Z couplings, with the result

$$V_{\bar\psi\psi Z} = \frac{g}{2\cos\theta_{\rm W}} \bar\psi \gamma_\mu \left[t^3_{\rm L}(1 - \gamma_5) + t^3_{\rm R}(1 + \gamma_5) - 2Q \sin^2\theta_{\rm W} \right] \psi Z^\mu \,, \tag{3.14}$$

where $V_{\bar\psi\psi Z}$ is a notation for the vertex. Once again, recall that in the minimal SM, $t^3_{\rm R} = 0$ and $t^3_{\rm L} = \pm 1/2$.

In order to derive the effective four-fermion interactions, which are equivalent at low energies to the CC and NC couplings given in (3.8) and (3.14), we anticipate that large masses, as observed experimentally, are provided for $W^\pm$ and Z by $\mathscr{L}_{\rm Higgs}$. For left–left CC couplings, when the square of the momentum transfer can be neglected (in comparison with m^2_W) in the propagator of Born diagrams with single W exchange (see, for example, the diagram for μ decay in Fig. 3.1), Eq. (3.8) implies

$$\mathscr{L}^{\rm C}_{\rm eff} \simeq \frac{g^2}{8 m^2_W} \left[\bar\psi \gamma_\mu (1 - \gamma_5) t^+_{\rm L} \psi \right] \left[\bar\psi \gamma^\mu (1 - \gamma_5) t^-_{\rm L} \psi \right] . \tag{3.15}$$

By specializing further in the case of doublet fields, such as $\nu_e - e^-$ or $\nu_\mu - \mu^-$, we obtain the tree-level relation of g with the Fermi coupling constant $G_{\rm F}$ precisely

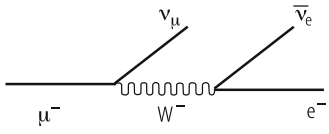

Fig. 3.1 Born diagram for μ decay

measured from μ decay [see (1.2) and (1.3)]:

$$\frac{G_{\rm F}}{\sqrt{2}} = \frac{g^2}{8m_W^2} \,. \tag{3.16}$$

Recalling that $g \sin\theta_{\rm W} = e$, we can also cast this relation in the form

$$m_W = \frac{\mu_{\rm Born}}{\sin\theta_{\rm W}} \,, \tag{3.17}$$

with

$$\mu_{\rm Born} = \left(\frac{\pi\alpha}{\sqrt{2}G_{\rm F}}\right)^{1/2} \simeq 37.2802\,{\rm GeV}\,, \tag{3.18}$$

where α is the QED fine-structure constant ($\alpha \equiv e^2/4\pi = 1/137.036$).

In the same way, for neutral currents, in the Born approximation, (3.14) yields the effective four-fermion interaction:

$$\mathscr{L}_{\rm eff}^{\rm NC} \simeq \sqrt{2}\, G_{\rm F}\rho_0 \bar{\psi}\gamma_\mu[\ldots]\psi\bar{\psi}\gamma^\mu[\ldots]\psi \,, \tag{3.19}$$

where

$$[\ldots] \equiv t_{\rm L}^3(1-\gamma_5) + t_{\rm R}^3(1+\gamma_5) - 2Q\sin^2\theta_{\rm W} \tag{3.20}$$

and

$$\rho_0 = \frac{m_W^2}{m_Z^2\cos^2\theta_{\rm W}} \,. \tag{3.21}$$

All couplings given in this section are valid at tree level, and are modified in higher orders of perturbation theory. In particular, the relations between m_W and $\sin\theta_{\rm W}$ [(3.17) and (3.18)] and the observed values of ρ ($\rho = \rho_0$ at tree level) in different NC processes, are altered by computable EW radiative corrections, as discussed in Sect. 3.11.

The partial width $\Gamma(W \to \bar{f}f')$ is given in the Born approximation by the simplest diagram in Fig. 3.2, and with $t_{\rm R} = 0$, one readily obtains from (3.8), in the limit of

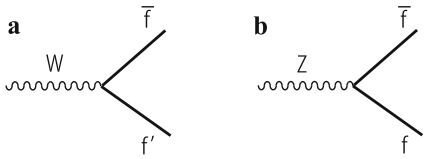

Fig. 3.2 Diagrams for (**a**) the W and (**b**) the Z widths in the Born approximation

neglecting the fermion masses and summing over all possible f' for a given f,

$$\Gamma(W \to \bar{f}f') = N_{\rm C}\frac{G_{\rm F}m_W^3}{6\pi\sqrt{2}} = N_{\rm C}\frac{\alpha m_W}{12\sin^2\theta_{\rm W}}\,, \tag{3.22}$$

where $N_{\rm C} = 3$ or 1 is the number of colours for quarks or leptons, respectively, and (3.12) and (3.16) have been used. Here and in the following expressions for the Z widths, the one-loop QCD corrections for the quark channels can be absorbed in a redefinition of $N_{\rm C}$:

$$N_{\rm C} \to 3\big[1 + \alpha_{\rm s}(m_Z)/\pi + \cdots\big]\,.$$

Note that the widths are particularly large because the rate already occurs at order g^2 or $G_{\rm F}$. The experimental values of the total W width and the leptonic branching ratio (the average of e, μ, and τ modes) are [307, 350] (see Sect. 3.11):

$$\Gamma_W = 2.085 \pm 0.042\,{\rm GeV}\,, \qquad B(W \to l\nu_l) = 10.80 \pm 0.09\,. \tag{3.23}$$

The branching ratio B is in very good agreement with the simple approximate formula, derived from (3.22):

$$B(W \to l\nu_l) \sim \frac{1}{2\times 3\times\big[1+\alpha_{\rm s}(m_Z^2)/\pi\big]+3} \sim 10.8\%\,. \tag{3.24}$$

The denominator corresponds to the sum of the final states $d'\bar{u}$, $s'\bar{c}$, $e^-\bar{\nu}_e$, $\mu^-\bar{\nu}_\mu$, $\tau^-\bar{\nu}_\tau$, where d' and s' are defined in (3.63).

For $t_{\rm R} = 0$, the Z coupling to fermions in (3.14) can be cast into the form

$$V_{\bar{\psi}_f\psi_f Z} = \frac{g}{2\cos\theta_{\rm W}}\bar{\psi}_f\gamma_\mu\big[g_{\rm V}^f - g_{\rm A}^f\gamma_5\big]\psi_f Z^\mu\,, \tag{3.25}$$

with

$$g_{\rm A}^f = t_{\rm L}^{3f}\,, \quad g_{\rm V}^f/g_{\rm A}^f = 1 - 4|Q_f|\sin^2\theta_{\rm W}\,, \tag{3.26}$$

and $t_{\rm L}^{3f} = \pm 1/2$ for up-type or down-type fermions. In terms of $g_{\rm A,V}$ given in (3.26) (the widths are proportional to $g_{\rm V}^2 + g_{\rm A}^2$), for negligible fermion masses, the partial width $\Gamma(Z \to \bar{f}f)$ in the Born approximation (see the diagram in Fig. 3.2) is given by

$$\begin{aligned}\Gamma(Z \to \bar{f}f) &= N_{\rm C}\frac{\alpha m_Z}{12\sin^2 2\theta_{\rm W}}\big[1 + (1 - 4|Q_f|\sin^2\theta_{\rm W})^2\big] \\ &= N_{\rm C}\rho_0\frac{G_{\rm F}m_Z^3}{24\pi\sqrt{2}}\big[1 + (1 - 4|Q_f|\sin^2\theta_{\rm W})^2\big]\,,\end{aligned} \tag{3.27}$$

where $\rho_0 = m_W^2/m_Z^2 \cos^2\theta_W$ is given in (3.52). The experimental values of the total Z width and the partial rates into charged leptons (average of e, μ, and τ), into hadrons and into invisible channels are [307, 350]

$$\begin{aligned} \Gamma_Z &= 2.4952 \pm 0.0023\,\text{GeV}\,, \quad \Gamma_{l^+l^-} = 83.984 \pm 0.086\,\text{MeV}\,, \\ \Gamma_h &= 1744.4 \pm 2.0\,\text{MeV}\,, \quad \Gamma_{\text{inv}} = 499.0 \pm 1.5\,\text{MeV}\,. \end{aligned} \tag{3.28}$$

The measured value of the Z invisible width, taking radiative corrections into account, leads to the determination of the number of light active neutrinos [307, 350]:

$$N_\nu = 2.9840 \pm 0.0082\,, \tag{3.29}$$

well compatible with the three known neutrinos ν_e, ν_μ, and ν_τ. Hence, there exist only the three known sequential generations of fermions (with light neutrinos), a result which also has important consequences in astrophysics and cosmology.

At the Z peak, besides total cross-sections, various types of asymmetries have been measured. The results of all asymmetry measurements are quoted in terms of the asymmetry parameter A_f, defined in terms of the effective coupling constants, g_V^f and g_A^f, as

$$A_f = 2\frac{g_V^f g_A^f}{g_V^{f2} + g_A^{f2}} = 2\frac{g_V^f/g_A^f}{1 + (g_V^f/g_A^f)^2}\,, \qquad A_{FB}^f = \frac{3}{4}A_e A_f\,. \tag{3.30}$$

The measurements are the forward–backward asymmetry ($A_{FB}^f = 3A_e A_f/4$), the tau polarization (A_τ) and its forward–backward asymmetry (A_e) measured at LEP, and also the left–right and left–right forward–backward asymmetry measured at SLC (A_e and A_f, respectively). Hence, the set of partial width and asymmetry results allows the extraction of the effective coupling constants: widths measure $(g_V^2 + g_A^2)$ and asymmetries measure g_V/g_A.

The top quark is heavy enough to be able to decay into a real bW pair, which is by far its dominant decay channel. The next mode, $t \to sW$, is suppressed in rate by a factor $|V_{ts}|^2 \sim 1.7 \times 10^{-3}$ [see (3.68)–(3.70)]. The associated width, neglecting m_b effects but including 1-loop QCD corrections in the limit $m_W = 0$, is given by (we have omitted a factor $|V_{tb}|^2$ that we set equal to 1) [253]

$$\Gamma(t \to bW^+) = \frac{G_F m_t^3}{8\pi\sqrt{2}}\left(1 - \frac{m_W^2}{m_t^2}\right)^2\left(1 + 2\frac{m_W^2}{m_t^2}\right)\left[1 - \frac{2\alpha_s(m_Z)}{3\pi}\left(\frac{2\pi^2}{3} - \frac{5}{2}\right) + \cdots\right]. \tag{3.31}$$

The top quark lifetime is so short, about 0.5×10^{-24} s, that it decays before hadronizing or forming toponium bound states.

3.4 Gauge Boson Self-Interactions

The gauge boson self-interactions can be derived from the $F_{\mu\nu}$ term in $\mathscr{L}_{\text{gauge}}$ using (3.9) and $W^{\pm} = (W^1 \pm \mathrm{i}W^2)/\sqrt{2}$. Defining the three-gauge-boson vertex as in Fig. 3.3 (with all incoming lines), we obtain

$$V_{W^-W^+V} = \mathrm{i}g_{W^-W^+V}\left[g_{\mu\nu}(p-q)_\lambda + g_{\mu\lambda}(r-p)_\nu + g_{\nu\lambda}(q-r)_\mu\right], \tag{3.32}$$

with $V \equiv \gamma, Z$ and

$$g_{W^-W^+\gamma} = g\sin\theta_{\mathrm{W}} = e\,, \qquad g_{W^-W^+Z} = g\cos\theta_{\mathrm{W}}\,. \tag{3.33}$$

Note that the photon coupling to the W is fixed by the electric charge, as imposed by QED gauge invariance. The ZWW coupling is larger by a factor of $\cot\theta_{\mathrm{W}}$. This form of the triple gauge vertex is very special: in general, there could be departures from the above SM expression, even if we restrict to Lorentz invariant, electromagnetic gauge symmetric, and C and P conserving couplings. In fact, some small corrections are already induced by the radiative corrections. But, in principle, the modifications induced by some new physics effect could be more important. The experimental testing of the triple gauge vertices has been done in the past, mainly at LEP2 and at the Tevatron [235], and now also at the LHC [319].

As a particularly important example, the cross-section and angular distributions for the process $e^+e^- \to W^+W^-$ have been studied at LEP2. In the Born approximation, the Feynman diagrams for the LEP2 process are shown in Fig. 3.4 [46]. Besides neutrino exchange, which only involves the well established charged

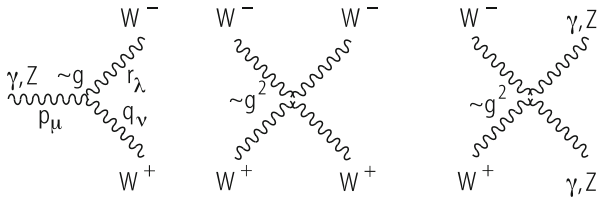

Fig. 3.3 The 3- and 4-gauge boson vertices. The cubic coupling is of order g and the quartic coupling of order g^2

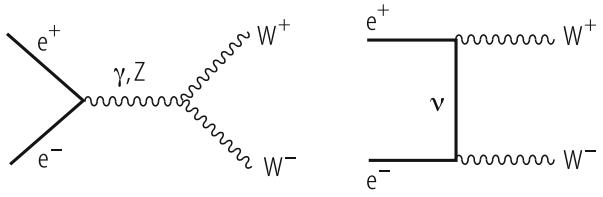

Fig. 3.4 Lowest order diagrams for $e^+e^- \to W^+W^-$

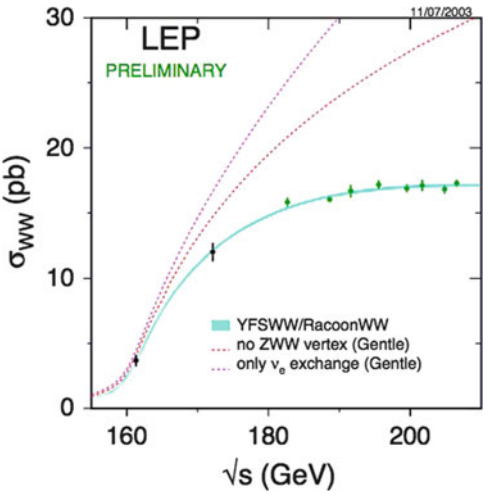

Fig. 3.5 Measured production cross-section for $e^+e^- \to W^+W^-$ compared to the SM and fictitious theories, not including trilinear gauge couplings, as indicated. From [281]

current vertex, the triple weak gauge vertices $V_{W^-W^+V}$ appear in the γ and Z exchange diagrams. The Higgs exchange is negligible because the electron mass is very small. The analytic cross-section formula in the Born approximation can be found, for example, in [307] (in the section entitled *Cross-section formulae for specific processes*). The experimental data are compared with the SM prediction in Fig. 3.5. Within the present accuracy, the agreement is good. Note that the sum of all three exchange amplitudes has a better high energy behaviour than its individual components. This is due to cancellations among the amplitudes implied by gauge invariance, connected to the fact that the theory is renormalizable (the cross-section can be seen as a contribution to the imaginary part of the $e^+e^- \to e^+e^-$ amplitude).

The quartic gauge coupling is proportional to $g^2\epsilon_{ABC}W^BW^C\epsilon_{ADE}W^DW^E$. Thus in the term with $A = 3$, we have four charged W particles. For $A = 1$ or 2, we have two charged W particles and two W^3 particles, each W_3 being a combination of γ and Z according to (3.10). With a little algebra the quartic vertex can be cast in the form

$$V_{WWVV} = \mathrm{i}g_{WWVV}\left(2g_{\mu\nu}g_{\lambda\rho} - g_{\mu\lambda}g_{\nu\rho} - g_{\mu\rho}g_{\nu\lambda}\right) , \tag{3.34}$$

where μ and ν refer to W^+W^+ in the $4W$ vertex and to VV in the $WWVV$ case, and

$$g_{WWWW} = g^2 , \quad g_{WW\gamma\gamma} = -e^2 , \quad g_{WW\gamma Z} = -eg\cos\theta_\mathrm{W} , \quad g_{WWZZ} = -g^2\cos^2\theta_\mathrm{W} . \tag{3.35}$$

In order to obtain these results for the vertex, the reader must duly take into account the factor of $-1/4$ in front of $F^2_{\mu\nu}$ in the Lagrangian and the statistical factors which are equal to 2 for each pair of identical particles (like W^+W^+ or $\gamma\gamma$, for example). As the quartic coupling is quadratic in g and hence small, it has not yet been possible to test it directly.

3.5 The Higgs Sector

We now turn to the Higgs sector of the EW Lagrangian [243]. Until recently, this simplest realization of the EW symmetry breaking was a pure conjecture. But in July 2012 the ATLAS and CMS Collaborations at the CERN LHC announced [2, 135] the discovery of a particle with mass $m_{\rm H} \sim 126\,{\rm GeV}$ that looks very much like the long sought Higgs particle. More precise measurements of its couplings and the proof that its spin is zero are necessary before the identification with the SM Higgs boson can be completely established. But the following description of the Higgs sector of the SM can now be read with this striking development in mind.

The Higgs Lagrangian is specified by the gauge principle and the requirement of renormalizability to be

$$\mathscr{L}_{\rm Higgs} = (D_\mu \phi)^\dagger (D^\mu \phi) - V(\phi^\dagger \phi) - \bar{\psi}_{\rm L} \Gamma \psi_{\rm R} \phi - \bar{\psi}_{\rm R} \Gamma^\dagger \psi_{\rm L} \phi^\dagger \,, \tag{3.36}$$

where ϕ is a column vector including all Higgs fields which generally transforms as a reducible representation of the gauge group $SU(2)_{\rm L} \otimes U(1)$. In the minimal SM, it is just a complex doublet. The quantities Γ (which include all coupling constants) are matrices that make the Yukawa couplings invariant under the Lorentz and gauge groups. The potential $V(\phi^\dagger \phi)$, symmetric under $SU(2)_{\rm L} \otimes U(1)$, contains at most quartic terms in ϕ so that the theory is renormalizable:

$$V(\phi^\dagger \phi) = -\mu^2 \phi^\dagger \phi + \frac{1}{2} \lambda (\phi^\dagger \phi)^2 \tag{3.37}$$

As discussed in Chap. 1, spontaneous symmetry breaking is induced if the minimum of V, which is the classical analogue of the quantum mechanical vacuum state, is not a single point but a whole orbit obtained for non-vanishing ϕ values. Precisely, we denote the vacuum expectation value (VEV) of ϕ, i.e., the position of the minimum, by v (which is a doublet):

$$\langle 0 | \phi(x) | 0 \rangle = v = \begin{pmatrix} 0 \\ v \end{pmatrix} \neq 0 \,. \tag{3.38}$$

The reader should be careful that, for economy of notation, the same symbol is used for the doublet and for the only nonzero component of the same doublet. The fermion mass matrix is obtained from the Yukawa couplings by replacing $\phi(x)$ by v :

$$M = \bar{\psi}_{\rm L} \mathscr{M} \psi_{\rm R} + \bar{\psi}_{\rm R} \mathscr{M}^\dagger \psi_{\rm L} \,, \tag{3.39}$$

with

$$\mathscr{M} = \Gamma v \,. \tag{3.40}$$

In the MSM, where all left fermions $\psi_{\rm L}$ are doublets and all right fermions $\psi_{\rm R}$ are singlets, only Higgs doublets can contribute to fermion masses. There are enough free couplings in Γ to ensure that a single complex Higgs doublet is indeed sufficient to generate the most general fermion mass matrix. It is important to observe that, by a suitable change of basis, we can always make the matrix $\mathscr{M}$ Hermitian (so that the mass matrix is γ_5-free) and diagonal. In fact, we can make separate unitary transformations on $\psi_{\rm L}$ and $\psi_{\rm R}$ according to

$$\psi'_{\rm L} = U\psi_{\rm L} \ , \quad \psi'_{\rm R} = W\psi_{\rm R} \ , \tag{3.41}$$

and consequently,

$$\mathscr{M} \to \mathscr{M}' = U^\dagger \mathscr{M} W \ . \tag{3.42}$$

This transformation produces different effects on mass terms and on the structure of the fermion couplings in $\mathscr{L}_{\rm symm}$, because both the kinetic terms and the couplings to gauge bosons do not mix L and R spinors. The combined effect of these unitary rotations leads to the phenomenon of mixing and, generically, to flavour-changing neutral currents (FCNC), as we shall see in Sect. 3.6.

If only one Higgs doublet is present, the change of basis that makes $\mathscr{M}$ diagonal will at the same time diagonalize the fermion–Higgs Yukawa couplings. Thus, in this case, no flavour-changing neutral Higgs vertices are present. This is not true, in general, when there are several Higgs doublets. But one Higgs doublet for each electric charge sector, i.e., one doublet coupled only to u-type quarks, one doublet to d-type quarks, one doublet to charged leptons, and possibly one for neutrino Dirac masses, would also be acceptable, because the mass matrices of fermions with different charges are diagonalized separately. For several Higgs doublets in a given charge sector, it is also possible to generate CP violation by complex phases in the Higgs couplings. In the presence of six quark flavours, this CP violation mechanism is not necessary. In fact, at the moment, the simplest model with only one Higgs doublet could be adequate for describing all observed phenomena.

We now consider the gauge boson masses and their couplings to the Higgs. These effects are induced by the $(D_\mu\phi)^\dagger(D^\mu\phi)$ term in $\mathscr{L}_{\rm Higgs}$ [see (3.36)], where

$$D_\mu\phi = \left(\partial_\mu + {\rm i}g\sum_{A=1}^{3} t^A W_\mu^A + {\rm i}g'\frac{Y}{2}B_\mu\right)\phi \ . \tag{3.43}$$

Here t^A and $Y/2$ are the $SU(2)\otimes U(1)$ generators in the reducible representation spanned by ϕ. Not only doublets, but all non-singlet Higgs representations can contribute to gauge boson masses. The condition that the photon remain massless is equivalent to the condition that the vacuum be electrically neutral:

$$Q|v\rangle = \left(t^3 + \frac{1}{2}Y\right)|v\rangle = 0 \ . \tag{3.44}$$

We now explicitly consider the case of a single Higgs doublet:

$$\phi = \begin{pmatrix} \phi^+ \\ \phi^0 \end{pmatrix} , \qquad v = \begin{pmatrix} 0 \\ v \end{pmatrix} . \tag{3.45}$$

The charged W mass is given by the quadratic terms in the W field arising from $\mathscr{L}_{\text{Higgs}}$, when $\phi(x)$ is replaced by v in (3.38). Recalling (3.7), we obtain

$$m_W^2 W_\mu^+ W^{-\mu} = g^2 \left| t^+ v/\sqrt{2} \right|^2 W_\mu^+ W^{-\mu} , \tag{3.46}$$

whilst for the Z mass we get [recalling (3.9)–(3.11)]

$$\frac{1}{2} m_Z^2 Z_\mu Z^\mu = \left| \left(g t^3 \cos\theta_{\text{W}} - g' \frac{Y}{2} \sin\theta_{\text{W}} \right) v \right|^2 Z_\mu Z^\mu , \tag{3.47}$$

where the factor of 1/2 on the left-hand side is the correct normalization for the definition of the mass of a neutral field. Using (3.44), relating the action of t^3 and $Y/2$ on the vacuum v, and (3.13), we obtain

$$\frac{1}{2} m_Z^2 = (g \cos\theta_{\text{W}} + g' \sin\theta_{\text{W}})^2 |t^3 v|^2 = \frac{g^2}{\cos^2\theta_{\text{W}}} |t^3 v|^2 . \tag{3.48}$$

For a Higgs doublet, as in (3.45), we have

$$|t^+ v|^2 = v^2 , \qquad |t^3 v|^2 = 1/4 v^2 , \tag{3.49}$$

so that

$$m_W^2 = \frac{1}{2} g^2 v^2 , \qquad m_Z^2 = \frac{g^2 v^2}{2 \cos^2\theta_{\text{W}}} . \tag{3.50}$$

Note that by using (3.16), we obtain

$$v = 2^{-3/4} G_{\text{F}}^{-1/2} = 174.1\,\text{GeV} . \tag{3.51}$$

It is also evident that, for Higgs doublets,

$$\rho_0 = \frac{m_W^2}{m_Z^2 \cos^2\theta_{\text{W}}} = 1 . \tag{3.52}$$

This relation is typical of one or more Higgs doublets and would be spoiled by the existence of Higgs triplets, etc. In general,

$$\rho_0 = \frac{\sum_i \left[(t_i)^2 - (t_i^3)^2 + t_i \right] v_i^2}{\sum_i 2 (t_i^3)^2 v_i^2} , \tag{3.53}$$

for several Higgs bosons with VEVs v_i, weak isospins t_i, and z-components t_i^3. These results are valid at the tree level and are modified by calculable EW radiative corrections, as discussed in Sect. 3.11.

The measured values of the W (combined from the LEP and Tevatron experiments) and Z masses (from LEP) are [307, 350]:

$$m_W = 80.385 \pm 0.015\,\text{GeV}\,, \qquad m_Z = 91.1876 \pm 0.0021\,\text{GeV}\,. \tag{3.54}$$

In the minimal version of the SM, only one Higgs doublet is present. Then the fermion–Higgs couplings are in proportion to the fermion masses. In fact, from the fermion f Yukawa couplings $g_{\phi\bar{f}f}(\bar{f}_\text{L}\phi f_\text{R} + \text{h.c.})$, the mass m_f is obtained by replacing ϕ by v, so that $m_f = g_{\phi\bar{f}f}v$. In the minimal SM, three out of the four Hermitian fields are removed from the physical spectrum by the Higgs mechanism and become the longitudinal modes of W^+, W^-, and Z. The fourth neutral Higgs is physical and should presumably be identified with the newly discovered particle at $\sim$126 GeV. If more doublets are present, two more charged and two more neutral Higgs scalars should be around for each additional doublet.

The couplings of the physical Higgs H can be simply obtained from $\mathscr{L}_\text{Higgs}$, by making the replacement (the remaining three Hermitian fields correspond to the would-be Goldstone bosons that become the longitudinal modes of $W^\pm$ and Z):

$$\phi(x) = \begin{pmatrix} \phi^+(x) \\ \phi^0(x) \end{pmatrix} \longrightarrow \begin{pmatrix} 0 \\ v + H/\sqrt{2} \end{pmatrix}\,, \tag{3.55}$$

so that $(D_\mu\phi)^\dagger(D^\mu\phi) = \partial_\mu H)^2/2 + \cdots$, with the results

$$\begin{aligned} \mathscr{L}[H,W,Z] = {} & g^2\frac{v}{\sqrt{2}}W_\mu^+W^{-\mu}H + \frac{g^2}{4}W_\mu^+W^{-\mu}H^2 \\ & + g^2\frac{v}{2\sqrt{2}\cos^2\theta_\text{W}}Z_\mu Z^\mu H + \frac{g^2}{8\cos^2\theta_\text{W}}Z_\mu Z^\mu H^2\,. \end{aligned} \tag{3.56}$$

Note that the trilinear couplings are nominally of order g^2, but the dimensionless coupling constant is actually of order g if we express the couplings in terms of the masses according to (3.50):

$$\begin{aligned} \mathscr{L}[H,W,Z] = {} & gm_W W_\mu^+W^{-\mu}H + \frac{g^2}{4}W_\mu^+W^{-\mu}H^2 \\ & + \frac{gm_Z}{2\cos^2\theta_\text{W}}Z_\mu Z^\mu H + \frac{g^2}{8\cos^2\theta_\text{W}}Z_\mu Z^\mu H^2\,. \end{aligned} \tag{3.57}$$

Thus the trilinear couplings of the Higgs to the gauge bosons are also proportional to the masses at fixed g [if instead G_F is kept fixed then, by (3.16), g is proportional to m_W, and the Higgs couplings are quadratic in m_W]. The quadrilinear couplings

are of order g^2. Recall that, to go from the Lagrangian to the Feynman rules for the vertices, the statistical factors must be taken into account. For example, the Feynman rule for the $ZZHH$ vertex is $ig_{\mu\nu}g^2/2\cos^2\theta_W$.

The generic coupling of H to a fermion of type f is given after diagonalization by

$$\mathscr{L}[H,\bar{\psi},\psi] = \frac{g_f}{\sqrt{2}}\bar{\psi}\psi H\ , \tag{3.58}$$

with

$$\frac{g_f}{\sqrt{2}} = \frac{m_f}{\sqrt{2}v} = 2^{1/4}G_F^{1/2}m_f\ . \tag{3.59}$$

The Higgs self-couplings are obtained from the potential in (3.37) by the replacement in (3.55). From the minimum condition

$$v = \sqrt{\frac{\mu^2}{\lambda}}\ , \tag{3.60}$$

one obtains

$$V = -\mu^2\left(v+\frac{H}{\sqrt{2}}\right)^2 + \frac{\mu^2}{2v^2}\left(v+\frac{H}{\sqrt{2}}\right)^4 = -\frac{\mu^2v^2}{2} + \mu^2H^2 + \frac{\mu^2}{\sqrt{2}v}H^3 + \frac{\mu^2}{8v^2}H^4\ , \tag{3.61}$$

The constant term can be omitted in our context. We see that the Higgs mass is positive [compare with (3.37)] and is given by

$$m_H^2 = 2\mu^2 = 2\lambda v^2\ . \tag{3.62}$$

By recalling the value of v in (3.51), we see that, for $m_H \sim 126\,\text{GeV}$, λ is small, in fact, $\lambda/2 \sim 0.13$. Note that $\lambda/2$ is the coefficient of ϕ^4 in (3.37), and the Higgs self-interaction is in the perturbative domain.

The difficulty in the Higgs search is due to the fact that it is heavy and coupled in proportion to mass: it is a heavy particle that must be radiated by another heavy particle. So a lot of phase space and luminosity are needed. At LEP2, the main process for Higgs production was the Higgs strahlung process $e^+e^- \to ZH$ shown in Fig. 3.6 [181]. The alternative process $e^+e^- \to H\nu\bar{\nu}$, via WW fusion, also shown in Fig. 3.6 [44], has a smaller cross-section at LEP2 energies, but would become important, even dominant, in higher energy e^+e^- colliders, like the ILC or CLIC (the corresponding ZZ fusion process has a much smaller cross-section). The analytic formulae for the cross-sections of both processes can be found, for example, in [46]. The direct experimental limit on m_H from LEP2 was $m_H \gtrsim 114\,\text{GeV}$ at 95% confidence level. The phenomenology of the SM Higgs particle and its production and detection at hadron colliders will be discussed in Sects. 3.13 and 3.16.

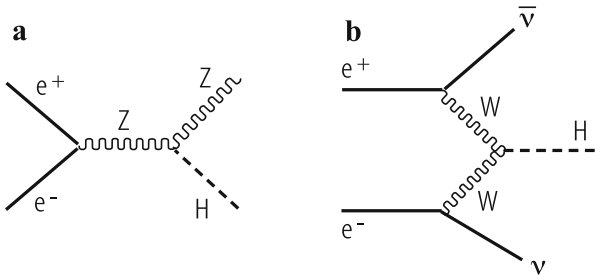

Fig. 3.6 Higgs production diagrams in the Born approximation for e^+e^- annihilation: (**a**) The Higgs strahlung process $e^+e^- \to ZH$, (**b**) the WW fusion process $e^+e^- \to H\nu\bar{\nu}$

3.6 The CKM Matrix and Flavour Physics

Weak charged current vertices are the only tree level interactions in the SM that change flavour. For example, by emission of a W^+, an up-type quark is turned into a down-type quark, or a ν_l neutrino is turned into a l^- charged lepton (all fermions are left-handed). If we start from an up quark that is a mass eigenstate, emission of a W^+ turns it into a down-type quark state d' (the weak isospin partner of u) which is not in general a mass eigenstate. The mass eigenstates and the weak eigenstates do not coincide, and a unitary transformation connects the two sets:

$$D' = \begin{pmatrix} d' \\ s' \\ b' \end{pmatrix} = V \begin{pmatrix} d \\ s \\ b \end{pmatrix} = VD \,, \tag{3.63}$$

where V is the Cabibbo–Kobayashi–Maskawa (CKM) matrix [121]. By analogy with D, we let U denote the column vector of the three up-quark mass eigenstates. Thus, in terms of mass eigenstates, the charged weak current of quarks is of the form

$$J_\mu^+ \propto \bar{U}\gamma_\mu(1-\gamma_5)t^+VD \,, \tag{3.64}$$

where

$$V = U_u^\dagger U_d \,. \tag{3.65}$$

Here U_u and U_d are the unitary matrices that operate on left-handed doublets in the diagonalization of the u and d quarks, respectively [see (3.41)]. Since V is unitary (i.e., $VV^\dagger = V^\dagger V = 1$) and commutes with T^2, T_3 and Q (because all d-type quarks have the same isospin and charge), the neutral current couplings are diagonal in both the primed and the unprimed basis. [If the down-type quark terms in the Z current are written in terms of weak isospin eigenvectors as $\bar{D}'\Gamma D'$, then by changing basis we get $\bar{D}V^\dagger\Gamma VD$, and V and Γ commute because, as can be seen from (3.20), Γ is made

of Dirac matrices and T_3 and Q generator matrices.] It follows that $\bar{D}'\Gamma D' = \bar{D}\Gamma D$. This is the GIM mechanism [226], which ensures natural flavour conservation of the neutral current couplings at the tree level.

For N generations of quarks, V is a $N \times N$ unitary matrix that depends on N^2 real numbers (N^2 complex entries with N^2 unitarity constraints). However, the $2N$ phases of up- and down-type quarks are not observable. Note that an overall phase drops away from the expression of the current in (3.64), so that only $2N-1$ phases can affect V. In total, V depends on $N^2-2N+1 = (N-1)^2$ real physical parameters. Similar counting gives $N(N-1)/2$ as the number of independent parameters in an orthogonal $N \times N$ matrix. This implies that in V we have $N(N-1)/2$ mixing angles and $(N-1)^2 - N(N-1)/2 = (N-1)(N-2)/2$ phases: for $N = 2$, one mixing angle (the Cabibbo angle θ_C) and no phases, for $N = 3$ three angles (θ_{12}, θ_{13}, and θ_{23}) and one phase φ, and so on.

Given the experimentally near-diagonal structure of V, a convenient parametrization is the one proposed by Maiani [286]. It can be cast in the form of a product of three independent 2×2 block matrices (s_{ij} and c_{ij} are shorthands for $\sin\theta_{ij}$ and $\cos\theta_{ij}$):

$$V = \begin{pmatrix} 1 & 0 & 0 \\ 0 & c_{23} & s_{23} \\ 0 & -s_{23} & c_{23} \end{pmatrix} \begin{pmatrix} c_{13} & 0 & s_{13}\mathrm{e}^{\mathrm{i}\varphi} \\ 0 & 1 & 0 \\ -s_{13}\mathrm{e}^{-\mathrm{i}\varphi} & 0 & c_{13} \end{pmatrix} \begin{pmatrix} c_{12} & s_{12} & 0 \\ -s_{12} & c_{12} & 0 \\ 0 & 0 & 1 \end{pmatrix} . \tag{3.66}$$

The advantage of this parametrization is that the three mixing angles are of different orders of magnitude. In fact, from experiment we know that $s_{12} \equiv \lambda$, $s_{23} \sim O(\lambda^2)$, and $s_{13} \sim O(\lambda^3)$, where $\lambda = \sin\theta_C$ is the sine of the Cabibbo angle, and, as an order of magnitude, s_{ij} can be expressed in terms of small powers of λ. More precisely, following Wolfenstein [370], one can set

$$s_{12} \equiv \lambda \,, \qquad s_{23} = A\lambda^2 \,, \qquad s_{13}\mathrm{e}^{-\mathrm{i}\phi} = A\lambda^3(\rho - \mathrm{i}\eta) \,. \tag{3.67}$$

As a result, by neglecting terms of higher order in λ, one can write

$$V = \begin{bmatrix} V_{ud} & V_{us} & V_{ub} \\ V_{cd} & V_{cs} & V_{cb} \\ V_{td} & V_{ts} & V_{tb} \end{bmatrix} \sim \begin{bmatrix} 1-\lambda^2/2 & \lambda & A\lambda^3(\rho - \mathrm{i}\eta) \\ -\lambda & 1-\lambda^2/2 & A\lambda^2 \\ A\lambda^3(1-\rho-\mathrm{i}\eta) & -A\lambda^2 & 1 \end{bmatrix} + O(\lambda^4). \tag{3.68}$$

It has become customary to make the replacement $\rho, \eta \to \bar{\rho}, \bar{\eta}$ with

$$\rho - \mathrm{i}\eta = \frac{\bar{\rho} - \mathrm{i}\bar{\eta}}{\sqrt{1-\lambda^2}} \sim (\bar{\rho} - \mathrm{i}\bar{\eta})\left(1 + \frac{\lambda^2}{2} + \cdots\right) . \tag{3.69}$$

The best values of the CKM parameters as obtained from experiment are continuously updated in [344, 355] (a survey of the current status of the CKM parameters can also be found in [307]). A Summer 2013 fit [355] led to the values

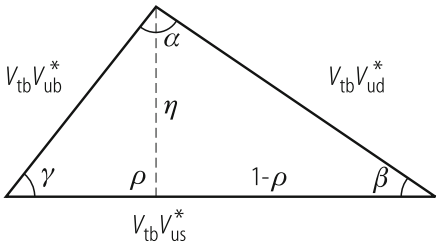

Fig. 3.7 The unitarity triangle corresponding to (3.71)

(compatible values, within stated errors, are given in [344]):

$$\begin{aligned} \lambda &= 0.22535 \pm 0.00065\,, \qquad A = 0.822 \pm 0.012\,, \\ \bar{\rho} &= 0.127 \pm 0.023\,, \qquad \bar{\eta} = 0.353 \pm 0.014\,. \end{aligned} \tag{3.70}$$

In the SM, the non-vanishing of the $\bar{\eta}$ parameter [related to the phase φ in (3.66) and (3.67)] is the only source of CP violation in the quark sector (we shall see that new sources of CP violation very likely arise from the neutrino sector). Unitarity of the CKM matrix V implies relations of the form $\sum_a V_{ba}V_{ca}^* = \delta_{bc}$.

In most cases these relations do not imply particularly instructive constraints on the Wolfenstein parameters. But when the three terms in the sum are of comparable magnitude, we get interesting information. The three numbers which must add to zero form a closed triangle in the complex plane (unitarity triangle), with sides of comparable length. This is the case for the *t*–*u* triangle shown in Fig. 3.7 (or, what is equivalent to a first approximation, for the *d*–*b* triangle):

$$V_{td}V_{ud}^* + V_{ts}V_{us}^* + V_{tb}V_{ub}^* = 0\,. \tag{3.71}$$

All terms are of order λ^3. For $\eta = 0$, the triangle would flatten down to vanishing area. In fact, the area J of the triangle, of order $J \sim \eta A^2\lambda^6$, is the Jarlskog invariant [251] (its value is independent of the parametrization). In the SM, in the quark sector, all CP violating observables must be proportional to J, hence to the area of the triangle or to η. Its experimental value is $J \sim (3.12 \pm 0.09) \times 10^{-5}$ [355].

Direct and by now very solid evidence for J being non-vanishing was first obtained from the measurements of ϵ and ϵ' in K decay. Additional direct evidence has more recently been collected from experiments on B decays at beauty factories, at the Tevatron and at the LHC (in particular by the LHCb experiment). Very recently searches for CP violation in D decays (negative so far) have been reported by the LHCb experiment [282]. The angles β (the most precisely measured), α, and γ have been determined with fair precision. The angle measurements and the available information on the magnitude of the sides, taken together, are in good agreement with the predictions from the SM unitary triangle (see Fig. 3.8) [344, 355]. Some alleged tensions are not convincing, either because of their poor statistical significance or because of lack of confirmation from different potentially

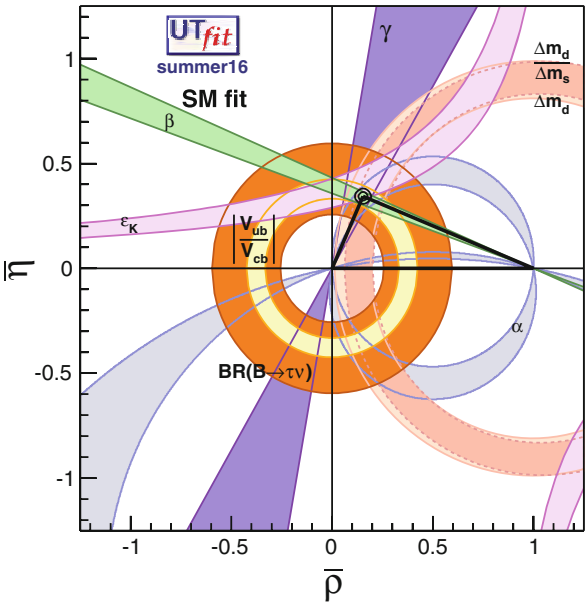

Fig. 3.8 Constraints in the $\bar{\rho}, \bar{\eta}$ plane, including the most recent data inputs in the global CKM fit. From [107] (with permission)

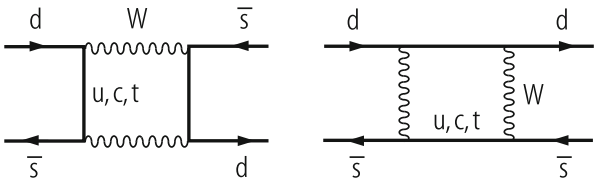

Fig. 3.9 Box diagrams describing K^0–$\bar{K}^0$ mixing at the quark level at 1-loop

sensitive experiments, or because the associated theoretical error estimates can be questioned.

As we have discussed, due to the GIM mechanism, there are no flavour-changing neutral current (FCNC) transitions at the tree level in the SM. Transitions with $|\Delta F| = 1, 2$ are induced at one-loop level. In particular, meson mixing, i.e., $M \to \bar{M}$ off-diagonal $|\Delta F| = 2$ mass matrix elements (with $M = K, D$, or B neutral mesons), are obtained from box diagrams. For example, in the case of K^0–$\bar{K}^0$ mixing, the relevant transition is $\bar{s}d \to s\bar{d}$ (see Fig. 3.9). In the internal quark lines, all up-type quarks are exchanged. In the amplitude, two vertices and the connecting propagator (with virtual four momentum p_μ) at one side contribute a factor ($u_i = u, c, t$):

$$F_{\text{GIM}} = \sum_i V^*_{u_i s} \frac{1}{\not{p} - m_{ui}} V_{u_i d} \,, \tag{3.72}$$

which, in the limit of equal m_{ui}, is clearly vanishing due to the unitarity of the CKM matrix V. Thus the result is proportional to mass differences.

For K^0–$\bar{K}^0$ mixing, the contribution of virtual u quarks is negligible due to the small value of m_u and the contribution of the t quark is also small due to the mixing factors $V_{ts}^* V_{td} \sim O(A^2\lambda^5)$. The dominant c quark contribution to the real part of the box diagram quark-level amplitude is approximately of the form (see, for example, [176]):

$$\mathrm{Re}\, H_{\mathrm{box}} = \frac{G_{\mathrm{F}}^2}{16\pi^2} m_c^2 \mathrm{Re}(V_{cs}^* V_{cd})^2 \eta_1 O^{\Delta s=2} \,, \tag{3.73}$$

where $\eta_1 \sim 0.85$ is a QCD correction factor and $O^{\Delta s=2} = \bar{d}_{\mathrm{L}} \gamma_\mu s_{\mathrm{L}} \bar{s}_{\mathrm{L}} \gamma_\mu d_{\mathrm{L}}$ is the relevant 4-quark dimension-6 operator. The η_1 factor arises from gluon exchanges among the quark legs of the 4-quark operator. Indeed the coefficients of the operator expansion, which arises when the heavy particles exchanged are integrated away, obey renormalization group equations, and the associated logarithms can be resummed. (The first calculation of resummed QCD corrections to weak non-leptonic amplitudes was carried out in [209]. For a pedagogical introduction see, for example, [116].) To obtain the K^0–$\bar{K}^0$ mixing amplitude, the matrix element of $O^{\Delta s=2}$ between meson states must be taken, and this is parametrized by a "B_K parameter", defined in such a way that $B_K = 1$ for vacuum state insertion between the two currents:

$$\left\langle K^0 | O^{\Delta s=2} | \bar{K}^0 \right\rangle = \frac{16}{3} f_K m_K^2 B_K \,, \tag{3.74}$$

where $B_K \sim 0.75$ (this is the renormalization group independent definition, usually denoted by $\hat{B}_K$) and $f_K \sim 113\,\mathrm{MeV}$, the kaon pseudoscalar constant, are best evaluated by QCD lattice simulations [348]. Clearly, additional non-perturbative terms must be added to the charm parton contribution in (3.73), some of them of $O(m_K^2/m_c^2)$, because the smallness of m_c makes a completely partonic dominance inadequate. In (3.73), the factor $O(m_c^2/m_W^2)$ is the "GIM suppression" factor [$1/m_W^2$ is hidden in G_{F} according to (3.16)].

For B mixing the dominant contribution is from the t quark. In this case, the partonic dominance is more realistic and the GIM factor $O(m_t^2/m_W^2)$ is actually larger than 1. More recently D mixing has also been observed [53]. In the corresponding box diagrams, down-type quarks are involved. But starting from $D \sim c\bar{u}$, the b quark contribution is strongly suppressed by the CKM angles, given that $V_{cb} V_{ub}^* \sim O(\lambda_C^5)$. The masses of the d and s quarks are too small for a partonic evaluation of the box diagram, and non-perturbative terms cannot be neglected. This makes a theoretical evaluation of mixing and CP violation effects for D mesons problematic.

All sorts of transitions with $|\Delta F| = 1$ are also induced at loop level. For example, an effective vertex $Z \to t\bar{c}$, which does not exist at tree level, is generated at 1-loop

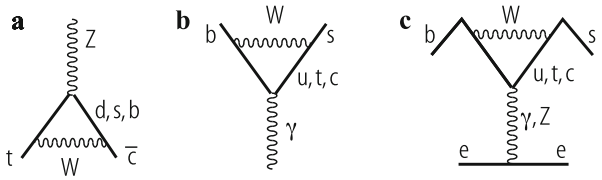

Fig. 3.10 Examples of $|\Delta F| = 1$ transitions at the quark level at 1-loop: (**a**) Diagram for a $Z \to t\bar{c}$ vertex, (**b**) $b \to s\gamma$, and (**c**) a "penguin" diagram for $b \to se^+e^-$

(see Fig. 3.10). Similarly, transitions involving photons or gluons are also possible, like $t \to cg$ or $b \to s\gamma$ (Fig. 3.10), or again $b \to sg$.

For light fermion exchange in the loop, the GIM suppression is also effective in $|\Delta F| = 1$ amplitudes. For example, analogous leptonic transitions like $\mu \to e\gamma$ or $\tau \to \mu\gamma$ also exist, but in the SM are extremely small and out of reach for experiments, because the tiny neutrino masses enter into the GIM suppression factor. But new physics effects could well make these rare lepton flavour-violating processes accessible to experiment. In fact, the present limits already pose stringent constraints on models of new physics. Of particular importance is the recent bound obtained by the MEG Collaboration at SIN, near Zurich, Switzerland, on the branching ratio for $\mu \to e\gamma$, viz., $B(\mu \to e\gamma) \lesssim 5.7 \times 10^{-13}$ at 90% [16].

The external Z, photon, or gluon can be attached to a pair of light fermions, giving rise to an effective four-fermion operator, as in "penguin diagrams" like the one shown in Fig. 3.10 for $b \to sl^+l^-$. The inclusive rate $B \to X_s\gamma$ (here B stands for B_d) with X_s a hadronic state containing a unit of strangeness corresponding to an s quark, has been precisely measured. The world average result for the branching ratio with $E_\gamma > 1.6\,\text{GeV}$ is [53]

$$B(B \to X_s\gamma)_{\text{exp}} = (3.55 \pm 0.26) \times 10^{-4} \,.$$

The theoretical prediction for this inclusive process is to a large extent free of uncertainties from hadronization effects and is accessible to perturbation theory as the b quark is heavy enough. The most complete result to order α_s^2 is at present from [86] (and references therein):

$$B(B \to X_s\gamma)_{\text{th}} = (2.98 \pm 0.26) \times 10^{-4} \,.$$

Note that the theoretical value has recently become smaller than the experimental value. The fair agreement between theory and experiment imposes stringent constraints on possible new physics effects.

Related processes are $B_{s,d} \to \mu^+\mu^-$. These decays are very rare in the SM, their predicted branching ratio being [117]

$$B(B_s \to \mu^+\mu^-) \sim (3.35 \pm 0.28) \times 10^{-9} \,, \quad B(B_d \to \mu^+\mu^-) \sim (1.07 \pm 0.10) \times 10^{-10} \,.$$

These very small expected branching ratios result because these decays are FCNC processes with helicity suppression in the purely leptonic final state (the decaying meson has spin zero and the muon pair is produced by vector exchange in the SM). Many models of new physics beyond the SM predict large deviations. Thus these processes represent very stringent tests of the SM.

Recently, the LHCb and CMS experiments have reached the sensitivity to observe the B_s mode. The LHCb result is [5]

$$B(B_s \to \mu^+\mu^-) = 2.9^{+1.1}_{-1.0} \times 10^{-9} ,$$

and the same paper sets the bound

$$B(B_d \to \mu^+\mu^-) \leq 7.4 \times 10^{-10} \quad \text{at 95\% confidence level} .$$

For the same decays, CMS has obtained [136]

$$B(B_s \to \mu^+\mu^-) = 3.0^{+1.0}_{-0.9} \times 10^{-9} ,$$

and

$$B(B_d \to \mu^+\mu^-) \leq 11 \times 10^{-10} \quad \text{at 95\% confidence level} .$$

The LHCb and CMS results have been combined [352] and give

$$B(B_s \to \mu^+\mu^-) = (2.9 \pm 0.7)^{-9} ,$$

in good agreement with the SM, and

$$B(B_d \to \mu^+\mu^-) = 3.6^{+1.6}_{-1.4} \times 10^{-10} ,$$

with the central value 1.7σ above the SM. Another very demanding test of the SM has been passed!

Among the exclusive processes of the $b \to s$ type, much interest is at present devoted to the channel $B \to K^*\mu^+\mu^-$ [4, 106]. The differential decay distribution depends on three angles and on the $\mu^+\mu^-$ invariant mass squared q^2. In general $12 + 12$ form factors enter into the decay distribution (12 in B decay and 12 in the CP conjugated $\bar{B}$ decay), and many observables can be defined. By suitable angular foldings and CP averages, the number of form factors is reduced. A sophisticated theoretical analysis allows one to identify and study a number of quantities that can be measured and are "clean", i.e., largely independent of hadronic form factor ambiguities [106]. For those observables most of the results agree with the SM predictions (based on a Wilson operator expansion in powers of $1/m_W$ and $1/m_b$, with coefficients depending on α_s), but a few discrepancies are observed. The significance, taking into account the number of observables studied

and the theoretical ambiguities (especially in the estimate of $1/m_b$ corrections), is not compelling, but a substantial activity is under way on both the experimental and the theoretical side (see, for example, [248]). Watch this space!

In conclusion, the CKM theory of quark mixing and CP violation has been precisely tested in the last decade and turns out to be very successful. The expected deviations from new physics at the EW scale have not yet appeared. The constraints on new physics from flavour phenomenology are extremely demanding: when adding higher dimensional effective operators to the SM, the flavour constraints generically lead to powers of very large suppression scales Λ in the denominators of the corresponding coefficients. In fact, in the SM, as we have discussed in this section, there are very powerful protections against flavour-changing neutral currents and CP violation effects, in particular through the smallness of quark mixing angles. In this respect the SM is very special and, as a consequence, if there is new physics, it must be highly non-generic in order to satisfy the present flavour constraints.

Only by requiring new physics to share the SM set of protections can one reduce the scale Λ down to $O(1)$ TeV. For example, the class of models with minimal flavour violation (MFV) [152], where the SM Yukawa couplings are the only flavour symmetry breaking terms also beyond the SM, have been much studied and represent a sort of extreme baseline. Alternative, less minimal models that are currently under study are based on a suitably broken $U(3)^3$ or $U(2)^3$ flavour symmetry (the cube refers to the $Q_{\mathrm{L}} = u_{\mathrm{L}}$, d_{L} doublet and the two u_{R} and d_{R} singlets, while $U(3)$ or $U(2)$ mix the three or the first two generations) [81].

3.7 Neutrino Mass and Mixing

In the minimal version of the SM, the right-handed neutrinos $\nu_{i\mathrm{R}}$, which have no gauge interactions, are not present at all. With no ν_{R}, no Dirac mass is possible for neutrinos. If lepton number conservation is also imposed, then no Majorana mass is allowed either, and as a consequence, all neutrinos are massless. But at present, from neutrino oscillation experiments, we know that at least two out of the three known neutrinos have non-vanishing masses (for reviews, see, for example, [36]): the two mass-squared differences measured from solar (Δm^2_{12}) and atmospheric oscillations (Δm^2_{23}) are given by $\Delta m^2_{12} \sim 8 \times 10^{-5}\,\mathrm{eV}^2$ and $\Delta m^2_{23} \sim 2.5 \times 10^{-3}\,\mathrm{eV}^2$ [200, 201, 229].

Neutrino oscillations only measure $|m_i^2|$ differences. Regarding the absolute values of each m_i we know that they are very small, with an upper limit of a fraction of an eV, obtained from the following:

- Laboratory experiments, e.g., tritium β decay near the end point, which gives $m_\nu \lesssim 2\,\mathrm{eV}$ [307].
- Absence of visible neutrinoless double β decay ($0\nu\beta\beta$). From Ge^{76}, it has been shown that $|m_{ee}| \lesssim 0.2$–$0.4\,\mathrm{eV}$ [21]. The range is from nuclear matrix element

ambiguities and m_{ee} is a combination of neutrino masses (for a review, see, for example, [373]). This result strongly disfavours, in a model-independent way, the claimed observation of $0\nu\beta\beta$ decay in Ge^{76} decays [267]. From Xe^{136}, one obtains the combined result $|m_{ee}| \lesssim 0.12$–$0.25\,\mathrm{eV}$ [69].

- Cosmological observations [175]. After the recent release of the Planck data, the quoted bounds for Σm_ν, the sum of (quasi-)stable neutrino masses, span a range, depending on the data set included and the cosmological priors, like $\Sigma m_\nu \lesssim 0.98$ or $\lesssim 0.32$ or $\lesssim 0.23$ [18] (assuming three degenerate neutrinos, these numbers have to be divided by 3 in order to obtain the limit on individual neutrino masses).

If $\nu_{i\mathrm{R}}$ are added to the minimal model and lepton number is imposed by hand, then neutrino masses would in general appear as Dirac masses, generated by the Higgs mechanism, as for any other fermion. But for Dirac neutrinos, to explain the extreme smallness of neutrino masses, one should allow for very small Yukawa couplings. However, we stress that, in the SM, baryon B and lepton L number conservation, which are not guaranteed by gauge symmetries (although this is the case for the electric charge Q), are understood as "accidental" symmetries. In fact the SM Lagrangian should contain all terms allowed by gauge symmetry and renormalizability, but the most general renormalizable Lagrangian (i.e., with operator dimension $d \leq 4$), built from the SM fields, compatible with the SM gauge symmetry, in the absence of $\nu_{i\mathrm{R}}$, is automatically B and L conserving. (However, non-perturbative instanton effects break the conservation of $B + L$ while preserving $B - L$, as discussed in Sect. 3.8.)

In the presence of $\nu_{i\mathrm{R}}$, this is no longer true, and the right-handed Majorana mass term is allowed:

$$M_{RR} = \bar{\nu}^{\mathrm{c}}_{i\mathrm{R}} M_{ij} \nu_{j\mathrm{R}} = \nu^{\mathrm{T}}_{i\mathrm{R}} C M_{ij} \nu_{j\mathrm{R}} \,, \tag{3.75}$$

where $\nu^{\mathrm{c}}_{i\mathrm{R}} = C\bar{\nu}^{\mathrm{T}}_{i\mathrm{R}}$ is the charge-conjugated neutrino field and C is the charge conjugation matrix in Dirac spinor space. The Majorana mass term is an operator of dimension $d = 3$ with $\Delta L = 2$. Since the $\nu_{i\mathrm{R}}$ are gauge singlets, the Majorana mass M_{RR} is fully allowed by the gauge symmetry and a coupling with the Higgs is not needed to generate this type of mass. As a consequence, the mass matrix entries M_{ij} do not need to be of the order of the EW symmetry breaking scale v, and could be much larger. If one starts from the Dirac and RR Majorana mass terms for neutrinos, the resulting mass matrix, in the L, R space, has the form

$$m_\nu = \begin{bmatrix} 0 & m_{\mathrm{D}} \\ m_{\mathrm{D}} & M \end{bmatrix} \,, \tag{3.76}$$

where m_{D} and M are the Dirac and Majorana mass matrices [M is the matrix M_{ij} in (3.75)]. The corresponding eigenvalues are three very heavy neutrinos with masses of order M and three light neutrinos with masses

$$m_\nu = -m^{\mathrm{T}}_{\mathrm{D}} M^{-1} m_{\mathrm{D}} \,, \tag{3.77}$$

which are possibly very small if M is large enough. This is the see-saw mechanism for neutrino masses [291]. Note that, if no ν_{iR} existed, a Majorana mass term could still be built out of ν_{jL}. But ν_{jL} have weak isospin 1/2, being part of the left-handed lepton doublet l. Thus, the left-handed Majorana mass term has total weak isospin equal to 1 and needs two Higgs fields to make a gauge invariant term. The resulting mass term, viz.,

$$O_5 = \frac{(Hl)_i^{\mathrm{T}} \lambda_{ij} (Hl)_j}{M} + \text{h.c.}, \tag{3.78}$$

with M a large scale (a priori comparable to the scale of M_{RR}) and λ a dimensionless coupling generically of $O(1)$, is a non-renormalizable operator of dimension 5, first pointed out by S. Weinberg [363]. The corresponding mass terms are of the order $m_\nu \sim \lambda v^2/M$, where v is the Higgs VEV, hence of the same generic order as the light neutrino masses from (3.77). Note that, in general, the neutrino mass matrix has the form

$$\mathbf{m}_\nu = \nu^{\mathrm{T}} m_\nu \nu \ , \tag{3.79}$$

as a consequence of the Majorana nature of neutrinos.

In conclusion, neutrino masses are believed to be small because neutrinos are Majorana particles with masses inversely proportional to the large scale M of energy where L non-conservation is induced. This corresponds to an important enlargement of the original minimal SM, where no ν_R was included and L conservation was imposed by hand (but this ansatz would be totally unsatisfactory because L conservation is true "accidentally" only at the renormalizable level, but is violated by non-renormalizable terms like the Weinberg operator and by instanton effects). Actually, L and B non-conservation are necessary if we want to explain baryogenesis and we have Grand Unified Theories (GUTs) in mind. It is interesting that the observed magnitudes of the mass-squared splittings of neutrinos are well compatible with a scale M remarkably close to the GUT scale, where L non-conservation is indeed naturally expected. In fact, for $m_\nu \approx \sqrt{\Delta m^2_{\text{atm}}} \approx 0.05$ eV (see Table 3.1) and $m_\nu \approx m_{\mathrm{D}}^2/M$ with $m_{\mathrm{D}} \approx v \approx 200\,\text{GeV}$, we find $M \approx 10^{15}$ GeV which indeed is an impressive indication for M_{GUT}.

Table 3.1 Fits to neutrino oscillation data from [229] (free fluxes, including short baseline reactor data)

Δm^2_{sun} (10^{-5} eV^2)	$7.45^{+0.19}_{-0.16}$
Δm^2_{atm} (10^{-3} eV^2)	2.417 ± 0.013 (-2.410 ± 0.062)
$\sin^2\theta_{12}$	0.306 ± 0.012
$\sin^2\theta_{23}$	$0.446 \pm 0.007 \bigoplus 0.587^{+0.032}_{-0.037}$
$\sin^2\theta_{13}$	$0.0229^{+0.0020}_{-0.0019}$
δ_{CP} (°)	265^{+56}_{-61}

The results for both the normal and the inverse (in brackets) hierarchies are shown

In the previous section, we discussed flavour mixing for quarks. But clearly, given that non-vanishing neutrino masses have been established, a similar mixing matrix is also introduced in the leptonic sector. We assume in the following that there are only two distinct neutrino oscillation frequencies, the atmospheric and the solar frequencies (both of them now also confirmed by experiments where neutrinos are generated on the Earth like K2K, KamLAND, and MINOS). At present the bulk of neutrino oscillation data are well reproduced in terms of three light neutrino species. However, some (so far not compelling) evidence for additional "sterile" neutrino species (i.e., not coupled to the weak interactions, as demanded by the LEP limit on the number of "active" neutrinos) are present in some data. We discuss here 3-neutrino mixing, which is in any case a good approximate framework to discuss neutrino oscillations, while for possible sterile neutrinos we refer to the comprehensive review in [8].

Neutrino oscillations are due to a misalignment between the flavour basis, i.e., $\nu' \equiv (\nu_e, \nu_\mu, \nu_\tau)$, where ν_e is the partner of the mass and flavour eigenstate e^- in a left-handed (LH) weak isospin $SU(2)$ doublet (similarly for ν_μ and ν_τ)) and the mass eigenstates $\nu \equiv (\nu_1, \nu_2, \nu_3)$ [36, 280, 312]:

$$\nu' = U\nu \ , \tag{3.80}$$

where U is the unitary $\times 3$ mixing matrix. Given the definition of U and the transformation properties of the effective light neutrino mass matrix $\mathbf{m_\nu}$ in (3.79), viz.,

$$\nu'^{\mathrm{T}} m_\nu \nu' = \nu^{\mathrm{T}} U^{\mathrm{T}} m_\nu U \nu \ , \qquad U^{\mathrm{T}} m_\nu U = \mathrm{Diag}\,(m_1, m_2, m_3) \equiv m_{\mathrm{diag}} \ , \tag{3.81}$$

we obtain the general form of m_ν (i.e., of the light ν mass matrix in the basis where the charged lepton mass is a diagonal matrix):

$$m_\nu = U^* m_{\mathrm{diag}} U^\dagger \ . \tag{3.82}$$

The matrix U can be parameterized in terms of three mixing angles θ_{12}, θ_{23}, and θ_{13} ($0 \le \theta_{ij} \le \pi/2$) and one phase φ ($0 \le \varphi \le 2\pi$) [122], exactly as for the quark mixing matrix V_{CKM}. The following definition of mixing angles can be adopted:

$$U = \begin{pmatrix} 1 & 0 & 0 \\ 0 & c_{23} & s_{23} \\ 0 & -s_{23} & c_{23} \end{pmatrix} \begin{pmatrix} c_{13} & 0 & s_{13}\mathrm{e}^{\mathrm{i}\varphi} \\ 0 & 1 & 0 \\ -s_{13}\mathrm{e}^{-\mathrm{i}\varphi} & 0 & c_{13} \end{pmatrix} \begin{pmatrix} c_{12} & s_{12} & 0 \\ -s_{12} & c_{12} & 0 \\ 0 & 0 & 1 \end{pmatrix} \ , \tag{3.83}$$

where $s_{ij} \equiv \sin\theta_{ij}$ and $c_{ij} \equiv \cos\theta_{ij}$. In addition, if ν are Majorana particles, we have two more phases [101] given by the relative phases among the Majorana masses m_1, m_2, and m_3. If we choose m_3 real and positive, these phases are carried by $m_{1,2} \equiv |m_{1,2}|\mathrm{e}^{\mathrm{i}\phi_{1,2}}$. Thus, in general, nine parameters are added to the SM when non-vanishing neutrino masses are included: three eigenvalues, three mixing angles, and three CP violating phases.

In our notation the two frequencies, $\Delta m_I^2/4E$ (I = sun, atm), are parametrized in terms of the ν mass eigenvalues by

$$\Delta m^2_{\rm sun} \equiv |\Delta m^2_{12}|\,, \qquad \Delta m^2_{\rm atm} \equiv |\Delta m^2_{23}|\,. \tag{3.84}$$

where $\Delta m^2_{12} = |m_2|^2 - |m_1|^2 > 0$ and $\Delta m^2_{23} = m_3^2 - |m_2|^2$. The numbering 1,2,3 corresponds to a definition of the frequencies and in principle may not coincide with the ordering from the lightest to the heaviest state. "Normal hierarchy" is the case where m_3 is the largest mass in absolute value, otherwise one has an "inverse hierarchy".

Very important developments occurred in the data in 2012. The value of the mixing angle θ_{13} was shown to be non-vanishing and its value is now known to fair accuracy. Several experiments were involved in the θ_{13} measurement and their results are reported in Fig. 3.11. The most precise result is from the Daya Bay reactor experiment in China:

$$\sin^2 2\theta_{13} = 0.090 \pm 0.012\,,\ \text{or}\ \sin^2\theta_{13} = 0.023 \pm 0.003\,,\ \text{or}\ \theta_{13} \sim 0.152 \pm 0.010\,. \tag{3.85}$$

Note that θ_{13} is somewhat smaller but of the same order as the Cabibbo angle $\theta_{\rm C}$. The present data on the oscillation parameters are summarized in Table 3.1 [229].

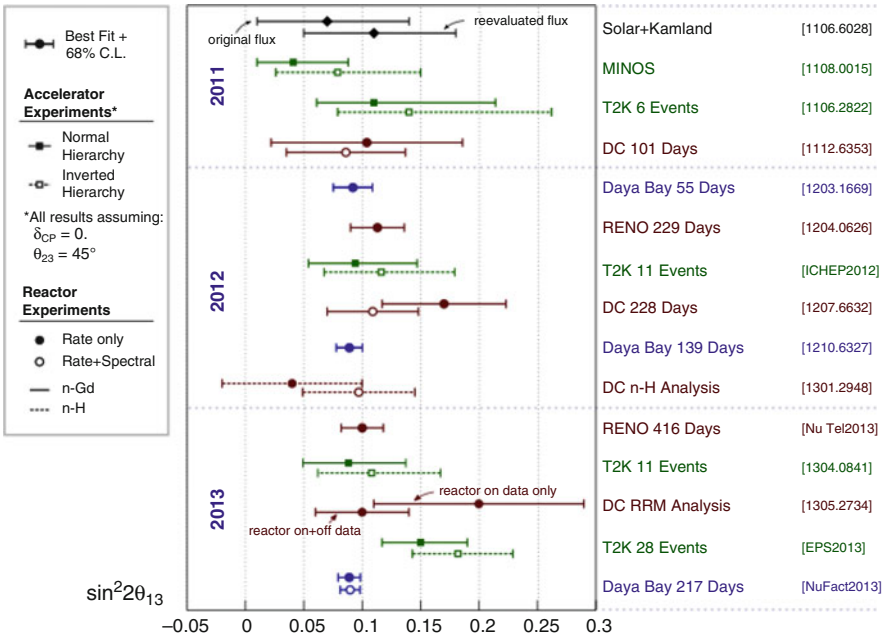

Fig. 3.11 Reactor angle measurements, updated to the NUFACT13 Conference, August 2013 [259], from the experiments T2K [12], MINOS [17], DOUBLE CHOOZ [13], Daya Bay [54], and RENO [23], for the normal (inverse) hierarchy. Figure credit: S. Jetter

Neutrino mixing is important because it could in principle provide new clues for the understanding of the flavour problem. Even more so since neutrino mixing angles show a pattern that is completely different from that of quark mixing: for quarks all mixing angles are small, while for neutrinos two angles are large (one is still compatible with the maximal value) and only the third one is small. In reality, it is frustrating that there has been no real illumination of the problem of flavour. Models can reproduce the data on neutrino mixing in a wide range of dynamical setups that goes from anarchy to discrete flavour symmetries (for reviews and references see, for example, [35, 37, 50–52, 264]), but we have not yet been able to single out a unique and convincing baseline for the understanding of fermion masses and mixings. Despite many interesting ideas and the formulation of many elegant models, the mysteries of the flavour structure of the three generations of fermions have not yet been unveiled.

3.8 Quantization and Renormalization of the Electroweak Theory

The Higgs mechanism gives masses to the Z, the $W^{\pm}$, and to fermions, while the Lagrangian density is still symmetric. In particular the gauge Ward identities and the symmetric form of the gauge currents are preserved. The validity of these relations is an essential ingredient for renormalizability. In the previous sections, we have specified the Feynman vertices in the "unitary" gauge, where only physical particles appear. However, as discussed in Chap. 1, in this gauge the massive gauge boson propagator would have a bad ultraviolet behaviour:

$$W_{\mu\nu} = \frac{-g_{\mu\nu} + q_\mu q_\nu / m_W^2}{q^2 - m_W^2} \,. \tag{3.86}$$

A formulation of the standard EW theory with good apparent ultraviolet behaviour can be obtained by introducing the renormalizable or R_ξ gauges [14], in analogy with the Abelian case discussed in detail in Chap. 1. One parametrizes the Higgs doublet as

$$\phi = \begin{pmatrix} \phi^+ \\ \phi^0 \end{pmatrix} = \begin{pmatrix} \phi_1 + \mathrm{i}\phi_2 \\ \phi_3 + \mathrm{i}\phi_4 \end{pmatrix} = \begin{pmatrix} -\mathrm{i}w^+ \\ v + (H + \mathrm{i}z)/\sqrt{2} \end{pmatrix} \,, \tag{3.87}$$

and similarly for $\phi^\dagger$, where w^- appears. The scalar fields $w^{\pm}$ and z are the pseudo-Goldstone bosons associated with the longitudinal modes of the physical vector bosons $W^{\pm}$ and Z. The R_ξ gauge fixing Lagrangian has the form

$$\Delta\mathscr{L}_{\mathrm{GF}} = -\frac{1}{\xi}\left|\partial^\mu W_\mu - \xi m_W w\right|^2 - \frac{1}{2\eta}(\partial^\mu Z_\mu - \eta m_Z z)^2 - \frac{1}{2\alpha}(\partial^\mu A_\mu)^2 \,. \tag{3.88}$$

The $W^{\pm}$ and Z propagators, as well as those of the scalars $w^{\pm}$ and z, have exactly the same general forms as for the Abelian case in (1.67)–(1.69), with parameters ξ and η, respectively (and the pseudo-Goldstone bosons $w^{\pm}$ and z have masses ξm_W and ηm_Z). In general, a set of associated ghost fields must be added, again in direct analogy with the treatment of R_ξ gauges in the Abelian case of Chap. 1. The complete Feynman rules for the standard EW theory can be found in a number of textbooks (see, for example, [137]).

The pseudo-Goldstone bosons $w^{\pm}$ and z are directly related to the longitudinal helicity states of the corresponding massive vector bosons $W^{\pm}$ and Z. This correspondence materializes in a very interesting "equivalence theorem": at high energies of order E, the amplitude for the emission of one or more longitudinal gauge bosons $V_{\rm L}$ (with $V = W, Z$) becomes equal (apart from terms reduced by powers of m_V/E) to the amplitude where each longitudinal gauge boson is replaced by the corresponding Goldstone field $w^{\pm}$ or z [149]. For example, consider top decay with a longitudinal W in the final state: $t \to bW^+_{\rm L}$. The equivalence theorem asserts that we can compute the dominant contribution to this rate from the simpler $t \to bw^+$ matrix element:

$$\Gamma(t \to bW^+_{\rm L}) = \Gamma(t \to bw^+)\left[1 + O(m_W^2/m_t^2)\right] . \tag{3.89}$$

In fact, one finds

$$\Gamma(t \to bw^+) = \frac{h_t^2}{32\pi} m_t = \frac{G_{\rm F} m_t^3}{8\pi\sqrt{2}} , \tag{3.90}$$

where $h_t = m_t/v$ is the Yukawa coupling of the top quark (numerically very close to 1), and we used $1/v^2 = 2\sqrt{2}G_{\rm F}$ [see (3.51)]. If we compare with (3.31), we see that this expression coincides with the total top width (i.e., including all polarizations for the W in the final state), computed at tree level, apart from terms reduced by powers of $O(m_W^2/m_t^2)$. In fact, the longitudinal W is dominant in the final state because $h_t^2 \gg g^2$. Similarly, the equivalence theorem can be applied to find the dominant terms at large $\sqrt{s}$ for the cross-section $e^+e^- \to W^+_{\rm L} W^-_{\rm L}$, or the leading contribution, in the limit $m_{\rm H} \gg m_V$, to the width for the decay $\Gamma(H \to VV)$.

The formalism of the R_ξ gauges is also very useful in proving that spontaneously broken gauge theories are renormalizable. In fact, the non-singular behaviour of propagators at large momenta is very suggestive of the result. Nevertheless, it is not at all a simple matter to prove this statement. The fundamental theorem that a gauge theory with spontaneous symmetry breaking and the Higgs mechanism is in general renormalizable was proven by 't Hooft and Veltman [278, 358].

For a chiral theory like the SM an additional complication arises from the existence of chiral anomalies. But this problem is avoided in the SM because the quantum numbers of the quarks and leptons in each generation imply a remarkable (and, from the point of view of the SM, mysterious) cancellation of the anomaly, as originally observed in [109]. In quantum field theory, one encounters an

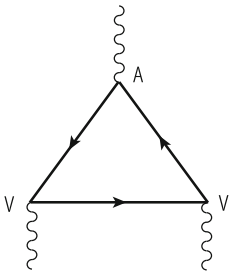

Fig. 3.12 Triangle diagram that generates the ABJ anomaly [19]

anomaly when a symmetry of the classical Lagrangian is broken by the process of quantization, regularization, and renormalization of the theory. Of direct relevance for the EW theory is the Adler–Bell–Jackiw (ABJ) chiral anomaly [19]. The classical Lagrangian of a theory with massless fermions is invariant under $U(1)$ chiral transformations $\psi\prime = \mathrm{e}^{\mathrm{i}\gamma_5\theta}\psi$ (see also Sect. 2.2.3). The associated axial Noether current is conserved at the classical level. But at the quantum level, chiral symmetry is broken due to the ABJ anomaly and the current is not conserved. The chiral breaking is produced by a clash between chiral symmetry, gauge invariance, and the regularization procedure.

The anomaly is generated by triangular fermion loops with one axial and two vector vertices (Fig. 3.12). For example, for the Z, the axial coupling is proportional to the third component of weak isospin t_3, while the vector coupling is proportional to a linear combination of t_3 and the electric charge Q. Thus in order for the chiral anomaly to vanish, all traces of the form $\mathrm{tr}\{t_3QQ\}$, $\mathrm{tr}\{t_3t_3Q\}$, $\mathrm{tr}\{t_3t_3t_3\}$ (and also $\mathrm{tr}\{t_+t_-t_3\}$ when charged currents are included) must vanish, where the trace is extended over all fermions in the theory that can circulate in the loop. Now all of these traces happen to vanish for each fermion family separately. For example, take $\mathrm{tr}\{t_3QQ\}$. In one family there are, with $t_3 = +1/2$, three colours of up quarks with charge $Q = +2/3$ and one neutrino with $Q = 0$ and, with $t_3 = -1/2$, three colours of down quarks with charge $Q = -1/3$ and one l^- with $Q = -1$. Thus we obtain

$$\mathrm{tr}\{t_3QQ\} = \frac{1}{2}\times 3\times\frac{4}{9} - \frac{1}{2}\times 3\times\frac{1}{9} - \frac{1}{2}\times 1 = 0\ .$$

This impressive cancellation suggests an interplay among weak isospin, charge, and colour quantum numbers, which appears as a miracle from the point of view of the low energy theory, but is in fact understandable from the point of view of the high energy theory. For example, in Grand Unified Theories (GUTs) (for reviews, see, for example, [315]) there are similar relations where charge quantization and colour are related: in the 5 of $SU(5)$, we have the content $(d, d, d, e^+, \bar{\nu})$ and the charge generator has a vanishing trace in each $SU(5)$ representation: the condition of unit determinant, represented by the letter S in the $SU(5)$ group name, translates into zero trace for the generators. Thus the charge of d quarks is $-1/3$ of the positron charge, because there are three colours. A whole family fits perfectly in one 16 dimensional

representation of $SO(10)$ which is anomaly free. So GUTs can naturally explain the cancellation of the chiral anomaly.

An important implication of chiral anomalies together with the topological properties of the vacuum in non-Abelian gauge theories is that the conservation of the charges associated with baryon (B) and lepton (L) numbers is broken by the anomaly [336], so that B and L conservation are actually violated in the standard electroweak theory (but $B - L$ remains conserved). B and L are conserved to all orders in the perturbative expansion, but the violation occurs via non-perturbative instanton effects [87] [The amplitude is proportional to the typical non-perturbative factor $\exp(-c/g^2)$, with c a constant and g the $SU(2)$ gauge coupling.] The corresponding effect is totally negligible at zero temperature T, but becomes relevant at temperatures close to the electroweak symmetry breaking scale, precisely at $T \sim O(\text{TeV})$. The non-conservation of $B + L$ and the conservation of $B - L$ near the weak scale plays a role in the theory of baryogenesis that aims quantitatively at explaining the observed matter–antimatter asymmetry in the Universe (for reviews and references, see, for example, [115]).

3.9 QED Tests: Lepton Anomalous Magnetic Moments

The most precise tests of the electroweak theory apply to the QED sector. Here we discuss the anomalous magnetic moments of the electron and the muon that are among the most precise measurements in the whole of physics. The magnetic moment μ and the spin $\mathbf{S}$ are related by $\mu = -ge\mathbf{S}/2m$, where g is the gyromagnetic ratio ($g = 2$ for a pointlike Dirac particle). The quantity $a = (g-2)/2$ measures the anomalous magnetic moment of the particle. Recently there have been new precise measurements of a_e and a_μ for the electron [242] and the muon [297]:

$$a_e^{\text{exp}} = 11\,596\,521\,807.3(2.8) \times 10^{-13}\,, \quad a_\mu^{\text{exp}} = 11\,659\,208.9(6.3) \times 10^{-10}\,. \tag{3.91}$$

The theoretical calculations in general contain a pure QED part plus the sum of hadronic and weak contribution terms:

$$a = a^{\text{QED}} + a^{\text{hadronic}} + a^{\text{weak}} = \sum_i C_i \left(\frac{\alpha}{\pi}\right)^i + a^{\text{hadronic}} + a^{\text{weak}}\,. \tag{3.92}$$

The QED part has been computed analytically for $i = 1, 2, 3$, while for $i = 4$ there is a numerical calculation with an error (see, for example, [266] and references therein). The complete numerical evaluation of $i = 5$ for the muon case was published in 2012 [59] as a new and impressive achievement by Kinoshita and his group. The hadronic contribution is from vacuum polarization insertions and from light-by-light scattering diagrams (see Fig. 3.13). The weak contribution is from W or Z exchange.

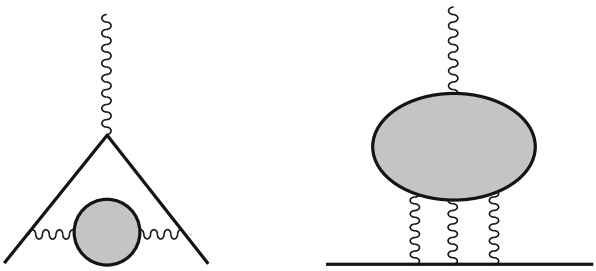

Fig. 3.13 Hadronic contributions to the anomalous magnetic moment: vacuum polarization (*left*) and light-by-light scattering (*right*)

For the electron case, the weak contribution is essentially negligible and the hadronic term $a_e^{\text{hadronic}} \sim (16.82 \pm 0.19) \times 10^{-13}$ does not introduce an important uncertainty. As a result this measurement can be used to obtain the most precise determination of the fine structure constant [59]:

$$\alpha^{-1} \sim 137.035\,999\,165\,7(340)\,, \tag{3.93}$$

In the muon case the experimental precision is less by about three orders of magnitude, but the sensitivity to new physics effects is typically increased by a factor $(m_\mu/m_e)^2 \sim 4 \times 10^4$. One mass factor arises because the effective operator needs a chirality flip and the second because, by definition, one must factor out the Bohr magneton $e/2m$. From the theory side, the QED term, using the value of α from a_e in (3.93), and the weak contribution [151] are affected by small errors and are given by

$$a_\mu^{\text{QED}} = (116\,584\,718.853 \pm 0.037) \times 10^{-11}\,, \quad a_\mu^{\text{weak}} = (154 \pm 2.0) \times 10^{-11}\,, \tag{3.94}$$

where all theoretical numbers are taken from [59].

The dominant ambiguities arise from the hadronic term. The lowest order (LO) vacuum polarization contribution can be evaluated from the measured cross-sections in $e^+e^- \to$ hadrons at low energy via dispersion relations (the largest contribution is from the $\pi\pi$ final state) [155, 239], with the result $a_\mu^{\text{LO}} \times 10^{-11} = 6949 \pm 43$. The higher order (HO) vacuum polarization contribution (from 2-loop diagrams containing a hadronic insertion) is given by $a_\mu^{\text{HO}} \times 10^{-11} = -98.4 \pm 0.7$ [239]. The contribution of the light-by-light (LbL) scattering diagrams is estimated to be $a_\mu^{\text{LBL}} \times 10^{-11} = 116 \pm 40$ [290]. Adding the above contributions, the total hadronic result is reported as

$$a_\mu^{\text{hadronic}} = (6967 \pm 59) \times 10^{-11}\,. \tag{3.95}$$

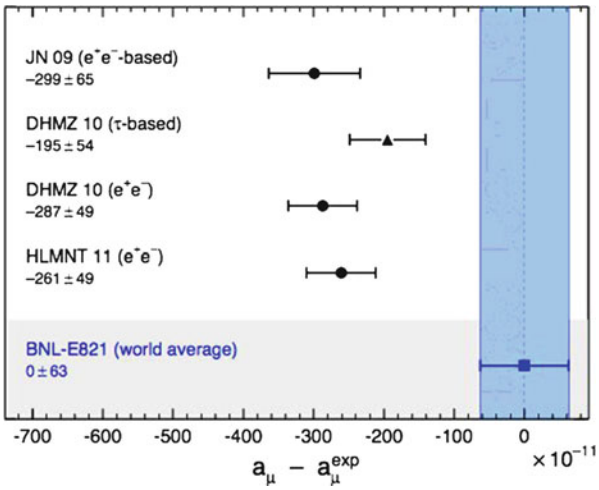

Fig. 3.14 Compilation of recently published results for a_μ (in units of 10^{-11}) [245]: JN [252], DHMZ [155], HLMNT [239]. Figure reproduced with permission. Copyright (c) 2012 by American Physical Society

At face value, this would lead to a 2.9σ deviation from the experimental value $a_\mu^{\rm exp}$ in (3.91):

$$a_\mu^{\rm exp} - a_\mu^{{\rm th}(e^+e^-)} = (249 \pm 87) \times 10^{-11}\,. \tag{3.96}$$

For a recent exchange on the significance of the discrepancy, see [88]. However, the error estimate in the LBL term, mainly a theoretical uncertainty, is not compelling, and it could well be somewhat larger (although probably not by so much as to make the discrepancy completely disappear). A minor puzzle is the fact that, using the conservation of the vector current (CVC) and isospin invariance, which are well established tools at low energy, $a_\mu^{\rm LO}$ can also be evaluated from τ decays. But the results on the hadronic contribution from e^+e^- and from τ decay, nominally of comparable accuracy, are still somewhat different (although the two are now closer than in the past), and the $g-2$ discrepancy would be attenuated if one took the τ result (see Fig. 3.14, which refers to the most recent results). Since it is difficult to find a theoretical reason for the e^+e^- vs τ difference, one must conclude that there is something which is not understood either in the data or in the assessment of theoretical errors. The prevailing view is to take the e^+e^- determination as the most directly reliable, which leads to (3.96), but some doubts remain. Finally, we note that, given the great accuracy of the a_μ measurement and the relative importance of the non-QED contributions, it is not unreasonable that a first signal of new physics would appear in this quantity.

3.10 Large Radiative Corrections to Electroweak Processes

Since the SM theory is renormalizable, higher order perturbative corrections can be reliably computed. Radiative corrections are very important for precision EW tests. The SM inherits all the successes of the old $V-A$ theory of charged currents and QED. Modern tests have focussed on neutral current processes, the W mass, and the measurement of triple gauge vertices. For Z physics and the W mass, the state-of-the-art computation of radiative corrections include the complete one-loop diagrams and selected dominant multi-loop corrections. In addition, some resummation techniques are also implemented, like Dyson resummation of vacuum polarization functions and important renormalization group improvements for large QED and QCD logarithms. We now discuss in more detail sets of large radiative corrections which are particularly significant (for reviews of radiative corrections for LEP1 physics, see, for example, [47], and for a more pedagogical description of LEP physics, see [338]).

Even leaving aside QCD corrections, an important set of quantitative contributions to the radiative corrections arise from large logarithms, e.g., terms of the form

$$\left(\frac{\alpha}{\pi}\ln\frac{m_Z}{m_{f_{ll}}}\right)^n ,$$

where f_{ll} is a light fermion. The sequences of leading and close-to-leading logarithms are fixed by well-known and consolidated techniques (β functions, anomalous dimensions, penguin-like diagrams, etc.). For example, large logarithms from pure QED effects dominate the running of α from m_e, the electron mass, up to m_Z. Similarly, large logarithms of the form

$$\left(\frac{\alpha}{\pi}\ln\frac{m_Z}{\mu}\right)^n$$

also enter, for example, in the relation between $\sin^2\theta_{\rm W}$ at the scales m_Z (LEP, SLC) and μ, e.g., the scale of low-energy neutral-current experiments. Furthermore, large logs from initial state radiation dramatically distort the line shape of the Z resonance, as observed at LEP1 and SLC, and this effect was accurately taken into account for the measurement of the Z mass and total width. The experimental accuracy on m_Z obtained at LEP1 is $\delta m_Z = \pm 2.1$ MeV.

Similarly, a measurement of the total width to an accuracy $\delta\Gamma = \pm 2.3$ MeV has been achieved. The prediction of the Z line shape in the SM to such an accuracy posed a formidable challenge to theory, and it has been successfully met. For the inclusive process $e^+e^- \to f\bar{f}X$, with $f \neq e$ (for a concise discussion, we leave Bhabha scattering aside) and X including photons and gluons, the physical cross-section can be written in the form of a convolution [47]:

$$\sigma(s) = \int_{z_0}^{1} {\rm d}z\, \hat{\sigma}(zs) G(z,s) , \tag{3.97}$$

where $\hat{\sigma}$ is the reduced cross-section, $G(z,s)$ is the radiator function, which describes the effect of initial-state radiation, and $\hat{\sigma}$ includes the purely weak corrections, the effect of final-state radiation (of both photons and gluons), and also non-factorizable terms (initial- and final-state radiation interferences, boxes, etc.) which, being small, can be treated in lowest order and effectively absorbed in a modified $\hat{\sigma}$. The radiator function $G(z,s)$ has an expansion of the form

$$G(z,s) = \delta(1-z) + \frac{\alpha}{\pi}(a_{11}L + a_{10}) + \left(\frac{\alpha}{\pi}\right)^2 (a_{22}L^2 + a_{11}L + a_{20}) + \cdots + \left(\frac{\alpha}{\pi}\right)^n \sum_{i=0}^{n} a_{ni}L^i \,, \tag{3.98}$$

where $L = \ln(s/m_e^2) \simeq 24.2$ for $\sqrt{s} \simeq m_Z$. All first- and second-order terms are known exactly. The sequence of leading and next-to-leading logs can be exponentiated (closely following the formalism of structure functions in QCD). For $m_Z \approx 91\,\text{GeV}$, the convolution displaces the peak by $+110\,\text{MeV}$, and reduces it by a factor of about 0.74. The exponentiation is important in that it amounts to an additional shift of about 14 MeV in the peak position with respect to the 1-loop radiative correction.

Among the one-loop EW radiative corrections, a remarkable class of contributions are those terms that increase quadratically with the top mass. The sensitivity of radiative corrections to m_t arises from the existence of these terms. The quadratic dependence on m_t (and on other possible widely broken isospin multiplets from new physics) arises because, in spontaneously broken gauge theories, heavy virtual particles do not decouple. On the contrary, in QED or QCD, the running of α and α_s at a scale Q is not affected by heavy quarks with mass $M \gg Q$. According to an intuitive decoupling theorem [60], diagrams with heavy virtual particles of mass M can be ignored at $Q \ll M$, provided that the couplings do not grow with M and that the theory with no heavy particles is still renormalizable. In the spontaneously broken EW gauge theories, both requirements are violated.

First, one important difference with respect to unbroken gauge theories is in the longitudinal modes of weak gauge bosons. These modes are generated by the Higgs mechanism, and their couplings grow with masses (as is also the case for the physical Higgs couplings). Second, the theory without the top quark is no longer renormalizable since the gauge symmetry is broken because the (t,b) doublet would not be complete (also the chiral anomaly would not be completely cancelled). With the observed value of m_t, the quantitative importance of the terms of order $G_F m_t^2/4\pi^2\sqrt{2}$ is substantial but not dominant (they are enhanced by a factor $m_t^2/m_W^2 \sim 5$ with respect to ordinary terms). Both the large logarithms and the $G_F m_t^2$ terms have a simple structure and are to a large extent universal, i.e., common to a wide class of processes. In particular, the $G_F m_t^2$ terms appear in vacuum polarization diagrams which are universal (virtual loops inserted in gauge boson internal lines are independent of the nature of the vertices on each side of the propagator) and in the $Z \to b\bar{b}$ vertex which is not. This vertex is specifically sensitive to the top

quark which, being the partner of the b quark in a doublet, runs in the loop. Instead, all types of heavy particles could in principle contribute to vacuum polarization diagrams. The study of universal vacuum polarization contributions, also called "oblique" corrections, and of top enhanced terms is important for an understanding of the pattern of radiative corrections. More generally, the important consequence of non-decoupling is that precision tests of the electroweak theory may a priori be sensitive to new physics, even if the new particles are too heavy for their direct production, but a posteriori no signal of deviation has clearly emerged.

While radiative corrections are quite sensitive to the top mass, they are unfortunately much less dependent on the Higgs mass. In fact, the dependence of one-loop diagrams on $m_{\rm H}$ is only logarithmic, viz., $\sim G_{\rm F} m_W^2 \log(m_H^2/m_W^2)$. Quadratic terms $\sim G_F^2 m_H^2$ only appear at two-loop level [356] and are too small to be detectable. The difference with the top case is that the splitting $m_t^2 - m_b^2$ is a direct breaking of the gauge symmetry that already affects the 1-loop corrections, while the Higgs couplings are "custodial" $SU(2)$ symmetric in lowest order.

3.11 Electroweak Precision Tests

For the analysis of electroweak data in the SM, one starts from the input parameters: as is the case in any renormalizable theory, masses and couplings have to be specified from outside. One can trade one parameter for another and this freedom is used to select the best measured ones as input parameters. Some of them, α, $G_{\rm F}$, and m_Z, are very precisely known, as we have seen, and some others, $m_{f_{\rm light}}$, m_t, and $\alpha_{\rm s}(m_Z)$ are less well determined, while $m_{\rm H}$ was largely unknown before the LHC. In this section we discuss the EW fit without the new input on $m_{\rm H}$ from the LHC, in order to compare the limits so derived on $m_{\rm H}$ with the LHC data. The LHC results will be discussed in the following sections. Among the light fermions, the quark masses are poorly known, but fortunately, for the calculation of radiative corrections, they can be replaced by $\alpha(m_Z)$, the value of the QED running coupling at the Z mass scale. The value of the hadronic contribution to the running, embodied in the value of $\Delta\alpha^{(5)}_{\rm had}(m_Z^2)$ (see Fig. 3.15 [350]) is obtained through dispersion relations from the data on $e^+e^- \to$ hadrons at moderate centre-of-mass energies. From the input parameters, one computes the radiative corrections to a sufficient accuracy to match the experimental accuracy. One then compares the theoretical predictions with the data for the numerous observables which have been measured [351], checks the consistency of the theory, and derives constraints on m_t, $\alpha_{\rm s}(m_Z)$, and $m_{\rm H}$.

The basic tree level relations

$$\frac{g^2}{8m_W^2} = \frac{G_{\rm F}}{\sqrt{2}}\,, \quad g^2 \sin^2\theta_{\rm W} = e^2 = 4\pi\alpha\,, \tag{3.99}$$

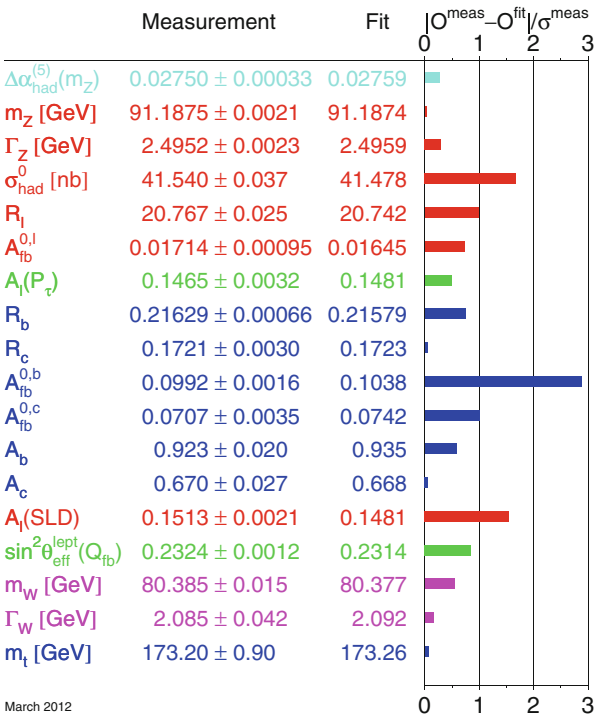

Fig. 3.15 Summary of electroweak precision measurements at high Q^2 [350]. The *first block* shows the Z-pole measurements. The *second block* shows additional results from other experiments: the mass and the width of the W boson measured at the Tevatron and at LEP2, the mass of the top quark measured at the Tevatron, and the contribution to α of the hadronic vacuum polarization. The SM fit results are also shown with the corresponding pulls (differences data and fits in units of standard deviations)

can be combined into

$$\sin^2\theta_{\mathrm{W}} = \frac{\pi\alpha}{\sqrt{2}G_{\mathrm{F}}m_W^2}\,. \tag{3.100}$$

Still at tree level, a different definition of $\sin^2\theta_{\mathrm{W}}$ comes from the gauge boson masses

$$\frac{m_W^2}{m_Z^2\cos^2\theta_{\mathrm{W}}} = \rho_0 = 1 \quad\Longrightarrow\quad \sin^2\theta_{\mathrm{W}} = 1 - \frac{m_W^2}{m_Z^2}\,, \tag{3.101}$$

where $\rho_0 = 1$, assuming that there are only Higgs doublets. The last two relations can be put into the convenient form

$$\left(1 - \frac{m_W^2}{m_Z^2}\right)\frac{m_W^2}{m_Z^2} = \frac{\pi\alpha}{\sqrt{2}G_{\mathrm{F}}m_Z^2}\,. \tag{3.102}$$

Beyond tree level, these relations are modified by radiative corrections:

$$\left(1-\frac{m_W^2}{m_Z^2}\right)\frac{m_W^2}{m_Z^2}=\frac{\pi\alpha(m_Z)}{\sqrt{2}G_{\rm F}m_Z^2}\frac{1}{1-\Delta r_W}\,,$$
$$\frac{m_W^2}{m_Z^2\cos^2\theta_{\rm W}}=1+\Delta\rho_m\,. \tag{3.103}$$

The Z and W masses are to be precisely defined, for example, in terms of the pole position in the respective propagators. Then in the first relation, the replacement of α with the running coupling at the Z mass $\alpha(m_Z)$ makes Δr_W completely determined at 1-loop by purely weak corrections ($G_{\rm F}$ is protected from logarithmic running as an indirect consequence of $V-A$ current conservation in the massless theory). This relation defines Δr_W unambiguously, once the meaning of $m_{W,Z}$ and $\alpha(m_Z)$ is specified (for example, $\bar{M}\bar{S}$). In contrast, in the second relation, $\Delta\rho_m$ depends on the definition of $\sin^2\theta_{\rm W}$ beyond the tree level. For LEP physics $\sin^2\theta_{\rm W}$ is usually defined from the $Z\to\mu^+\mu^-$ effective vertex. At the tree level, the vector and axial-vector couplings $g_{\rm V}^\mu$ and $g_{\rm A}^\mu$ are given in (3.26). Beyond the tree level a corrected vertex can be written down in terms of modified effective couplings. Then $\sin^2\theta_{\rm W}\equiv\sin^2\theta_{\rm eff}$ is generally defined through the muon vertex:

$$\frac{g_{\rm V}^\mu}{g_{\rm A}^\mu}=1\text{–}4\sin^2\theta_{\rm eff}\,,\quad \sin^2\theta_{\rm eff}=(1+\Delta k)s_0^2\,,\quad s_0^2c_0^2=\frac{\pi\alpha(m_Z)}{\sqrt{2}G_{\rm F}m_Z^2}\,,\quad g_{\rm A}^{\mu 2}=\frac{1}{4}(1+\Delta\rho)\,. \tag{3.104}$$

We see that s_0^2 and c_0^2 are "improved" Born approximations (by including the running of α) for $\sin^2\theta_{\rm eff}$ and $\cos^2\theta_{\rm eff}$. Actually, since lepton universality is only broken by masses in the SM, and is in agreement with experiment within the present accuracy, the muon channel can in practice be replaced with the average over charged leptons.

We can write a symbolic equation that summarizes the status of what has been computed up to now for the radiative corrections Δr_W [70], $\Delta\rho$ [193], and Δk [71] (listing some recent work on each item from which older references can be retrieved):

$$\Delta r_W,\Delta\rho,\Delta k=g^2(1+\alpha_{\rm s})+g^2\frac{m_t^2}{m_W^2}(\alpha_s^2+\alpha_s^3)+g^4+g^4\frac{m_t^4}{m_W^4}\alpha_{\rm s}+g^6\frac{m_t^6}{m_W^6}+\cdots\,. \tag{3.105}$$

The meaning of this relation is that the one loop terms of order g^2 are completely known, together with their first order QCD corrections, while the second and third order QCD corrections are only known for the g^2 terms enhanced by m_t^2/m_W^2, the two-loop terms of order g^4 are completely known, and for $\Delta\rho$ alone, the terms $g^4\alpha_{\rm s}$ enhanced by the ratio m_t^4/m_W^4 and the terms $g^6\frac{m_t^6}{m_W^6}$ are also computed.

In the SM, the quantities Δr_W, $\Delta\rho$, Δk, for sufficiently large m_t, are all dominated by quadratic terms in m_t of order $G_F m_t^2$. The quantity $\Delta\rho_m$ is not independent and can be expressed in terms of them. As new physics can more easily be disentangled if not masked by large conventional m_t effects, it is convenient to keep $\Delta\rho$, while trading Δr_W and Δk for two quantities with no contributions of order $G_F m_t^2$. One thus introduces the following linear combinations (epsilon parameters) [48]:

$$\begin{aligned}
\epsilon_1 &= \Delta\rho \,, \\
\epsilon_2 &= c_0^2\Delta\rho + \frac{s_0^2}{c_0^2 - s_0^2}\Delta r_W - 2s_0^2\Delta k \,, \\
\epsilon_3 &= c_0^2\Delta\rho + (c_0^2 - s_0^2)\Delta k \,.
\end{aligned} \tag{3.106}$$

The quantities ϵ_2 and ϵ_3 no longer contain terms of order $G_F m_t^2$, but only logarithmic terms in m_t. The leading terms for large Higgs mass, which are logarithmic, are contained in ϵ_1 and ϵ_3. To complete the set of top-enhanced radiative corrections one adds ϵ_b, defined from the loop corrections to the $Zb\bar{b}$ vertex. One modifies g_V^b and g_A^b as follows:

$$g_A^b = -\frac{1}{2}\left(1 + \frac{\Delta\rho}{2}\right)(1 + \epsilon_b) \,, \qquad \frac{g_V^b}{g_A^b} = \frac{1 - \frac{4}{3}\sin^2\theta_{\rm eff} + \epsilon_b}{1 + \epsilon_b} \,. \tag{3.107}$$

ϵ_b can be measured from $R_b = \Gamma(Z \to b\bar{b})/\Gamma(Z \to \text{hadrons})$ (see Fig. 3.15). This is clearly not the most general deviation from the SM in the $Z \to b\bar{b}$ vertex, but ϵ_b is the quantity where the large m_t corrections are located in the SM. Thus, summarizing, in the SM one has the following "large" asymptotic contributions:

$$\begin{aligned}
\epsilon_1 &= \frac{3G_F m_t^2}{8\pi^2\sqrt{2}} - \frac{3G_F m_W^2}{4\pi^2\sqrt{2}}\tan^2\theta_W \ln\frac{m_H}{m_Z} + \cdots \,, \\
\epsilon_2 &= -\frac{G_F m_W^2}{2\pi^2\sqrt{2}}\ln\frac{m_t}{m_Z} + \cdots \,, \\
\epsilon_3 &= \frac{G_F m_W^2}{12\pi^2\sqrt{2}}\ln\frac{m_H}{m_Z} - \frac{G_F m_W^2}{6\pi^2\sqrt{2}}\ln\frac{m_t}{m_Z} + \cdots \,, \\
\epsilon_b &= -\frac{G_F m_t^2}{4\pi^2\sqrt{2}} + \cdots \,,
\end{aligned} \tag{3.108}$$

The ϵ_i parameters vanish in the limit where only tree level SM effects are kept plus pure QED and/or QCD corrections. So they describe the effects of quantum corrections (i.e., loops) from weak interactions. A similar set of parameters are the S, T, U parameters [310]: the shifts induced by new physics on S, T, and U are proportional to those induced on ϵ_3, ϵ_1, and ϵ_2, respectively. In principle, with no

model dependence, one can measure the four ϵ_i from the basic observables of LEP physics $\Gamma(Z \to \mu^+\mu^-)$, $A_{\rm FB}^{\mu}$, and R_b on the Z peak plus m_W. With increasing model dependence, one can include other measurements in the fit for the ϵ_i. For example, one can use lepton universality to average the μ with the e and τ final states, or include all lepton asymmetries and so on. The present experimental values of the ϵ_i, obtained from a fit of all LEP1-SLD measurements plus m_W, are [142]

$$\begin{aligned} \epsilon_1 \times 10^3 &= 5.6 \pm 1.0\,, \qquad \epsilon_2 \times 10^3 = -7.8 \pm 0.9\,, \\ \epsilon_3 \times 10^3 &= 5.6 \pm 0.9\,, \qquad \epsilon_b \times 10^3 = -5.8 \pm 1.3\,. \end{aligned} \tag{3.109}$$

Note that the ϵ parameters are of order a few 10^{-3} and are known with an accuracy in the range 15–30%. These values are in agreement with the predictions of the SM with a 126 GeV Higgs [142]:

$$\begin{aligned} \epsilon_1^{\rm SM} \times 10^3 &= 5.21 \pm 0.08\,, \qquad \epsilon_2^{\rm SM} \times 10^3 = -7.37 \pm 0.03\,, \\ \epsilon_3^{\rm SM} \times 10^3 &= 5.279 \pm 0.004\,, \qquad \epsilon_b^{\rm SM} \times 10^3 = -6.94 \pm 0.15\,. \end{aligned} \tag{3.110}$$

All models of new physics must be compared with these findings and pass this difficult test.

3.12 Results of the SM Analysis of Precision Tests

The electroweak Z pole measurements, combining the results of all the experiments, plus the W mass and width and the top mass m_t, are summarised in Fig 3.15, as of March 2012 [350]. The primary rates are given by the pole cross-sections for the various final states σ^0, and ratios thereof correspond to ratios of partial decay widths:

$$\sigma_{\rm h}^0 = \frac{12\pi}{m_Z^2}\,\frac{\Gamma_{ee}\Gamma_{\rm h}}{\Gamma_Z^2}\,, \qquad R_{\rm l}^0 = \frac{\sigma_{\rm h}^0}{\sigma_{\rm l}^0} = \frac{\Gamma_{\rm h}}{\Gamma_{\rm ll}}\,, \qquad R_q^0 = \frac{\Gamma_{q\bar{q}}}{\Gamma_{\rm h}}\,. \tag{3.111}$$

Here $\Gamma_{\rm ll}$ is the partial decay width for a pair of massless charged leptons. The partial decay width for a given fermion species contains information about the effective vector and axial-vector coupling constants of the neutral weak current:

$$\Gamma_{ff} = N_{\rm C}^f \frac{G_{\rm F} m_Z^3}{6\sqrt{2}\pi}\left(g_{{\rm a}f}^2 C_{{\rm A}f} + g_{{\rm v}f}^2 C_{{\rm V}f}\right) + \Delta_{\rm ew/QCD}\,, \tag{3.112}$$

where $N_{\rm C}^f$ is the QCD colour factor, $C_{\{{\rm A,V}\}f}$ are final-state QCD/QED correction factors, also absorbing imaginary contributions to the effective coupling constants,

g_{af} and g_{vf} are the real parts of the effective couplings, and Δ contains non-factorisable mixed corrections.

Besides total cross-sections, various types of asymmetries have been measured. The results of all asymmetry measurements are quoted in terms of the asymmetry parameter A_f, defined in terms of the real parts of the effective coupling constants g_{af} and g_{vf} by

$$A_f = 2\frac{g_{vf}g_{af}}{g_{vf}^2 + g_{af}^2} = 2\frac{g_{vf}/g_{af}}{1 + (g_{vf}/g_{af})^2} , \qquad A_{FB}^{0,f} = \frac{3}{4}A_e A_f . \tag{3.113}$$

The measurements are the forward–backward asymmetry ($A_{FB}^{0,f}$), the tau polarization (A_τ) and its forward–backward asymmetry (A_e) measured at LEP, as well as the left–right and left–right forward–backward asymmetry measured at SLC (A_e and A_f, respectively). Hence the set of partial width and asymmetry results allows the extraction of the effective coupling constants.

The various asymmetries determine the effective electroweak mixing angle for leptons with highest sensitivity (see Fig. 3.16). The weighted average of these results, including small correlations, is

$$\sin^2\theta_{\text{eff}} = 0.23153 \pm 0.00016 , \tag{3.114}$$

Note, however, that this average has a χ^2 of 11.8 for 5 degrees of freedom, corresponding to a probability of a few %. The χ^2 is pushed up by the two most precise measurements of $\sin^2\theta_{\text{eff}}$, namely those derived from the measurements of A_l by SLD, dominated by the left–right asymmetry A_{LR}^0, and measurements of the forward–backward asymmetry $A_{FB}^{0,b}$ measured in $b\bar{b}$ production at LEP, which differ by about 3σ.

We now extend the discussion of the SM fit of the data. One can think of different types of fit, depending on which experimental results are included or which answers one wants to obtain. For example, in Table 3.2 we present in column 1 a fit of all Z pole data plus m_W and Γ_W (this is interesting as it shows the value of m_t obtained

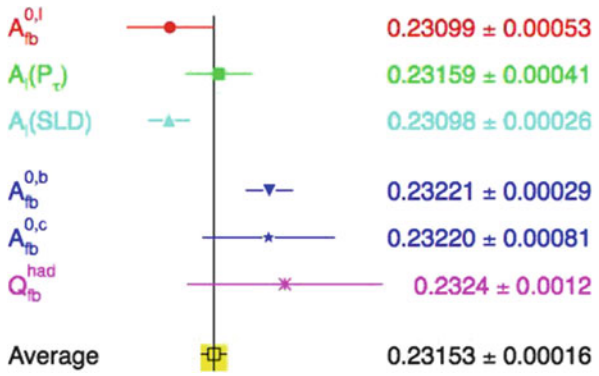

Fig. 3.16 Summary of $\sin^2\theta_{\text{eff}}$ precision measurements at high Q^2 [350]

Table 3.2 Standard Model fits of electroweak data [350]

Fit	1	2	3
Measurements	m_W, Γ_W	m_t	m_t, m_W, Γ_W
m_t (GeV)	$178.1^{+10.9}_{-7.8}$	173.2 ± 0.9	173.26 ± 0.89
$m_{\rm H}$ (GeV)	148^{+237}_{-81}	122^{+59}_{-41}	94^{+29}_{-24}
log $[m_{\rm H}({\rm GeV})]$	$2.17 \pm +0.38$	2.09 ± 0.17	1.97 ± 0.12
$\alpha_{\rm s}(m_Z)$	0.1190 ± 0.0028	0.1191 ± 0.0027	0.1185 ± 0.0026
m_W (MeV)	80381 ± 13	80363 ± 20	80377 ± 12

All fits use the Z pole results and $\Delta\alpha^{(5)}_{\rm had}(m_Z^2)$, as listed in Fig. 3.15. In addition, the measurements listed at the top of each column are included in that case. The fitted W mass is also shown [350] (the directly measured value is $m_W = 80\,385 \pm 15\,{\rm MeV}$)

indirectly from radiative corrections, to be compared with the value of m_t measured in production experiments), in column 2, a fit of all Z pole data plus m_t (here it is m_W which is indirectly determined), and finally, in column 3, a fit of all the data listed in Fig. 3.15 (which is the most relevant fit for constraining $m_{\rm H}$).

From the fit in column 1 we see that the extracted value of m_t is in good agreement with the direct measurement (see Fig 3.15). Similarly, we see that the experimental measurement of m_W is larger by about one standard deviation with respect to the value from the fit in column 2. We have seen that quantum corrections depend only logarithmically on $m_{\rm H}$. In spite of this small sensitivity, the measurements are still precise enough to obtain a quantitative indication of the mass range. From the fit in column 3 we obtain

$$\log_{10} m_{\rm H}\,({\rm GeV}) = 1.97 \pm 0.12\,, \quad \text{or } m_{\rm H} = 94^{+29}_{-24}\,{\rm GeV}\,.$$

This result on the Higgs mass is truly remarkable. The value of $\log_{10} m_{\rm H}$ (GeV) is compatible with the small window between ~ 2 and ~ 3 which is allowed, on the one side, by the direct search limit $m_{\rm H} > 114\,{\rm GeV}$ from LEP2 [350], and on the other side by the theoretical upper limit on the Higgs mass in the minimal SM, $m_{\rm H} \lesssim 600$–$800\,{\rm GeV}$ [320], to be discussed in Sect. 3.13.

Thus the whole picture of a perturbative theory with a fundamental Higgs is well supported by the data on radiative corrections. It is important that there is a clear indication for a particularly light Higgs: at 95% confidence level $m_{\rm H} \lesssim 152\,{\rm GeV}$ (which becomes $m_{\rm H} \lesssim 171\,{\rm GeV}$, including the input from the LEP2 direct search result). This was quite encouraging for the LHC search for the Higgs particle. More generally, if the Higgs couplings are removed from the Lagrangian, the resulting theory is non-renormalizable. A cutoff Λ must be introduced. In the quantum corrections, $\log m_{\rm H}$ is then replaced by $\log \Lambda$ plus a constant. The precise determination of the associated finite terms would be lost (that is, the value of the mass in the denominator in the argument of the logarithm). A heavy Higgs would need some unfortunate accident: the finite terms, different in the new theory from those of the SM, should by chance compensate for the heavy Higgs in a few

key parameters of the radiative corrections (mainly ϵ_1 and ϵ_3, see, for example, [48]). Alternatively, additional new physics, for example in the form of effective contact terms added to the minimal SM Lagrangian, should accidentally do the compensation, which again needs some sort of conspiracy.

To the list of precision tests of the SM, one should add the results on low energy tests obtained from neutrino and antineutrino deep inelastic scattering (NuTeV [353]), parity violation in Cs atoms (APV [274]), and the recent measurement of the parity-violating asymmetry in Moller scattering [354]. When these experimental results are compared with the SM predictions, the agreement is good except for the NuTeV result, which differs by three standard deviations. The NuTeV measurement is quoted as a measurement of $\sin^2\theta_{\rm W} = 1 - m_W^2/m_Z^2$ from the ratio of neutral to charged current deep inelastic cross-sections from ν_μ and $\bar{\nu}_\mu$ using the Fermilab beams. But it has been argued, and it is now generally accepted, that the NuTeV anomaly probably simply arises from an underestimation of the theoretical uncertainty in the QCD analysis needed to extract $\sin^2\theta_{\rm W}$. In fact, the lowest order QCD parton formalism upon which the analysis has been based is too crude to match the experimental accuracy.

When confronted with these results, the SM performs rather well on the whole, so that it is fair to say that no clear indication for new physics emerges from the data. However, as already mentioned, one problem is that the two most precise measurements of $\sin^2\theta_{\rm eff}$ from $A_{\rm LR}$ and $A_{\rm FB}^b$ differ by about 3σ. In general, there appears to be a discrepancy between $\sin^2\theta_{\rm eff}$ measured from leptonic asymmetries, denoted $(\sin^2\theta_{\rm eff})_{\rm l}$, and from hadronic asymmetries, denoted $(\sin^2\theta_{\rm eff})_{\rm h}$. In fact, the result from $A_{\rm LR}$ is in good agreement with the leptonic asymmetries measured at LEP, while all hadronic asymmetries, though their errors are large, are better compatible with the result of $A_{\rm FB}^b$. These two results for $\sin^2\theta_{\rm eff}$ are shown in Fig. 3.17 [210]. Each of them is plotted at the $m_{\rm H}$ value that would correspond to it given the central value of m_t. Of course, the value for $m_{\rm H}$ indicated by each $\sin^2\theta_{\rm eff}$ has a horizontal ambiguity determined by the measurement error and the width of the $\pm 1\sigma$ band for m_t.

Even taking this spread into account, it is clear that the implications for $m_{\rm H}$ are significantly different. One might imagine that some new physics effect could be hidden in the $Zb\bar{b}$ vertex. For instance, for the top quark mass there could be other non-decoupling effects from new heavy states or a mixing of the b quark with some other heavy quark. However, it is well known that this discrepancy is not easily explained in terms of any new physics effect in the $Zb\bar{b}$ vertex. A rather large change with respect to the SM of the b quark right-handed coupling to the Z is needed in order to reproduce the measured discrepancy (in fact, a $\sim 30\%$ change in the right-handed coupling), an effect too large to be a loop effect, but which could be produced at the tree level, e.g., by mixing of the b quark with a new heavy vector-like quark [140], or some mixing of the Z with ad hoc heavy states [170]. But then this effect should normally also appear in the direct measurement of A_b performed at SLD using the left–right polarized b asymmetry, even within the moderate accuracy of this result. The measurements of neither A_b at SLD nor R_b confirm the need for

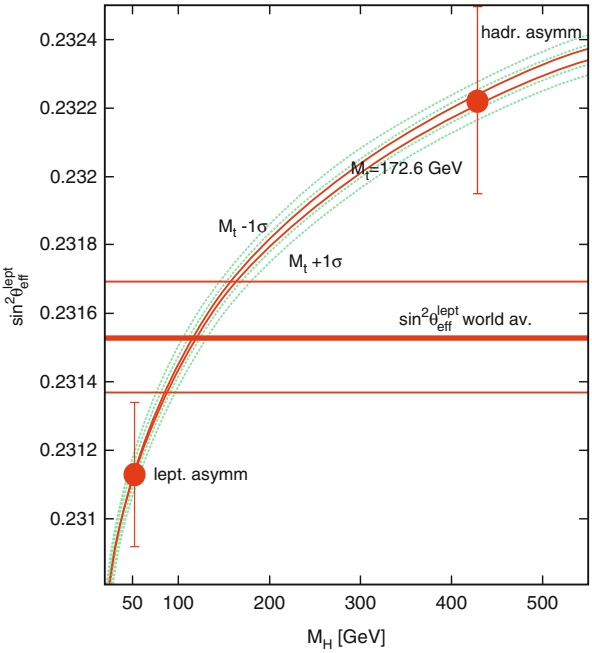

Fig. 3.17 The data for $\sin^2\theta_{\rm eff}^{\rm lept}$ are plotted vs $m_{\rm H}$. The theoretical prediction for the measured value of m_t is also shown. For presentation purposes the measured points are each shown at the $m_{\rm H}$ value that would ideally correspond to it, given the central value of m_t. Adapted from [210]. New version courtesy of P. Gambino

such a large effect (recently a numerical calculation of NLO corrections to R_b [204] appeared at first to indicate a rather large result, but in the end the full correction turned out to be rather small). Alternatively, the observed discrepancy could simply be due to a large statistical fluctuation or an unknown experimental problem. As a consequence of this problem, the ambiguity in the measured value of $\sin^2\theta_{\rm eff}$ is in practice greater than the nominal error, reported in (3.114), obtained from averaging all the existing determinations, and the interpretation of precision tests is less sharp than it would otherwise be.

We have already observed that the experimental value of m_W (with good agreement between LEP and the Tevatron) is a bit high compared to the SM prediction (see Fig. 3.18). The value of $m_{\rm H}$ indicated by m_W is on the low side, just in the same interval as for $\sin^2\theta_{\rm eff}^{\rm lept}$ measured from leptonic asymmetries.

In conclusion, the experimental information on the Higgs sector, obtained from EW precision tests at LEP1 and 2 and the Tevatron can be summarized as follows. First, the relation $M_W^2 = M_Z^2\cos^2\theta_{\rm W}$ in (3.52), modified by small, computable radiative corrections, has been demonstrated experimentally. This relation means that the effective Higgs (be it fundamental or composite) is indeed a weak isospin doublet. The direct lower limit $m_{\rm H} \gtrsim 114.5\,\text{GeV}$ (at 95% confidence level) was

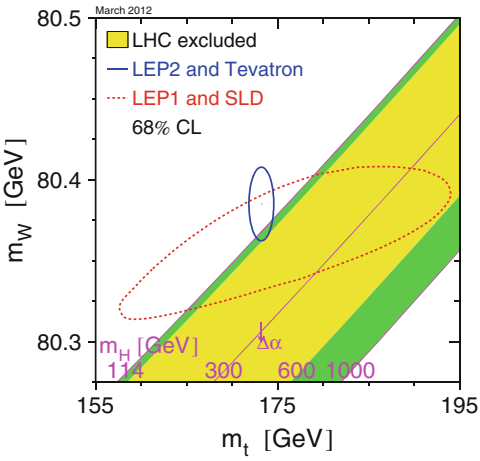

Fig. 3.18 The data for m_W are plotted vs m_t [350]

obtained from searches at LEP2. When compared to the data on precision EW tests, the radiative corrections computed in the SM lead to a clear indication of a light Higgs, not too far from the direct LEP2 lower bound. The upper limit for m_{H} in the SM from the EW tests depends on the value of the top quark mass m_t. The CDF and D0 combined value after Run II is at present $m_t = 173.2 \pm 0.9\,\mathrm{GeV}$ [350]. As a consequence, the limit on m_{H} from the LEP and Tevatron measurements is rather stringent [350]: $m_{\mathrm{H}} < 171\,\mathrm{GeV}$ (at 95% confidence level, after including the information from the 114.5 GeV direct bound).

3.13 The Search for the SM Higgs

The Higgs problem is really central in particle physics today. On the one hand, the experimental verification of the Standard Model (SM) cannot be considered complete until the structure of the Higgs sector has been established by experiment. On the other hand, the Higgs is also related to most of the major problems of particle physics, like the flavour problem and the hierarchy problem, the latter strongly suggesting the need for new physics near the weak scale (something that so far has not been found). In its turn, the discovery of new physics could throw light on the nature of dark matter. It was already clear before the LHC that some sort of Higgs mechanism is at work. The W or the Z with longitudinal polarization that we observe are not present in an unbroken gauge theory (massless spin-1 particles, like the photon, are transversely polarized): the longitudinal degrees of freedom for the W or the Z are borrowed from the Higgs sector and hence provide evidence for it.

Furthermore, it has been precisely established at LEP that the gauge symmetry is unbroken in the vertices of the theory: all currents and charges are indeed symmetric. Yet there is obvious evidence that the symmetry is instead badly broken in the

masses. Not only do the W and the Z have large masses, but the large splitting of, for example, the t–b doublet shows that even a global weak $SU(2)$ is not at all respected by the fermion spectrum. This is a clear signal of spontaneous symmetry breaking and the implementation of spontaneous symmetry breaking in a gauge theory is via the Higgs mechanism.

The big questions are about the nature and the properties of the Higgs particle(s). The search for the Higgs boson and for possible new physics that could accompany it was the main goal of the LHC from the start. On the Higgs the LHC should answer the following questions: do some Higgs particles exist? And if so, which ones: a single doublet, more doublets, additional singlets? SM Higgs or SUSY Higgses? Fundamental or composite (of fermions, of WW, or other)? Pseudo-Goldstone bosons of an enlarged symmetry? A manifestation of large extra dimensions (fifth component of a gauge boson, an effect of orbifolding or of boundary conditions, or other)? Or some combination of the above, or something so far unthought of? By now we have a candidate Higgs boson that really looks like the simplest realization of the Higgs mechanism, as described by the minimal SM Higgs. In the following we first consider the a priori expectations for the Higgs sector and then the profile of the Higgs candidate discovered at the LHC.

3.14 Theoretical Bounds on the SM Higgs Mass

A strong argument indicating that the solution of the Higgs problem may not be too far away (that is, either discovering the Higgs or finding the new physics that complicates the picture) is the fact that, in the absence of a Higgs particle or any alternative mechanism, violations of unitarity appear in some scattering amplitudes at energies in the few TeV range [279]. In particular, amplitudes involving longitudinal gauge bosons (those most directly related to the Higgs sector) are affected. For example, at tree level, in the absence of Higgs exchange and for $s \gg m_Z^2$, one obtains

$$A(W_L^+ W_L^- \to Z_L Z_L)_{\text{no Higgs}} \sim \mathrm{i}\frac{s}{v^2} \,. \tag{3.115}$$

In the SM this unacceptable large energy behaviour is quenched by the Higgs exchange diagram contribution

$$A(W_L^+ W_L^- \to Z_L Z_L)_{\text{Higgs}} \sim -\mathrm{i}\frac{s^2}{v^2(s - m_H^2)} \,. \tag{3.116}$$

Thus the total result in the SM is

$$A(W_L^+ W_L^- \to Z_L Z_L)_{SM} \sim -i\frac{s m_H^2}{v^2(s - m_H^2)} \,, \tag{3.117}$$

which at high energies saturates at a constant value. To be compatible with unitarity bounds, one needs $m_{\rm H}^2 < 4\pi\sqrt{2}/G_{\rm F}$ or $m_{\rm H} < 1.5\,{\rm TeV}$. This is an important theorem that guarantees that either the Higgs boson(s) or new physics or both must be present in the few TeV energy range.

It is well known that, as described in [241] and references therein, in the SM with only one Higgs doublet an upper bound on $m_{\rm H}$ (with mild dependence on m_t and the QCD coupling $\alpha_{\rm s}$) is obtained from the requirement that the perturbative description of the theory remains valid up to a large energy scale Λ where the SM model breaks down and new physics appears. Similarly, a lower bound on $m_{\rm H}$ can be derived from the requirement of vacuum stability [38, 123, 323] (or, in milder form, a requirement of moderate instability, compatible with the lifetime of the Universe [160, 249]). The Higgs mass enters because it fixes the initial value of the quartic Higgs coupling λ in its running up to the large scale Λ. We now briefly recall the derivation of these limits.

The upper limit on the Higgs mass in the SM is clearly important for an a priori assessment of the chances of success for the LHC as an accelerator designed to solve the Higgs problem. One way to estimate the upper limit [241] is to require that the Landau pole associated with the non-asymptotically free behaviour of the $\lambda\phi^4$ theory does not occur below the scale Λ. The running of $\lambda(\Lambda)$ at one loop is given by

$$\frac{{\rm d}\lambda}{{\rm d}t} = \frac{3}{4\pi^2}\left[\lambda^2 + 3\lambda h_t^2 - 9h_t^4 + \text{small gauge and Yukawa terms}\right], \tag{3.118}$$

with the normalization such that at $t = 0$, $\lambda = \lambda_0 = m_H^2/2v^2$, from the minimum condition in (3.60), and the top Yukawa coupling is given by $h_t^0 = m_t/v$. The initial value of λ at the weak scale increases with $m_{\rm H}$ and the derivative is positive at large λ because of the positive λ^2 term (the $\lambda\varphi^4$ theory is not asymptotically free), which overwhelms the negative top Yukawa term. Thus, if $m_{\rm H}$ is too large, the point where λ computed from the perturbative beta function becomes infinite (the Landau pole) occurs at too low an energy. Of course, in the vicinity of the Landau pole the 2-loop evaluation of the beta function is not reliable. Indeed, the limit indicates the frontier of the domain where the theory is well described by the perturbative expansion. Thus the quantitative evaluation of the limit is only indicative, although it has been to some extent supported by simulations of the Higgs sector of the EW theory on the lattice. For the upper limit on $m_{\rm H}$, one finds [241]

$$m_{\rm H} \lesssim 180\,{\rm GeV} \ \text{ for } \Lambda \sim M_{\rm GUT}\text{–}M_{\rm Planck}\,, \quad m_{\rm H} \lesssim 0.5\text{–}0.8\,{\rm TeV} \ \text{ for } \Lambda \sim 1\,{\rm TeV}\,. \tag{3.119}$$

As for a lower limit on the SM Higgs mass, a possible instability of the Higgs potential $V[\phi]$ is generated by the quantum loop corrections to the classical expression for $V[\phi]$. At large ϕ the derivative $V'[\phi]$ could become negative and the potential would become unbound from below. The one-loop corrections to $V[\phi]$ in the SM are well known and change the dominant term at large ϕ according to

$\lambda\phi^4 \to (\lambda + \gamma \log \phi^2/\Lambda^2)\phi^4$. This one-loop approximation is not enough in this case, because it fails at large enough ϕ, when $\gamma \log \phi^2/\Lambda^2$ becomes of order 1. The renormalization group improved version of the corrected potential leads to the replacement $\lambda\phi^4 \to \lambda(\Lambda)\phi'^4(\Lambda)$, where $\lambda(\Lambda)$ is the running coupling and $\phi'(\mu) = \phi \exp \int^t \gamma(t')\mathrm{d}t'$, with $\gamma(t)$ an anomalous dimension function, $t = \log \Lambda/v$, and v the vacuum expectation value $v = (2\sqrt{2}G_\mathrm{F})^{-1/2}$. As a result, the positivity condition for the potential amounts to the requirement that the running coupling $\lambda(\Lambda)$ should never become negative.

A more precise calculation, which also takes into account the quadratic term in the potential, confirms that the requirement of positive $\lambda(\Lambda)$ leads to the correct bound down to scales Λ as low as ~ 1 TeV. We see that, for m_H small and m_t fixed at its measured value, λ decreases with t and can become negative. If one requires λ to remain positive up to $\Lambda = 10^{16}$–10^{19} GeV, then the resulting bound on m_H in the SM with only one Higgs doublet, obtained from a recent state-of-the-art calculation [118, 160] is given by

$$m_\mathrm{H}\,(\mathrm{GeV}) > 129.6 + 2.0\left[\frac{m_t\,(\mathrm{GeV}) - 173.35}{0.7}\right] - 0.5\frac{\alpha_\mathrm{s}(m_Z) - 0.1184}{0.0007} \pm 0.3\ . \tag{3.120}$$

The estimate of the ambiguity associated with m_t can be questioned: is the definition of mass as measured at the Tevatron relevant for this calculation [25]? Note that this limit is avoided in models with more Higgs doublets. In that case the limit, applies to some average mass, but the lightest Higgs particle can be well below, as is the case in the minimal SUSY extension of the SM (MSSM).

In conclusion, for $m_t \sim 173$ GeV, only a small range of values for m_H is allowed, viz., $130 < m_\mathrm{H} <\sim 180$ GeV, if the SM holds and the vacuum is absolutely stable up to an energy scale $\Lambda \sim M_\mathrm{GUT}$ or M_Planck. For Higgs masses below this range, one can still have a domain where the SM is viable because the vacuum can be unstable, but with a lifetime longer than the age of the Universe [111, 118, 160]. We shall come back to this later (see Fig. 3.21).

3.15 SM Higgs Decays

The total width and the branching ratios for the SM Higgs as a function of m_H are given in Fig. 3.19 [169]. Since the couplings of the Higgs particle are proportional to masses, when m_H increases, the Higgs particle becomes strongly coupled. This is reflected in the sharp rise of the total width with m_H. For m_H in the range 114–130 GeV, the width is below 5 MeV, much less than the widths of the W or the Z, which have a comparable mass. The dominant channel for such a Higgs is $H \to b\bar{b}$. In the Born approximation, the partial width into a fermion pair is given

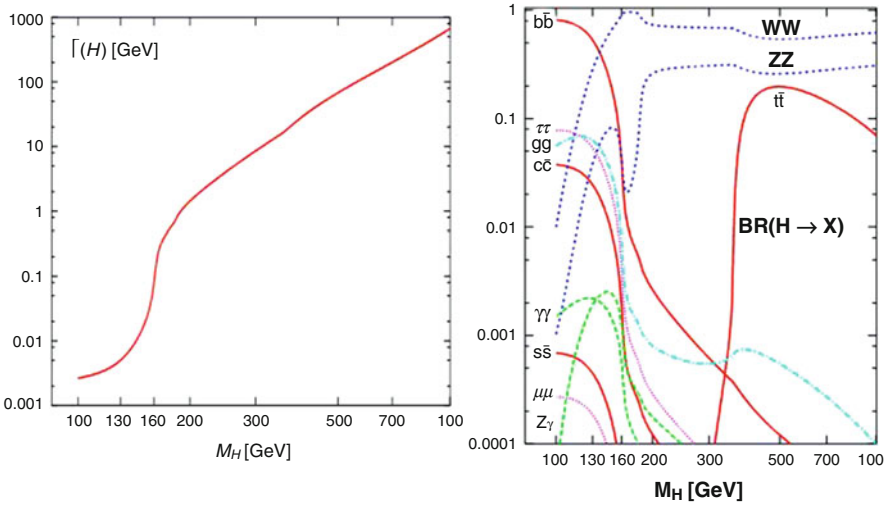

Fig. 3.19 *Left*: The total width of the SM Higgs boson as a function of the mass. *Right*: The branching ratios of the SM Higgs boson as a function of the mass (*solid line* fermions, *dashed line* bosons) [169]

by [169, 238]

$$\Gamma(H \to f\bar{f}) = N_{\mathrm{C}} \frac{G_{\mathrm{F}}}{4\pi\sqrt{2}} m_{\mathrm{H}} m_f^2 \beta_f^3 \,, \tag{3.121}$$

where $\beta_f = (1 - 4m_f^2/m_{\mathrm{H}}^2)^{1/2}$. The factor of β^3 appears because parity requires the fermion pair to be in a p-state of orbital angular momentum for a scalar Higgs (with parity $P = +1$). This factor would be β for a pseudoscalar Higgs boson. We see that the width is suppressed by a factor m_f^2/m_{H}^2 (the Higgs coupling is proportional to the fermion mass) with respect to the natural size $G_{\mathrm{F}} m_{\mathrm{H}}^3$ for the width of a particle of mass m_{H} decaying through a diagram with only one weak vertex.

A glance at the branching ratios shows that the branching ratio into τ pairs is larger by more than a factor of 2 with respect to the $c\bar{c}$ channel. This is at first sight surprising because the colour factor N_{C} favours the quark channels and the masses of τ leptons and D mesons are quite similar. This is due to the fact that the QCD corrections replace the charm mass at the scale of charm with the charm mass at the scale m_{H}, which is lower by about a factor of 2.5. The masses run logarithmically in QCD, similarly to the coupling constant. The corresponding logs are already present in the 1-loop QCD correction, which amounts to the replacement

$$m_q^2 \longrightarrow m_q^2 \left[1 + \frac{2\alpha_{\mathrm{s}}}{\pi} \left(\log \frac{m_q^2}{m_{\mathrm{H}}^2} + \frac{3}{2} \right) \right] \sim m_q^2(m_{\mathrm{H}}^2) \,.$$

The Higgs width increases sharply as the WW threshold is approached. For decay into a real pair of V bosons, with $V = W, Z$, one obtains in the Born approximation [169, 238]

$$\Gamma(H \to VV) = \frac{G_F m_H^3}{16\pi\sqrt{2}} \delta_V \beta_V (1 - 4x + 12x^2) \,, \tag{3.122}$$

where $\beta_V = \sqrt{1-4x}$ with $x = m_V^2/m_H^2$ and $\delta_W = 2$, $\delta_Z = 1$. Well above threshold, the VV channels are dominant and the total width, given approximately by

$$\Gamma_H \sim 0.5 \text{ TeV} \left(\frac{m_H}{1 \text{ TeV}}\right)^3 \,, \tag{3.123}$$

becomes very large, signalling that the Higgs sector is becoming strongly interacting, if we recall the upper limit on the SM Higgs mass in (3.119). The VV dominates over the $t\bar{t}$ because of the β threshold factors, which disfavour the fermion channel, and at large m_H, by the cubic versus linear behaviour with m_H of the partial widths for VV versus $t\bar{t}$. Below the VV threshold, the decays into virtual V particles is important: VV^* and V^*V^*. Note in particular the dip in the ZZ branching ratio just below the ZZ threshold. This is due to the fact that the W is lighter than the Z and the opening of its threshold depletes all other branching ratios. When the ZZ threshold is also passed, the ZZ branching fraction then comes back to the ratio of approximately 1:2 with the WW channel (just the number of degrees of freedom, i.e., two Hermitian fields for the W, one for the Z). The decay channels into $\gamma\gamma$, $Z\gamma$, and gg proceed through loop diagrams, with the contributions from W (only for $\gamma\gamma$ and $Z\gamma$) and from fermion loops (for all) (Fig. 3.20).

We reproduce here the results for $\Gamma(H \to \gamma\gamma)$ and $\Gamma(H \to gg)$ [169, 238]:

$$\Gamma(H \to \gamma\gamma) = \frac{G_F \alpha^2 m_H^3}{128\pi^3\sqrt{2}} \left| A_W(\tau_W) + \sum_f N_C Q_f^2 A_f(\tau_f) \right|^2 \,, \tag{3.124}$$

$$\Gamma(H \to gg) = \frac{G_F \alpha_s^2 m_H^3}{64\pi^3\sqrt{2}} \left| \sum_{f=Q} A_f(\tau_f) \right|^2 \,, \tag{3.125}$$

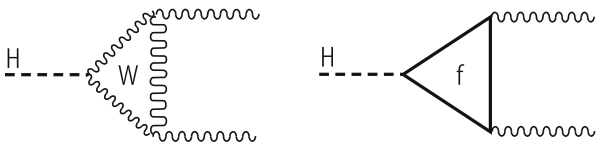

Fig. 3.20 Typical one-loop diagrams for Higgs decay into $\gamma\gamma$, $Z\gamma$, and for only the quark loop, gg

where $\tau_i = m_{\rm H}^2/4m_i^2$ and

$$A_f(\tau) = \frac{2}{\tau^2}\big[\tau + (\tau-1)f(\tau)\big]\,, \quad A_W(\tau) = -\frac{1}{\tau^2}\big[2\tau^2 + 3\tau + 3(2\tau-1)f(\tau)\big]\,, \tag{3.126}$$

with

$$f(\tau) = \begin{cases} \arcsin^2\sqrt{\tau} & \text{for } \tau \le 1\,, \\ -\dfrac{1}{4}\left(\log\dfrac{1+\sqrt{1-\tau^{-1}}}{1-\sqrt{1-\tau^{-1}}} - {\rm i}\pi\right)^2 & \text{for } \tau > 1\,. \end{cases} \tag{3.127}$$

For $H \to \gamma\gamma$ (as well as for $H \to Z\gamma$), the W loop is the dominant contribution at small and moderate $m_{\rm H}$. We recall that the $\gamma\gamma$ mode is a possible channel for Higgs discovery only for $m_{\rm H}$ near its lower bound (i.e., for $114 < m_{\rm H} < 150\,{\rm GeV}$). In this domain of $m_{\rm H}$, we have $\Gamma(H \to \gamma\gamma) \sim 6$–$23\,{\rm KeV}$. For example, in the limit $m_{\rm H} \ll 2m_i$, or $\tau \to 0$, we have $A_W(0) = -7$ and $A_f(0) = 4/3$. The two contributions become comparable only for $m_{\rm H} \sim 650\,{\rm GeV}$, where the two amplitudes, still of opposite sign, nearly cancel. The top loop is dominant among fermions (lighter fermions are suppressed by $m_f^2/m_{\rm H}^2$ modulo logs), and as we have seen, it approaches a constant for large m_t. Thus the fermion loop amplitude for the Higgs would be sensitive to effects from very heavy fermions. In particular, the $H \to gg$ effective vertex would be sensitive to all possible very heavy coloured quarks (of course, there is no W loop in this case, and the top quark gives the dominant contribution in the loop). As discussed in Chap. 2, the $gg \to H$ vertex provides one of the main production channels for the Higgs boson at hadron colliders, while another important channel at present is WH associate production.

3.16 The Higgs Discovery at the LHC

On 4 July 2012 at CERN, the ATLAS and CMS Collaborations [341, 345] announced the observation of a particle with mass around 126 GeV that, within the present accuracy, does indeed look like the SM Higgs boson. This is a great breakthrough which, by itself, already makes an adequate return for the LHC investment. With the Higgs discovery, the main building block for the experimental validation of the SM is now in place. The Higgs discovery is the last milestone in the long history (some 130 years) of the development of a field theory of fundamental interactions (apart from quantum gravity), starting with the Maxwell equations of classical electrodynamics, going through the great revolutions of relativity and quantum mechanics, then the formulation of quantum electrodynamics (QED) and the gradual buildup of the gauge part of the Standard Model, and finally completed with the tentative description of the electroweak (EW) symmetry breaking sector of

the SM in terms of a simple formulation of the Englert–Brout–Higgs mechanism [189].

The other extremely important result from the LHC at 7 and 8 TeV center-of-mass energy is that no new physics signals have been seen so far. This negative result is certainly less exciting than a positive discovery, but it is a crucial new input which, if confirmed in the future LHC runs at 13 and 14 TeV, will be instrumental in redirecting our perspective of the field. In this section we summarize the relevant data on the Higgs signal as they are known at present, while the analysis of the data from the 2012 LHC run is still in progress.

The Higgs particle has been observed by ATLAS and CMS in five channels $\gamma\gamma$, ZZ^*, WW^*, $b\bar{b}$, and $\tau^+\tau^-$. If we also include the Tevatron experiments, especially important for the $b\bar{b}$ channel, the combined evidence is by now totally convincing. The ATLAS (CMS) combined values for the mass, in GeV$/c^2$, are $m_{\rm H} = 125.5\pm0.6$ ($m_{\rm H} = 125.7\pm0.4$). This light Higgs is what one expects from a direct interpretation of EW precision tests [73, 142, 350]. The possibility of a "conspiracy" (the Higgs is heavy, but it falsely appears to be light because of confusing new physics effects) has been discarded: the EW precision tests of the SM tell the truth and in fact, consistently, no "conspirators", namely no new particles, have been seen around.

As shown in the previous section, the observed value of $m_{\rm H}$ is a bit too low for the SM to be valid up to the Planck mass with an absolutely stable vacuum [see (3.120)], but it corresponds to a metastable value with a lifetime longer than the age of the universe, so that the SM may well be valid up to the Planck mass (if one is ready to accept the immense fine-tuning that this option implies, as discussed in Sect. 3.17). This is shown in Fig. 3.21, where the stability domains are shown as functions of m_t and $m_{\rm H}$, as obtained from a recent state-of-the-art evaluation of the relevant boundaries [118, 160]. It is puzzling to find that, with the measured values of the top and Higgs masses and the strong coupling constant, the evolution of the Higgs quartic coupling ends up in a narrow metastability wedge at very high energies. This criticality looks intriguing, and is perhaps telling us something.

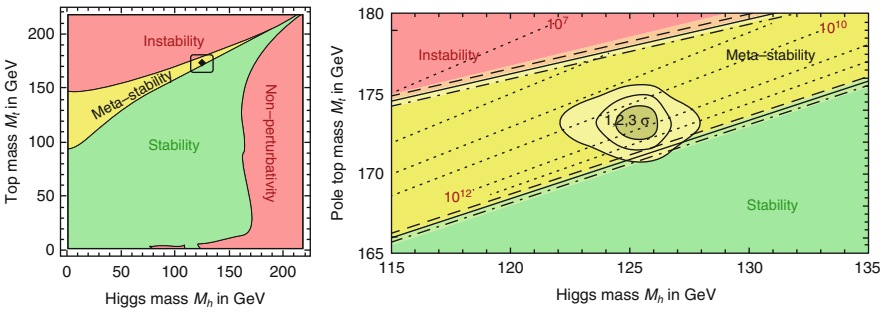

Fig. 3.21 Vacuum stability domains in the SM for the observed values of m_t and $m_{\rm H}$ [118, 160]. *Right*: Expanded view of the most relevant domain in the m_t–$m_{\rm H}$ plane. *Dotted contour lines* show the scale Λ in GeV where the instability sets in, for $\alpha_{\rm s}(m_Z) = 0.1184$

In order to be sure that this is the SM Higgs boson, one must confirm that the spin-parity is 0^+ and that the couplings are as predicted by the theory. It is also essential to search for possible additional Higgs states, such as those predicted in supersymmetric extensions of the SM. As for the spin (see, for example, [179]), the existence of the $H \to \gamma\gamma$ mode proves that the spin cannot be 1, and must be either 0 or 2, in the assumption of an s-wave decay. The $b\bar{b}$ and $\tau^+\tau^-$ modes are compatible with both possibilities. With large enough statistics the spin-parity can be determined from the distributions of $H \to ZZ^* \to 4$ leptons, or $WW^* \to 4$ leptons. Information can also be obtained from the HZ invariant mass distributions in the associated production [179]. The existing data already appear to strongly favour a $J^P = 0^+$ state against 0^-, $1^{+/-}$, or 2^+ [68]. We do not expect surprises on the spin-parity assignment because, if different, then all the Lagrangian vertices would be changed and the profile of the SM Higgs particle would be completely altered.

The tree level couplings of the Higgs are proportional to masses, and as a consequence are very hierarchical. The loop effective vertices to $\gamma\gamma$ and gg, g being the gluon, are also completely specified in the SM, where no states heavier than the top quark exist and contribute in the loop. This means that the SM Higgs couplings are predicted to exhibit a very special and very pronounced pattern (see Fig. 3.22) which would be extremely difficult to fake by a random particle. In fact, only a dilaton, a particle coupled to the energy–momentum tensor, could come close to simulating a Higgs particle, at least for the H tree level couplings, although in general there would be a common proportionality factor in the couplings. The hierarchy of couplings is reflected in the branching ratios and the rates of production channels, as can be seen in Fig. 3.23. The combined signal strengths (which, modulo acceptance and selection cut deformations, correspond to $\mu = \sigma Br/(\sigma Br)_{\rm SM}$) are obtained as $\mu = 0.8 \pm 0.14$ by CMS and $\mu = 1.30 \pm 0.20$ by ATLAS. Taken together these numbers constitute a triumph for the SM!

Within the somewhat limited present accuracy (October 2013), the measured Higgs couplings are in reasonable agreement (at about a 20% accuracy) with the

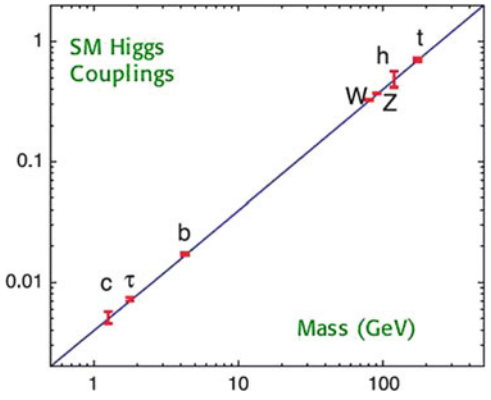

Fig. 3.22 Predicted couplings of the SM Higgs

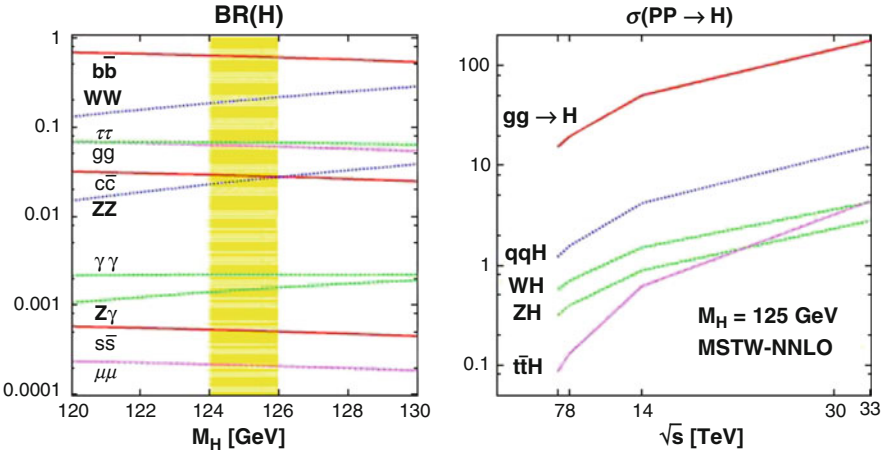

Fig. 3.23 Branching ratios of the SM Higgs boson in the mass range $m_{\mathrm{H}} = 120$–$130\,\mathrm{GeV}$ (*left*) and its production cross-sections at the LHC for various center-of-mass energies (*right*) [168]

sharp predictions of the SM. Great interest was excited by a hint of an enhanced Higgs signal in $\gamma\gamma$, but if we put the ATLAS and CMS data together, the evidence appears now to have evaporated. All included, if the CERN particle is not the SM Higgs, it must be a very close relative! Still it would be really astonishing if the H couplings were exactly those of the minimal SM, meaning that no new physics distortions reach an appreciable level of contribution.

Thus, it becomes a firm priority to establish a roadmap for measuring the H couplings as precisely as possible. The planning of new machines beyond the LHC has already started. Meanwhile strategies for analyzing the already available and the forthcoming data in terms of suitable effective Lagrangians have been formulated (see, for example, [222] and references therein). A very simple test is to introduce a universal factor multiplying all $H\bar{\psi}\psi$ couplings to fermions, denoted by c, and another factor a multiplying the HWW and HZZ vertices. Both a and c are 1 in the SM limit. All existing data on production times branching ratios are compared with the a- and c-distorted formulae to obtain the best fit values of these parameters (see [72, 194, 218] and references therein). At present this fit is performed routinely by the experimental collaborations [66, 260], each using its own data (see Fig. 3.24). But theorists have not refrained from abusively combining the data from both experiments and the result is well in agreement with the SM, as shown in Fig. 3.25 [194, 218].

Actually, a more ambitious fit in terms of seven parameters has also been performed [194] with a common factor like a for couplings to WW and ZZ, three separate c-factors c_t, c_b, and c_τ for u-type and d-type quarks and for charged leptons, and three parameters c_{gg}, $c_{\gamma\gamma}$, and $c_{Z\gamma}$ for additional gluon–gluon, γ–γ and Z–γ terms, respectively. In the SM $a = c_t = c_b = c_\tau = 1$ and $c_{gg} = c_{\gamma\gamma} = c_{Z\gamma} = 0$. The present data allow a meaningful determination of all seven parameters which

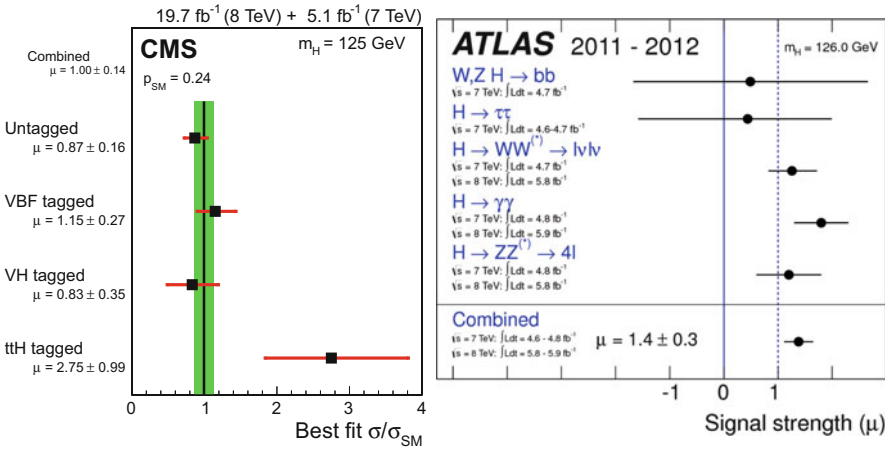

Fig. 3.24 Measured H couplings compared with the SM predictions by the CMS [260] (2016 updated version, included with permission) and ATLAS [66] collaborations (earlier 2013 version, when these lectures were written, included with permission). For a 2016 update of the ATLAS plot, see [3]

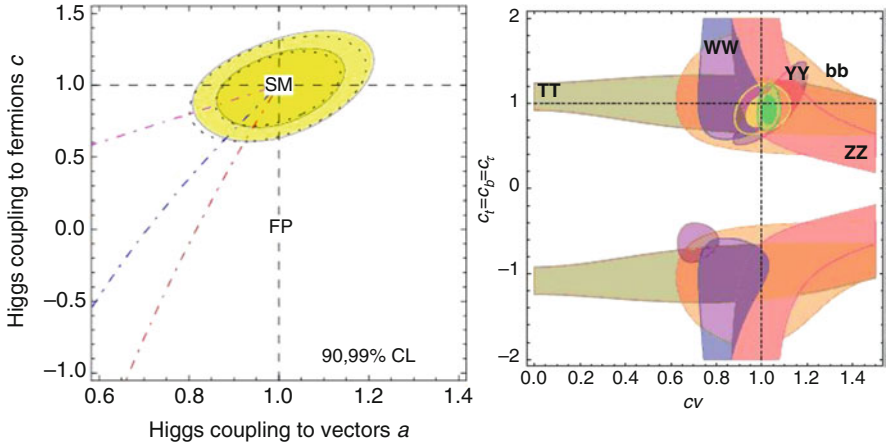

Fig. 3.25 Fit of the Higgs boson couplings obtained from the (unofficially) combined ATLAS and CMS data assuming common rescaling factors a and c with respect to the SM prediction for couplings to vector bosons and fermions, respectively. *Left*: From [218]. *Dashed lines* correspond to different versions of composite Higgs models. The *dashed vertical line*, marked FP (fermiophobic) corresponds to $a = 1$ and $c = 1 - \xi$. Then *from bottom to top* $c = (1 - 3\xi)/a$, $c = (1 - 2\xi)/a$, $a = c = \sqrt{1 - \xi}$, with ξ defined in Sect. 3.17. *Right*: From [194], with $c_t = c_b = c_\tau = c$ and $c_V = a$

turns out to be in agreement with the SM [194]. For example, in the MSSM, at the tree level, $a = \sin(\beta - \alpha)$, for fermions the u- and d-type quark couplings are different: $c_t = \cos\alpha/\sin\beta$ and $c_b = -\sin\alpha/\cos\beta = c_\tau$. At the tree level (but radiative corrections are in many cases necessary for a realistic description), the α

angle is related to the A, Z masses and to β by $\tan 2\alpha = \tan 2\beta (m_A^2 - m_Z^2)/(m_A^2 + m_Z^2)$. If c_t is enhanced, c_b is suppressed. In the limit of large m_A, $a = \sin(\beta - \alpha) \to 1$.

In conclusion it really appears that the Higgs sector of the minimal SM, with good approximation, is realized in nature. Apparently, what was considered just as a toy model, a temporary addendum to the gauge part of the SM, presumably to be replaced by a more complex reality and likely to be accompanied by new physics, has now been experimentally established as the actual realization of the EW symmetry breaking (at least to a very good approximation). If the role of the newly discovered particle in the EW symmetry breaking is confirmed, it will be the only known example in physics of a fundamental, weakly coupled, scalar particle with vacuum expectation value (VEV). We know many composite types of Higgs-like particles, like the Cooper pairs of superconductivity or the quark condensates that break the chiral symmetry of massless QCD, but the Higgs found at the LHC is the only possibly elementary one. This is a death blow not only to Higgsless models, to straightforward technicolor models, and to other unsophisticated strongly interacting Higgs sector models, but actually a threat to all models without fast enough decoupling, in the sense that, if new physics comes in a model with decoupling, the absence of new particles at the LHC helps to explain why large corrections to the H couplings are not observed.

3.17 Limitations of the Standard Model

No signal of new physics has been found, either by direct production of new particles at the LHC, or in the electroweak precision tests, or in flavour physics. Given the success of the SM, why are we not satisfied with this theory? Once the Higgs particle has been found, why don't we declare particle physics closed? The reason is that there are both conceptual problems and phenomenological indications for physics beyond the SM. On the conceptual side the most obvious problems are that quantum gravity is not included in the SM and that the famous hierarchy (or naturalness or fine-tuning) problem remains open. Among the main phenomenological hints for new physics we can list coupling unification, dark matter, neutrino masses (discussed in Sect. 3.7), baryogenesis, and the cosmological vacuum energy. At accelerator experiments, the most plausible departure from the SM is the muon anomalous magnetic moment which, as discussed in Sect. 3.9, shows a deviation by about 3 σ, but some caution should be applied since a large fraction of the uncertainty is of theoretical origin, in particular that due to the hadronic contribution to light–light scattering [245].

The computed evolution with energy of the effective SM gauge couplings clearly points towards the unification of the electroweak and strong forces (GUTs) at scales of energy $M_{\rm GUT} \sim 10^{15}$–10^{16} GeV [315], which are close to the scale of quantum gravity, $M_{\rm Planck} \sim 10^{19}$ GeV. The crossing of the three gauge couplings at a single

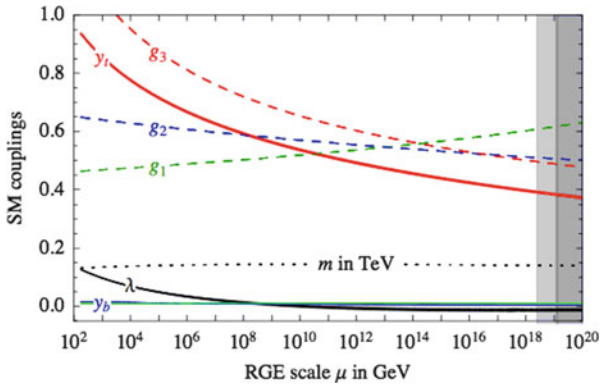

Fig. 3.26 Renormalisation of the SM gauge couplings $g_1 = \sqrt{5/3}g_Y$, g_2, g_3, of the *top*, *bottom*, and τ couplings (y_t, y_b, y_τ), of the Higgs quartic coupling λ, and of the Higgs mass parameter m. In the figure, y_b and y_τ are not easily distinguished. All parameters are defined in the $\bar{M}\bar{S}$ scheme [118]

point is not perfect in the SM and is much better in the supersymmetric extensions of the SM. But still the matching is sufficiently close in the SM (see Fig. 3.26, [118]) that one can imagine some atypical threshold effect at the GUT scale to fix the apparent residual mismatch. One is led to imagine a unified theory of all interactions, also including gravity (at present superstrings [231] provide the best attempt at such a theory).

Thus GUTs and the realm of quantum gravity set a very distant energy horizon that modern particle theory cannot ignore. Can the SM without new physics be valid up to such high energies? One can imagine that some obvious problems of the SM could be postponed to the more fundamental theory at the Planck mass. For example, the explanation of the three generations of fermions and the understanding of fermion masses and mixing angles can be postponed. But other problems must find their solution in the low energy theory. In particular, the structure of the SM could not naturally explain the relative smallness of the weak scale of mass, set by the Higgs mechanism at $v \sim 1/\sqrt{G_F} \sim 250\,\text{GeV}$, where G_F is the Fermi coupling constant. This so-called hierarchy problem [219] is due to the instability of the SM with respect to quantum corrections. In fact, nobody can believe that the SM is the definitive, complete theory but, rather, we all believe it is only an effective low energy theory.

The dominant terms at low energy correspond to the SM renormalizable Lagrangian, but additional non-renormalizable terms should be added which are suppressed by powers (modulo logs) of the large scale Λ, where physics beyond the SM becomes relevant (for simplicity we write down only one such scale of new physics, but there could be different levels). The complete Lagrangian takes the

general form

$$\mathscr{L} = O(\Lambda^4) + O(\Lambda^2)\mathscr{L}_2 + O(\Lambda)\mathscr{L}_3 + O(1)\mathscr{L}_4 + O(1/\Lambda)\mathscr{L}_5 + O(1/\Lambda^2)\mathscr{L}_6 + \cdots \,. \tag{3.128}$$

Here $\mathscr{L}_\mathrm{D}$ are Lagrangian vertices of operator dimension D. In particular $\mathscr{L}_2 = \Phi^\dagger\Phi$ is a scalar mass term, $\mathscr{L}_3 = \bar{\Psi}\Psi$ is a fermion mass term (which in the SM only appears after EW symmetry breaking), $\mathscr{L}_4$ describes all dimension-4 gauge and Higgs interactions, $\mathscr{L}_5$ is the Weinberg operator [363] (with two lepton doublets and two Higgs fields) which leads to neutrino masses (see Sect. 3.7), and $\mathscr{L}_6$ includes 4-fermion operators (among others). The first line in (3.128) corresponds to the renormalizable part (that is, what we usually call the SM). The baseline power of the large scale Λ in the coefficient of each $\mathscr{L}_\mathrm{D}$ vertex is fixed by dimensions. A deviation from the baseline power can only be naturally expected if some symmetry or some dynamical principle justifies a suppression. For example, for the fermion mass terms, we know that all Dirac masses vanish in the limit of gauge invariance and only arise when the Higgs VEV v breaks the EW symmetry. The fermion masses also break chiral symmetry. Thus the fermion mass coefficient is not linear in Λ modulo logs, but actually behaves as $v \log \Lambda$. An exceptional case is the Majorana mass term of right-handed neutrinos ν_R, $M_\mathrm{RR}\,\bar{\nu}_\mathrm{R}^\mathrm{c}\nu_\mathrm{R}$, which is lepton number non-conserving but gauge invariant (because ν_R is a gauge singlet). In fact, in this case one expects $M_\mathrm{RR} \sim \Lambda$. As another example, proton decay arises from a 4-fermion operator in $\mathscr{L}_6$, suppressed by $1/\Lambda^2$, where in this case Λ could be identified with the large mass of lepto-quark gauge bosons that appear in GUTs.

The hierarchy problem arises because the coefficient of $\mathscr{L}_2$ is not suppressed by any symmetry. This term, which appears in the Higgs potential, fixes the scale of the Higgs VEV and of all related masses. Since empirically the Higgs mass is light, (and by naturalness, it should be of $O(\Lambda)$, we would expect Λ, i.e., some form of new physics, to appear near the TeV scale. The hierarchy problem can be put in very practical terms (the "little hierarchy problem"): loop corrections to the Higgs mass squared are quadratic in the cutoff Λ, which can be interpreted as the scale of new physics.

The most pressing problem is from the top loop. With $m_\mathrm{h}^2 = m_\mathrm{bare}^2 + \delta m_\mathrm{h}^2$, the top loop gives

$$\delta m_{\mathrm{h}|\mathrm{top}}^2 \sim -\frac{3G_\mathrm{F}}{2\sqrt{2}\pi^2} m_t^2 \Lambda^2 \sim -(0.2\Lambda)^2 \,. \tag{3.129}$$

If we demand that the correction not exceed the light Higgs mass observed by experiment (that is, we exclude an unexplained fine-tuning), Λ must be close, $\Lambda \sim O(1\ \mathrm{TeV})$. Similar constraints also arise from the quadratic Λ dependence of loops with exchanges of gauge bosons and scalars, which, however, lead to less pressing bounds. So the hierarchy problem strongly indicates that new physics must be very close (in particular the mechanism that quenches or compensates the top

loop). The restoration of naturalness would occur if new physics implemented an approximate symmetry implying the cancellation of the Λ^2 coefficient. Actually, this new physics must be rather special, because it must be very close, while its effects are not yet clearly visible, either in precision electroweak tests (the "LEP paradox" [80]), or in flavour-changing processes and CP violation.

It is important to note that, although the hierarchy problem is directly related to the quadratic divergences in the scalar sector of the SM, the problem can actually be formulated without any reference to divergences, directly in terms of renormalized quantities. After renormalization, the hierarchy problem is manifested by the quadratic sensitivity of μ^2 to the physics at high energy scales. If there is a threshold at high energy, where some particles of mass M coupled to the Higgs sector can be produced and contribute in loops, then the renormalized running mass μ will evolve slowly (i.e., logarithmically according to the relevant beta functions [195]) up to M and there, as an effect of the matching conditions at the threshold, rapidly jump to become of order M (see, for example, [79]). In fact, in Fig. 3.26, we see that, under the assumption of no thresholds, the running Higgs mass m evolves slowly, starting from the observed low energy value, up to very high energies. In the presence of a threshold at M one needs a fine-tuning of order μ^2/M^2 in order to fix the running mass at low energy to the observed value.

Thus for naturalness either new thresholds appear endowed with a mechanism for the cancellation of the sensitivity or they had better not appear at all. But certainly there is the Planck mass, connected to the onset of quantum gravity, which sets an unavoidable threshold. One possible point of view is that there are no new thresholds up to M_{Planck} (at the price of giving up GUTs, among other things) but, miraculously, there is a hidden mechanism in quantum gravity that solves the fine-tuning problem related to the Planck mass [221, 322]. For this one would need to solve all phenomenological problems, like dark matter, baryogenesis, and so on, with physics below the EW scale. Possible ways to do so are discussed in [322]. This point of view is extreme, but allegedly not yet ruled out.

The main classes of orthodox solutions to the hierarchy problem are:

- Supersymmetry [302]. In the limit of exact boson–fermion symmetry, quadratic bosonic divergences cancel so that only log divergences remain. However, exact SUSY is clearly unrealistic. For approximate SUSY (with soft breaking terms and R-parity conservation), which is the basis for most practical models, Λ^2 is essentially replaced by the splitting of SUSY multiplets, $\Lambda^2 \sim m^2_{\text{SUSY}} - m^2_{\text{ord}}$, with m_{ord} the SM particle masses. In particular, the top loop is quenched by partial cancellation with s-top exchange, so the s-top cannot be too heavy. After the bounds from the LHC, the present emphasis is to build SUSY models where naturalness is restored not too far from the weak scale, but the related new physics is arranged in such a way that it would not have been visible so far. The simplest ingredients introduced in order to decrease the fine tuning are either the assumption of a split spectrum with heavy first two generations of squarks (for some recent work along this line see, for example, [271]) or the enlargement of

the Higgs sector of the MSSM by adding a singlet Higgs field (see, for example, [196] on next-to-minimal SUSY SM or NMSSM) or both.

- A strongly interacting EW symmetry-breaking sector. The archetypal model of this class is technicolor, where the Higgs is a condensate of new fermions [332]. In these theories there is no fundamental scalar Higgs field, hence no quadratic divergences associated with the μ^2 mass in the scalar potential. But this mechanism needs a very strong binding force, $\Lambda_{\rm TC} \sim 10^3 \Lambda_{\rm QCD}$. It is difficult to arrange for such a nearby strong force not to show up in precision tests. Hence, this class of models was abandoned after LEP, although some special classes of models have been devised a posteriori, like walking TC, top-color assisted TC, etc. [246] (for reviews see, for example, [275]). But the simplest Higgs observed at the LHC has now eliminated another score of these models. Modern strongly interacting models, like little Higgs models [63] [in these models extra symmetries allow $m_{\rm h} \neq 0$ only at two-loop level, so that Λ can be as large as $O(10$ TeV$)$], or composite Higgs models [223, 258] (where non-perturbative dynamics modifies the linear realization of the gauge symmetry and the Higgs has both elementary and composite components) are more sophisticated. All models in this class share the idea that the Higgs is light because it is the pseudo-Goldstone boson of an enlarged global symmetry of the theory, for example $SO(5)$ broken down to $SO(4)$. There is a gap between the mass of the Higgs (similar to a pion) and the scale f where new physics appears in the form of resonances (similar to the ρ, etc.). The ratio $\xi = v^2/f^2$ defines a degree of compositeness that interpolates between the SM at $\xi = 0$ up to technicolor at $\xi = 1$. Precision EW tests impose $\xi < 0.05$–0.2. In these models the bad quadratic behaviour from the top loop is softened by the exchange of new vector-like fermions with charge 2/3, or even with exotic charges like 5/3 (see, for example, [143, 295]).
- Extra dimensions [62, 314] (for pedagogical introductions, see, for example, [331]). The idea is that $M_{\rm Planck}$ appears very large, or equivalently that gravity appears very weak, because we are fooled by hidden extra dimensions, so that either the real gravity scale is reduced down to a lower scale, even possibly down to $O(1$ TeV$)$ or the intensity of gravity is redshifted away by an exponential warping factor [314]. This possibility is very exciting in itself and it is really remarkable that it is compatible with experiment. It provides a very rich framework with many different scenarios.
- The anthropic evasion of the problem. The observed value of the cosmological constant Λ also poses a tremendous, unsolved naturalness problem [205]. Yet the value of Λ is close to the Weinberg upper bound for galaxy formation [364]. Possibly our Universe is just one of infinitely many bubbles (a multiverse) continuously created from the vacuum by quantum fluctuations. Different physics takes place in different universes according to the multitude of string theory solutions [177] ($\sim 10^{500}$). Perhaps we live in a very unlikely universe, but the only one that allows our existence [61, 220, 318]. Personally, I find the application of the anthropic principle to the SM hierarchy problem somewhat excessive. After all,

one can find plenty of models that easily reduce the fine tuning from 10^{14} to 10^{2}: why make our universe so terribly unlikely? If we add, say, supersymmetry to the SM, does the universe become less fit for our existence? In the multiverse, there should be plenty of less finely tuned universes where more natural solutions are realized and which are still suitable for us to live in them. By comparison, the case of the cosmological constant is very different: the context is not as fully specified as the one for the SM (quantum gravity, string cosmology, branes in extra dimensions, wormholes through different universes, and so on). Further, while there are many natural extensions of the SM, so far there is no natural theory of the cosmological constant.

It is true that the data impose a substantial amount of apparent fine tuning, and our criterion of naturalness has certainly failed so far, so that we are now lacking a reliable argument to tell us where precisely the new physics threshold is located. On the other hand, many of us remain confident that some new physics will appear not too far from the weak scale.

While I remain skeptical I would like to sketch here one possibility of how the SM can be extended in agreement with the anthropic idea. If we completely ignore the fine-tuning problem and only want to reproduce, in a way compatible with GUTs, the most compelling data that demand new physics beyond the SM, a possible scenario is the following. The SM spectrum is completed by the recently discovered light Higgs and there is no other new physics in the LHC range (how sad!). In particular there is no SUSY in this model. At the GUT scale of $M_{\rm GUT} \geq 10^{16}\,$GeV, the unifying group is $SO(10)$, broken at an intermediate scale, typically $M_{\rm int} \sim 10^{10}$–10^{12} down to a subgroup like the Pati–Salam group $SU(4) \bigotimes SU(2)_{\rm L} \bigotimes SU(2)_{\rm R}$ or $SU(3) \bigotimes U(1) \bigotimes SU(2)_{\rm L} \bigotimes SU(2)_{\rm R}$ [98]. Note that, in general, unification in $SU(5)$ would not work because we need a group of rank larger than 4 to allow for (at least) two-step breaking: this is needed, in the absence of SUSY, to restore coupling unification and to avoid a too fast proton decay. An alternative is to assume some ad hoc intermediate threshold to modify the evolution towards unification [224].

The dark matter problem is one of the strongest pieces of evidence for new physics. In this model it should be solved by axions [262, 263, 309]. It must be said that axions have the problem that their mass has to be fixed ad hoc to reproduce the observed amount of dark matter. In this respect, the WIMP (weakly interacting massive particle) solution, like the neutralinos in SUSY models, is much more attractive. Lepton number violation, Majorana neutrinos, and the see-saw mechanism give rise to neutrino mass and mixing. Baryogenesis occurs through leptogenesis [115]. One should one day observe proton decay and neutrino-less beta decay. None of the alleged indications for new physics at colliders would survive (in particular, even the claimed muon $g-2$ [297] discrepancy should be attributed, if not to an experimental problem, to an underestimate of the theoretical uncertainties, or otherwise to some specific addition to the above model [257]). This model is in line with the non-observation of the decay $\mu \to e\gamma$ at MEG [16], of the electric dipole

moment of the neutron [75], etc. It is a very important challenge to experiment to falsify such a scenario by establishing firm evidence for new physics at the LHC or at some other "low energy" experiment.

In 2015 the LHC will restart at 13–14 TeV and in the following years should collect a much larger statistical sample than available at present at 7–8 TeV. From the above discussion it is clear that it is extremely important for the future of particle physics to know whether the extraordinary and unexpected success of the SM, including the Higgs sector, will continue, or whether clear signals of new physics will finally appear, as we very much hope.

Open Access This chapter is licensed under the terms of the Creative Commons Attribution 4.0 International License (http://creativecommons.org/licenses/by/4.0/), which permits use, sharing, adaptation, distribution and reproduction in any medium or format, as long as you give appropriate credit to the original author(s) and the source, provide a link to the Creative Commons license and indicate if changes were made.

The images or other third party material in this chapter are included in the chapter's Creative Commons license, unless indicated otherwise in a credit line to the material. If material is not included in the chapter's Creative Commons license and your intended use is not permitted by statutory regulation or exceeds the permitted use, you will need to obtain permission directly from the copyright holder.

References

1. Aad, G., et al., [ATLAS Collaboration]: Eur. Phys. J. C 72, 2039 (2012). ArXiv:1203.4211; and talk by Giordani, M.P., [ATLAS Collaboration], presented at ICHEP 2012, Melbourne (2012)
2. Aad, G., et al., [ATLAS Collab.]: Phys. Lett. B 716, 1 (2012). ArXiv:1207.7214
3. Aad, G., et al., ATLAS and CMS Collaborations: JHEP 1608, 045 (2016). arXiv:1606.02266 [hep-ex]
4. Aaij, R., et al., LHCb Collaboration: (2013). ArXiv:1304.6325; (2013). ArXiv:1308.1707; Chatrchyan, S., et al., CMS Collaboration: (2013). ArXiv:1308.3409
5. Aaij, R., et al., LHCb Collaboration: Phys. Rev. Lett. 111, 101805 (2013). ArXiv:1307.5024
6. Aaltonen, T., et al., [CDF Collaboration]: Phys. Rev. D 83, 112003 (2011). ArXiv:1101.0034; CDF note 10807
7. Aaltonen, T., et al., [CDF Collaboration]: (2013). ArXiv:1306.2357
8. Abazajian, K.N., et al.: (2012). ArXiv:1204.5379
9. Abazov, V.M., et al., [D0 Collaboration]: Phys. Rev. D 84, 112005 (2011). ArXiv:1107.4995
10. Abbate, R., Fickinger, M., Hoang, A.H., Mateu, V., Stewart, I.W.: Phys. Rev. D 83, 074021 (2011). ArXiv:1006.3080
11. Abbate, R., Fickinger, M., Hoang, A.H., Mateu, V., Stewart, I.W.: Phys. Rev. D 86, 094002 (2012). ArXiv:1204.5746
12. Abe, K., et al., T2K Collaboration: Phys. Rev. Lett. 107, 041801 (2011). ArXiv:1106.2822
13. Abe, Y., et al., DOUBLE-CHOOZ Collaboration: (2011). ArXiv:1112.6353
14. Abers, E.S., Lee, B.W.: Phys. Rep. 9, 1 (1973)
15. Abulencia, A., et al., CDF Collaboration: Phys. Rev. D 74, 072005 (2006); Phys. Rev. D 74, 072006 (2006); Abazov, V.M., et al., the D0 Collaboration: Phys. Rev. D 74, 112004 (2006)
16. Adam, J., et al., MEG Collaboration: (2013). ArXiv:1303.0754
17. Adamson, P., et al., MINOS Collaboration: Phys. Rev. Lett. 107, 181802 (2011). ArXiv:1108.0015
18. Ade, P.A.R., et al., Planck Collaboration: (2013). ArXiv:1303.5076
19. Adler, S.L.: Phys. Rev. 177, 24261 (969); Adler, S.L., Bardeen, W.A.: Phys. Rev. 182, 1517 (1969); Bell, J.S., Jackiw, R.: Nuovo Cim. A 60, 47 (1969); Bardeen, W.A.: Phys. Rev. 184, 1848 (1969)
20. Aglietti, U., Bonciani, R., Degrassi, G., Vicini, A.: Phys. Lett. B 595, 432 (2004); Degrassi, G., Maltoni, F.: Phys. Lett. B 600, 255 (2004)
21. Agostini, M., et al.: GERDA Collaboration, Phys. Rev. Lett. 111, 122503 (2013)
22. Ahmed, M.A., Ross, G.G.: Nucl. Phys. B 111, 441 (1976)
23. Ahn, J.K., et al., RENO Collaboration: (2012). ArXiv:1204.0626

© The Author(s) 2017

G. Altarelli, *Collider Physics within the Standard Model*,
Lecture Notes in Physics 937, DOI 10.1007/978-3-319-51920-3

24. Aidala, C.A., Bass, S.D., Hasch, D., Mallot, G.K.: (2012). ArXiv:1209.2803; Burkardt, M., Miller, C.A., Nowak, W.D.: Rep. Prog. Phys. 73, 016201 (2010)
25. Alekhin, S., Djouadi, A., Moch, S.: Phys. Lett. B 716, 214 (2012). ArXiv:1207.0980
26. Alekhin, S., Blumlein, J., Moch, S.: ArXiv:1202.2281 [hep-ph]
27. Alekhin, S., Djouadi, A., Moch, S.: (2012). ArXiv:1207.0980; see also Beneke, M., Falgari, P., Klein, S., Schwinn, C.: (2011). ArXiv:1112.4606
28. Altarelli, G.: Proceedings of the International Conference on High Energy Physics, Geneva, vol. 2, p. 727 (1979)
29. Altarelli, G.: Phys. Rep. 81, 1 (1982)
30. Altarelli, G.: Annu. Rev. Nucl. Part. Sci. 39, 357 (1989)
31. Altarelli, G.: In: Zichichi, A. (ed.) Proceedings of the E. Majorana Summer School, Erice. Plenum, New York (1995); Beneke, M., Braun, V.M.: In: Shifman, M. (ed.) Handbook of QCD, vol. 3, p. 1719. World Scientific, Singapore (2001)
32. Altarelli, G.: Gauge theories and the standard model. In: Landolt-Boernstein I 21A: Elementary Particles, vol. 2. Springer, Berlin (2008)
33. Altarelli, G., QCD: The theory of strong interactions. In: Landolt-Boernstein I 21A: Elementary Particles, vol. 4. Springer, Berlin (2008)
34. Altarelli, G.: The standard model of electroweak interactions. In: Landolt-Boernstein I 21A: Elementary Particles, vol. 3. Springer, Berlin (2008)
35. Altarelli, G.: (2012). ArXiv:1210.3467
36. Altarelli, G., Feruglio, F.: New J. Phys. 6, 106 (2004). hep-ph/0405048; Mohapatra, R.N., Smirnov, A.Y.: Annu. Rev. Nucl. Part. Sci. 56, 569 (2006). hep-ph/0603118; Grimus, W., PoS P2GC, 001 (2006). hep-ph/0612311; Gonzalez-Garcia, M.C., Maltoni, M.: Phys. Rep. 460, 1 (2008). ArXiv:0704.1800
37. Altarelli, G., Feruglio, F.: Rev. Mod. Phys. 82, 2701–2729 (2010). ArXiv:1002.0211
38. Altarelli, G., Isidori, G.: Phys. Lett. B 337, 141 (1994); Casas, J.A., Espinosa, J.R., Quirós, M.: Phys. Lett. B 342, 171 (1995); Casas, J.A., et al.: Nucl. Phys. B 436, 3 (1995); B 439, 466 (1995); Carena, M., Wagner, C.E.M.: Nucl. Phys. B 452, 45 (1995)
39. Altarelli, G., Martinelli, G.: Phys. Lett. B 76, 89 (1978)
40. Altarelli, G., Parisi, G.: Nucl. Phys. B 126, 298 (1977)
41. Altarelli, G., Ross, G.G.: Phys. Lett. B 212, 391 (1988); Efremov, A.V., Terayev, O.V.: In: Proceedings of the Czech Hadron Symposium, p. 302 (1988); Carlitz, R.D., Collins, J.C., Mueller, A.H.: Phys. Lett. B 214, 229 (1988); Altarelli, G., Lampe, B.: Z. Phys. C 47, 315 (1990)
42. Altarelli, G., Ellis, R.K., Martinelli, G.: Nucl. Phys. B 143, 521 (1978); Altarelli, G., Ellis, R.K., Martinelli, G.: Nucl. Phys. B 146, 544 (1978); Nucl. Phys. B 157, 461 (1979)
43. Altarelli, G., Ellis, R.K., Greco, M., Martinelli, G.: Nucl. Phys. B 246, 12 (1984); Altarelli, G., Ellis, R.K., Martinelli, G.: Z. Phys. C 27, 617 (1985)
44. Altarelli, G., Mele, B., Pitolli, F.: Nucl. Phys. B 287, 205 (1987)
45. Altarelli, G., Nason, P., Ridolfi, G.: Z. Phys. C 68, 257 (1995)
46. Altarelli, G., Sjostrand, T., Zwirner, F.: Physics at LEP2, CERN Report 96-01 (1996). LEP2
47. Altarelli, G., Kleiss, R., Verzegnassi, C. (eds.): *Z* Physics at LEP1 (CERN 89-08, Geneva, 1989), vols. 1–3; Precision Calculations for the *Z* Resonance, ed. by Bardin, D., Hollik, W., Passarino, G., CERN Rep 95-03 (1995); Vysotskii, M.I., Novikov, V.A., Okun, L.B., Rozanov, A.N.: hep-ph/9606253 or Phys. Usp. 39, 503–538 (1996)
48. Altarelli, G., Barbieri, R., Caravaglios, F.: Int. J. Mod. Phys. A 13, 1031 (1998) and references therein
49. Altarelli, G., Ball, R., Forte, S.: Nucl. Phys. B 799, 199 (2008). ArXiv:0802.0032
50. Altarelli, G., Feruglio, F., Merlo, L.: (2012). ArXiv:1205.5133
51. Altarelli, G., Feruglio, F., Merlo, L., Stamou, E.: (2012). ArXiv:1205.4670
52. Altarelli, G., Feruglio, F., Masina, I., Merlo, L.: (2012). ArXiv:1207.0587
53. Amhis, Y., et al., the Heavy Flavor Averaging Group: (2012). ArXiv:1207.1158; Aaij, R., et al., LHCb Collaboration: (2012). ArXiv:1211.1230
54. An, F.P., et al., DAYA-BAY Collaboration: (2012). ArXiv:1203.1669

55. Anastasiou, C., Dixon, L.J., Melnikov, K., Petriello, F.: Phys. Rev. D 69, 094008 (2004). hep-ph/0312266
56. Anastasiou, C., Melnikov, K., Petriello, F.: Nucl. Phys. B 724, 197 (2005); Ravindran, V., Smith, J., van Neerven, W.L.: hep-ph/0608308
57. Anastasiou, C., Melnikov, K., Petriello, F.: Phys. Rev. D 72, 097302 (2005). hep-ph/0509014
58. Anderson, P.W.: Phys. Rev. 112, 1900 (1958); Phys. Rev. 130, 439 (1963)
59. Aoyama, T., Hayakawa, M., Kinoshita, T., Nio, N.: (2012). ArXiv:1205.5368; ArXiv:1205.5370
60. Appelquist, T., Carazzone, J.: Phys. Rev. D 11, 2856 (1975)
61. Arkani-Hamed, N., Dimopoulos, S.: JHEP 0506, 073 (2005). hep-th/0405159; Arkani-Hamed, N., et al.: Nucl. Phys. B 709, 3 (2005). hep-ph/0409232; Giudice, G., Romanino, A.: Nucl. Phys. B 699, 65 (2004); erratum ibid. B 706, 65 (2005); hep-ph/0406088; Arkani-Hamed, N., Dimopoulos, S., Kachru, S.: hep-ph/0501082; Giudice, G., Rattazzi, R.: Nucl. Phys. B 757, 19 (2006). hep-ph/0606105
62. Arkani-Hamed, N., Dimopoulos, S., Dvali, G.: Phys. Lett. B 429, 263 (1998). hep-ph/9803315; Antoniadis, I., Arkani-Hamed, N., Dimopoulos, S., Dvali, G.R.: Phys. Lett. B 436, 257 (1998). hep-ph/9804398; Arkani-Hamed, N., Hall, L.J., Smith, D.R., Weiner, N.: Phys. Rev. D 62 (2000). hep-ph/9912453; Giudice, G.F., Rattazzi, R., Wells, J.D.: Nucl. Phys. B 544, 3 (1999). hep-ph/9811291; Han, T., Lykken, J.D., Zhang, R.-J.: Phys. Rev. D 59, 105006 (1999). hep-ph/9811350; Hewett, J.L.: Phys. Rev. Lett. 82, 4765 (1999)
63. Arkani-Hamed, N., et al.: JHEP 0208, 021 (2002). hep-ph/0206020; Arkani-Hamed, N., Cohen, A., Katz, E., Nelson, A.: JHEP 0207, 034 (2002). hep-ph/0206021; Schmaltz, M., Tucker-Smith, D.: Annu. Rev. Nucl. Part. Sci. 55, 229 (2005). hep-ph/0502182; Perelstein, M.: Prog. Part. Nucl. Phys. 58, 247 (2007). hep-ph/0512128; Perelstein, M., Peskin, M.E., Pierce, A.: Phys. Rev. D 69, 075002 (2004). hep-ph/0310039
64. Arnold, P., Kauffman, R.: Nucl. Phys. B 349, 381 (1991); Ladinsky, G.A., Yuan, C.P.: Phys. Rev. D 50, 4239 (1994); Ellis, R.K., Veseli, S.: Nucl. Phys. B 511, 649 (1998)
65. Ashman, J., et al., EMC Collaboration: Phys. Lett. B 206, 364 (1988)
66. Atlas Collaboration: Coupling properties of the new Higgs-like boson observed with the ATLAS detector at the LHC. CERN Council Open Symposium: European Strategy for Particle Physics, Krakow, Poland, 10–12 September 2012. ATLAS-CONF-20122127 (2012)
67. ATLAS Collaboration: Eur. Phys. J. C 71, 1846 (2011). ArXiv:1109.6833; CMS Collaboration: JHEP 04, 084 (2012). ArXiv:1202.4617
68. ATLAS Collaboration ATLAS-CONF-2013-034: Phys. Lett. B 726, 88 (2013). ArXiv:1307.1427; ATLAS Collaboration ATLAS-CONF-2013-034: Phys. Lett. 726, 120 (2013). ArXiv:1307.1432; CMS Collaboration: PAS HIG-13-005; Landsberg, G.: Proceedings of EPS-HEP Conference, Stockholm (2013). ArXiv:1310.5705
69. Auger, M., et al., (EXO Collaboration): Phys. Rev. Lett. 109, 032505 (2012); Gando, A., et al., KamLAND-Zen Collaboration: ArXiv:1211.3863
70. Awramik, M., Czakon, M.: Phys. Rev. Lett. 89, 241801 (2002). hep-ph/0208113; Onishchenko, A., Veretin, O.: Phys. Lett. B 551, 111 (2003). hep-ph/0209010; Awramik, M., Czakon, M., Onishchenko, A., Veretin, O.: Phys. Rev. D 68, 053004 (2003). hep-ph/0209084; Awramik, M., Czakon, M.: Phys. Lett. B 568, 48 (2003). hep-ph/0305248; Freitas, A., Hollik, W., Walter, W., Weiglein, G.: Phys. Lett. B 495, 338 (2000); erratum ibid. B 570, 260 (2003). hep-ph/0007091; Freitas, A., Hollik, W., Walter, W., Weiglein, G.: Nucl. Phys. B 632, 189 (2002). erratum ibid. B 666, 305 (2003). hep-ph/0202131
71. Awramik, M., Czakon, M., Freitas, A., Weiglein, G.: Phys. Rev. Lett. 93, 201805 (2004). hep-ph/0407317; Awramik, M., Czakon, M., Freitas, A.: (2006). hep-ph/0608099; Phys. Lett. B 642, 563 (2006). hep-ph/0605339; Hollik, W., Meier, U., Uccirati, S.: Nucl. Phys. B 731, 213 (2005). hep-ph/0507158; Nucl. Phys. B 765, 154 (2007). hep-ph/0610312
72. Azatov, A., Galloway, J.: (2006). ArXiv:1212.1380; Hollik, W., Meler, U., Uccirati, S.: Nucl. Phys. B **731**, 213 (2005); Nucl. Phys. B **765**, 154 (2007)
73. Baak, M., et al., Gfitter group: (2012). ArXiv:1209.2716

74. Baikov, P.A., Chetyrkin, K.G., Kuhn, J.H.: Phys. Rev. Lett. 101, 012002 (2008). ArXiv:0801.1821; Phys. Rev. Lett. 104, 132004 (2010). ArXiv:1001.3606; Baikov, A., Chetyrkin, K.G., Kuhn, J.H., Rittinger, J.: ArXiv:1210.3594
75. Baker, C.A., et al.: Phys. Rev. Lett. 97, 131801 (2006). hep-ex/0602020v3
76. Ball, R.D., et al.: Phys. Lett. B 707, 66 (2012). ArXiv:1110.2483
77. Banfi, A., Dasgupta, M.: JHEP 0401, 027 (2004); Idilbi, A., Ji, X.-d.: Phys. Rev. D 72, 054016 (2005). hep-ph/0501006; Bolzoni, P., Forte, S., Ridolfi, G.: Nucl. Phys. B 731, 85 (2005); Delenda, Y., Appleby, R., Dasgupta, M., Banfi, A.: JHEP 0612, 044 (2006); Bolzoni, P.: Phys. Lett. B 643, 325 (2006); Mert, S., Aybat, Dixon, L.J., Sterman, G.: Phys. Rev. D 74, 074004 (2006); Dokshitzer, Yu.L., Marchesini, G.: JHEP 0601, 007 (2006); Laenen, E., Magnea, L.: Phys. Lett. B 632, 270 (2006); Lee, C., Sterman, G.: Phys. Rev. D 75, 014022 (2007); Becher, T., Neubert, M.: Phys. Rev. Lett. 97, 082001 (2006). hep-ph/0605050; de Florian, D., Vogelsang, W.: ArXiv:0704.1677; Chay, J., Kim, C.: Phys. Rev. D 75, 016003 (2007). hep-ph/0511066; Becher, T., Neubert, M., Pecjak, B.D.: JHEP 0701, 076 (2007). ArXiv:0607228; Abbate, R., Forte, S., Ridolfi, G.: ArXiv:0707.2452; Becher, T., Neubert, M., Xu, G.: JHEP 0807, 030 (2008). ArXiv:0710.0680; Ahrens, V., Becher, T., Neubert, M., Yang, L.L.: Phys. Rev. D 79, 033013 (2009); ArXiv:0808.3008; Bonvini, M., Forte, S., Ridolfi, G.: Nucl. Phys. B 808, 347 (2009). ArXiv:0807.3830; Nucl. Phys. B 847, 93 (2011). ArXiv:1009.5691; Bonvini, M., Ghezzi, M., Ridolfi, G.: Nucl. Phys. B 861, 337 (2012); ArXiv:1201.6364
78. Banfi, A., Salam, G.P., Zanderighi, G.: JHEP 0503, 073 (2005)
79. Barbieri, R.: (2013). ArXiv:1309.3473
80. Barbieri, R., Strumia, A.: (2000). hep-ph/0007265
81. Barbieri, R., et al.: Eur. Phys. J. C 71, 1725 (2011). ArXiv:1105.2296; JHEP 1207, 181 (2012). ArXiv:1203.4218; ArXiv:1206.1327; ArXiv:1211.5085; Crivellin, A., Hofer, L., Nierste, U.: PoS EPS-HEP2011, 145 (2011); Buras, A.J., Girrbach, J.: JHEP 1301, 007 (2013). ArXiv:1206.3878
82. Bardeen, W.A., Buras, A.J., Duke, D.W., Muta, T.: Phys. Rev. D 18, 3998 (1978)
83. Bauer, D., (for the CDF and D0 Collaborations): Nucl. Phys. B (Proc. Suppl.) 156, 226 (2006)
84. Bauer, C.W., Fleming, S., Luke, M.E.: Phys. Rev. D 63, 014006 (2000). hep-ph/0005275; Bauer, C.W., et al.: Phys. Rev. D 63, 114020 (2001). hep-ph/0011336; Bauer, C.W., Stewart, I.W.: Phys. Lett. B 516, 134 (2001). hep-ph/0107001; Bauer, C.W., Pirjol, D., Stewart, I.W.: Phys. Rev. D 65, 054022 (2002). hep-ph/0109045;
85. Bazavov, A., et al.: Phys. Rev. D 85, 054503 (2012). ArXiv:1111.1710
86. Becher, T., Neubert, M.: Phys. Rev. Lett. 98, 022003 (2007). hep-ph 0610067; see also Misiak, M., et al.: Phys. Rev. Lett. 98, 022002 (2007). hep-ph/0609232
87. Belavin, A., Polyakov, A., Shvarts, A., Tyupkin, Y.: Phys. Lett. B 59, 85 (1975)
88. Benayoun, M., David, P., Del Buono, L., Jegerlehner, F.: (2012). ArXiv:1210.7184; Davier, M., Malaescu, B.: (2013). ArXiv:1306.6374
89. Beneke, M., Boito, D., Jamin, M.: (2012). ArXiv:1210.8038
90. Beneke, M., Jamin, M., JHEP 0809, 044 (2008). ArXiv:0806.3156; Davier, M., et al., Eur. Phys. J. C 56, 305 (2008). ArXiv:0803.0979; Maltman, K., Yavin, T.: Phys. Rev. D 78, 094020 (2008). ArXiv:0807.0650; Narison, S.: Phys. Lett. B 673, 30 (2009). ArXiv:0901.3823; Caprini, I., Fischer, J., Eur. Phys. J. C 64, 35 (2009); ArXiv:0906.5211; Phys. Rev. D 84, 054019 (2011). ArXiv:1106.5336S; Abbas, G., Ananthanarayan, B., Caprini, I., Fischer, J.: Phys. Rev. D 87, 014008 (2013). ArXiv:1211.4316; Menke, S.: ArXiv:0904.1796; Pich, A.: ArXiv:1107.1123; Magradze, B.A.: ArXiv:1112.5958; Abbas, G., et al.: ArXiv:1202.2672; Boito, D., et al.: Phys. Rev. D 84, 113006 (2011). ArXiv:1110.1127; Boito, D., et al.: ArXiv:1203.3146
91. Berends, F.A., Giele, W.: Nucl. Phys. B 294, 700 (1987); Mangano, M.L., Parke, S.J., Xu, Z.: Nucl. Phys. B 298, 653 (1988)
92. Berger, C., et al.: Phys. Rev. D 78, 036003 (2008). ArXiv:0803.4180; ArXiv:0912.4927; Bern, Z., et al.: ArXiv:1210.6684
93. Berger, C.F., et al.: Phys. Rev. D 82, 074002 (2010). ArXiv:1004.1659

94. Berger, C.F., et al.: Phys. Rev. Lett. 106, 092001 (2011). ArXiv:1009.2338; Ita, H., et al.: Phys. Rev. D 85, 031501 (2012). ArXiv:1108.2229
95. Bern, Z., Dixon, L.J., Kosower, D.A.: Annu. Rev. Nucl. Part. Sci. 46, 109 (1996). hep-ph/9602280 and references therein
96. Bern, Z., Forde, D., Kosower, D.A., Mastrolia, P.: Phys. Rev. D 72, 025006 (2005)
97. Bern, Z., et al., Phys. Rev. D 88, 014025 (2013). ArXiv:1304.1253
98. Bertolini, S., Di Luzio, L., Malinsky, M.: (2012). ArXiv:1205.5637 and references therein
99. Bethke, S.: (2009). ArXiv:0908.1135
100. Bevilacqua, G., Czakon, M., Papadopoulos, C.G., Worek, M.: Phys. Rev. Lett. 104, 162002 (2010). ArXiv:1002.4009; Phys. Rev. D 84, 114017 (2011); ArXiv:1108.2851
101. Bilenky, S.M., Hosek, J., Petcov, S.T.: Phys. Lett. B 94, 495 (1980); Schechter, J., Valle, J.W.F.: Phys. Rev. D 22, 2227 (1980); Doi, M., et al.: Phys. Lett. B 102, 323 (1981)
102. Bjorken, J.D., Drell, S.: Relativistic Quantum Mechanics/Fields, vols. I, II. McGraw-Hill, New York (1965)
103. Bloch, F., Nordsieck, H.: Phys. Rev. 52, 54 (1937)
104. Blumlein, J., Bottcher, H.: Nucl. Phys. B 841, 205–230 (2010). ArXiv:1005.3113
105. Blumlein, J., Bottcher, H., Guffanti, A.: Nucl. Phys. B 774, 182 (2007). ArXiv:0607200 [hep-ph]
106. Bobeth, C., Hiller, G., van Dyk, D.: JHEP 1107, 067 (2011). ArXiv:1105.0376; Beaujean, F., Bobeth, C., van Dyk, D., Wacker, C.: JHEP 1208, 030 (2012). ArXiv:1205.1838; Bobeth, C., Hiller, G., van Dyk, D.: Phys. Rev. D 87, 034016 (2013). ArXiv:1212.2321; Descotes-Genon, S., Matias, J., Virto, J.: Phys. Rev. D 88, 074002 (2013). ArXiv:1307.5683 and references therein
107. Bona, M., [UTFit Collaboration]: UPdates from the UTfit on the Unitarity Triangle analysis. In: ICHEP 2016, Chicago (2016)
108. Bonciani, R., Catani, S., Mangano, M.L., Nason, P.: Nucl. Phys. B 529, 424 (1998) and references therein
109. Bouchiat, C., Iliopoulos, J., Meyer, P.: Phys. Lett. B 38, 519 (1972)
110. Bozzi, G., Catani, S., de Florian, D., Grazzini, M.: Phys. Lett. B 564, 65 (2003); Nucl. Phys. B 737, 73 (2006); Kulesza, A., Sterman, G., Vogelsang, W.: Phys. Rev. D 69, 014012 (2004)
111. Branchina, V., Messina, E.: (2013). ArXiv:1307.5193
112. Brandt, R., Preparata, G.: Nucl. Phys. B 27, 541 (1971)
113. Bredenstein, A., Denner, A., Dittmaier, S., Pozzorini, S.: Phys. Rev. Lett. 103, 012002 (2009). ArXiv:0905.0110; JHEP 1003, 021 (2010). ArXiv:1001.4006; Bevilacqua, G., et al.: JHEP 0909, 109 (2009). ArXiv:0907.4723
114. Britto, R., Cachazo, F., Feng, B.: Nucl. Phys. B 715, 499 (2005). hep-th/0412308; Britto, R., Cachazo, F., Feng, B., Witten, E.: Phys. Rev. Lett. 94, 181602 (2005). hep-th/0501052
115. Buchmuller, W., Peccei, R.D., Yanagida, T.: Annu. Rev. Nucl. Part. Sci. 55, 311 (2005). hep-ph 0502169; Fong, C.S., Nardi, E., Riotto, A.: Adv. High Energy Phys. 2012, 158303 (2012). ArXiv:1301.3062; Buchmuller, W.: ArXiv:1212.3554
116. Buras, A.J.: Lect. Notes Phys. 558, 65 (2000). hep-ph/9901409
117. Buras, A.J., Girrbach, J., Guadagnoli, D., Isidori, G.: Eur. Phys. J. C 72, 2172 (2012). ArXiv:1208.0934; Buras, A.J., Fleischer, R., Girrbach, J., Knegjens, R., JHEP 07, 077 (2013). ArXiv:1303.3820; see also Amhis, Y., et al., (Heavy Flavor Averaging Group): ArXiv:1207.1158
118. Buttazzo, D., Degrassi, G., Giardino, P.P., Giudice, G.F., Sala, F., Salvio, A., Strumia, A.: JHEP 1312, 089 (2013). doi:10.1007; JHEP 12, 089 (2013). arXiv:1307.3536 [hep-ph]
119. Butterworth, J.M., Dissertori, G., Salam, G.P.: Annu. Rev. Nucl. Part. Sci. 62, 387 (2012). doi:10.1146/annurev-nucl-102711-094913, arXiv:1202.0583 [hep-ex]
120. Cabibbo, N.: Phys. Rev. Lett. 10, 531 (1963)
121. Cabibbo, N.: Phys. Rev. Lett. 10, 531 (1963); Kobayashi, M., Maskawa, T.: Prog. Theor. Phys. 49, 652 (1973)
122. Cabibbo, N.: Phys. Lett. B 72, 333 (1978)
123. Cabibbo, N., Maiani, L., Parisi, G., Petronzio, R.: Nucl. Phys. B 158, 295 (1979)

124. Cacciari, M., Greco, M.: Nucl. Phys. B 421, 530 (1994); Cacciari, M., Greco, M., Nason, P., JHEP 9805, 007 (1998)
125. Cacciari, M., et al., JHEP 0404, 068 (2004); Cacciari, M., et al., JHEP 0407, 033 (2004)
126. Cacciari, M., Salam, G.P., Soyez, G.: JHEP 0804, 005 (2008). ArXiv:0802.1188
127. Cacciari, M., et al.: Phys. Lett. B 710, 612, (2012). ArXiv:1111.5869
128. Cachazo, F., Svrcek, P.: PoS RTN2005:004 (2005). hep-th/0504194; Dixon, L.J.: In: Proceedings of the EPS International Europhysics Conference on High Energy Physics, Lisbon, Portugal, 2005, PoS HEP2005:405 (2006). hep-ph/0512111 and references therein
129. Campbell, J.M., Ellis, R.K.: JHEP 1207, 052 (2012). ArXiv:1204.5678
130. Campbell, J.M., Huston, J.W., Stirling, W.J.: Rep. Prog. Phys. 70, 89 (2007)
131. Caswell, W.E.: Phys. Rev. Lett. 33, 244 (1974); Jones, D.R.T.: Nucl. Phys. B 75, 531 (1974); Egorian, E., Tarasov, O.V.: Theor. Math. Phys. 41, 863 (1979). [Teor. Mat. Fiz. 41 (1979) 26]
132. Catani, S., Dokshitzer, Y.L., Seymour, M.H., Webber, B.R.: Nucl. Phys. B 406, 187 (1993) and references therein; Ellis, S.D., Soper, D.E.: Phys. Rev. D 48, 3160 (1993). hep-ph/9305266
133. Catani, S., de Florian, D., Grazzini, M.: JHEP 0105, 025 (2001); JHEP 0201, 015 (2002); Harlander, R.V.: Phys. Lett. B 492, 74 (2000); Ravindran, V., Smith, J., van Neerven, W.L.: Nucl. Phys. B 704, 332 (2005); Harlander, R.V., Kilgore, W.B.: Phys. Rev. D 64, 013015 (2001); Harlander, R.V., Kilgore, W.B.: Phys. Rev. Lett. 88, 201801 (2002); Anastasiou, C., Melnikov, K.: Nucl. Phys. B 646, 220 (2002); Ravindran, V., Smith, J., van Neerven, W.L.: Nucl. Phys. B 665, 325 (2003)
134. Catani, S., de Florian, D., Grazzini, M., Nason, P.: JHEP 0307, 028 (2003); Moch, S., Vogt, A.: Phys. Lett. B 631, 48 (2005); Ravindran, V.: Nucl. Phys. B 752, 173 (2006) (and references therein)
135. Chatrchyan, S., et al., [CMS Collab.]: Phys. Lett. B 716, 30 (2012). ArXiv:1207:7235
136. Chatrchyan, S., et al., CMS Collaboration: Phys. Rev. Lett. 111, 101804 (2013). ArXiv:1307.5025
137. Cheng, T.-P., Li, L.-F.: Gauge Theory of Elementary Particle Physics. Oxford University Press, Oxford (1988); Bailin, D., Love, A.: Introduction to Gauge Field Theory, Revised edition. CRC, Boca Raton, FL (1993); Bardin, D.Y., Passarino, G.: The Standard Model in the Making: Precision Study of the Electroweak Interactions. Clarendon, Oxford (1999); Aitchison, I.J.R., Hey, A.J.G.: Gauge Theories in Particle Physics. Taylor and Francis, London (2003)
138. Chetyrkin, K.G., Kataev, A.L., Tkachev, F.V.: Phys. Lett. B 85, 277 (1979); Dine, M., Sapirstein, J.: Phys. Rev. Lett. 43, 688 (1979); Celmaster, W., Gonsalves, R.J.: Phys. Rev. Lett. 44, 560 (1979); Phys. Rev. D 21, 3772 (1980)
139. Chetyrkin, K., Kniehl, B., Steinhauser, M.: Phys. Rev. Lett. 79, 353 (1997)
140. Choudhury, D., Tait, T.M.P., Wagner, C.E.M.: Phys. Rev. D 65, 053002 (2002). hep-ph/0109097
141. Ciafaloni, M., Colferai, D., Salam, G.P., Stasto, A.M.: Phys. Lett. B 587, 87 (2004); see also Salam, G.P.: hep-ph/0501097; White, C.D., Thorne, R.S.: hep-ph/0611204
142. Ciuchini, M., Franco, E., Mishima, S., Silvestrini, L.: (2013). ArXiv:1306.4644
143. CMS Collaboration: CMS PAS B2G-12-012 (2012)
144. CMS Collaboration: (2011). CMS-PAS-TOP-11-030; and talk by Chwalek, T., [CMS Collaboration]: Presented at ICHEP 2012, Melbourne (2012)
145. Coleman, S., Gross, D.: Phys. Rev. Lett. 31, 851 (1973)
146. Collins, J.C., Soper, D.E., Sterman, G.: Nucl. Phys. B 261, 104 (1985); a review by the same authors can be found in Perturbative QCD, edited by Mueller, A.H., World Scientific, Singapore (1989); Bodwin, G.T.: Phys. Rev. D 31, 2616 (1985); erratum D 34, 3932 (1986); Nucl. Phys. B 308, 833 (1988); Phys. Lett. B 438, 184 (1998). hep-ph/9806234
147. Combridge, B.L., Kripfganz, J., Ranft, J.: Phys. Lett. B 70, 234 (1977)
148. Commins, E.D.: Weak Interactions. McGraw Hill, New York (1973); Okun, L.V.: Leptons and Quarks. North Holland, Amsterdam (1982); Bailin, D.: Weak Interactions, 2nd edn. Hilger, Bristol (1982); Georgi, H.M.: Weak and Modern Particle Theory. Benjamin, Menlo Park, CA (1984)

149. Cornwall, J.M., Levin, D.N., Tiktopoulos, G.: Phys. Rev. D 10, 1145 (1974); Vayonakis, C.E.: Lett. Nuovo Cim. 17, 383 (1976); Lee, B.W., Quigg, C., Thacker, H.: Phys. Rev. D 16, 1519 (1977); Chanowitz, M.S., Gaillard, M.K.: Nucl. Phys. B 261, 379 (1985)
150. Czakon, M., Fiedler, P., Mitov, A., Rojo, A.: (2013). ArXiv:1305.3892; See also: Baernreuther, P., Czakon, M., Mitov, A.: Phys. Rev. Lett. 109, 132001 (2012). ArXiv:1204.5201; Czakon, M., Mitov, A.: JHEP 1212, 054 (2012). ArXiv:1207.0236; JHEP 1301, 080 (2013). ArXiv:1210.6832; Czakon, M., Fiedler, P., Mitov, A.: Phys. Rev. Lett. 110, 252004 (2013). ArXiv:1303.6254
151. Czarnecki, A., Krause, B., Marciano, W.J.: Phys. Rev. Lett. 76, 3267 (1996); Knecht, M., Peris, S., Perrottet, M., De, E., Rafael, J.: High Energy Phys. 11, 003 (2002); Czarnecki, A., Marciano, W.J., Vainshtein, A.: Phys. Rev. D 67, 073006 (2003)
152. D'Ambrosio, G., Giudice, G.F., Isidori, G., Strumia, A.: Nucl. Phys. B 645, 155 (2002). hep-ph/0207036; Buras, A.J.: Acta Phys. Polon. B 34, 5615 (2003). hep-ph/0310208
153. Dasgupta, M., Salam, G.P.: Phys. Lett. B 512, 323 (2001); Dasgupta, M., Salam, G.P.: J. Phys. G 30, R143 (2004); Banfi, A., Corcella, G., Dasgupta, M., Delenda, Y., Salam, G.P., Zanderighi, G.: (2005). hep-ph/0508096; Forshaw, J.R., Kyrieleis, A., Seymour, M.H.: JHEP 0608, 059 (2006)
154. Dasgupta, M., Salam, G.P., J. Phys. G. 30, R143 (2004). hep-ph/0312283; Biebel, O.: Phys. Rep. 3450, 165 (2001); Kluth, S.: Rep. Prog. Phys. 69, 1771 (2006). hep-ex/0603011
155. Davier, M., Hoecker, A., Malaescu, B., Zhang, Z.: Eur. Phys. J. C 71, 1515 (2011). ArXiv:1010.4180
156. Dawson, S.: Nucl. Phys. B 359, 283 (1991); Djouadi, A., Spira, M., Zerwas, P.M.: Phys. Lett. B 264, 440 (1991); Spira, M., Djouadi, A., Graudenz, D., Zerwas, P.: Nucl. Phys. B 453, 17 (1995)
157. de Boer, W., Sander, C.: Phys. Lett. B 585, 276 (2004)
158. de Florian, D., Grazzini, M., Kunszt, Z.: Phys. Rev. Lett. 82, 5209 (1999); Ravindran, V., Smith, J., Van Neerven, W.L.: Nucl. Phys. B 634, 247 (2002); Glosser, C.J., Schmidt, C.R.: JHEP 0212, 016 (2002)
159. de Florian, D., Sassot, R., Stratmann, M., Vogelsang, W.: Phys. Rev. D 80, 034030 (2009). ArXiv:0904.3821; ArXiv:1112.0904
160. Degrassi, G., et al.: JHEP 1208, 098 (2012). ArXiv:1205.6497
161. Denner, A., Dittmaier, S., Kallweit, S., Pozzorini, S.: Phys. Rev. Lett. 106, 052001 (2011). ArXiv:1012.3975; Bevilacqua, G., et al.: JHEP 1102, 083 (2011). ArXiv:1012.4230
162. DeTar, C.E., Heller, U.M.: Eur. Phys. J. A. 41, 405 (2009). ArXiv:0905.2949
163. Dinsdale, M., Ternick, M., Weinzierl, S.: JHEP 0603, 056 (2006). hep-ph/0602204
164. Dissertori, G., et al.: JHEP 0908, 036 (2009). ArXiv:0906.3436
165. Dittmaier, S., et al.: Handbook of LHC Higgs Cross Sections (2011). ArXiv:1101.0593, (2012). ArXiv:1201.3084
166. Dixon, L.: Talk at ICHEP 2012, Melbourne (2012)
167. Dixon, L.J., Glover, E.W.N., Khoze, V.V.: JHEP 0412, 015 (2004); Badger, S.D., Glover, E.W.N., Khoze, V.V.: JHEP 0503, 023 (2005); Badger, S.D., Glover, E.W.N., Risager, K.: Acta Phys. Polon. B 38, 2273–2278 (2007)
168. Djouadi, A.: Eur. Phys. J. C 73, 2498 (2013) doi:10.1140/epjc/s10052-013-2498-3. arXiv:1208.3436 [hep-ph]
169. Djouadi, A.: (2005). hep-ph/0503172; (2012). ArXiv:1203.4199
170. Djouadi, A., Moreau, G., Richard, F.: (2006). hep-ph/0610173
171. Dokshitzer, Yu.L.: Sov. Phys. JETP 46, 641 (1977)
172. Dokshitzer, Yu.: J. Phys. G 17, 1572 (1991); Brown, N., Stirling, W.J.: Z. Phys. C 53, 629 (1992)
173. Dokshitzer, Y.L., Khoze, V.A.: Basics of Perturbative QCD. Frontieres, Gif-sur-Yvette (1991); Muta, T.: Foundation of Quantum Chromodynamics: An Introduction to Perturbative Methods in Gauge Theories, 3rd edn. World Scientific, Singapore (2009); Yndurain, F.J.: The Theory of Quark and Gluon Interactions, 4th edn. Springer, Berlin (2006); Altarelli, G.: The Development of Perturbative QCD. World Scientific, Singapore (1994); Greiner,

W., Schramm, S., Stein, E.: Quantum Chromodynamics, 3rd edn. Springer, Berlin (2007); Shifman, M. (eds.): At the Frontier of Particle Physics: Handbook of QCD, vols. 1–4. World Scientific, Singapore (2001); Ellis, R.K., Stirling, W.J., Webber, B.R.: QCD and Collider Physics. Cambridge Monographs. Cambridge University Press, Cambridge (2003); Dissertori, G., Knowles, I., Schmelling, M.: Quantum Chromodynamics: High Energy Experiments and Theory. Oxford University Press, Oxford (2003); Narison, S.: QCD as a Theory of Hadrons: From Partons to Confinement. Cambridge Monographs. Cambridge University Press, Cambridge (2007); Collins, J.C.: Foundations of Perturbative QCD. Cambridge Monographs. Cambridge University Press, Cambridge (2011)
174. Dokshitzer, Y.L., Leder, G.D., Moretti, S., Webber, B.R.: JHEP 9708, 001 (1997). hep-ph/9707323; Wobisch, M., Wengler, T.: hep-ph/9907280
175. Dolgov, A.D.: Phys. Rep. 370, 333 (2002). hep-ph/0202122; Lesgourgues, J., Pastor, S.: Phys. Rep. 429, 307–379 (2006); ArXiv:astro-ph/0603494; ArXiv:1212.6154
176. Donoghue, J.F., Golowich, E., Holstein, B.: Dynamics of the Standard Model. Cambridge University Press, Cambridge (1992)
177. Douglas, M.R.: (2006). hep-th/0602266; (2012). ArXiv:1204.6626
178. Eichten, E., Hill, B.: Phys. Lett. B 234, 511 (1990); Georgi, H.: Phys. Lett. B 240, 447 (1990); Grinstein, B.: Nucl. Phys. B 339, 253 (1990); Mannel, T., Roberts, W., Ryzak, Z.: Nucl. Phys. B 368, 204 (1992)
179. Ellis, J., Hwang, D.S.: JHEP 1209, 071 (2012). ArXiv:1202.6660; Ellis, J., Hwang, D.S., Sanz, V., You, T.: ArXiv:1208.6002; ArXiv:1210.5229
180. Ellis, R.K., Sexton, J.C.: Nucl. Phys. B 269, 445 (1986); Aversa, F., Chiappetta, P., Greco, M., Guillet, J.P.: Nucl. Phys. B 327, 105 (1989); Phys. Rev. Lett. 65, 401 (1990); Ellis, S.D., Kunszt, Z., Soper, D.E.: Phys. Rev. Lett. 64, 2121 (1990); Kunszt, Z., Soper, D.E.: Phys. Rev. D 46, 192 (1992); Giele, W.T., Glover, E.W.N., Kosower, D.A.: Nucl. Phys. B 403, 633 (1993)
181. Ellis, J., Gaillard, J.M., Nanopoulos, D.V.: Nucl. Phys. B 106, 292 (1976); Bjorken, J.D.: SLAC Report 198 (1976)
182. Ellis, J., Gaillard, M., Nanopoulos, D.: Nucl. Phys. B 106, 292 (1976)
183. Ellis, R.K., Martinelli, G., Petronzio, R.: Nucl. Phys. B 211, 106 (1983); Arnold, P., Reno, M.H.: Nucl. Phys. B 319, 37 (1989); erratum B 330, 284 (1990); Arnold, P., Ellis, R.K., Reno, M.H.: Phys. Rev. D 40, 912 (1989); Gonsalves, R., Pawlowski, J., Wai, C.F.: Phys. Rev. D 40, 2245 (1989)
184. Ellis, R.K., Giele, W.T., Zanderighi, G.: Phys. Rev. D 72, 054018 (2005); erratum D 74, 079902 (2006); Campbell, J.M., Ellis, R.K., Zanderighi, G.: JHEP 0610, 028 (2006); Anastasiou, C., et al.: JHEP 0701, 082 (2007); Davatz, G., et al.: JHEP 0607, 037 (2006); Catani, S., Grazzini, M.: Phys. Rev. Lett. 98, 222002 (2007); Anastasiou, C., Dissertori, G., Stoeckli, F.: ArXiv:0707.2373; Balázs, C., Berger, E.L., Nadolsky, P.M., Yuan, C.-P.: hep-ph/0702003. ArXiv:0704.0001; Ciccolini, M., Denner, A., Dittmaier, S.: ArXiv:0707.0381; Furlan, E.: JHEP 1110, 115 (2011). ArXiv:1106.4024; Anastasiou, C., et al.: ArXiv:1202.3638; Bonvini, M., Forte, S., Ridolfi, G.: Phys. Rev. Lett. 109, 102002 (2012). ArXiv:1204.5473; Grazzini, M., Sargsyan, H.: JHEP (2013). ArXiv:1306.4581
185. Ellis, S.D., et al.: Prog. Part. Nucl. Phys. 60, 484 (2008). ArXiv:0712.2447
186. Ellis, R.K., Giele, W.T., Kunszt, Z., Melnikov, K.: Nucl. Phys. B 822, 270 (2009). ArXiv:0806.3467
187. Ellis, R.K., Melnikov, K., Zanderighi, G.: Phys. Rev. D 80, 094002 (2009). ArXiv:0906;1445; JHEP 0904, 077 (2009). ArXiv:0901.4101; Melnikov, K., Zanderighi, G.: Phys. Rev. D 81, 074025 (2010). ArXiv:0910.3671; Berger, F., et al.: Phys. Rev. Lett. 102, 222001 (2009). ArXiv:0902.2760; Berger, C.F., et al.: Phys. Rev. D 80, 074036 (2009). ArXiv:0907.1984
188. Ellis, R.K., Kunszt, Z., Melnikov, K., Zanderighi, G.: Phys. Rep. 518, 141 (2012). ArXiv:1105.4319
189. Englert, F., Brout, R.: Phys. Rev. Lett. 13, 321 (1964); Higgs, P.W.: Phys. Lett. 12, 132 (1964); Phys. Rev. Lett. 13, 508 (1964)
190. Ermolaev, B.I., Greco, M., Troyan, S.I.: (2009). ArXiv:0905.2841 and references therein

191. Fadin, V.S., Lipatov, L.N.: Phys. Lett. B 429, 127 (1998); B 429, 127 (1998); Fadin, V.S., et al.: Phys. Lett. B 359, 181 (1995); B 387, 593 (1996); Nucl. Phys. B 406, 259 (1993); Phys. Rev. D 50, 5893 (1994); Phys. Lett. B 389, 737 (1996); Nucl. Phys. B 477, 767 (1996); Phys. Lett. B 415, 97 (1997); B 422, 287 (1998); Camici, G., Ciafaloni, M.: Phys. Lett. B 412, 396 (1997); Phys. Lett. B 430, 349 (1998); del Duca, V., Phys. Rev. D 54, 989 (1996); D 54, 4474 (1996); del Duca, V., Schmidt, C.R.: Phys. Rev. D 57, 4069 (1998); Bern, Z., del Duca, V., Schmidt, C.R.: Phys. Lett. B 445, 168 (1998)
192. Fahri, E.: Phys. Rev. Lett. 39, 1587 (1977)
193. Faisst, M., Kuhn, J.H., Seidensticker, T., Veretin, O.: Nucl. Phys. B 665, 649 (2003). hep-ph/0302275; Chetyrkin, K.G., Faisst, M., Kuhn, J.H., Maierhofer, P., Sturm, C.: Phys. Rev. Lett. 97, 102003 (2006). hep-ph/0605201; Boughezal, R., Czakon, M.: Nucl. Phys. B 755, 221 (2006). hep-ph/0606232
194. Falkowski, A., Riva, F., Urbano, A.: JHEP 1311, 111 (2013). arXiv:1303.1812 [hep-ph]
195. Farina, M., Pappadopulo, D., Strumia, A.: (2013). ArXiv:1303.7244
196. Fayet, P.: Nucl. Phys. B 90, 104 (1975); Ellwanger, U., Hugonie, C., Teixeira, A.M.: Phys. Rep. 496, 1 (2010). ArXiv:0910.1785; Maniatis, M.: Int. J. Mod. Phys. A 25, 3505 (2010); Hall, L.J., Pinner, D., Ruderman, J.T.: JHEP 1204, 131 (2012). ArXiv:1112.2703; Agashe, K., Cui, Y., Franceschini, R.: JHEP 1302, 031 (2013). ArXiv:1209.2115; Athron, P., Binjonaid, M., King, S.F.: ArXiv:1302.5291; Barbieri, R., et al.: ArXiv:1307.4937
197. Feynman, R.: Acta Phys. Pol. 24, 697 (1963); De Witt, B.: Phys. Rev. 162, 1195, 1239 (1967); Faddeev, L.D., Popov, V.N.: Phys. Lett. B 25, 29 (1967)
198. Floratos, E.G., Ross, D.A., Sachrajda, C.T.: Nucl. Phys. B 129, 66 (1977); B 139, 545 (1978); B 152, 493 (1979); Gonzales-Arroyo, A., Lopez, C., Yndurain, F.J.: Nucl. Phys. B 153, 161 (1979); Curci, G., Furmanski, W., Petronzio, R.: Nucl. Phys. B 175, 27 (1980); Furmanski, W., Petronzio, R.: Phys. Lett. B 97, 438 (1980); Floratos, E.G., Lacaze, R., Kounnas, C.: Phys. Lett. B 99, 89, 285 (1981); Herrod, R.T., Wada, S.: Z. Phys. C 9, 351 (1981)
199. Fodor, Z., Katz, S.D.: arXiv:0908.3341; Acta Phys. Polon. B 42, 2791 (2009)
200. Fogli, G., et al.: (2012). ArXiv:1205.5254
201. Forero, D., Tortola, M., Valle, J.: (2012). ArXiv:1205.4018
202. Forte, S., Ridolfi, G.: Nucl. Phys. B 650, 229 (2003); Moch, S., Vermaseren, J.A.M., Vogt, A.: Nucl. Phys. B 726, 317 (2005). hep-ph/0506288; Becher, T., Neubert, M., Pecjak, B.D.: JHEP 0701, 076 (2007). hep-ph/0607228
203. Frederix, R., et al.: Phys. Lett. B 701, 427 (2011). ArXiv:1104.5613
204. Freitas, A., Huang, Y.-C.: JHEP 1208, 050 (2012); erratum ibid 1305, 074 (2013); 1310, 044 (2013). ArXiv:1205.0299
205. Frieman, J., Turner, M., Huterer, D.: Annu. Rev. Astron. Astrophys. 46, 385 (2008). ArXiv:0803.0982
206. Frixione, S., Webber, B.R.: JHEP 06, 029 (2002). hep-ph/0204244; hep-ph/0612272 and references therein
207. Fujikawa, K., Lee, B.W., Sanda, A.: Phys. Rev. D 6, 2923 (1972); Yao, Y.P.: Phys. Rev. D 7, 1647 (1973)
208. Fukaya, H., et al.: Phys. Rev. D 83, 074501 (2011). ArXiv:1012.4052
209. Gaillard, M.K., Lee, B.W.: Phys. Rev. Lett. 33, 108 (1974); Altarelli, G., Maiani, L.: Phys. Lett. B 52, 351 (1974)
210. Gambino, P.: Int. J. Mod. Phys. A 19, 808 (2004). hep-ph/0311257
211. Gardi, E., Korchemsky, G.P., Ross, D.A., Tafat, S.: Nucl. Phys. B 636, 385 (2002). hep-ph/0203161; Gardi, E., Roberts, R.G.: Nucl. Phys. B 653, 227 (2003). hep-ph/0210429
212. Gasser, J.: Nucl. Phys. Proc. Suppl. 86, 257 (2000). hep-ph/9912548
213. Gehrmann-De Ridder, A., Gehrmann, T., Glover, E.W.N., Heinrich, G.: Phys. Rev. Lett. 99, 132002 (2007). ArXiv:0707.1285; JHEP 0711, 058 (2007). ArXiv:0710.0346; Phys. Rev. Lett. 100, 172001 (2008). ArXiv:0802.0813; JHEP 0712, 094 (2007). ArXiv:0711.4711
214. Gell-Mann, M.: Phys. Lett. 8, 214 (1964); Zweig, G.: CERN TH 401 and 412 (1964); Greenberg, O.W.: Phys. Rev. Lett. 13, 598 (1964)

215. Gell-Mann, M.: Acta Phys. Austriaca Suppl. IX, 733 (1972); Fritzsch, H., Gell-Mann, M.: In: Proceedings of XVI International Conference on High Energy Physics, Chicago-Batavia (1972); Fritzsch, H., Gell-Mann, M., Leutwyler, H.: Phys. Lett. B 47, 365 (1973)
216. Georgi, H., Glashow, S., Machacek, M., Nanopoulos, D.: Phys. Rev. Lett. 40, 692 (1978)
217. Georgiou, G., Khoze, V.V.: JHEP 0405, 015 (2004); Wu, J.B., Zhu, C.J.: JHEP 0409, 063 (2004); Georgiou, G., Glover, E.W.N., Khoze, V.V.: JHEP 0407, 048 (2004)
218. Giardino, P.P., Kannike, K., Masina, I., Raidal, M., Strumia, A.: JHEP 1405, 046 (2014). arXiv:1303.3570 [hep-ph]
219. Gildener, E.: Phys. Rev. D 14, 1667 (1976); Gildener, E., Weinberg, S.: Phys. Rev. D 13, 3333 (1976); Maiani, L.: In: Davier, M., et al. (eds.) Proceedings of the Summer School on Particle Physics, Gif-sur-Yvette, 3–7 September 1979, IN2P3, Paris (1979); t'Hooft, G.: In: Proceedings of the 1979 Cargese Institute on Recent Developments in Gauge Theories, p. 135. Plenum, New York (1980); Veltman, M.: Acta Phys. Polon. B 12, 437 (1981); Witten, E.: Nucl. Phys. B 188, 513 (1981); Phys. Lett. B 105, 267 (1981)
220. Giudice, G.: In: Kane, G., Pierce, A.: Perspectives on LHC Physics. World Scientific, Singapore (2008). ArXiv:0801.2562
221. Giudice, G.: Proceedings of EPS-HEP Conference, Stockholm (2013). ArXiv:1307.7879
222. Giudice, G.F., Grojean, C., Pomarol, A., Rattazzi, R.: JHEP 0706, 045 (2007). hep-ph/0703164; Alonso, R., et al.: ArXiv:1212.3305; Contino, R., et al.: ArXiv:1303.3876; Pomarol, A., Riva, F.: ArXiv:1308.2803 and references therein
223. Giudice, G.F., Grojean, C., Pomarol, A., Rattazzi, R.: JHEP 0706, 045 (2007). hep-ph/0703164; Csaki, C., Falkowski, A., Weiler, A.: JHEP 0809, 008 (2008). ArXiv:0804.1954; Contino, R.: ArXiv:1005.4269; Barbieri, R., et al.: ArXiv:1211.5085; Keren-Zur, B., et al.: Nucl. Phys. B 867, 429 (2013). ArXiv:1205.5803
224. Giudice, G.F., Rattazzi, R., Strumia, A.: Phys. Lett. B 715, 142 (2012). ArXiv:1204.5465
225. Glashow, S.L.: Nucl. Phys. 22, 579 (1961)
226. Glashow, S.L., Iliopoulos, J., Maiani, L.: Phys. Rev. 96, 1285 (1970)
227. Gleisberg, T., et al.: JHEP 0402, 056 (2004). hep-ph/0311263; Gleisberg, T., et al.: JHEP 0902, 007 (2009). ArXiv:0811.4622; Krauss, F., Kuhn, R., Soff, G.: JHEP 0202, 044 (2002). hep-ph/0109036; Gleisberg, T., Krauss, F.: Eur. Phys. J. C 53, 501 (2008). ArXiv:0709.2881
228. Goldstone, J.: Nuovo Cim. 19, 154 (1961); Goldstone, J., Salam, A., Weinberg, S.: Phys. Rev. 127, 965 (1962)
229. Gonzalez-Garcia, M.C., Maltoni, M., Salvado, J., Schwetz, T.: (2012). ArXiv:1209.3023
230. Gorishny, S.G., Kataev, A.L., Larin, S.A.: Phys. Lett. B 259, 144 (1991); Surguladze, L.R., Samuel, M.A.: Phys. Rev. Lett. 66, 560 (1991)
231. Green, M.B., Schwarz, J.H., Witten, E.: Superstring Theory. Cambridge University Press, Cambridge (1987)
232. Greiner, N., Guffanti, A., Reiter, T., Reuter, J.: Phys. Rev. Lett. 107, 102002 (2011). ArXiv:1105.3624
233. Gribov, V.N., Lipatov, L.N.: Sov. J. Nucl. Phys. 15, 438 (1972)
234. Gross, D., Wilczek, F.: Phys. Rev. Lett. 30, 1343 (1973); Phys. Rev. D 8, 3633 (1973); Politzer, H.D.: Phys. Rev. Lett. 30, 1346 (1973)
235. Grunewald, M., Gurtu, A., Particle Data Group, Beringer, J., et al.: Phys. Rev. D 86, 010001 (2012)
236. Guralnik, G.S., Hagen, C.R., Kibble, T.W.B.: Phys. Rev. Lett. 13, 585 (1964)
237. H1 Collaboration: Eur. Phys. J. C 71, 1579 (2011). ArXiv:1012.4355
238. Haber, H.E., Kane, G., Dawson, S., Gunion, J.F.: The Higgs Hunter's Guide. Westview, Boulder, CO (1990)
239. Hagiwara, K., Liao, R., Martin, A.D., Nomura, D., Teubner, T.: J. Phys. G 38, 085003 (2011)
240. Hamberg, R., van Neerven, W.L., Matsuura, T.: Nucl. Phys. B 359, 343 (1991); erratum ibid. B 644, 403–404 (2002); van Neerven, W.L., Zijlstra, E.B.: Nucl. Phys. B 382, 11 (1992)
241. Hambye, T., Riesselmann, K.: Phys. Rev. D 55, 7255 (1997)
242. Hanneke, D., Fogwell, S., Gabrielse, G.: Phys. Rev. Lett. 100, 120801 (2008); Hanneke, D., Fogwell Hoogerheide, S., Gabrielse, G.: Phys. Rev. A 83, 052122 (2011)

243. Higgs, P.W.: Phys. Rev. 145, 1156 (1966)
244. Hirai, M., Kumano, S.: Nucl. Phys. B 813, 106–122 (2009). ArXiv:0808.0413
245. Hoecker, A., Marciano, W.: The Muon Anomalous Magnetic Moment, in [307]
246. Holdom, R.: Phys. Rev. D 24, 1441 (1981); Phys. Lett. B 150, 301 (1985); Appelquist, T., Karabali, D., Wijewardhana, L.C.R.: Phys. Rev. Lett. 57, 957 (1986); Appelquist, T., Wijewardhana, L.C.R.: Phys. Rev. D 36, 568 (1987); Yamawaki, K., Bando, M., Matumoto, K.: Phys. Rev. Lett. 56, 1335 (1986); Akiba, T., Yanagida, T.: Phys. (1986); Hill, C.T.: Phys. Lett. B 345, 483 (1995); Lane, K.D., Mrenna, S.: Phys. Rev. D 67, 115011 (2003)
247. Hollik, W., Pagani, D.: Phys. Rev. D 84, 093003 (2011). ArXiv:1107.2606; Kuhn, J.H., Rodrigo, G.: JHEP 1201, 063 (2012). ArXiv:1109.6830; Manohar, A.V., Trott, M.: Phys. Lett. B 711, 313 (2012). ArXiv:1201.3926; Bernreuther, W., Si, Z.-G.: ArXiv:1205.6580
248. Hurth, T., Mahmoudi, F.: Nucl. Phys. B 865, 461 (2012). ArXiv:1207.0688; Altmannshofer, W., Straub, D.M.: ArXiv:1308.1501; Gauld, R., Goertz, F., Haisch, U.: ArXiv:1308.1959; ArXiv:1310.1082; Buras, A.J., Girrbach, J.: ArXiv:1309.2466
249. Isidori, G., Ridolfi, G., Strumia, A.: Nucl. Phys. B 609, 387 (2001)
250. Itzykson, C., Zuber, J.: Introduction to Quantum Field Theory. McGraw-Hill, New York, (1980); Cheng, T.P., Li, L.F.: Gauge Theory of Elementary Particle Physics. Oxford University Press, New York (1984); Peskin, M.E., Schroeder, D.V.: An Introduction to Quantum Field Theory. Perseus Books, Cambridge, MA (1995); Weinberg, S.: The Quantum Theory of Fields, vols. I, II. Cambridge University Press, Cambridge, MA (1996); Zee, A.: Quantum Field Theory in a Nutshell. Princeton University Press, Princeton, NJ (2003)
251. Jarlskog, C.: Phys. Rev. Lett. 55, 1039 (1985)
252. Jegerlehner, F., Nyffeler, A.: Phys. Rep. 477, 1 (2009). ArXiv:0902.3360s
253. Jezabek, M., Kuhn, J.H.: Nucl. Phys. B 314, 1 (1989)
254. Jimenez-Delgado, P., Reya, E.: Phys. Rev. D 79, 074023 (2009). ArXiv:0810.4274
255. Kaczmarak, O., Karsch, F., Laermann, E., Lutgemeier, M.: Phys. Rev. D 62, 034021 (2000). ArXiv:hep-lat/9908010
256. Kaczmarek, O., Karsch, F., Zantow, F., Petreczky, P.: Phys. Rev. D 70, 074505 (2004); erratum ibid. D 72, 059903 (2005); hep-lat/0406036 and references therein
257. Kannike, K., et al.: (2011). ArXiv:1111.2551
258. Kaplan, D.B., Georgi, H.: Phys. Lett. B 136, 183 (1984); Dimopoulos, S., Preskill, J.: Nucl. Phys. B 199, 206 (1982); Banks, T.: Nucl. Phys. B 243, 125 (1984); Kaplan, D.B., Georgi, H., Dimopoulos, S.: Phys. Lett. B 136, 187 (1984); Georgi, H., Kaplan, D.B., Galison, P.: Phys. Lett. B 143, 152 (1984); Georgi, H., Kaplan, D.B.: Phys. Lett. B 145, 216 (1984); Dugan, M.J., Georgi, H., Kaplan, D.B.: Nucl. Phys. B 254, 299 (1985)
259. Kettell, S.: Talk at NuFact 2013. IHEP, Beijing (2013)
260. Khachatryan, V., et al., CMS Collaboration: Eur. Phys. J. C 75(5), 212 (2015). doi:10.1140/epjc/s10052-015-3351-7. arXiv:1412.8662 [hep-ex]
261. Kibble, T.W.B.: Phys. Rev. 155, 1554 (1967)
262. Kim, J.E., AIP Conf. Proc. 1200, 83 (2010). ArXiv:0909.3908
263. Kim, J.E., Carosi, G.: Rev. Mod. Phys. 82, 557 (2010). ArXiv:0807.3125
264. King, S.F., Luhn, C.: (2013). ArXiv:1301.1340
265. Kinoshita, T.: J. Math. Phys. 3, 650 (1962); Lee, T.D., Nauenberg, M.: Phys. Rev. 133, 1549 (1964)
266. Kinoshita, T., Nio, N.: Phys. Rev. D 73, 013003 (2006)
267. Klapdor-Kleingrothaus, H.V., Krivosheina, I.V.: Mod. Phys. Lett. A 21, 1547 (2006)
268. Kluth, S.: Rep. Prog. Phys. 69, 1771 (2006)
269. Kobayashi, M., Maskawa, T.: Prog. Theor. Phys. 49, 652 (1973)
270. Kramer, M., Laenen, E., Spira, M.: Nucl. Phys. B 511, 523 (1998)
271. Kribs, G.D., Martin, A., Menon, A.: ArXiv:1305.1313; Krizka, K., Kumar, A., Morrissey, D.E.: ArXiv:1212.4856; Auzzi, R., Giveon, A., Gudnason, S.B., Shacham, T.: JHEP 1301, 169 (2013). ArXiv:1208.6263; Espinosa, J.R., Grojean, C., Sanz, V., Trott, M.: JHEP 1212, 077 (2012). ArXiv:1207.7355; Han, Z., Katz, A., Krohn, D., Reece, M.: JHEP 1208, 083 (2012). ArXiv:1205.5808; Lee, H.M., Sanzand, V., Trott, M.: JHEP 1205, 139 (2012).

ArXiv:1204.0802; Bai, Y., Cheng, H.-C., Gallicchio, J., Gu, J.: JHEP 1207, 110 (2012). ArXiv:1203.4813; Allanach, B., Gripaios, B.: JHEP 1205, 062 (2012). ArXiv:1202.6616; Larsen, G., Nomura, Y., Roberts, H.L.: JHEP 1206, 032 (2012). ArXiv:1202.6339; Buchmueller, O., Marrouche, J.: ArXiv:1304.2185; Bi, X.-J., Yan, Q.-S., Yin, P.-F.: Phys. Rev. D 85, 035005 (2012). ArXiv:1111.2250; Papucci, M., Ruderman, J.T., Weiler, A.: ArXiv:1110.6926; Brust, C., Katz, A., Lawrence, S., Sundrum, R., JHEP 1203, 103 (2012). ArXiv:1110.6670; Arganda, E., Diaz-Cruz, J.L., Szynkman, A.: Eur. Phys. J. C 73, 2384 (2013). ArXiv:1211.0163; Phys. Lett. B 722, 100 (2013). ArXiv:1301.0708; Cao, J., Han, C., Wu, L., Yang, J.M., Zhang, Y.: JHEP 1211, 039 (2012). ArXiv:1206.3865; Hardy, E.: ArXiv:1306.1534; Baer, H., et al.: ArXiv:1306.3148; ArXiv:1306.4183; ArXiv:1310.4858

272. Kronfeld, A.S.: Annu. Rev. Nucl. Part. Sci. 62, 265 (2012). doi:10.1146/annurev-nucl-102711-094942. arXiv:1203.1204 [hep-lat]
273. Kubar-Andre, J., Paige, F.: Phys. Rev. D 19, 221 (1979)
274. Kuchiev, M.Yu., Flambaum, V.V.: (2003). hep-ph/0305053
275. Lane, K.: (2002). hep-ph/0202255; Chivukula, R.S.: (2000). hep-ph/0011264
276. Langacker, P.: The Standard Model and Beyond. CRC, Boca Raton, FL (2010); Paschos, E.A.: Electroweak Theory. Cambridge University Press, Cambridge, 2007; Becchi, C.M., Ridolfi, G.: An Introduction to Relativistic Processes and the Standard Model of Electroweak Interactions. Springer, Berlin (2006); Horejsi, J.: Fundamentals of Electroweak Theory. Karolinum, Prague (2002); Barbieri, R.: Lectures on the ElectroWeak Interactions. Publications of the Scuola Normale Superiore, Pisa (2007)
277. Leader, E., Sidorov, A.V., Stamenov, D.B.: Phys. Rev. D 82, 114018 (2010). ArXiv:1010.0574
278. Lee, B.W., Zinn-Justin, J.: Phys. Rev. D 5, 3121, 3137 (1972); 7, 1049 (1973)
279. Lee, B.W., Quigg, C., Thacker, H.B.: Phys. Rev. D 16, 1519 (1977)
280. Lee, B.W., Pakvasa, S., Shrock, R., Sugawara, H.: Phys. Rev. Lett. 38, 937 (1977); Lee, B.W., Shrock, R.: Phys. Rev. D 16, 1444 (1977)
281. LEPEWWG, figures included with permission. See also Schael, S., et al.: ALEPH and DELPHI and L3 and OPAL and LEP Electroweak Collaborations. Phys. Rep. 532, 119 (2013). doi:10.1016/j.physrep.2013.07.004 arXiv:1302.3415 [hep-ex]
282. LHCb Collaboration: (2013). ArXiv:1309.6534 and PAPER-2013-054
283. Lipatov, L.N.: Sov. J. Nucl. Phys. 20, 94 (1975)
284. Lipatov, L.N.: Sov. J. Nucl. Phys. 23, 338 (1976); Fadin, V.S., Kuraev, E.A., Lipatov, L.N.: Phys. Lett. B 60, 50 (1975); Sov. Phys. JETP 44, 443 (1976); 45, 199 (1977); Balitski, Y.Y., Lipatov, L.N.: Sov. J. Nucl. Phys. 28, 822 (1978)
285. Lombard, V.: Moriond QCD (2013). ArXiv:1305.3773
286. Maiani, L.: Proceedings of International Symposium on Lepton and Photon Interactions at High Energy, Hamburg (1977)
287. Martin, A.D., Stirling, W.J., Thorne, R.S., Watt, G.: Eur. Phys. J. C 64, 653 (2009). ArXiv:0905.3531
288. McNeile, C., et al., [HPQCD Collab.]: Phys. Rev. D 82, 034512 (2010) ArXiv:1004.4285; Davies, C.T.H., et al., [HPQCD Collab., UKQCD Collab., and MILC Collab.]: Phys. Rev. Lett. 92, 022001 (2004). ArXiv:0304004; Mason, Q., et al., [HPQCD and UKQCD Collaborations]: Phys. Rev. Lett. 95, 052002 (2005). hep-lat/0503005; Maltman, K., et al.: Phys. Rev. D 78, 114504 (2008). ArXiv:0807.2020; Aoki, S., et al., [PACS-CS Collab.]: JHEP 0910, 053 (2009). ArXiv:0906.3906; Shintani, E., et al., [JLQCD Collab.]: Phys. Rev. D 82, 074505 (2010). ArXiv:1002.0371; Blossier, B., et al., [ETM Collab.]: ArXiv:1201.5770
289. Melia, T., Melnikov, K., Rontsch, R., Zanderighi, G., JHEP 1012, 053 (2010). ArXiv:1007.5313; Phys. Rev. D 83, 114043 (2011). ArXiv:1104.2327; Greiner, N., et al.: Phys. Lett. B 713, 277 (2012). ArXiv:1202.6004; Denner, A., Hosekova, L., Kallweit, S. ArXiv:1209.2389; Jager, B., Zanderighi, G.: JHEP 1111, 055 (2011). ArXiv:1108.0864
290. Melnikov, K., Vainshtein, A.: Phys. Rev. D 70, 113006 (2004); Bijnens, J., Prades, J.: Mod. Phys. Lett. A 22, 767 (2007); Prades, J., de Rafael, E., Vainshtein, A.: In: Roberts, B.L., Marciano, W.J. (eds.) Lepton Dipole Moments, pp. 303–319. World Scientific, Singapore, (2009); Nyffeler, A.: Phys. Rev. D 79, 073012 (2009)

291. Minkowski, P.: Phys. Lett. B 67, 421 (1977); Yanagida, T.: In: Proceedings of the Workshop on Unified Theory and Baryon Number in the Universe, KEK (1979); Glashow, S.L.: In: Levy, M., et al. (eds.) Quarks and Leptons. Cargèse. Plenum, New York (1980); Gell-Mann, M., Ramond, P., Slansky, R.: In: Supergravity. Stony Brook, New York (1979); Mohapatra, R.N., Senjanovic, G.: Phys. Rev. Lett. 44, 912 (1980)
292. Moch, S., Vermaseren, J.A.M., Vogt, A.: Nucl. Phys. B 688, 101 (2004). hep-ph/0403192; Vogt, A., Moch, S., Vermaseren, J.A.M.: Nucl. Phys. B 691, 129 (2004). hep-ph/0404111; Vermaseren, J.A.M., Vogt, A., Moch, S.: Nucl. Phys. B 724, 3 (2005). hep-ph/0504242
293. Moch, S., Vermaseren, J.A.M., Vogt, A.: Phys. Lett. B 606, 123 (2005). hep-ph/0411112
294. Moretti, S., Lonnblad, L., Sjostrand, T.: JHEP 9808, 001 (1998). hep-ph/9804296
295. Mrazek, J., Wulzer, A.: Phys. Rev. D 81, 075006; Dissertori, G., et al., JHEP 1009, 019 (2010). ArXiv:1005.4414; Contino, R., Servant, G.: JHEP 06, 026 (2008). ArXiv:0801.1679; Vignaroli, N., JHEP 1207, 158 (2012). ArXiv:1204.0468; De Simone, A., et al.: ArXiv:1211.5663; Buchkremer, M., Cacciapaglia, G., Deandrea, A., Panizzi, L.: ArXiv:1305.4172; Grojean, C., Matsedonskyi, O., Panico, G.: ArXiv:1306.4655
296. Muller, B., Schukraft, J., Wyslouch, B.: Annu. Rev. Nucl. Part. Sci. 62, 361 (2012). doi:10.1146/annurev-nucl-102711-094910. arXiv:1202.3233 [hep-ex]
297. Muon g-2 Collab., Bennett, G.W., et al.: Phys. Rev. D 73, 072003 (2006); Roberts, B.L.: Chin. Phys. C 34, 741 (2010)
298. Narison, S.: QCD Spectral Sum Rules. World Scientific Lecture Notes in Physics, vol. 26, p. 1. World Scientific, Singapore (1989)
299. Nason, P.: JHEP 0411, 040 (2004). hep-ph/0409146; Frixione, S., Nason, P., Oleari, C.: JHEP 11, 070 (2007). ArXiv:0709.2092; Alioli, S., Nason, P., Oleari, C., Re, E.: JHEP 1006, 043 (2010). ArXiv:1002.2581
300. Nason, P., Dawson, S., Ellis, R.K.: Nucl. Phys. B 303, 607 (1988); Beenakker, W., Kuijf, H., van Neerven, W.L., Smith, J.: Phys. Rev. D 40, 54 (1989); Nason, P., Dawson, S., Ellis, R.K.: Nucl. Phys. B 327, 49 (1989); erratum ibid. B 335, 260 (1989); Mangano, M.L., Nason, P., Ridolfi, G.: Nucl. Phys. B 373, 295 (1992)
301. Neubert, M.: Phys. Rep. 245, 259 (1994). hep-ph/9306320; Manohar, A.V., Wise, M.B.: Camb. Monogr. Part. Phys. Nucl. Phys. Cosmol. 10, 1 (2000)
302. Nilles, H.P.: Phys. Rep. C 110, 1 (1984); Haber, H.E., Kane, G.L.: Phys. Rep. C 117, 75 (1985); Barbieri, R.: Riv. Nuovo Cim. 11, 1 (1988); Martin, S.P.: hep-ph/9709356; Drees, M., Godbole, R., Roy, P.: Theory and Phenomenology of Sparticles. World Scientific, Singapore (2004); Aitchinson, I.: Supersymmetry in Particle Physics: An Elementary Introduction. Cambridge University Press, Cambridge (2007)
303. NNPDF Collaboration, Ball, R.D., et al.: Nucl. Phys. B 874, 36 (2013). ArXiv:1303.7236
304. Ossola, G., Papadopoulos, C.G., Pittau, R.: Nucl. Phys. B 763, 147 (2007). hep-ph/0609007; JHEP 0803, 042 (2008). ArXiv:0711.3596; JHEP 0805, 004 (2008). ArXiv:0802.1876
305. Parke, S.J., Taylor, T.R.: Phys. Rev. Lett. 56, 2459 (1986)
306. Particle Data group, Yao, W.-M., et al.: J. Phys. G 33, 1 (2006)
307. Particle Data Group, Beringer, J., et al.: Phys. Rev. D 86, 010001 (2012)
308. Peccei, R.D.: In: Jarlskog, C. (ed.) CP Violation. Advanced Series on Directions in High Energy Physics, p. 503. World Scientific, Singapore (1989)
309. Peccei, R.D., Quinn, H.R.: Phys. Rev. Lett. 38, 1440 (1977); Phys. Rev. D 16, 1791 (1977); Weinberg, S.: Phys. Rev. Lett. 40, 223 (1978); Wilczek, F.: Phys. Rev. Lett. 40, 279 (1978)
310. Peskin, M.E., Takeuchi, T.: Phys. Rev. Lett. 65, 964 (1990); Phys. Rev. D 46, 381 (1991)
311. Pich, A.: (2013). ArXiv:1303.2262
312. Pontecorvo, B., Sov. Phys. JETP 6, 429 (1957); Zh. Eksp. Teor. Fiz. 33, 549 (1957); Maki, Z., Nakagawa, M., Sakata, S.: Prog. Theor. Phys. 28, 870 (1962); Sov. Phys. JETP 26, 984 (1968); Zh. Eksp. Teor. Fiz. 53, 1717 (1968); Gribov, V.N., Pontecorvo, B.: Phys. Lett. B 28, 493 (1969)
313. Quigg, C.: Annu. Rev. Nucl. Part. Sci. 59, 505 (2009). ArXiv:0905.3187
314. Randall, L., Sundrum, R.: Phys. Rev. Lett. 83, 3370 (1999); 83, 4690 (1999); Goldberger, W.D., Wise, M.B.: Phys. Rev. Lett. 83, 4922 (1999)

315. Ross, G.G.: Grand Unified Theories. Benjamin, Reading, MA (1985); Mohapatra, R.N.: Unification and Supersymmetry. Springer, Berlin (1986); Raby, S.: in [307]; Masiero, A., Vempati, S.K., Vives, O.: ArXiv:0711.2903
316. Salam, A.: In: Svartholm, N. (ed.) Elementary Particle Theory, p. 367. Almquist and Wiksells, Stockholm (1969)
317. Salam, G.P.: Eur. Phys. J. C 67, 637 (2010). ArXiv:0906.1833
318. Schellekens, A.N.: (2013). ArXiv:1306.5083
319. See, for example, https://twiki.cern.ch/twiki/bin/view/CMSPublic/PhysicsResultsSMPaTGC. Accessed 2013
320. See, for example, Lindner, M.: Z. Phys. 31, 295 (1986); Hambye, T., Riesselmann, K.: Phys. Rev. D55, 7255 (1997). hep-ph/9610272
321. See, for example, Kamenik, J.F., Shu, J., Zupan, J.: (2011). ArXiv:1107.5257; Drobnak, J., et al.: (2012). ArXiv:1209.4872
322. Shaposhnikov, M.: (2007). ArXiv:0708.3550; Canetti, L., Drewes, M., Shaposhnikov, M.: (2012). ArXiv:1204.3902; Canetti, L., Drewes, M., Frossard, T., Shaposhnikov, M.: (2012). ArXiv:1208.4607
323. Sher, M.: Phys. Rep. 179, 273 (1989); Phys. Lett. B 317, 159 (1993)
324. Shifman, M.: (2013). ArXiv:1310.1966 and references therein
325. Shifman, M., Vainshtein, A., Zakharov, V.: Nucl. Phys. B 147, 385 (1979)
326. Sissakian, A., Shevchenko, O., Ivanov, O.: Eur. Phys. J. C 65, 413 (2010). ArXiv:0908.3296
327. Stelzer-Chilton, O.: Hadron Collider Physics Symposium, Kyoto (2012); see also supplement to Phys. Rev. Lett. 112, 191802 (2014)
328. Stenzel, H.: JHEP 0507, 0132 (2005)
329. Sterman, G.: Nucl. Phys. B 281, 310 (1987); Catani, S., Trentadue, L.: Nucl. Phys. B 327, 323 (1989); Kidonakis, N., Sterman, G.: Nucl. Phys. B 505, 321 (1997)
330. Sudakov, V.V.: Sov. Phys. JETP 3, 75 (1956); Dokshitzer, Yu., Dyakonov, D., Troyan, S.: Phys. Lett. B 76, 290 (1978); Phys. Rep. 58, 269 (1980); Parisi, G., Petronzio, R.: Nucl. Phys. B 154, 427 (1979); Curci, G., Greco, M., Srivastava, Y.: Phys. Rev. Lett. 43 (1979); Nucl. Phys. B 159, 451 (1979); Collins, J., Soper, D.: Nucl. Phys. B 139, 381 (1981); B 194, 445 (1982); B 197, 446 (1982); Kodaira, J., Trentadue, L.: Phys. Lett. B 112, 66 (1982); B 123, 335 (1983); Collins, J., Soper, D., Sterman, G.: Nucl. Phys. B 250, 199 (1985); Davies, C., Webber, B., Stirling, J.: Nucl. Phys. B 256, 413 (1985)
331. Sundrum, R.: (2005). hep-th/0508134; Rattazzi, R.: (2006). hep-ph/ 0607055
332. Susskind, L.: Phys. Rev. D 20, 2619 (1979); Dimopoulos, S., Susskind, L.: Nucl. Phys. B 155, 237 (1979); Eichten, E., Lane, K.D., Phys. Lett. B 90, 125 (1980)
333. 't Hooft, G., Veltman, M.: Nucl. Phys. B 44, 189 (1972); Bollini, C.G., Giambiagi, J.J.: Nuovo Cimento 12B 20 (1972); Ashmore, J.F.: Nuovo Cimento Lett. 4, 289 (1972); Cicuta, G.M., Montaldi, E.: Nuovo Cimento Lett. 4, 329 (1972)
334. 't Hooft, G., Veltman, M.: Nucl. Phys. B 44, 189 (1972); Bollini, C.G., Giambiagi, J.J.: Phys. Lett. B 40, 566 (1972); Ashmore, J.F.: Nuovo Cim. Lett. 4, 289 (1972); Cicuta, G.M., Montaldi, E.: Nuovo Cim. Lett. 4, 329 (1972)
335. 't Hooft, G.: Nucl. Phys. B 61, 455 (1973)
336. 't Hooft, G.: Phys. Rev. Lett. 37, 8 (1976); Phys. Rev. D 14, 3432 (1976); erratum ibid. D 18, 2199 (1978)
337. Tarasov, O.V., Vladimirov, A.A., Zharkov, A.Yu.: Phys. Lett. B 93, 429 (1980)
338. Tenchini, R., Verzegnassi, C.: The Physics of the Z and W Bosons. World Scientific, Singapore (2008)
339. The ATLAS Collaboration: ATLAS-CONF-2012-024, 031,097,134 and 149 (2012)
340. The ATLAS Collaboration: ATLAS-CONF-2011-129; Guimares, J.: Talk at the ICHEP'12 Conference, Melbourne (2012)
341. The ATLAS Collaboration: Phys. Lett. B 716, 1 (2012). ArXiv:1207.7214 (2012)
342. The ATLAS Collaboration: ATL-PHYS-PUB-2011-01 (2011). https://atlas.web.cern.ch/Atlas/GROUPS/PHYSICS/PUBNOTES/ATL-PHYS-PUB-2011-013

343. The ATLAS Collaboration: Phys. Rev. D 85, 012005 (2012). ArXiv:1108.6308; Phys. Lett. B 705, 415 (2011). ArXiv:1107.2381; the CMS Collaboration, Phys. Rev. D 85, 032002 (2012). ArXiv:1110.4973 Phys. Rev. D 65, 112003 (2002); Phys. Rev. D 70, 074008 (2004); the D0 Collaboration, Phys. Rev. Lett. 87, 251805 (2001); Phys. Rev. Lett. 84, 2786 (2000)
344. The CKM Fitter Group: http://ckmfitter.in2p3.fr/. Accessed 2013
345. The CMS Collaboration, Aad, G., et al.: Phys. Lett. B. (2012). ArXiv:1207.7235
346. The CMS Collaboration: JHEP 1305, 065 (2013). ArXiv:1302.0508; Eur. Phys. J. C 73, 2386 (2013). ArXiv:1301.5755; Phys. Lett. B 720, 83 (2013). ArXiv:1212.6682, top-12-006, 007, arXiv:1602.09024
347. The D0 collaboration: Phys. Rev. Lett. 84, 2792 (2000); Phys. Rev. D 61, 032004 (2000); see also the CDF Collaboration, Phys. Rev. Lett. 84, 845 (2000)
348. The FLAG Working Group, Colangelo, G., et al.: (2010). ArXiv:1011.4408
349. The H1, ZEUS Collaborations: JHEP 1001, 109 (2010). ArXiv:0911.0884
350. The LEP Electroweak Working Group: http://lepewwg.web.cern.ch/LEPEWWG/. Accessed 2013
351. The LEP and SLD Collaborations: Phys. Rep. 427, 257 (2006). hep-ex/0509008
352. The LHCb and CMS Collaborations: LHCb-CONF-2013-012 (2013)
353. The NuTeV Collaboration, Zeller, G.P., et al.: Phys. Rev. Lett. 88, 091802 (2002)
354. The SLAC E158 Collaboration, Anthony, P.L., et al.: (2003). hep-ex/0312035, (2004). hep-ex/0403010
355. The Unitary Triangle Fit Group: http://www.utfit.org. Accessed 2013
356. van der Bij, J., Veltman, M.J.G.: Nucl. Phys. B 231, 205 (1984)
357. van Ritbergen, T., Vermaseren, J.A.M., Larin, S.A.: Phys. Lett. B 400, 379 (1997); see also Czakon, M.: Nucl. Phys. B 710, 485 (2005)
358. Veltman, M.: Nucl. Phys. B 21, 288 (1970); 't Hooft, G.: Nucl. Phys. B 33, 173 (1971); 35, 167 (1971)
359. Weinberg, S.: Phys. Rev. Lett. 19, 1264 (1967)
360. Weinberg, S.: Phys. Rev. Lett. 31, 494 (1973)
361. Weinberg, S.: Phys. Rev. D 11, 3583 (1975)
362. Weinberg, S.: Phys. A 96, 327 (1979); Gasser, J., Leutwyler, H.: Ann. Phys. 158, 142 (1984); Nucl. Phys. B 250, 465 (1985); Bijnens, J., Ecker, G., Gasser, J.: The Second DAΦNE Physics Handbook (Frascati, 1995). hep-ph/9411232; Bijnens, J., Meissner, U.: hep-ph/9901381; Ecker, G.: hep-ph/9805500, hep-ph/0011026; Leutwyler, H.: hep-ph/9609465, hep-ph/0008124; Pich, A.: hep-ph/9806303; de Rafael, E.: hep-ph/9502254; Maiani, L., Pancheri, G., Paver, N.: The Second DAΦNE Physics Handbook (Frascati, 1995); Ecker, G.: Prog. Part. Nucl. Phys. 35, 1 (1995); Colangelo, G., Isidori, G.: hep-ph/0101264
363. Weinberg, S.: Phys. Rev. D 22, 1694 (1980)
364. Weinberg, S.: Phys. Rev. Lett. 59, 2607 (1987)
365. Wilson, K.: Phys. Rev. 179, 1499 (1969)
366. Wilson, K.G.: Phys. Rev. D 10, 2445 (1974)
367. Witten, E.: Nucl. Phys. B 156, 269 (1979); Veneziano, G.: Nucl. Phys. B 159, 213 (1979)
368. Witten, E.: Commun. Math. Phys. 252, 189 (2004). hep-th/0312171
369. Wobisch, M., Britzger, D., Kluge, T., Rabbertz, K., Stober, F., (the Fast NLO Collaboration): (2011). ArXiv:1109.1310
370. Wolfenstein, L.: Phys. Rev. Lett. 51, 1945 (1983)
371. Yang, C.N., Mills, R.: Phys. Rev. 96, 191 (1954)
372. Zijlstra, E.B., van Neerven, W.L.: Phys. Lett. B 273, 476 (1991); Phys. Lett. B 297, 377 (1992); Guillen, J.S., et al.: Nucl. Phys. B 353, 337 (1991)
373. Zuber, K.: Acta Phys. Polon. B 37, 1905–1921 (2006). nucl-ex/0610007